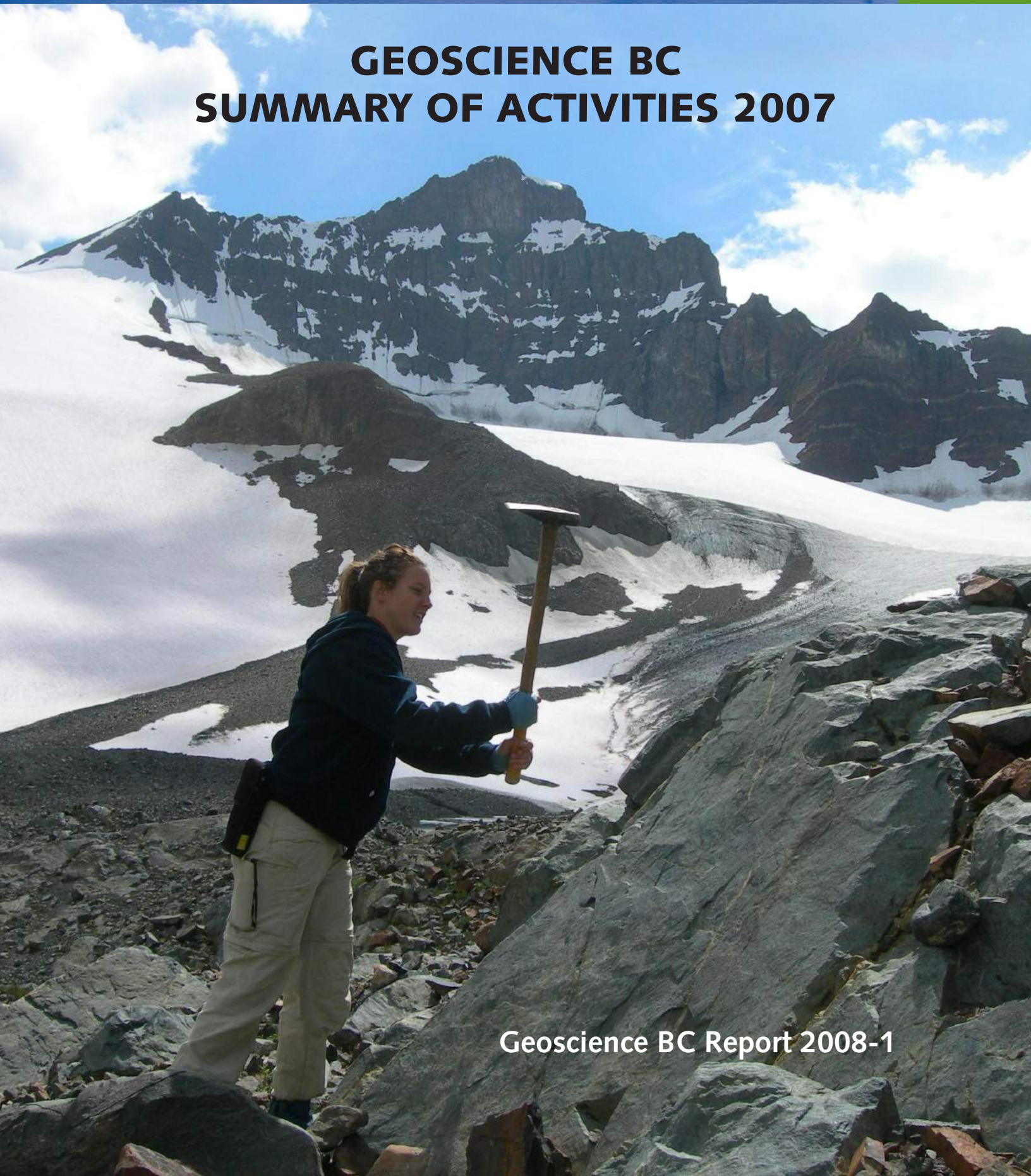




GEOSCIENCE BC SUMMARY OF ACTIVITIES 2007





GEOSCIENCE BC SUMMARY OF ACTIVITIES 2007

© 2008 by Geoscience BC

All rights reserved. Electronic edition published 2008.

This publication is also available, free of charge, as colour digital files in Adobe Acrobat® PDF format from the Geoscience BC website: <http://www.geosciencebc.com/s/DataReleases.asp>.

Every reasonable effort is made to ensure the accuracy of the information contained in this report, but Geoscience BC does not assume any liability for errors that may occur. Source references are included in the report and users should verify critical information.

When using information from this publication in other publications or presentations, due acknowledgment should be given to Geoscience BC. The recommended reference is included on the title page of each paper. The complete volume should be referenced as follows:

Geoscience BC (2008): Geoscience BC Summary of Activities 2007; Geoscience BC, Report 2008-1, 150 p.

ISSN 1916-2960 Summary of Activities (Geoscience BC)

Cover photo: Erin Looby collecting andesite samples in the shadow of RCAF peak.

Photo credit: Lucy Hollis, 2007

Foreword

Geoscience BC Overview

Geoscience BC (GBC) is a unique, industry-led, industry-focused, not-for-profit geoscience organization. Since its inception in April 2005 with a start-up grant from the Provincial Government of British Columbia, GBC has pursued its mandate of attracting new exploration investment to British Columbia through a combination of GBC-led initiatives and funding of partnership projects. The majority of GBC's partnership projects are identified through an annual Request for Proposals (RFP) process. Geoscience BC-led geophysical and geochemical surveys have been developed by GBC staff and the Project Team, and undertaken by means of contracts awarded through a call for bids, or sole-sourced where specific technical expertise was required.

Geoscience BC obtains industry input into project planning through our Project Team of highly respected consultants and our Technical Advisory Committee of dedicated industry volunteers and government geoscientists, who advise GBC's Board on project priorities and review proposals received in response to the RFPs.

To date, GBC has supported 35 partnership projects with an investment of \$5.8 million, which has been matched by almost \$5.4 million in partners' funds. These projects include mineral deposit studies and mapping projects, geochemical studies, examinations of Chilcotin basalt cover in interior BC, development of a physical rock properties database, and numerous oil and gas-related projects in the intermontane basins.

Geoscience BC is committed to the development of the next generation of exploration geoscientists. GBC's contributions to partnership projects based at academic institutions exceed \$1.6 million to date. All of these projects have involved training and education opportunities for graduate and/or undergraduate students. Many of GBC's partnership projects with government also include training for geoscience students. In 2007, GBC awarded ten \$5000 scholarships to geoscience graduate students across Canada and in Australia, who are working on exploration-related geoscience research projects in BC.

Geoscience BC has also supported extensive additions to the Province of British Columbia's geological, geochemical and geophysical databases (*see* listing below of data and reports released in 2007). Figures 1 and 2 illustrate the locations of GBC-supported geochemical and geophysical surveys.

Geoscience BC's QUEST Project, initiated in June 2007 and partnered with the Northern Development Initiative

Trust, represents an additional \$5 million investment in new minerals-related geoscience data (*see* below and papers in this volume).

Geoscience BC Summary of Activities 2007

Geoscience BC is pleased to present the results of 2007 geoscience studies and surveys in this first edition of the *Geoscience BC Summary of Activities*. The volume is divided into three sections and contains a total of sixteen articles, prepared by industry consultants and contractors, university-based researchers and government geoscientists.

QUEST

The first section of the volume contains two brief overview papers on the geophysical and geochemical surveys underway as part of Geoscience BC's QUEST (QUesnellia EXploration STRategy) Project in central BC. The QUEST Project is a \$5 million program of new geoscience data collection and compilation designed to stimulate exploration interest and investment in BC's interior, specifically in the highly prospective Quesnel Terrane, where the bedrock is obscured by glacial cover.

Barnett and Kowalczyk (from BW Mining and PK Geophysics, respectively), members of GBC's Project Team, outline the survey design for the QUEST airborne geophysical surveys. They include an overview of existing publicly available regional geophysical datasets (airborne magnetic and ground gravity) from the Geoscience Data Repository at Natural Resources Canada, and an outline of the rationale for new airborne electromagnetic (EM) and airborne gravity geophysical surveys for the project area. In addition, they include a preliminary perspective view of stacked sections from a small area of the EM survey, illustrating some of the possible bedrock features observed in the data.

Jackaman and Balfour (the former from Noble Exploration Services and a member of GBC's Project Team, the latter a private consultant based in Cranbrook) provide a summary of the QUEST geochemical program, which covers an area of more than 95 000 km². The program includes a new reconnaissance Regional Geochemical Survey of NTS sheet 0930 (a 10 500 km² area), infill lake sediment sampling over an area of 19 000 km² from north of Quesnel to Mount Milligan, and reanalysis of almost 4500 stream and almost 500 lake sediment pulps from government archives of regional geochemical samples stored in Ottawa (by the Geological Survey of Canada) and Victoria (by the BC Geological Survey).

Mineral Projects

The second section of the volume contains nine papers on mineral exploration–related geoscience projects supported by Geoscience BC.

Andrews and Russell, from the University of British Columbia (UBC), provide an update on their investigations of cover thicknesses across the Southern Interior Plateau. They summarize their work to date on the Chilcotin Group basalts, and information from the provincial water well database, to help constrain the thickness of both Quaternary drift and basalt cover in the interior.

Blevings et al., also from UBC, summarize their work on understanding the controls on copper and gold mineralization along the contacts between the northeastern Coast Belt

and the Coast Plutonic Complex in the Taseko Lakes region. Their paper includes short summaries of previous project work; new descriptions of several important mineral occurrences in the study area; and outline plans for additional work to constrain the pressure, temperature and age of the mineralization and develop a metallogenic model for the region. This work forms part of an M.Sc. thesis by the first author.

Fecova et al., from Simon Fraser University (SFU) and UBC, provide a summary of new geological mapping in the Nootka Sound area and their studies of new mafic-ultramafic layered intrusions identified during the course of their mapping and mineral deposit investigations in the area. This work, being completed as part of an M.Sc. thesis by the first author, has generated considerable new industry interest in this area of Vancouver Island.

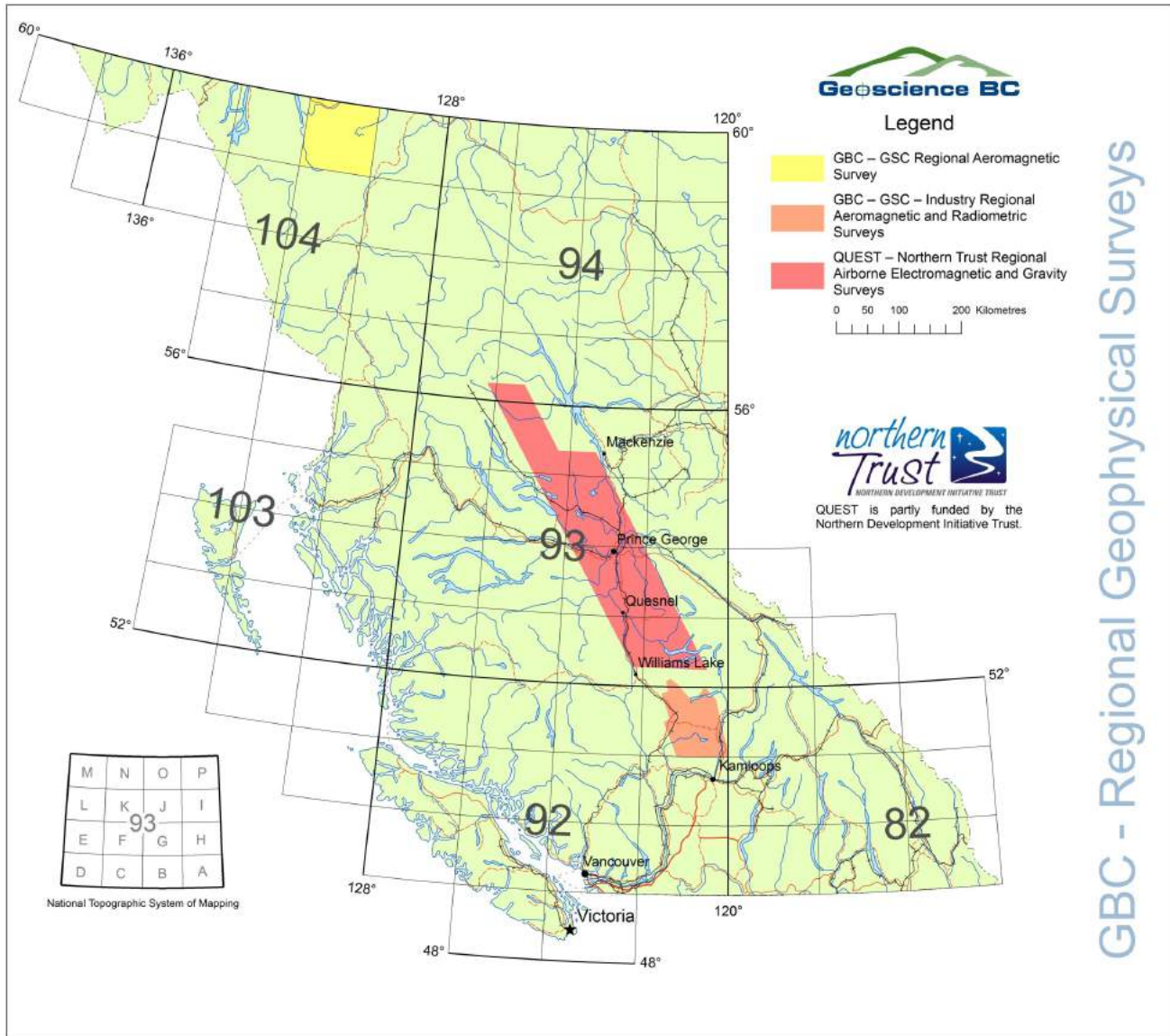


Figure 1. Locations of Geoscience BC–supported airborne geophysical surveys undertaken since April 2005.

Hart et al., from the University of Western Australia, with colleagues from the United States Geological Survey and UBC, provide critical new geochronological information for the Bralorne-Pioneer camp in the Bridge River mining district of southwestern BC. Their investigations of the timing of gold introduction and relationships to other mineralizing and intrusive events in the area have important implications for our understanding of the metallogeny of the region.

Hollis et al., from UBC, are also undertaking mineral deposit studies in the Taseko Lakes area (*see* Blevings et al.), examining the porphyritic intrusions and related copper showings in the region. This project, being undertaken as an M.Sc. by the first author, aims to develop a geological framework for the formation of the showings and their relationship to models of porphyry deposit formation.

Kilby and Kilby continue to provide leading-edge public access and analysis tools for remote-sensing imagery as applied to mineral exploration in BC. Their paper presents a summary of the Hyperspectral Demonstration Project, undertaken on behalf of Geoscience BC in 2007 to provide samples of airborne hyperspectral images over eight exploration and mining sites in BC. The new imagery will be made available through the MapPlace website of the BC Ministry of Energy, Mines and Petroleum Resources (MEMPR). The new imagery will be incorporated into the Image Analysis Toolbox and can be utilized with the Landsat, ASTER and other datasets on MapPlace.

Ruks and Mortensen, from UBC, have undertaken an intensive examination of the geological setting of volcanogenic massive sulphide (VMS) occurrences and their relationship to exhalitive iron formation in the Sicker Group of the Port

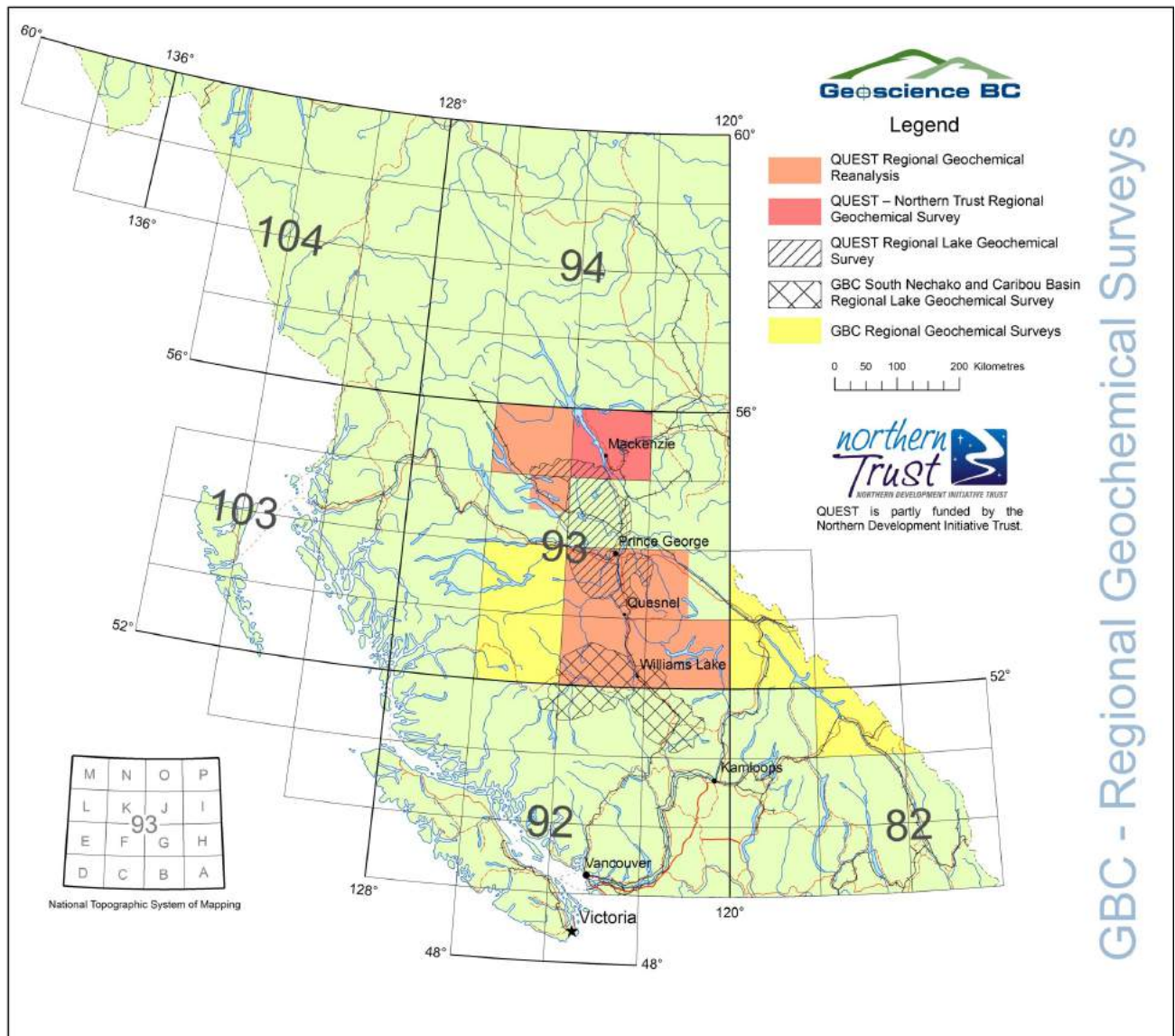


Figure 2. Locations of Geoscience BC-supported regional geochemical surveys undertaken since April 2005.

Alberni area on southern Vancouver Island. They report two new sulphide occurrences identified during the course of their mapping, and the implications of their mapping work for VMS exploration in the area. The first author is pursuing Ph.D. studies at UBC.

Smith et al., from University of Nevada–Reno (UNR), and colleagues at Adanac Molybdenum Corporation are examining the potential linkages between gold-depleted porphyry molybdenum deposits and ‘intrusion-hosted’ gold deposits. Their studies are focused on the Adanac Molybdenum property in the Atlin area. The paper presents detailed rock descriptions and whole-rock and trace-element geochemistry of a representative sample suite from the Adanac deposit, and represents part of the first author’s graduate work at UNR.

Tosdal et al., from the Mineral Deposits Research Unit (MDRU) at UBC, and colleagues from the Centre for Excellence in Ore Deposits Research (CODES) at the University of Tasmania and from industry report on a component of the CODES-MDRU Alkalic Porphyry Project. This paper summarizes the hydrothermal breccias observed in ore zones of the silica-undersaturated alkali copper-gold porphyry mineralization at Mount Polley, between Williams Lake and Quesnel in the Quesnel Terrane. This project includes contributions from numerous graduate students, including the second author, who is undertaking an M.Sc. at MDRU, and the third author, who is pursuing a Ph.D. at CODES.

Oil and Gas Projects

The third section of this volume comprises five papers summarizing Geoscience BC–supported contributions to oil and gas exploration geoscience projects in BC.

Cassidy et al., from the Geological Survey of Canada (GSC) and the University of Victoria (UVic), are undertaking a passive seismic study of the Nechako Basin to help assess the hydrocarbon and mineral potential of the basin and develop a better understanding of the crustal architecture in this region. Seven seismic stations were deployed in 2006, and results will complement planned active-source seismic and magnetotelluric studies planned and underway in the area. This research is being undertaken as part of an M.Sc. thesis by the third author.

Gagnon and Waldron, from the University of Alberta, are continuing their investigations of the evolution of the Bowser Basin in northwestern BC. They are concentrating on providing new detailed stratigraphic observations of the Hazelton Group–Bowser Lake Group transition, exhibited in a continuous exposure across the Ashman Ridge section, located approximately 40 km west of Smithers. Their aim is to develop a clearer understanding of this stratigraphic transition, which has implications for both mineral and hy-

drocarbon exploration. The first author is presently pursuing Ph.D. studies.

Hayward and Calvert, from SFU, have re-evaluated the stratigraphy and structure of the southeastern Nechako Basin from a reinterpretation of the Canadian Hunter 1980s seismic reflection profiles, including tomographic velocity modelling. They are integrating the seismic interpretations with relevant geological and geophysical data, including well logs, geology and potential-field data, to create new, more detailed interpretations of the basin. The results of this work will provide key constraints on collection and interpretation of new seismic data.

Mustard et al., from SFU, the University of Wisconsin–Eau Claire (UWEC) and the GSC, report on the second year of their study of the Jackass Mountain Group and its potential as a hydrocarbon reservoir system in the Nechako Basin. Their work aims to develop a better understanding of regional facies patterns and basin architecture within the Nechako Basin. Their paper presents a summary of the 2007 field observations and an overview of their regional sampling program and future work. This project is supporting M.Sc. theses by the third and fourth authors at SFU, and a B.Sc. project next year at UWEC.

Spratt et al., from Geoscience BC, GSC and MEMPR, have re-examined 20-year old magnetotelluric (MT) data from within the Nechako Basin and initiated new MT data collection in the south-central part of the basin. Their work indicates that the MT method may be an important tool for understanding shallow structures and mapping the boundaries of the basin and structures within the basin. The 2007 survey has collected both audiomagnetotelluric (AMT) and broadband magnetotelluric (BBMT) data from within the Nechako Basin.

Geoscience BC Publications 2007

New Geoscience BC data sets and reports released in 2007 include:

- twenty-three technical articles in the joint *Geological Fieldwork 2006* volume, copublished with the BC Geological Survey;
- **high-resolution airborne magnetic data for the Jennings River area (NTS 104O)**, funded by GBC and managed by and jointly released with Natural Resources Canada (NRCan);
- **airborne gamma-ray spectrometric and magnetic data for the Bonaparte Lake area (parts of NTS 092P and 093A)**, released in partnership with NRCan’s Targeted Geoscience Initiative III, Candorado Operating Company Limited, Amarc Resources Limited and GWR Resources Limited;
- **‘Skeena Arch Metallogenic Data and Map, Compilation of NTS Map Sheets 093E, L, M; South**

Half of 094D, East Half of 103I and Southeast Corner of 103P by D.G. MacIntyre;

- **‘A Comparative Assessment of Soil Geochemical Methods for Detecting Buried Mineral Deposits – 3Ts Au-Ag Prospect, Central British Columbia’** by S.J. Cook and C.E. Dunn;
- **‘Regional Drainage Sediment and Water Geochemical Data, South Nechako Basin and Cariboo Basin, Central British Columbia (parts of NTS 092N, O, P, 093A and B)’**, by W. Jackaman, which contains new lake sediment and water data covering more than 16 000 km² of previously unsurveyed ground in central BC;
- **‘Geoscience BC Mountain Pine Beetle Data Repository Version 1.0’** by W. Jackaman, which compiles publicly available multimedia regional geochemical information for the core of the Mountain Pine Beetle Infestation Area of BC;
- **‘Halogens in Surface Exploration Geochemistry: Evaluation and Development of Methods for Detecting Buried Mineral Deposits’** by C.E. Dunn, S.J. Cook and G.E.M. Hall; and
- four new 1:50 000 scale bedrock geology maps, available from the Geological Survey of Canada: **‘Geology,**

Tahtsa Peak (93 E/12), British Columbia’; **‘Geology, parts of Chikamin Mountain and Troitsa Lake (93 E/06 and 11), British Columbia’;** **‘Geology, Tsaytis River (93 E/05), British Columbia’;** and **‘Geology, Kitlope Lake (east part) (93 E/04), British Columbia’;** all by J.B. Mahoney, J.W. Haggart, R.L. Hooper, L.S. Snyder, G.J. Woodsworth.

Acknowledgments

Geoscience BC would like to acknowledge our Technical Advisory Committee of volunteers from the mineral and oil and gas exploration industries, our project proponents, and our government geoscience partners in the BC Geological Survey and the Resource and Development Geoscience branches for all their contributions to this volume and other Geoscience BC projects. RnD Technical is also acknowledged for their high-quality work in editing and assembling this volume.

In addition, Geoscience BC would like to thank the Northern Development Initiative Trust, based in Prince George, who provided Geoscience BC with a grant to fund part of the QUEST Project.

C.D. (‘Lyn’) Anglin
President and CEO

Garth Kirkham
Vice President – Industry Liaison

Christa Sluggett
Project Geologist and Communications Co-ordinator
Geoscience BC

www.geosciencebc.com

Contents

QUEST Project

- Barnett, C.T. and Kowalczyk, P.L.:** Airborne electromagnetics and airborne gravity in the QUEST project area, Williams Lake to Mackenzie, British Columbia. 1
- Jackaman, W. and Balfour, J.S.:** QUEST Project geochemistry: field surveys and data reanalysis, central British Columbia. 7

Minerals Projects

- Andrews, G.D.M. and Russell, J.K.:** Cover thickness across the southern Interior Plateau, British Columbia: constraints from water-well records 11
- Blevings, S.K., Kennedy, L.A. and Hickey, K.A.:** Controls on copper and gold mineralization along the contact between the Coast Plutonic Complex and the southeast Coast Belt, Taseko Lakes region, southwestern British Columbia. 21
- Fecova, K., Marshall, D., Staples, R., Xue, G., Ullrich, T.D. and Close, S.:** Layered intrusions and regional geology of the Nootka Sound area, Vancouver Island, British Columbia. 35
- Hart, C.J.R., Goldfarb, R.J., Ullrich, T.D. and Friedman, R.:** Gold, granites and geochronology: timing of formation of the Bralorne-Pioneer gold orebodies and the Bendor batholith, southwestern British Columbia. . . . 47
- Hollis, L., Hickey, K. and Kennedy, L.A.:** Mineralization and alteration associated with an hypothesized copper (molybdenum) porphyry system in the Taseko Lakes area, southwestern British Columbia 55
- Kilby, W.E. and Kilby, C.E.:** Hyperspectral Imagery Demonstration Project, British Columbia 67

- Ruks, T. and Mortensen, J.K.:** Geological setting of volcanogenic massive sulphide occurrences in the Middle Paleozoic Sicker Group of the Cowichan Lake uplift, southern Vancouver Island, British Columbia 77
- Smith, J.L., Arehart, G.B. and Pinsent, R.:** New models for mineral exploration in British Columbia: is there a continuum between porphyry molybdenum deposits and intrusion-hosted gold deposits? 93
- Tosdal, R.M., Jackson, M., Pass, H.E., Rees, C., Simpson, K.A., Cooke, D.R., Chamberlain, C.M. and Ferreira, L.:** Hydrothermal breccia in the Mount Polley alkaline porphyry copper-gold deposit, British Columbia 105

Oil and Gas Projects

- Cassidy, J.F., Al-Khoubbi, I. and Kim, H.S.:** Mapping the structure of the Nechako Basin using passive source seismology. 115
- Gagnon, J-F. and Waldron, J.W.F.:** Ashman Ridge section revisited: new insights for the evolution of the Bowser Basin, northwestern British Columbia. 121
- Hayward, N. and Calvert, A.J.:** Structure of the southeastern Nechako Basin, south-central British Columbia: preliminary results of seismic interpretation and first-arrival tomographic modelling 129
- Mustard, P.S., Mahoney, J.B., Goodin, J.R., MacLaurin, C.I. and Haggart, J.W.:** New studies of the Lower Cretaceous Jackass Mountain Group on the southern margin of the Nechako Basin, south-central British Columbia: progress and preliminary observations . . . 135
- Spratt, J., Craven, J., Shareef, S., Ferri, F. and Riddell, J.:** Designing a test survey in the Nechako Basin, south-central British Columbia to determine the usefulness of the magnetotelluric method in oil and gas exploration 145

Airborne Electromagnetics and Airborne Gravity in the QUEST Project Area, Williams Lake to Mackenzie, British Columbia (parts of NTS 093A, B, G, H, J, K, N, O; 094C, D)

C.T. Barnett, BW Mining, Boulder, Colorado, USA, colin@bwmining.com

P.L. Kowalczyk, PK Geophysics Inc., Vancouver, BC

Barnett, C.T. and Kowalczyk, P.L. (2008): Airborne electromagnetics and airborne gravity in the QUEST Project area, Williams Lake to Mackenzie, British Columbia (parts of NTS 093A, B, G, H, J, K, N, O; 094C, D); in Geoscience BC, Summary of Activities 2007, Geoscience BC, Report 2008-1, p. 1–6.

Introduction

Geoscience BC's QUEST Project (QUesnellia EXploration STRategy) is designed to stimulate mineral exploration in the drift-covered section of the Quesnellia Terrane between Williams Lake and Mackenzie, British Columbia. This is a belt of highly prospective rocks that to date has had little exploration because of the till and lacustrine cover left by retreating glaciers (Logan et al., 2007).

At the northern and southern ends of the QUEST Project area, the Quaternary cover is thinner, and several important deposits have been discovered. At the southern end are the Gibraltar porphyry copper and the Mt. Polley porphyry copper-gold deposits, and at the northern end is the Mt. Milligan copper-gold porphyry deposit. A number of recent mineral discoveries have also been made further north from Mt. Milligan. An extension to the original QUEST survey area has been funded by the Northern Development Initiative Trust, based in Prince George, that will help stimulate further exploration to the northwest.

Geoscience BC's QUEST Project will compile publicly available topographic, watershed, surficial and bedrock geology, geophysical, geochemical, mineral deposit and road access data for an area of approximately 150 000 km², centred on Prince George (Figure 1). Geoscience BC is also collecting approximately 2 100 new lake and sediment samples to increase the density of geochemical sampling north and west of Prince George (Jackaman and Balfour, 2008). In addition, new airborne gravity and electromagnetic surveys are being flown

Keywords: *airborne gravity, airborne electromagnetics, regional geophysical surveys, porphyry copper-gold deposits, target generation, Quesnellia Terrane, QUEST Project.*

This publication is also available, free of charge, as colour digital files in Adobe Acrobat® PDF format from the Geoscience BC website: <http://www.geosciencebc.com/s/DataReleases.asp>.



Figure 1. Location of the QUEST Project area, showing the outline of new airborne gravity and electromagnetic surveys being conducted in the QUEST Project. Note that any new deposits found in this area will be close to existing infrastructure.

to help map the bedrock geology under the glacial drift and to provide a framework for further exploration in this area.

Surficial Geology and Regional Geophysics

Figure 2 shows the surface geology of the QUEST Project area, based on the 1:1 000 000 geological map published by the BC Geological Survey (Massey et al., 2005). It can be seen that large areas of this map are pale yellow, which represents the Quaternary cover. Until recently it was thought that the thickness of the glacial overburden would make the exploitation of any new discovery uneconomic. Review of water well data and observations made during recent geological mapping suggests that the Quaternary cover may

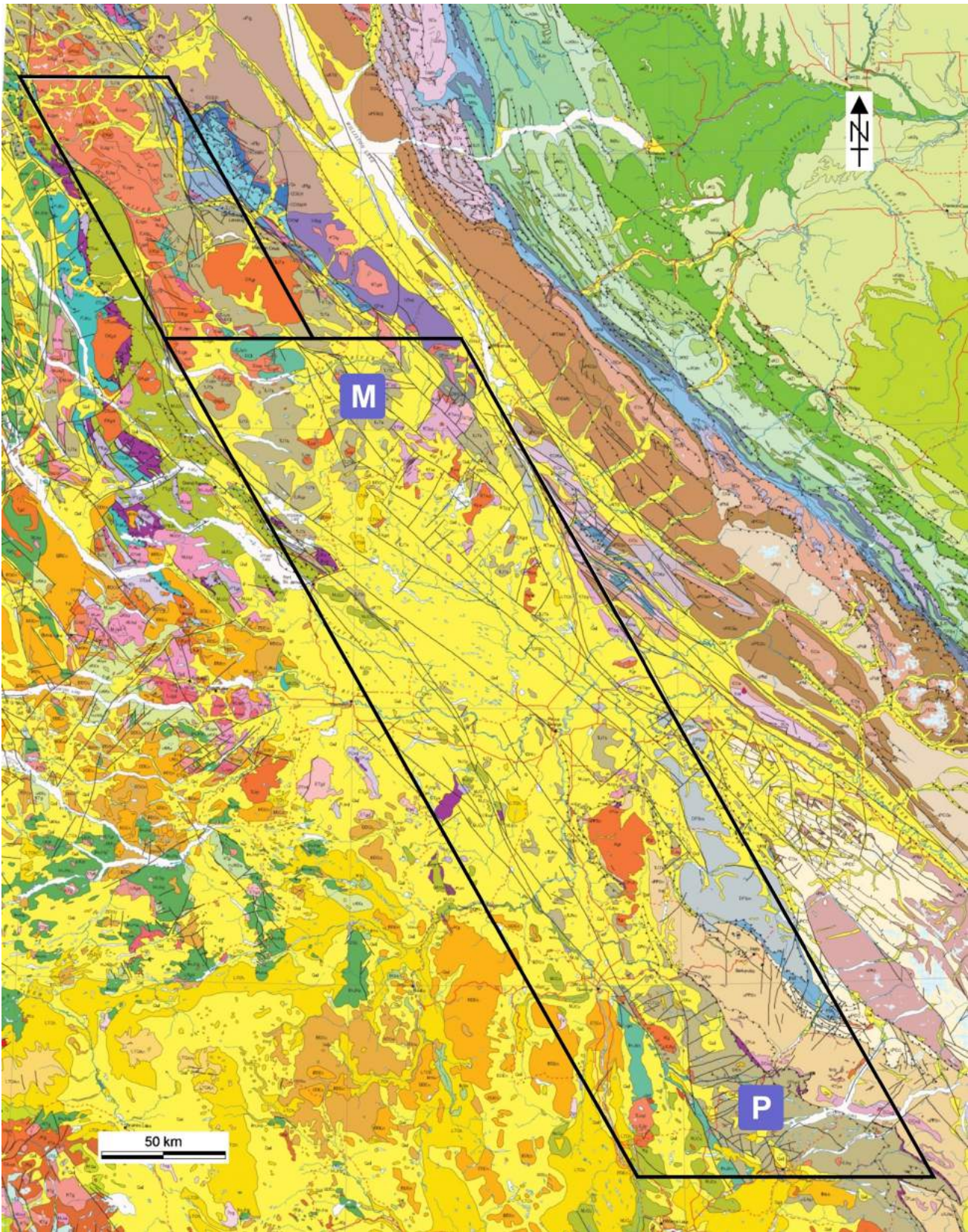


Figure 2. Surficial geological map of the QUEST Project area, showing the outline of the QUEST airborne gravity and electromagnetic surveys. The pale yellow areas represent the Quaternary overburden. Mt. Milligan is marked with an 'M', while Mt. Polley is marked with a 'P'. The smaller block to the northwest outlines the extension to the original QUEST geophysical survey area that was funded by a grant from the Northern Development Initiative Trust.

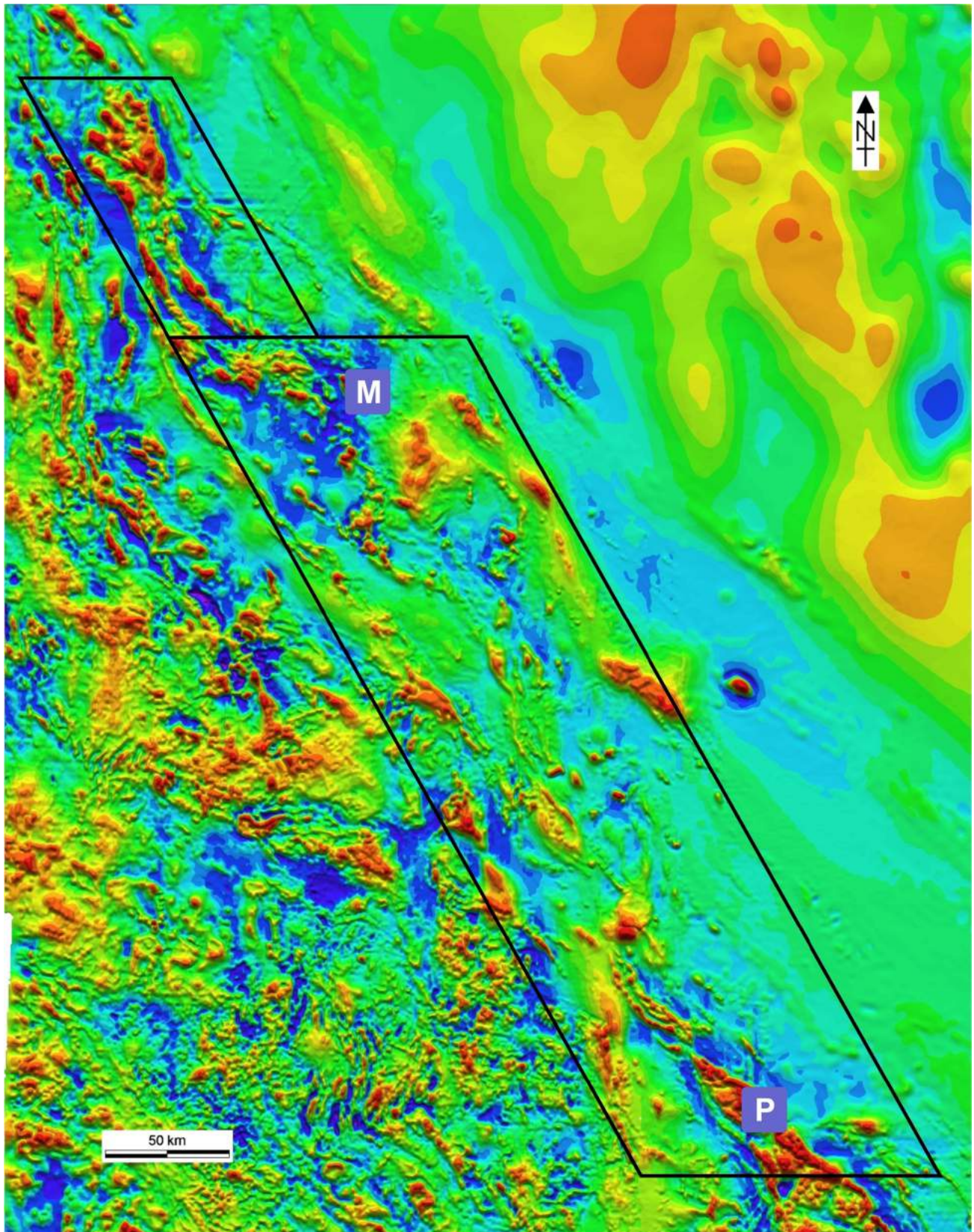


Figure 3. Reduced-to-pole magnetic image of the QUEST Project area, showing the outline of the QUEST airborne gravity and electromagnetic surveys. The grid interval for these data is about 250 m.

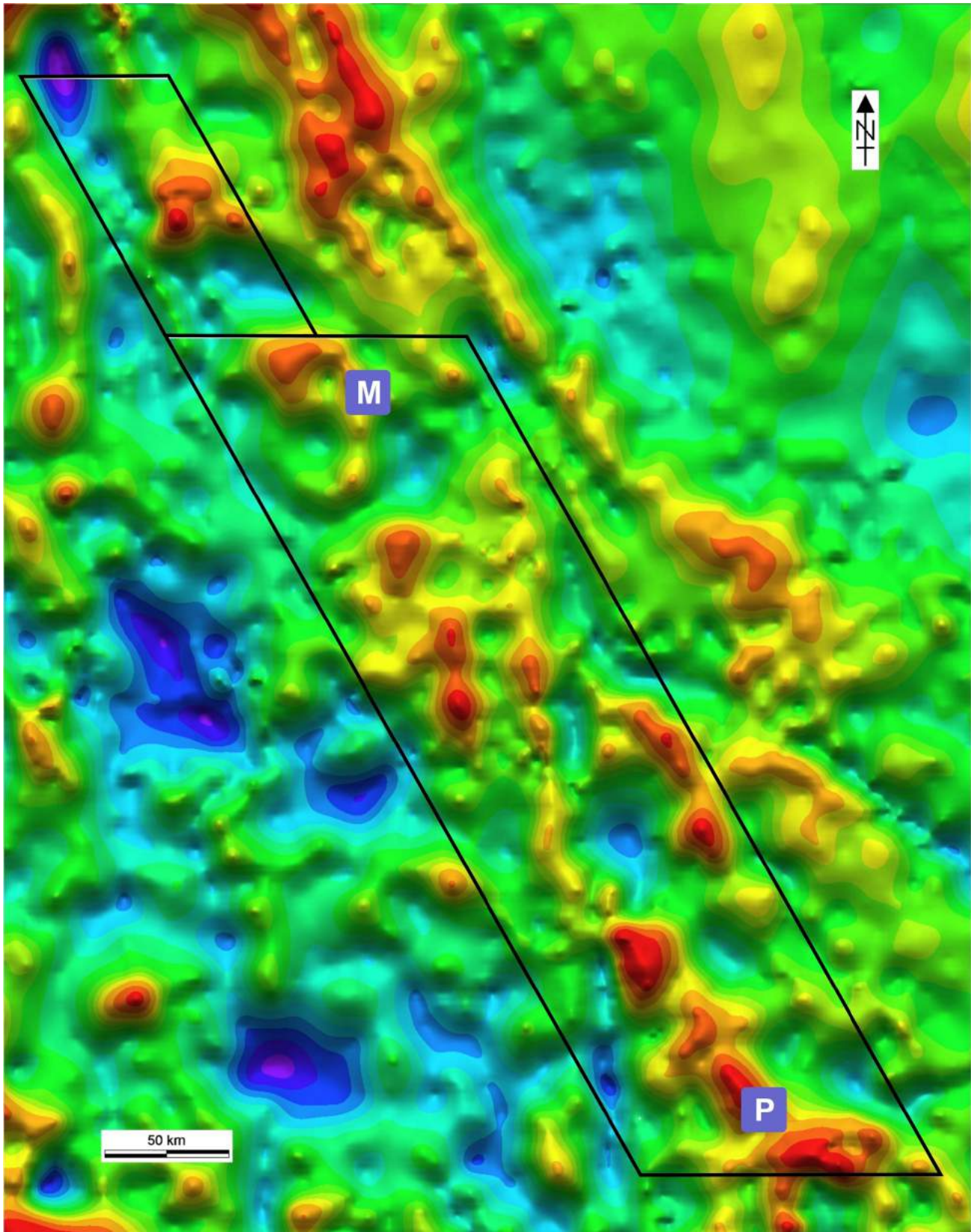


Figure 4. Isostatic residual gravity image of the QUEST Project area, showing the outline of the QUEST airborne gravity and electromagnetic surveys. The grid interval for these data is about 2 500 m.

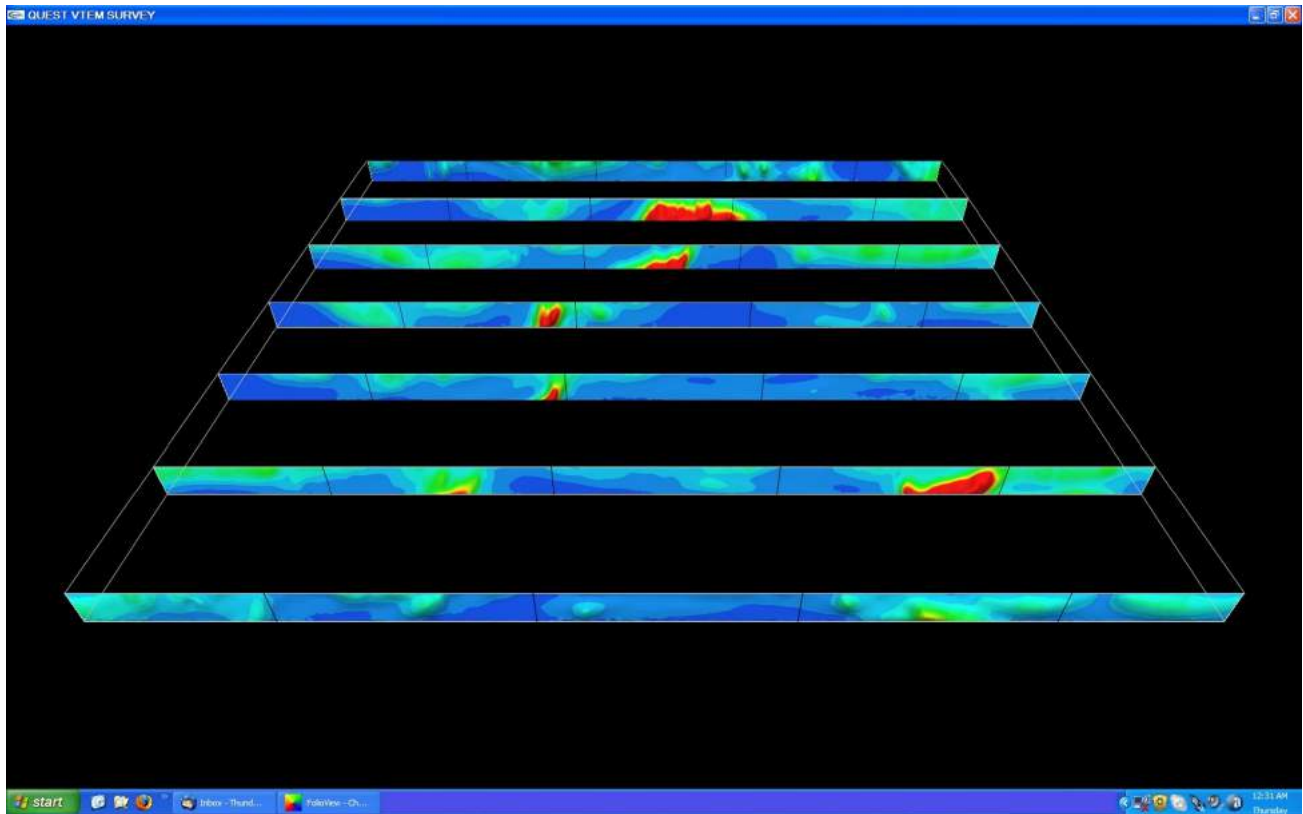


Figure 5. Perspective view of stacked airborne electromagnetic sections from a portion of the QUEST Project area. Resistive areas are shown in blue, while overburden conductors are highlighted in green and probable bedrock conductors, in red. The line spacing between the EM sections is 4000 m. Image produced by BW Mining, Boulder, Colorado.

not be as thick as previously assumed over much of the area (Andrews and Russell, 2008).

Figures 3 and 4 show the existing aeromagnetic and gravity datasets for the QUEST Project area that are available from Natural Resource Canada's Geoscience Data Repository (<http://www.gdr.nrcan.gc.ca/>). The majority of the magnetic surveys were flown on east-west flight lines at a line spacing of 805 m, which permits the data to be gridded at an interval of 250 m. The gravity readings were collected at an average station spacing of 10 km, which permits the data to be gridded only at a relatively coarse interval of 2 500 m. Nonetheless, both these datasets contain useful information. It can be seen, for example, that Mt. Polley (P) and Mt. Milligan (M) are spatially associated with magnetic and gravity highs, which are related to the Late Triassic and Early Jurassic alkalic intrusions that host these deposits.

New Airborne Geophysical Surveys

Although the existing aeromagnetic dataset could certainly be improved by flying lower and more closely spaced lines, it was felt that the existing data provide an adequate framework for exploration in this area. Geoscience BC's Project Development Team concluded that a greater advantage would be gained from an airborne gravity survey to im-

prove the density of the existing ground stations, and an airborne electromagnetic survey to map conductivity. In combination, these data should complement the existing aeromagnetic dataset.

Figures 1 to 4 show the outline of the two new airborne surveys, which were designed to cover an area of approximately 46 000 km² in one field season. The gravity survey will be flown at a line spacing of 2 km to permit gridding the data at 500 m, which should result in a five-fold improvement over the existing data. The electromagnetic survey was flown at a line spacing of 4 km. The two surveys are being flown on matching east-west lines with the hope of mapping cross structures as well as the regional trend of the northwest-trending geology. Every second line will therefore contain both detailed gravity and EM traverses.

The gravity survey is currently in progress, and is being flown with the Sander AIRGrav fixed-wing system. The airborne gravity survey should map the plutons at depth, which are expected to be important controls for any porphyry copper or copper-gold deposits, and differentiate lithologies in the subsurface geology based on their density.

The electromagnetic survey was completed in late October, and was flown with the Geotech VTEM helicopter-borne

system. This electromagnetic system was selected for the QUEST Project as it has the power to penetrate the Quaternary cover, in order to map the basement conductivity and to provide an indication of areas where the cover is thinner and hence of greater possible economic interest to the exploration industry.

The VTEM data are still being processed, but the initial results indicate that the system is seeing through the Quaternary overburden and picking up discrete conductors in the bedrock. Figure 5 shows a perspective view of stacked vertical time sections of the VTEM data for a small portion of the QUEST Project. Areas shown in blue are resistive, while areas shown in green are more conductive and typically represent the glacial till. A number of discrete conductors are shown in red. These are just preliminary sections, designed for quality-control purposes rather than interpretation, and a rigorous inversion of the data will be carried out in due course.

Conclusions

Geoscience BC's QUEST Project was initiated to add to the geoscience knowledge of, and to stimulate exploration interest in, the covered areas of the Quesnel Terrane in central BC. An airborne electromagnetic survey on a 4 km line spacing has been completed and an airborne gravity survey on a 2 km line spacing has been initiated over Geoscience BC's QUEST Project area. The processing of the electromagnetic data is in hand, and the data should be ready for release in January 2008. The airborne gravity survey is still in progress, and the data will be released as soon as possible after the completion of the survey. The new airborne gravity and electromagnetic survey data will complement the existing ground-based gravity data and airborne magnetic data available through NRCan's Geoscience Data Repository. The QUEST geophysical surveys are supported by the new geochemical data being made available as a part of the

QUEST Project and by the existing geological, geophysical, remote sensing and topographic data.

Ultimately, QUEST's goal is to stimulate new exploration activity in the area, and to accelerate the rate of new mineral discoveries, hopefully resulting in the development of one or more new mines in the area. The new airborne surveys will complement the existing airborne magnetic information. The airborne geophysics, along with the detailed topography, water well data and ground observations, should provide a powerful data set to map the thickness of the Quaternary. To assist with the identification of economic deposits, an integrated folio of maps representing the multiple layers of exploration data sets will also be produced. In addition, over the coming year, Geoscience BC intends to work with geologists in government, academia and industry to develop revised interpretations of the subcropping geology using the results of the new QUEST geophysics and geochemistry.

References

- Andrews, G.D.M. and Russell, J.K. (2008): Cover thicknesses across the southern Interior Plateau, British Columbia (NTS sheets 92N, O, P, and 93A, B, C, F, and G): constraints from water well records; *in* Geoscience BC Summary of Activities 2007, Geoscience BC, Report 2008-1, p. 11–20.
- Jackaman, W. and Balfour, J.S. (2008): QUEST Project geochemistry: field surveys and data re-analysis (parts of NTS 93A, B, G, H, J, K, N and O); *in* Geoscience BC Summary of Activities 2007, Geoscience BC, Report 2008-1, p. 7–10.
- Logan, J., Ullrich, T., Friedman, R., Mihalynuk, M. and Sciarizza, P. (2007): Quesnel Arc – porphyry setting, potential and discoveries; *in* Abstract Volume, Mineral Exploration Roundup '07, Vancouver, British Columbia, Association for Mineral Exploration British Columbia, p. 4.
- Massey, N.W.D., MacIntyre, D.G., Desjardins, P.J. and Cooney, R.T. (2005): Geology of British Columbia; British Columbia Geological Survey, Geoscience Map 2005-3, scale 1:1 000 000.

QUEST Project Geochemistry: Field Surveys and Data Reanalysis, Central British Columbia (parts of NTS 093A, B, G, H, J, K, N, O)

W. Jackaman, Noble Exploration Services Ltd., Sooke, BC, wjackaman@shaw.ca

J.S. Balfour, Consultant, Cranbrook, BC

Jackaman, W. and Balfour, J.S. (2008): QUEST Project geochemistry: field surveys and data reanalysis, central British Columbia (parts of NTS 093A, B, G, H, J, K, N, O); in Geoscience BC Summary of Activities 2007, Geoscience BC, Report 2008-1, p. 7–10.

Introduction

During the 2007 field season, several exploration geochemistry activities were completed, as part of Geoscience BC's QUEST Project, in the Prince George area in central British Columbia (Figure 1). These included the reanalysis of 4940 sediment pulps from previous government-funded regional geochemical surveys conducted within the QUEST Project area (parts of NTS 093A, B, G, H, K, N), an infill lake sediment geochemical survey covering an area of more than 19 000 km² also within the QUEST Project area (parts of NTS 093G, J, K, N, O) and a reconnaissance-scale stream sediment geochemical survey of the Pine Pass area (NTS 093O).

When released in early 2008, this work will represent one of the largest infusions of publicly available geochemical information into the provincial geochemical database. The release will include field and analytical results for 7327 samples covering an area in excess of 95 000 km².

The results of these surveys will provide new regional drainage sediment and water geochemical information in an underexplored and geologically poorly understood region of central BC. The work will significantly enhance existing geochemical information and complement other geoscience initiatives such as the new electromagnetic and gravity surveys being flown as part of the QUEST Project. It also provides immediate economic opportunities to local service providers and potential long-term benefits from increased mineral exploration.

QUEST Reanalysis Project

Administrators of the National Geochemical Reconnaissance (NGR) and BC Regional Geochemical Survey (RGS) programs had the foresight to preserve portions of samples collected during drainage sediment surveys completed

Keywords: Interior Plateau, Pine Pass, mineral exploration, geochemistry, multi-element, reanalysis, stream sediment, lake sediment, lake water, gold, copper, porphyry deposit

This publication is also available, free of charge, as colour digital files in Adobe Acrobat® PDF format from the Geoscience BC website: <http://www.geosciencebc.com/s/DataReleases.asp>.

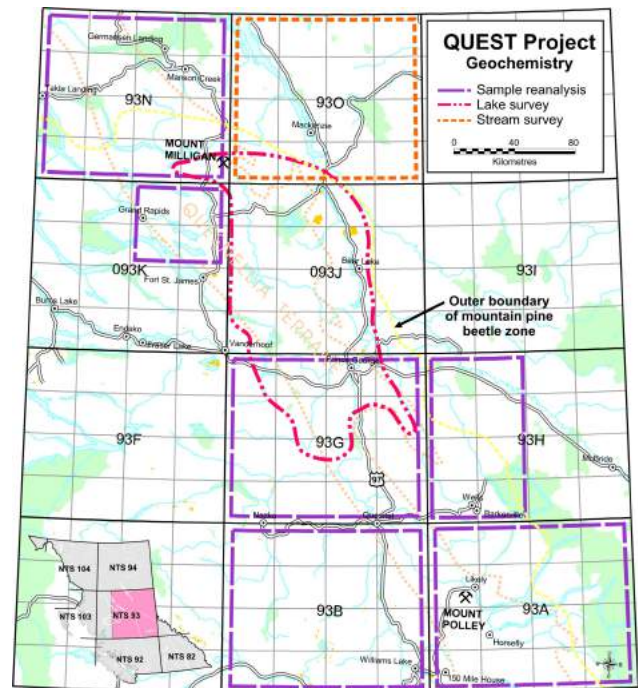


Figure 1. Location of survey areas in central British Columbia.

from 1976 to 1985. The archived material has provided the opportunity to reanalyze samples using up-to-date analytical techniques. In the early 1990s, over 24 000 samples collected throughout BC from 1976 to 1985 were reanalyzed by instrumental neutron activation analysis (INAA) for gold and a number of other metals not previously determined (Jackaman et al., 1991; Jackaman, 1992). This type of work has provided important new analytical information at improved detection levels and has significantly enhanced the utility of the provincial geochemical database.

As part of the QUEST Project initiative, archived samples are now being reanalyzed by inductively coupled plasma mass spectrometry (ICP-MS). This technique will not only provide a wide range of new analytical information at improved detection levels, but also provide greater data compatibility with survey analytical methods currently being employed. A total of 4452 stream sediment pulps have been

selected for this project and cover NTS map sheets 093A, B, G, H, N (Lett, 2005), plus 488 lake sediment pulps from NTS map sheet 093K (Cook et al., 1999). Samples from the 1985 survey completed in the McLeod Lake (NTS 093J) map sheet were reanalyzed by ICP-MS in 2006 (Lett and Bluemel, 2006). It should be noted that although efforts have been made to include all samples from the target survey areas, there are gaps in the data due to missing sample material.

Drainage sediment pulps from previous NGR and RGS programs are currently stored at facilities in Ottawa and Victoria. Custodians of the collection are Natural Resources Canada (NRCan) and the BC Geological Survey (BCGS). Most of the samples are stored by NTS map sheet designation in sample ID order and include original analytical duplicate and control reference samples. A total of 1 g of material was transferred from storage containers to prelabelled sample envelopes and shipped to Acme Analytical Laboratories Ltd. (Vancouver) for analysis. A complete list of elements and analytical detection limits is provided in Table 1.

Table 1. Detection limits for sediment samples analyzed by ICP-MS.

Element	Detection		
		limit	Units
Aluminum	Al	0.01	%
Antimony	Sb	0.02	ppm
Arsenic	As	0.1	ppm
Barium	Ba	0.5	ppm
Bismuth	Bi	0.02	ppm
Cadmium	Cd	0.01	ppm
Calcium	Ca	0.01	%
Chromium	Cr	0.5	ppm
Cobalt	Co	0.1	ppm
Copper	Cu	0.01	ppm
Gallium	Ga	0.2	ppm
Iron	Fe	0.01	%
Lanthanum	La	0.5	ppm
Lead	Pb	0.01	ppm
Magnesium	Mg	0.01	%
Manganese	Mn	1	ppm
Mercury	Hg	5	ppb
Molybdenum	Mo	0.01	ppm
Nickel	Ni	0.1	ppm
Phosphorous	P	0.001	%
Potassium	K	0.01	%
Scandium	Sc	0.1	ppm
Selenium	Se	0.1	ppm
Silver	Ag	2	ppb
Sodium	Na	0.001	%
Strontium	Sr	0.5	ppm
Sulphur	S	0.02	%
Tellurium	Te	0.02	ppm
Thallium	Tl	0.02	ppm
Thorium	Th	0.1	ppm
Titanium	Ti	0.001	%
Tungsten	W	0.1	ppm
Uranium	U	0.1	ppm
Vanadium	V	2	ppm
Zinc	Zn	0.1	ppm

QUEST Lake Sediment Infill Survey

The 2007 QUEST Project geochemical survey covers the northeast corner of the Interior Plateau and is bounded by Mount Milligan in the north, Fort St. James in the west, Highway 97 to the east and Quesnel in the south. The relatively subdued topography varies from exposed grasslands to rolling hills covered with pine and spruce forests (Figure 2). The upland surface of the plateau is favourably dotted with numerous lakes and ponds. Although much of the area was the site of stream sediment survey, the characteristic low relief and disorganized drainage systems of the area make lake sediment an ideal infill sample medium. Methods and specifications utilized in the 2007 project are based on standard lake sediment geochemical survey strategies used elsewhere in Canada for the NGR program (Friske, 1991), as well as prior orientation studies and regional lake sediment surveys completed in BC (Cook, 1997; Jackaman, 2006, 2007).

Helicopter-supported sample collection was carried out in August 2007, during which 1962 lake sediment and water samples were systematically collected from 1854 sites. Average sample site density was one site per 9 km² over the 19 000 km² survey area. Field duplicate sediment and water samples were routinely collected in each analytical block of 20 samples. Combined with the existing stream sediment sampling, site density becomes one site per 5 km².

Lake sites were accessed using a float-equipped Bell Jet Ranger helicopter. The sampling crews collected sediment material with a torpedo-style sampler and water samples were saved in 250 mL bottles. Field observations and site locations were recorded for each site. Samples were successfully collected from most of the lakes targeted in the survey area. However, some of the smaller ponds were not sampled due to poor sampling conditions, and samples were not collected from several very large and deep lakes. In general, lake-bottom samples sent for analysis represent a 35 cm section of material obtained from immediately below the water-sediment interface. Samples typically consisted of organic gels (gyttja) with varying amounts of inorganic sediment and organic matter. Organic gels are the target sample medium as element concentrations tend to be higher and more consistent compared to concentrations in other media, high and consistent loss-on-ignition (LOI) content minimizes the influence of this factor on element distributions, and a relatively deep-water environment is chemically more stable than a shallow-water environment (Friske, 1991).

After drying, each sample was pulverized in a ceramic ring mill to approximately –150 mesh (100 µm), and two analytical splits were extracted from the material. To monitor and assess accuracy and precision of analytical results, control reference material and analytical duplicate samples were



Figure 2. Typical lake sample site, located north of Mount Milligan, British Columbia.

Table 2. Detection limits for sediment samples analyzed by instrumental neutron activation analysis (INAA), loss-on-ignition (LOI) and fluorine (F). Detection limits for fluoride, conductivity and pH of water samples.

Element	Detection		Units
		limit	
Antimony	Sb	0.1	ppm
Arsenic	As	0.5	ppm
Barium	Ba	50	ppm
Bromine	Br	0.5	ppm
Cerium	Ce	5	ppm
Cesium	Cs	0.5	ppm
Chromium	Cr	20	ppm
Cobalt	Co	5	ppm
Europium	Eu	1	ppm
Gold	Au	2	ppb
Hafnium	Hf	1	ppm
Iron	Fe	0.2	%
Lanthanum	La	2	ppm
Lutetium	Lu	0.2	ppm
Rubidium	Rb	5	ppm
Samarium	Sm	0.1	ppm
Scandium	Sc	0.2	ppm
Sodium	Na	0.02	%
Tantalum	Ta	0.5	ppm
Terbium	Tb	0.5	ppm
Thorium	Th	0.2	ppm
Tungsten	W	1	ppm
Uranium	U	0.2	ppm
Ytterbium	Yb	2	ppm
Sample weight	Wt	0.01	g
Fluorine	F	10	ppm
Loss-on-ignition	LOI	0.1	%
pH	pH		
Conductivity	CND	0.01	µS

routinely inserted into each block of 20 sediment samples. The sediment samples will be analyzed for base and precious metals, pathfinder elements and rare earth elements by INAA and ICP-MS. Loss-on-ignition and fluorine will also be determined for sediment material. Fluoride, conductivity and pH will be determined for the water samples. A complete list of elements and analytical detection limits is provided in Tables 1 and 2.

QUEST Stream Sediment Survey

A new reconnaissance-scale stream sediment and water survey of the Pine Pass area (NTS map sheet 0930) was completed in 2007. The survey was conducted by CME

Managing Consultants Inc. and funding was provided by the Northern Development Initiative Trust. Methods and specifications utilized during the work were based on standard regional geochemical survey strategies used elsewhere in BC (Lett, 2005).

The survey area surrounds the community of Mackenzie and is dissected by the Rocky Mountain Trench. To the east, the survey area lies within the Foreland belt, which is composed equally of Upper Proterozoic and Paleozoic sedimentary rocks of the ancestral North America terrane. Lying in the Omineca belt, the southwest portion of the survey area is underlain by Upper Proterozoic and Paleozoic rocks of the Cassiar and Slide Mountain terranes. The survey area contains 50 documented mineral occurrences with coal and limestone being the primary types found (MINFILE, 2007).

In the western portion of the survey area, the Omineca Mountains are characterized by forested rounded summits and in the eastern portion are the moderately rugged mountains of the Hart Ranges and Rocky Mountain Foothills. Dissected by numerous actively flowing creeks and rivers, the area contains abundant sample sites to support a regional stream sediment and water survey. Fine-grained stream sediment is the preferred sample medium in these types of mountainous regions due to its widespread availability, ease of collection and its ability to provide representative geochemical data for the drainage basin upstream from the sample site.

Ground- and helicopter-supported sampling was conducted during August and September 2007. A total of 908 stream sediment and water samples were collected from 854 sites at an average density of one site per 12 km² over the 10 500 km² survey area. In general, 1–2 kg samples were collected from actively flowing primary or secondary drainages with catchment areas of less than 10 km². The –80 mesh (180 µm) fraction of the sediment samples will be analyzed for base and precious metals, pathfinder elements and rare earth elements by INAA and ICP-MS. Loss-on-ignition and fluorine will also be determined for sediment material. Fluoride, conductivity and pH will be determined for the water samples. A complete list of elements and analytical detection limits is provided in Tables 1 and 2.

Release Details

Reconnaissance-scale drainage sediment and water surveys are recognized as an important mineral exploration tool. Results from these types of activities are directly responsible for follow-up mineral exploration that is valued in the millions of dollars and has been credited with the discovery of numerous mineral prospects. Data from the 2007 QUEST Project initiatives will stimulate mineral exploration by presenting new geochemical information for an underexplored area that is considered to have a high potential for future discoveries of copper and copper-gold deposits, such as those at the Gibraltar and Mount Polley mines.

Survey results will include survey descriptions and details regarding survey methods; analytical and field data listings; summary statistics; sample location maps; and maps for individual elements. The publications will be released on a CD as PDF files and will include all raw digital data files used in the production process. The digital data packages are currently scheduled to be released in January 2008.

Acknowledgments

The authors would like to acknowledge J. Faulkner for his excellent helicopter flying abilities; S. Reichheld, S. Webb, K. Beaulieu and E. Jackaman for their tireless contributions both on the ground and in the air; C. Nass and the rest of the CME crew for their efforts in the Pine Pass survey; the many support services located in and around the Fort St. James, Prince George and Mackenzie communities that contributed to the completion of the surveys. Thanks to

P. Friske and M. McCurdy of Natural Resources Canada and R. Lett of the BC Geological Survey for their contributions. T. Höy is also thanked for his editorial comments and suggestions.

References

- Cook, S.J. (1997): Regional and property-scale application of lake sediment geochemistry in the search for buried mineral deposits in the southern Nechako Plateau area, British Columbia; *in* Interior Plateau Geoscience Project: Summary of Geological, Geochemical and Geophysical Studies, L.J. Diakow and J.M. Newell (ed.), Geological Survey of Canada, Open File 3448 and BC Ministry of Energy, Mines and Petroleum Resources, Paper 1997-2, p. 175–203.
- Cook, S.J., Jackaman, W., Lett, R.E.W., McCurdy, W. and Day, S.J. (1999): Regional lake water geochemistry of the Nechako Plateau, central British Columbia (NTS 93F/02,03; 93K/09,10,15,16; 93L/09, 16; 93M/01, 02, 07, 08); BC Ministry of Energy, Mines and Petroleum Resources, Open File 1999-5.
- Friske, P.W.B. (1991): The application of lake sediment geochemistry in mineral exploration; *in* Exploration Geochemistry Workshop, Geological Survey of Canada, Open File 2390, p. 4.1–4.2.
- Jackaman, W. (1992): 1992 regional geochemical survey program: review of activities; *in* Geological Fieldwork 1992, BC Ministry of Energy, Mines and Petroleum Resources, Paper 1993-1, p. 401–405.
- Jackaman, W. (2006): Regional drainage sediment and water geochemical data, Anahim Lake and Nechako River, central British Columbia (NTS 93C and 93F); Geoscience BC, Report 2006-4, 463 p.
- Jackaman, W. (2007): Regional drainage sediment and water geochemical data, South Nechako Basin and Cariboo Basin, central British Columbia (parts of NTS 92N, O, P, 93A, B); Geoscience BC, Report 2007-6, 332 p.
- Jackaman, W., Matysek, P.F. and Cook, S.J. (1991): The regional geochemical survey program: summary of activities; *in* Geological Fieldwork 1991, BC Ministry of Energy, Mines and Petroleum Resources, Paper 1992-2, p. 307–318.
- Lett, R.E.W. (2005): Regional geochemical survey database on CD; BC Ministry of Energy, Mines and Petroleum Resources, Geofile 2005-17.
- Lett, R.E.W. and Bluemel, B. (2006): Re-analysis of regional geochemical survey stream sediment samples from the McLeod Lake area (NTS map sheet 093J); BC Ministry of Energy, Mines and Petroleum Resources, Geofile 2006-09, 220 p.
- MINFILE (2007): MINFILE BC mineral deposits database; BC Ministry of Energy, Mines and Petroleum Resources, URL <<http://www.em.gov.bc.ca/Mining/Geolsurv/Minfile/>> [October 2007].

Cover Thickness across the Southern Interior Plateau, British Columbia (NTS 092O, P; 093A, B, C, F): Constraints from Water-Well Records

G.D.M. Andrews, Volcanology and Petrology Laboratory, Department of Earth and Ocean Sciences, University of British Columbia, Vancouver, BC, gandrews@eos.ubc.ca

J.K. Russell, Volcanology and Petrology Laboratory, Department of Earth and Ocean Sciences, University of British Columbia, Vancouver, BC

Andrews, G.D.M. and Russell, J.K. (2008): Cover thickness across the southern Interior Plateau, British Columbia (NTS 092O, P; 093A, B, C, F): constraints from water-well records; *in* Geoscience BC Summary of Activities 2007, Geoscience BC, Report 2008-1, p. 11–20.

Introduction

Basalts of the Chilcotin Group (CG), situated in the southern Interior Plateau physiographic region of central British Columbia, cover an area of over 30 000 km² (Figure 1). Their distribution is entirely within the region of BC that is most affected by mountain pine beetle (MPB) infestation (Figure 1). The CG is typically underlain by Paleozoic and Mesozoic basement rocks with high potential for Cu-Au-Mo deposits (e.g., Quesnel Trough), Eocene volcanic successions that host epithermal Au deposits (e.g., Blackdome), and Jurassic and Cretaceous sedimentary rocks of the Nechako Basin with hydrocarbon and possible mineral potential. In addition, the CG is itself, extensively overlain by late Quaternary glacial deposits of variable and unknown thickness.

The distribution of known mineral resources and prospects on the periphery of the CG (e.g., Blackdome, Gibraltar, Mount Polley, Prosperity and Vidette) makes the potential for unexploited mineral resources extending beneath the CG compelling (e.g., Mihalynuk, 2007a). However, there is currently little coherent data on the spatial distribution (e.g., thicknesses), the lithostratigraphy (facies variations) and physical properties (density, porosity, magnetic susceptibility and conductivity) of the CG and overlying Quaternary deposits. The incompleteness of geoscience information is one of the greatest impediments to successful exploration for resources beneath the CG. One aspect of this incomplete dataset is the depth through cover (glacial and CG) to basement, which is largely unknown. Previous workers have suggested that the CG can reach a thickness of ~200 m and averages ~100 m in thickness (e.g., Mathews, 1989); however, the authors have suggested that the CG is comparatively thin (<50 m) across most of its distribution and only thick (>100 m) in paleochannels (An-

draws and Russell, 2007). This initial hypothesis is supported by field observations from key vertical sections exposed in present-day drainages and canyons (e.g., Farrell et al., 2007; Gordee et al., 2007) and from analysis of volcanic facies and map unit geometries (Andrews and Russell, 2007; Gordee et al., 2007).

Herein is the analysis of geological information (lithology, thickness) available from the WELLS database, as it pertains to the southern Interior Plateau. This database comprises depth and lithology information recorded as water wells were drilled and is maintained by the BC Ministry of Environment (2007). In addition, thickness estimates for the CG from exposed sections and hydrocarbon exploration wells are included. This work forms part of Geoscience BC project 2006-003, which aims to produce 3-D facies and thickness models for the CG that can be used to 1) extrapolate regional geology, metallogeny and structure beneath the CG cover; 2) find windows to the basement and identify the basement geology; 3) delineate areas where the CG is thin or absent; and 4) provide a 3-D representation of physical property variations to allow the signature of the CG to be accurately stripped from total-field geophysical datasets.

Geological Setting

The Neogene Chilcotin Group (28–1 Ma) of south-central BC covers an area of over 30 000 km² (Figure 1), beneath an extensive blanket of Quaternary deposits. The region is characterized by moderately dissected, valley-incised plateaus, mainly composed of basaltic successions varying in thickness from 5 to 200 m (Andrews and Russell, 2007). Estimates of total volume are as high as 3500 km³ (Bevier, 1983; Mathews, 1989). The CG basalts are typically flat to shallow dipping, massive to columnar jointed, olivine-phyric basalt lavas with lesser volumes of pillow basalt and hyaloclastite (Gordee et al., 2007), occasional red-weathering paleosols (Farrell et al., 2007) and rare, intercalated felsic tephra (Mathews, 1989).

Keywords: Chilcotin Group, water wells, thickness models, GIS, paleotopography, Interior Plateau, Quaternary deposits

This publication is also available, free of charge, as colour digital files in Adobe Acrobat® PDF format from the Geoscience BC website: <http://www.geosciencebc.com/s/DataReleases.asp>.

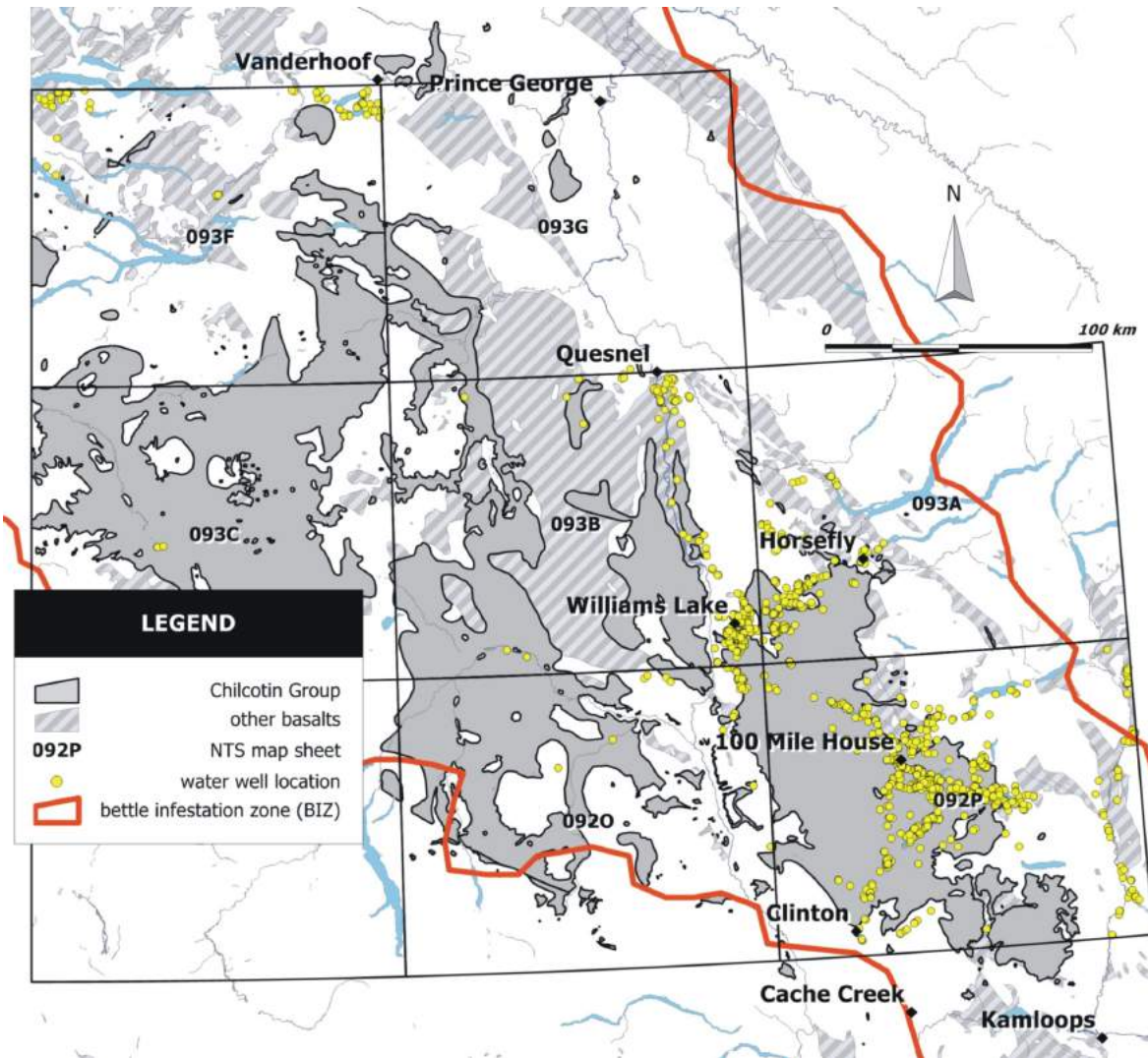


Figure 1. Simplified geological map of the southern Interior Plateau (NTS 0920, P, 093A, B, C, F) depicting the distribution of the Chilcotin Group and adjacent basaltic and basalt-hosting stratigraphic units (Massey et al., 2005a, b), major settlements and the margin of the mountain pine beetle infestation zone (BIZ). The locations of the water wells analyzed are shown as yellow dots.

The CG unconformably overlies a diverse range of rock types and stratigraphic packages, potentially the most economically important of which are the

- Upper Paleozoic limestone and phyllite of the Cache Creek Terrane;
- Triassic volcanic (including basalt) and volcanoclastic rocks of the Nicola Group (Quesnel Trough) that host granitic intrusions and extensive Cu-Au-Mo mineralization;
- Mesozoic marine sedimentary deposits of the Nechako Basin;
- Lower Eocene clastic sedimentary, volcanic (including basalt) and volcanoclastic rocks that host localized epithermal Au deposits; and
- Upper Eocene, Oligocene and Lower Miocene sandstone and shale.

The sub-CG basement geology is observed in windows through the basalt, however, the combination of areally extensive, glacially derived, surficial Quaternary deposits and the CG means that such windows are far apart. The consequence is that the basement geology cannot be extrapolated with a large degree of confidence beneath these cover units.

Analysis of Water-Well Records

Rationale

The widespread distribution of Quaternary surficial deposits precludes direct observation of the CG basalt for much of the Interior Plateau. In many instances, the distribution and the thickness of the underlying basalts is completely unknown; the basalts are assumed to be uniform in thickness and distributed everywhere beneath the surficial de-

posits. However, the recent work of Gordee et al. (2007) and Farrell et al. (2007) has led Andrews and Russell (2007) to propose that the CG is relatively thin; on average (<50 m) and is only thick (>100 m) in paleochannels. This suggests that under the extensive Quaternary cover, the CG may be very thin (<25 m) or absent, despite existing regional geological maps indicating otherwise. This hypothesis has been partly confirmed by a preliminary GIS study (Mihalynuk, 2007b). To test this hypothesis further and to attempt to map the basement beneath the CG, over 8000 water-well records have been examined to extract lithological and thickness data.

Methodology

The top-most bedrock lithology has been identified and vertical thickness estimates of the CG have been collected from outcrops (i.e., measured vertical sections) and publicly maintained databases (i.e., WELLS database, BC Ministry of Environment [2007] and well reports, BC Ministry of Energy, Mines and Petroleum Resources [2007]).

Water-Well Records

Water-well records were obtained from the WELLS database, which contains in excess of 88 000 records covering all of BC. For the study area (NTS 092O, P; 093A, B, C, F), there are records for over 8000 water wells, of which 1773 penetrate into bedrock (Figure 1). Only those wells that record lithological information and penetrate the bedrock are included in this analysis. The full array of geographic, hydrological and lithological data was downloaded, edited and entered into a Microsoft Excel® spreadsheet (Table 1). The well name, well location, drift thickness, bedrock type, minimum basalt thickness and maximum basalt thickness were recorded for each record.

In addition to the lithological and thickness data, a qualitative assessment of the lithological interpretation of each recorded unit was made; specifically, a certainty from 0 to 3 was ascribed, where 3 is the maximum confidence and 0 denotes no confidence in the identification of the rock type intersected. For example, a well report including ‘bedrock’ is assigned a certainty rank of 0 (it offers no information on rock type); in contrast a report including ‘hard vesicular ba-

salt’ is assigned a rank of 3 (positive identification of basalt). A ‘black rock’ is assigned a rank of 1 and a ‘grey volcanic rock’ is assigned a rank of 2. It should be noted that

- The identification of ‘basalt’ does not necessarily indicate CG basalt.
- Lithological descriptions are provided by water-well drillers who may not be (and probably are not) qualified geologists. Therefore, any inferences made on these descriptions must not be taken as accurate geological observations.
- The certainty ranking is wholly qualitative. The authors have used their experience of the known geology in the area, and their personal judgment, in assigning rankings. For example, an alternating sequence of ‘black volcanic rock and red breccia’ is assigned a rank of 3 and is inferred to be a subsurface expression of the Chasm lithofacies within the CG (Farrell et al., 2007).

The water wells recorded are primarily domestic or agricultural water sources, and therefore, their distributions are strongly heterogeneous and clustered around population centres (e.g., 100 Mile House and Williams Lake) and along major highways. As a result, there are minimal (<50) well records for NTS 092O, and 093C and F. Collation of well records for NTS 093G (Prince George) is ongoing and they are not included in this analysis.

Results

The results of the analysis are presented as a series of simplified geological maps with coloured dots representing each well. The size of dots is an indication of the certainty ranking; in contrast, dot colour reflects the unit thickness, except in one figure where colour indicates rock type.

Quaternary Deposits — Drift

All the well records analyzed ($n = 1773$) provide an estimate of the maximum thickness of drift encountered. In the analysis, ‘unconsolidated deposits’, ‘glacial sediment’, ‘mud’, ‘clay’, ‘sand’, ‘gravel’, ‘rocks’, ‘boulders’ and ‘till’ were assigned to ‘drift’. Drift thickness distributions are summarized in Figure 2, which shows the widespread presence of 11–50 m thick drift across NTS 092P, and 093A

Table 1. Example of the Microsoft Excel® data table created for water-well records from the WELLS database (Ministry of Environment, 2007). The well records are supplied in imperial units and are converted to metric in the Microsoft Excel® spreadsheet. Note that this is example data only and does not correspond to real well data.

NTS sheet	Water-well no.	Water-well depth (m)	Drift thickness (m)	Minimum bedrock thickness (m)	Topmost rock type	Certainty ranking	Minimum basalt thickness (m)	Rock type below basalt
092O	28269	33	8	25	basalt	2	23	granite
092O	46586	58	35	23	unknown	n/a	0	n/a
092O	54137	66	33	33	basalt	1	33	?
092O	30723	54	52	2	basalt	2	2	?
092O	55724	112	15	97	granite	1	n/a	n/a

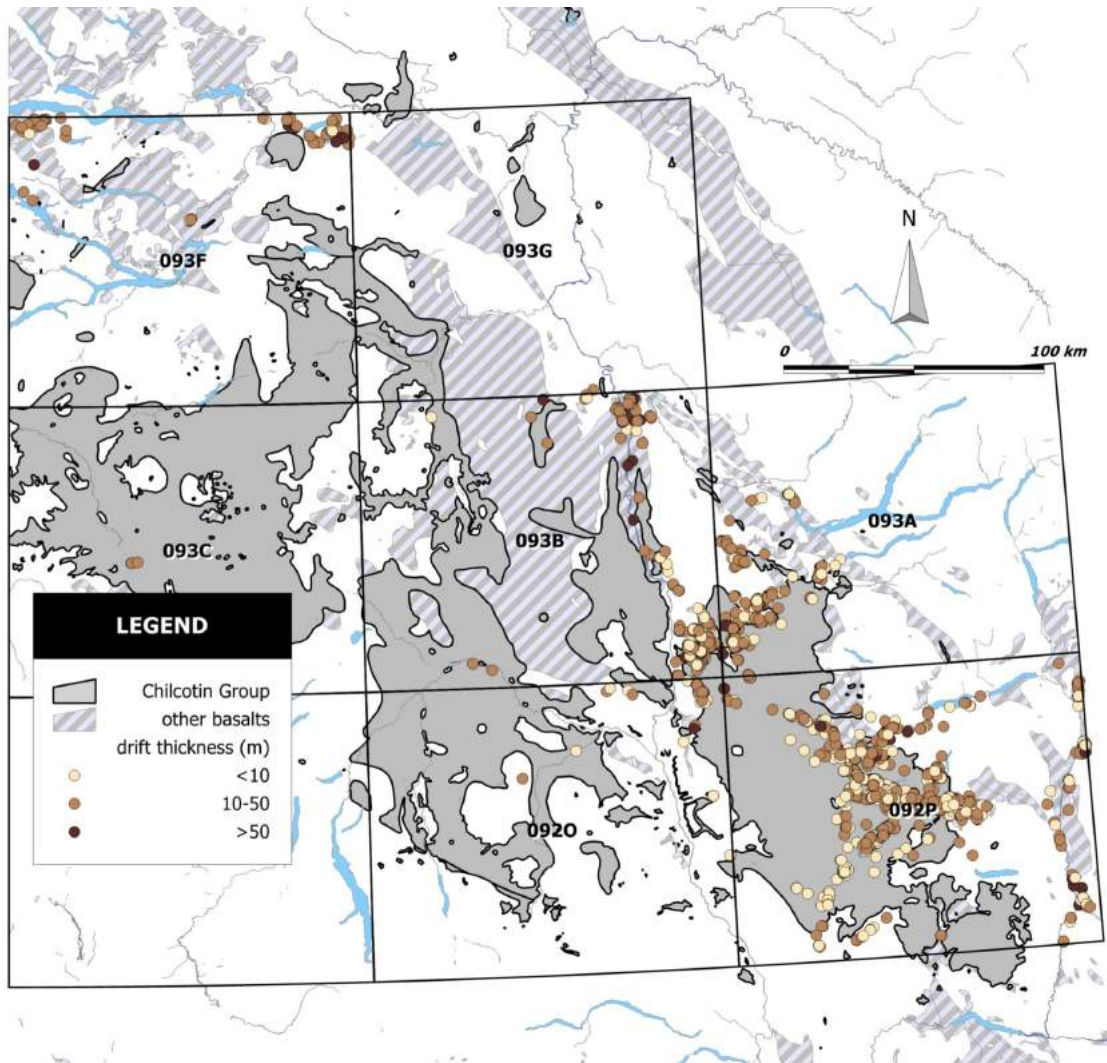


Figure 2. Quaternary drift thickness, southern Interior Plateau, BC (bedrock geology after Massey et al., 2005a, b).

and B. Drift less than 10 m thick is typical in the southwestern parts of NTS 092P around Clinton and in the areas bounding the Quesnel Highland around Horsefly (NTS

093A). Drift greater than 50 m thick is only extensive along the Fraser River valley between Quesnel and Williams Lake (NTS 093B). A preponderance of moderate thickness drift is demonstrated in Figure 3, where 66% of well reports record drift <70 m thick and 95% are <180 m (mainly around Williams Lake).

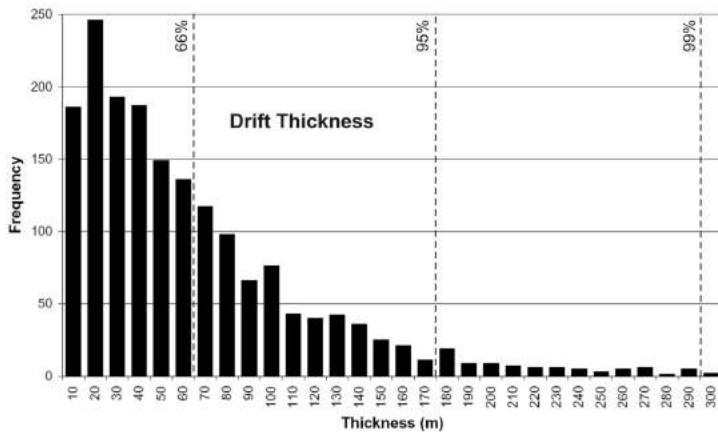


Figure 3. Histogram of drift thickness, southern Interior Plateau, BC. Note that the 66th, 95th and 99th percentiles are indicated.

Basalt

Most (1759) water wells penetrate bedrock that is inferred to be basalt in this study. The locations of those wells are displayed in Figure 1. Note that some of the wells displayed ($\leq 20\%$) are located outside the margins of the CG; rather, several wells are located on pre- or post-Chilcotin Group bedrock that is, or may include, basalt (e.g., Triassic Nicola Group, Quaternary Wells-Grey basalt lavas). It is, however, impossible to distinguish between basalts of different stratigraphic pack-

ages. The majority of wells intercepting basalt correspond with mapped basalt occurrences with the exception of the cluster of 11 wells west of Prince George (NTS 093F), where basaltic bedrock appears to be present at ≤ 50 m depth.

Basalt thickness data is presented as both minimum thickness ($n = 1585$ wells) and maximum (i.e., true) thickness ($n = 174$ wells). Minimum thickness estimates come from those wells that penetrate into basalt and stop; therefore they only provide a minimum thickness constraint. In contrast, maximum thickness estimates come from wells that penetrate through basalt into a sub-basalt rock type.

The locations of minimum thickness estimates ($n = 1585$ wells) are displayed in Figure 4, where thicknesses are differentiated into unequal bins of <10 m, 10–50 m and >50 m. These bin sizes were chosen to best demonstrate critical basalt thicknesses pertaining to exploration and possible exploitation; where very thin basalt is effectively invisible to

seismic and gravity survey, and where thick basalt is highly unfavourable for blind drilling or open-pit extraction. Wells penetrating into thick (>50 m thick) basalt are concentrated almost exclusively in the central portion of NTS 092P, under the town of 100 Mile House (minimum thickness 186 m) and immediately to the east (minimum thickness 124 m; Figure 4).

In addition, minimum basalt thickness derived from water-well records is supplemented by several field observations (measurement of vertical exposures). Although the number of measured sections included is small ($n = 18$ wells), they are located in areas not otherwise represented by water-well records, for example, along river valleys in NTS 0920 and 093B (Figure 4).

The locations of maximum thickness estimates ($n = 174$ wells) and supplementary field observations ($n = 6$ wells) and hydrocarbon exploration wells ($n = 1$ well) are displayed in Figure 5. Again, thickness bins of <10 m, 10–

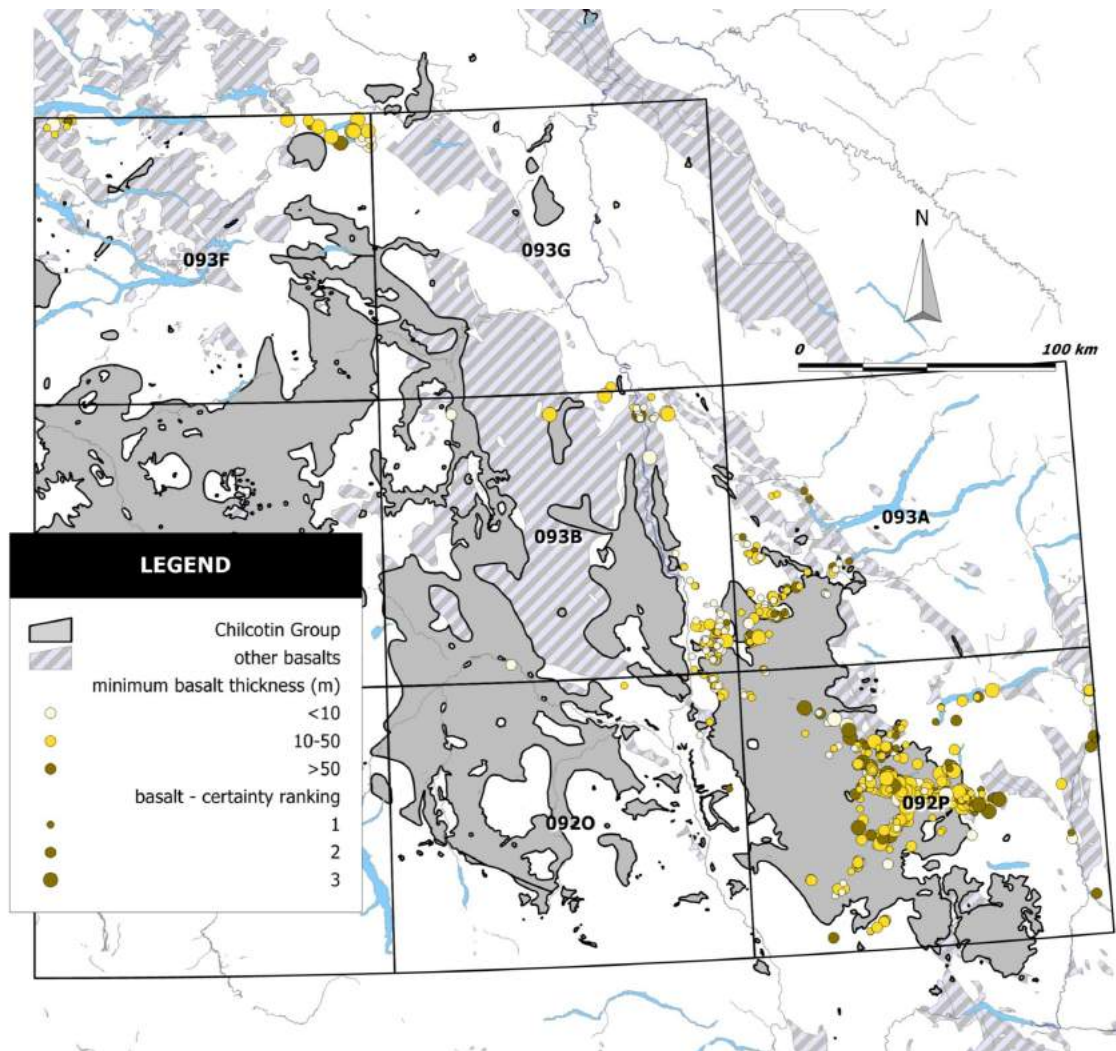


Figure 4. Minimum basalt thickness, southern Interior Plateau, BC (geology after Massey et al., 2005a, b).

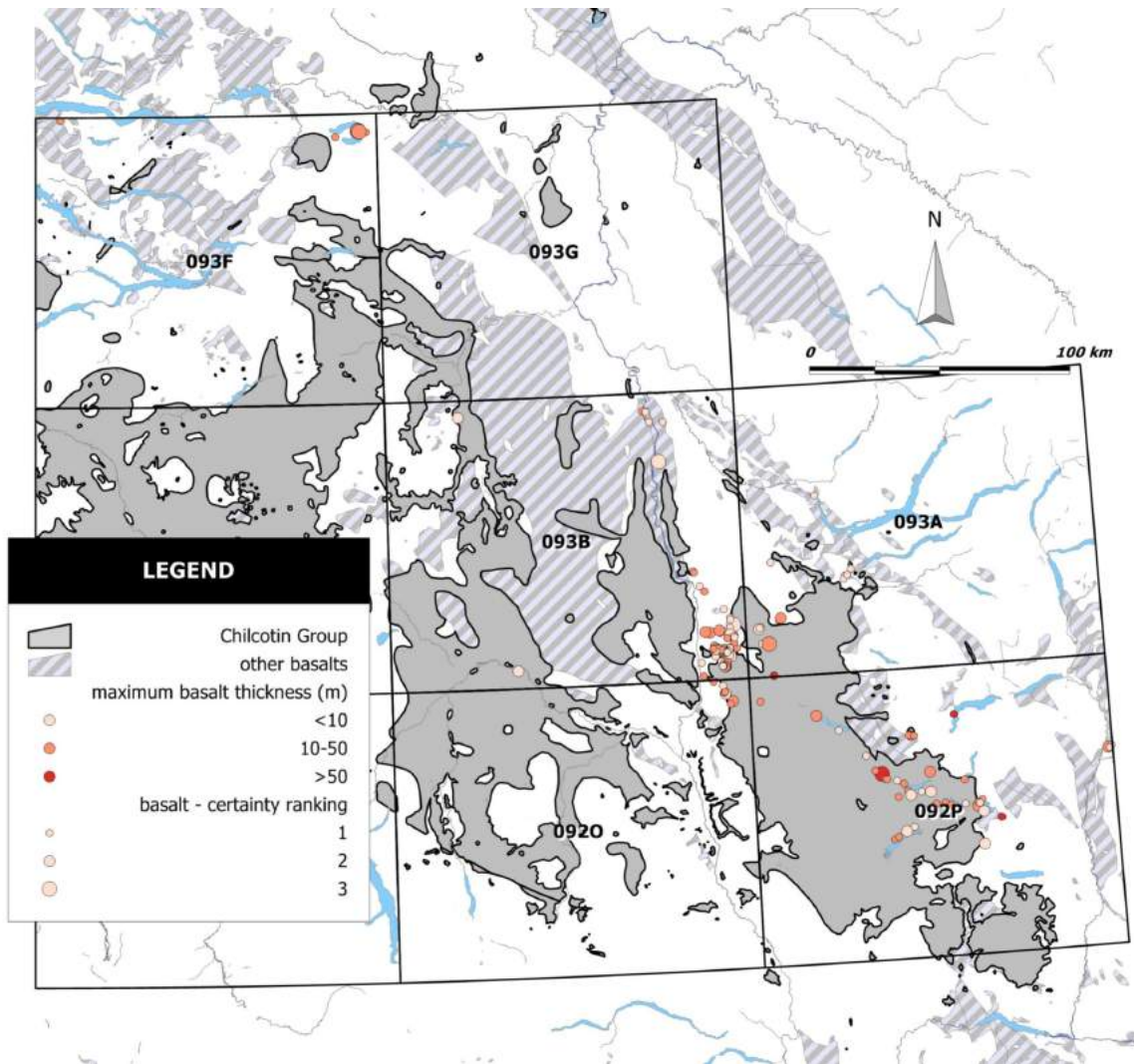


Figure 5. Maximum basalt thickness, southern Interior Plateau, BC (geology after Massey et al., 2005a, b).

50 m and >50 m are used. With far fewer maximum estimates than minimum estimates, the wells included tend to cluster more strongly around 100 Mile House (NTS 092P) and Williams Lake (NTS 093B); however, the thickest sections are still situated around 100 Mile House.

Not surprisingly, the typical maximum true thickness is less than that recorded in minimum thickness estimates because it is easier to penetrate through thinner basalt. The maximum true thickness recorded is 164 m (at 100 Mile House) and the mean is 16.2 m; 66% of basalt layers intercepted are <20 m thick and 95% are <50 m (Figure 6A). Thin basalt layers (≤ 20 m thick) are generally found around Williams Lake (Figure 5), between Williams Lake and 100 Mile House (NTS 092P) and central portions of NTS 093B. Minimum basalt thickness estimates are generally greater (Figure 6B): 66% of basalt layers intercepted are <40 m thick and 95% are <80 m thick; it is noteworthy that even mini-

um estimates still strongly suggest that the basalt layers are thinner than previously inferred.

Sub-Basalt and Other Rock Types

Non-basalt rock types encountered beneath Quaternary drift ($n = 714$ wells) and basalt ($n = 174$ wells) were recorded and are displayed in Figure 7. Rock types are presented as

- unknown/not classified (e.g., ‘bedrock’, ‘white rock’);
- clastic sedimentary (e.g., ‘shale’, ‘sandstone’, ‘conglomerate’);
- plutonic (e.g., ‘granite’, ‘diorite’);
- limestone; and
- metamorphic (e.g., ‘schist’, ‘chlorite rock’).

Clastic sedimentary rocks are prevalent across NTS 092P, and 093A and B, although it is not possible to correlate them to specific stratigraphic units or ages. Limestone, plutonic rocks and metamorphic rocks are restricted to NTS

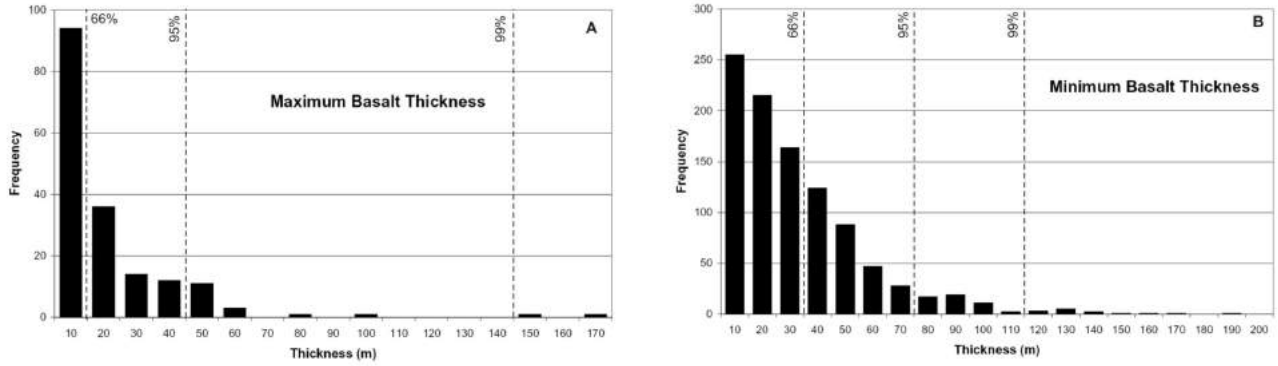


Figure 6. Histogram of basalt thickness, southern Interior Plateau, BC: A) maximum basalt thickness; B) minimum basalt thickness. Note that the 66th, 95th and 99th percentiles are indicated.

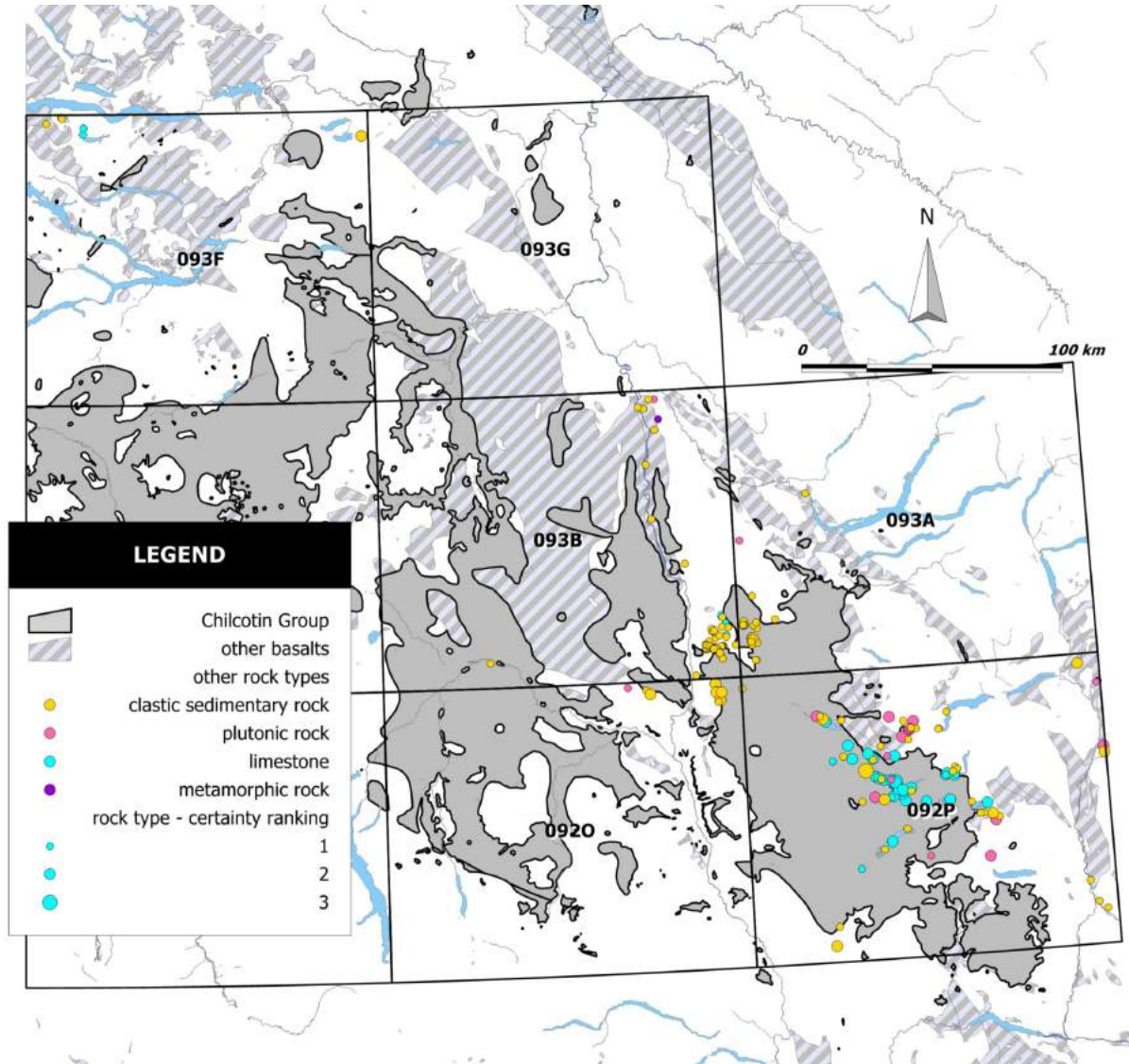


Figure 7. Non-basalt rock types encountered below drift and/or basalt (bedrock geology *after* Massey et al., 2005a, b).

092P, where they possibly represent the basement geology along the inferred margin between the Cache Creek Terrane (limestone-dominated) and the Quesnel Terrane (granite-hosting), beneath 100 Mile House. Known geology is probably represented by granite-penetrating wells east of 100 Mile House (NTS 092P; possibly the Takomane batholith) and limestone-penetrating wells near Clinton (NTS 092P). Elsewhere, the abundant clastic sedimentary rocks between Williams Lake and Quesnel probably represents the Upper Eocene–Lower Miocene succession along the Fraser River (Rouse and Mathews, 1979).

The occurrence of clastic sedimentary rocks, plutonic rocks and limestone as the uppermost bedrock within the presently mapped boundaries of the CG (Figure 7) indicates the presence of previously undetected basement windows. These are most common in the central portions of NTS 092P, the southwestern corner of NTS 093A and the southeastern corner of NTS 093B; areas where the typical basalt thickness is <50 m.

Discussion

The Thickness of the Chilcotin Group

Analysis of water-well records supports the assertion (Andrews and Russell, 2007) that the Chilcotin Group is typically thin (<50 m thick, probably <25 m thick; Figures 4–6) across most of its mapped distribution, and moreover, that in many areas its actual subdrift distribution is very patchy. Most of the thickest sections (>50 m) recorded are restricted to the central and southern parts of NTS 092P, where several water wells are located beyond the presently mapped boundary of the CG, where in fact they may penetrate into older, Eocene basalt (Endako Group).

Previously, Andrews and Russell (2007) proposed that significant thickness variations within the CG were the result of paleotopography, with thick sections filling ancient drainage systems and thin sections covering, or partially covering, ancient high ground. The variations in maximum CG thickness, revealed by analysis of water-well records, may be explained in this way, for example the thickest sections (>150 m thick) and many of the thinnest sections (<5 m) and basement windows (i.e., 0 m thickness of CG) are found adjacent to one another under the town of 100 Mile House (NTS 092P). It is not possible to positively identify paleodrainage systems by the analysis of water-well records alone, the number of wells is too low and they are not distributed widely enough. However, further detailed fieldwork to understand the architecture of the CG through studying its component lithofacies assemblages may allow this hypothesis to be tested and paleodrainages to be mapped.

Exploration Potential Beneath the Chilcotin Group

The unconstrained thicknesses and areal distributions of the Chilcotin Group and overlying Quaternary deposits have impeded mineral and hydrocarbon exploration for decades. The general consensus has been that the CG is uniformly thick (i.e., >100 m thick) everywhere across its mapped distribution (e.g., Bevier, 1983; Mathews, 1989). This common wisdom is based largely on a few thick but well-exposed outcrops around the margins of, and within, the Interior Plateau. Overestimation of the thickness of the CG, and therefore, the depth to basement, has discouraged conventional exploration activity (e.g., prospecting, staking, geochemical sampling) and has also discouraged higher cost exploration activities (drilling, geophysical surveys; e.g., Mihalyuk 2007a). Indeed, if geophysical surveys (e.g., seismic, gravity, aeromagnetic, radiometric) are to be useful to exploration they will require either 1) accurate estimation of CG thickness to produce realistic geophysical models and/or 2) complex data processing to remove the CG.

In this paper, evidence is presented in support of the hypothesis (Andrews and Russell, 2007) that the CG is generally thin (<50 m thick; probably <25 m thick) across most of its known and inferred distribution. Furthermore, it was found that excessively thick CG (>100 m) is localized, and appears to be restricted to the 100 Mile House area. The observation that the CG is generally thin across a large area increases the likelihood of basement windows being close to surface, and therefore more accessible to blind-drilling and identification by soil-, lake- and bio-geochemical surveys. Moreover, these observations further constrain the thickness of the CG in NTS 092P, and 093A and B; therefore, there is hope that these observations can be extrapolated across the remainder of the CG.

These results and interpretations of the thickness of the CG should be incorporated in ongoing and future research and exploration projects in areas underlain, or possibly underlain, by the CG. The authors believe that by incorporating their findings, exploration projects can be enhanced, and new areas of the Interior Plateau can be added to the provincial exploration portfolio.

Conclusions

- 1) The Chilcotin Group is typically <25 m thick across the area represented by the well records analyzed.
- 2) Localized sections that are >100 m thick are encountered in NTS 092P, some or all may include older basalt in addition to the CG.
- 3) A diverse range of basement rock types are identified at the bedrock-drift interface (in the absence of CG) and immediately below the CG. This suggests that

- the basement is widely accessible (<50 m depth) through drift only, or through drift and thin CG in many areas;
 - the areal distribution of the CG under Quaternary cover is overestimated; and
 - basement windows are more common, and larger, than previously thought.
- 4) Quaternary drift is typically <50 m thick across the area surveyed. Sections that are >50 m thick may be of interest to industrial mineral companies.
- 5) The realization that the CG is typically thin should be incorporated into exploration projects, allowing for simpler and cheaper geophysical and geochemical surveys, and increasing the area likely to be prospective.

Acknowledgments

This study was funded by the Geoscience BC Grant-In-Aid program for project 2006-003: *Mapping the Resource Potential Beneath the Chilcotin Flood Basalts (CFB): Volcanic Lithofacies Constraints on Geophysical Surveys*. The authors also acknowledge logistical support and assistance from the Geological Survey of Canada through the Targeted Geoscience Initiative 3 program. This work benefited from advice and helpful discussions with D. Allen and her graduate students M. Toews and J. Liggett at Simon Fraser University, C. Sluggett, B. Anderson, S. Brown, J. Dohaney and summer laboratory assistants L. Holmes, M. Russell and N. Schwartzman. This manuscript was reviewed by G. Chalmers, University of British Columbia.

References

- Andrews, G.D.M. and Russell, J.K. (2007): Mineral exploration potential beneath the Chilcotin Group, south-central BC: preliminary insights from volcanic facies analysis; *in* Geological Fieldwork 2006, BC Ministry of Energy, Mines and Petroleum Resources, Paper 2007-1 and Geoscience BC, Report 2007-1, p. 229–238.
- BC Ministry of Energy, Mines and Petroleum Resources (2007): Oil and gas well reports; BC Ministry of Energy, Mines and Petroleum Resources website, URL <http://www.em.gov.bc.ca/subwebs/oilandgas/petroleum_geology/wellreports/wellreports.htm> [October 2007].
- BC Ministry of Environment (2007): WELLS database; BC Ministry of Environment website, URL <<http://www.aardvark.gov.bc.ca/apps/wells/jsp/public/indexreports.jsp>> [September 2007].
- Bevier, M.L. (1983): Regional stratigraphy and age of Chilcotin Group basalts, south-central BC; *Canadian Journal of Earth Sciences*, v. 20, p. 515–524.
- Farrell, R-E., Andrews, G.D.M., Anderson, B. and Russell, J.K. (2007): Chasm and Dog Creek lithofacies, internal architecture of the Chilcotin Group basalt, Bonaparte Lake map area, British Columbia; Geological Survey of Canada, Current Research 2007-A5, 11 p.
- Gordec, S.M., Andrews, G.D.M., Simpson, K. and Russell, J.K. (2007): Sub-aqueous, channel-confined volcanism: Bull Canyon Provincial Park, BC; *in* Geological Fieldwork 2006, BC Ministry of Energy, Mines and Petroleum Resources, Paper 2007-1 and Geoscience BC, Report 2007-1, p. 285–290.
- Massey, N.W.D., MacIntyre, D.G., Desjardins, P.J. and Cooney, R.T. (2005a): Digital geology map of British Columbia – tile NM10 southwest British Columbia; BC Ministry of Energy, Mines and Petroleum Resources, Geofile 2005-3, scale 1:250 000.
- Massey, N.W.D., MacIntyre, D.G., Desjardins, P.J. and Cooney, R.T. (2005b): Digital geology map of British Columbia – tile NN10 central British Columbia; BC Ministry of Energy, Mines and Petroleum Resources, Geofile 2005-6, scale 1:250 000.
- Mathews, W.H. (1989): Neogene Chilcotin basalts in south-central BC; *Canadian Journal of Earth Sciences*, v. 26, p. 969–982.
- Mihalynuk, M.G. (2007a): Evaluation of mineral inventories and mineral exploration deficit of the Interior Plateau beetle infestation zone (BIZ), south-central British Columbia; *in* Geological Fieldwork 2006, BC Ministry of Energy, Mines and Petroleum Resources, Paper 2007-1 and Geoscience BC, Report 2007-1, p. 137–142.
- Mihalynuk, M.G. (2007b): Neogene and Quaternary Chilcotin Group cover rocks in the Interior Plateau, south-central British Columbia: a preliminary 3-D thickness model; *in* Geological Fieldwork 2006, BC Ministry of Energy, Mines and Petroleum Resources, Paper 2007-1 and Geoscience BC, Report 2007-1, p. 143–148.
- Rouse, G.E. and Mathews, W.H. (1979): Tertiary geology and palynology of the Quesnel area, British Columbia; *Bulletin of Canadian Petroleum Geology*, v. 28, p. 418–445.

Controls on Copper and Gold Mineralization along the Contact between the Coast Plutonic Complex and the Southeast Coast Belt, Taseko Lakes Region, Southwestern British Columbia (NTS 092O/04)

S.K. Blevings, Department of Earth and Ocean Sciences, University of British Columbia, Vancouver, BC; sblevings@eos.ubc.ca

L.A. Kennedy, Department of Earth and Ocean Sciences, University of British Columbia, Vancouver, BC

K.A. Hickey, Department of Earth and Ocean Sciences, University of British Columbia, Vancouver, BC

Blevings, S.K., Kennedy, L.A. and Hickey, K.A. (2008): Controls on copper and gold mineralization along the contact between the Coast Plutonic Complex and the southeast Coast Belt, Taseko Lakes region (NTS 092O/04), southwestern British Columbia; *in* Geoscience BC Summary of Activities 2007, Geoscience BC, Report 2008-1, p. 21–34.

Introduction

The Taseko Lakes region is located in southwestern British Columbia, approximately 215 km north of Vancouver (Figure 1), and straddles the boundary of the southeast and southwest Coast geomorphological belts (Figure 2). The geology of the region is dominated by intermediate intrusive, volcanic, volcanoclastic and clastic rocks that have undergone at least three phases of brittle deformation. Several mineral occurrences in the region are located within the southeast Coast Belt proximal to its contact with the Coast Plutonic Complex. The mineral occurrences include vein deposits and magmatic-hydrothermal systems, and are integral to the regional evolution of the eastern margin of the Coast Plutonic Complex (Figure 1). Numerous mineralized zones are present in the district, including the Bralorne (MINFILE 092JNE 001), Pioneer Mines (MINFILE 092JNE 004) and Prosperity (MINFILE 092O 041) deposits. Additional prospects, which are the subjects of this contribution, include the Pellaire, Empress and Taylor-Windfall mineral occurrences.

To date, the relationship between faulting and mineralization has not been established for the Taseko Lakes region. As a result, the link between the structural history of the area and its mineral occurrences is poorly understood. A two-year M.Sc. project is in progress, integrating field mapping and laboratory analyses, to address this issue. The overall goals of this project are 1) to characterize the mineralization and alteration pres-



Figure 1. Map of British Columbia (*modified from* MapPlace, 2006), showing the location of Vancouver, Taseko Lakes, the Coast Plutonic Complex, and selected porphyry and vein-hosted deposits that occur immediately east of the Coast Plutonic Complex. The deposits shown formed between the Late Triassic and the Late Cretaceous (MacMillan et al., 1991; MINFILE, 2007).

ent at three mineral occurrences in the Taseko Lakes area (Empress, Taylor-Windfall and Pellaire occurrences) proximal to the Coast Plutonic Complex; 2) to characterize the chronology of fault generation in the region by determining the kinematics of the faults and, in doing so, to evaluate the importance of structural controls on mineralization; and 3) to determine the timing and physical-chemical conditions of hydrothermal fluids (e.g., temperature, depth of emplacement and likely fluid source) for each of the three mineral occurrences. These results will be integrated to

Keywords: *Cu porphyry, epithermal, Coast Plutonic Complex, southeast Coast Belt, Taseko Lakes*

This publication is also available, free of charge, as colour digital files in Adobe Acrobat® PDF format from the Geoscience BC website: <http://www.geosciencebc.com/s/DataReleases.asp>.

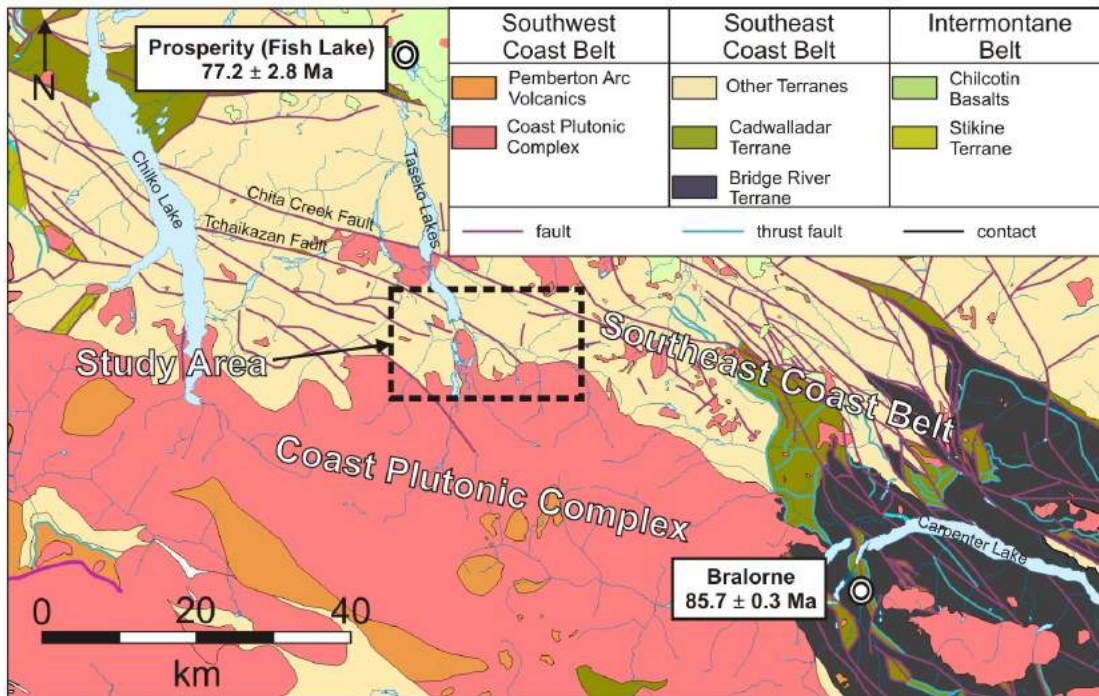


Figure 2. Geologic map (*modified from MapPlace, 2006*) of the Taseko Lakes area, showing the Coast Plutonic Complex and southeast Coast Belt as well as the approximate ages and locations of the Bralorne and Prosperity Deposits (MINFILE, 2007).

develop a coherent structural model for the mineralizing system(s) in the Taseko Lakes region.

This report provides an update from results presented by Hollis et al. (2007) and documents results from the second field season (2007) and preliminary laboratory results. Mapping in 2007 focused mainly on areas to the southeast of Taseko Lakes, with emphasis on the Mount McLeod batholith, the Tchaikazan fault (the major strike-slip fault in the area) and the known mineral occurrences in the region (Figure 3). The goals of this phase of the research are 1) to characterize the alteration and mineralization of three mineral occurrences in the area (Pellaire, Taylor-Windfall and Empress); 2) to determine any genetic relationships among the occurrences, the Tchaikazan fault and the Coast Plutonic Complex; and 3) to develop a model for the formation of the occurrences and address any links among them. In order to achieve these goals, the recent fieldwork entailed large scale mapping (1:10 000 scale) of the northern contact zone of the Mount McLeod batholith near the Spokane–Mount McLure, Pellaire, Taylor-Windfall and Empress occurrences. Additionally, more detailed mapping (1:5 000 scale) and sampling of rock types, structures, alteration and mineralization were also carried out in the area of the three occurrences. Drill core from previous exploration programs at the Empress and Taylor-Windfall occurrences was logged and sampled in detail. Field mapping and core logging involved distinguishing the different intrusive, extrusive and sedimentary rocks present in the area, and char-

acterizing the style, intensity and distribution of hydrothermal alteration and mineralization at the three occurrences. Samples collected in the field have been submitted for petrographic thin sections, fluid inclusion analysis and geochronological dating (U-Pb and Ar-Ar). These results will be reported in the future. Alteration mapping of clay minerals has been aided by the application of short-wave infrared (SWIR) analysis of hand samples following the field season.

Regional Geology

The Taseko Lakes region straddles the boundary between the southeast and southwest Coast Belt, which together comprise the southern Coast Belt in the Canadian Cordillera (Monger and Journeay, 1994; Umhoefer et al., 2002). The southeast Coast Belt consists mainly of late Paleozoic to Mesozoic volcanic arc rocks and clastic basinal lithotectonic assemblages (Scharizza et al., 1997; Umhoefer et al., 2002). In contrast, the southwest Coast Belt is dominated by Middle Jurassic to Late Cretaceous plutonic rocks of the Coast Plutonic Complex (Friedman and Armstrong, 1995).

The southern Coast Belt separates the Intermontane Superterrane to the east from the Insular Superterrane to the west. The Intermontane Superterrane is composed of the smaller Cache Creek, Quesnel and Stikine terranes, and was accreted to the western margin of North America during the Early to Middle Jurassic (Monger et al., 1982).

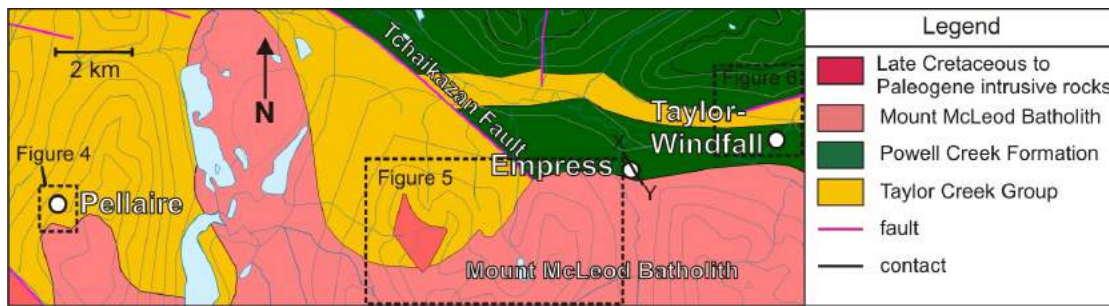


Figure 3. Geologic map (modified from MapPlace, 2006) showing the locations of the Mount McLeod batholith, Tchaikazan fault and mineral occurrences in the area south of Taseko Lakes. Locations of subsequent figures are also denoted. Line XY denotes the approximate location of the cross-section shown in Figure 6.

Likewise, the Insular Superterrane is composed of the smaller Wrangellia and Alexander terranes, and is believed to have accreted to the western margin of North America during latest Jurassic to the mid-Cretaceous (Monger et al., 1982; Schiarizza et al., 1997; Israel et al., 2006). The southeast Coast Belt is an overlap assemblage, representing the geologic material present between the Insular and Intermontane superterranes at the time of the accretion of the Insular Superterrane (Monger and Journeay, 1994). The southeast Coast Belt consists of the smaller Bridge River, Cadwallader and Methow oceanic terranes.

An extensive system of northwest-trending faults dominates the structural architecture of the Taseko Lakes area. These faults are dominantly strike-slip and contractional faults that developed during at least three phases of transpressional deformation from the mid-Cretaceous to the Tertiary (Schiarizza et al., 1997; Israel et al., 2006). Steeply dipping, sinistral, strike-slip faults are interpreted to represent the earliest deformation phase (D₁). These sinistral faults are interpreted as high-strain, but are discontinuous along strike (Israel et al., 2006; Hollis et al., 2007). Contractional faults formed during the second phase of deformation in the Late Cretaceous (Rusmore and Woodsworth, 1991, 1994). This shortening is characterized by mainly north- to northeast-verging thrust faults, believed to have developed during the accretion of the Insular Superterrane to the western margin of North America and interpreted to be a part of the Waddington Thrust Belt (Rusmore and Woodsworth, 1991). Eocene, dextral, strike-slip faults are the largest and dominant structures in the region, and appear to cut all other faults (Schiarizza et al., 1997). The largest of these are the Tchaikazan and Twin Creek faults.

The Taseko Lakes region is bounded to the south by the Mount McLeod batholith, which is part of the Coast Plutonic Complex and is dated at 103.8 ± 0.5 Ma (Israel et al., 2006). This batholith intrudes stratigraphic units of the southeast Coast Belt previously classified as the Taylor Creek Group (Schiarizza et al., 1997). The Tchaikazan fault runs through the centre of the study area and offsets all ob-

served rock types. The areas north of the Tchaikazan fault are dominated by the Powell Creek Formation, but also include units of the Taylor Creek Group.

Results From First Field Season

The objectives of the first year of the project were 1) to characterize the geology and geologic structures of the Taseko Lakes area, 2) to place age constraints on identified rock types and faults in the study area, and (3) to identify any structural controls on mineralization in the area (Hollis et al., 2007). Results from the first mapping season and subsequent laboratory studies include the following:

- 1) Broad compositional similarities between the stratigraphic rock units in the area suggest that no single unit possesses an apparent greater capacity to react with mineralizing fluids resulting in precipitation of ore minerals from solution.
- 2) Andesitic dikes as young as 22 Ma (Ar-Ar of hornblende) in the area indicate that magmatism was active in the area until Miocene time.
- 3) Sinistral shear zones belonging to D₁ are lithologically heterogeneous, and host variable alteration but negligible mineralization. Ar-Ar dates from shear fabrics defined by muscovite, biotite and illite provide cooling ages of 96.77 ± 0.92, 91.98 ± 0.75 and 88.15 ± 0.57 Ma, respectively.
- 4) Thrust faults belonging to D₂ host mylonitic fabrics, propylitic (chlorite, epidote, carbonate) alteration and minor mineralization (pyrite, chalcopyrite). An Ar-Ar date of illite from the mylonitic fabrics provides a cooling age of 60.53 ± 0.33 Ma, which may represent the late stages of movement along the fault zone.
- 5) Dextral strike-slip faults belonging to D₃ are characterized by brittle deformation and appear to host no significant mineralization or alteration. No fault material was suitable for geochronology, but regional correlations suggest that these faults were active during Eocene time.

Short Wavelength Infrared Analysis

Short wavelength infrared (SWIR) analysis can be performed on samples in the field with the use of the portable infrared mineral analyzer (PIMA). A PIMA allows for speedy identification of hydrothermal and clay minerals, which ultimately allows the mapping of different zones of hydrothermal alteration when individual mineral species are indiscernible (Herrmann et al., 2001). The short wavelength infrared range consists of electromagnetic wavelengths from 1 300 to 2 500 nm. This range incorporates fundamental absorption features of OH, H₂O, CO₃, NH₄, AlOH, FeOH and MgOH. From the relative magnitude of these absorption features, relative abundances of many hydrothermal alteration minerals can be estimated (Thompson et al., 1999). SWIR measurements for this project were made using a TerraSpec[®] SWIR spectrometer from Analytical Spectral Devices, Inc.

Areas Studied in Second Field Season

Pellaire Gold Deposit

The Pellaire gold deposit is classified as a polymetallic vein-hosted deposit by Holtby (1988). This deposit was mapped at a scale of 1:5 000, to determine the structural controls on the mineralization and to collect samples of veins and wallrock for laboratory analyses in order to place constraints on temperature, depth and age of mineralization. Results from these studies will potentially provide insights into any temporal and genetic links present between mineralization at the Pellaire and the other showings in the area.

Pellaire is a past-producing gold-silver deposit located approximately 7 km south-southwest of Upper Taseko Lake (Figure 3). The deposit occurs at the contact of the Falls River succession with the Mount McLeod batholith (Hollis et al., 2007). Mineralization occurs in quartz veins that are hosted in south-verging thrust faults (Pezzot, 2005). Ore minerals include pyrite, chalcopyrite, galena, sphalerite, arsenopyrite, tetrahedrite and hessite. The majority of the gold in the deposit is associated with hessite. Hydrothermal alteration in the area is not intense or widespread, but is dominated by muscovite, illite, ankerite and jarosite. Probable geological reserves are 30 841 tonnes grading 22.9 grams per tonne gold and 78.8 grams per tonne silver (Holtby, 1988).

The Falls River succession was defined by Israel et al. (2006). Prior to this it was included in the Taylor Creek Group (Jeletzky and Tipper, 1968; McLaren, 1990; Schiarizza et al., 1997). The succession consists of intermediate, coherent and clastic volcanic units with subordinate amounts of sedimentary rocks, typified by siltstone and shale. At the Pellaire deposit, it is intruded by the Mount McLeod batholith to the south (Figure 4). A minimum age

of deposition for the Falls River succession is 103.8 ± 0.5 Ma, based on a uranium-lead zircon age from the Mount McLeod batholith (Israel et al., 2006).

The Mount McLeod batholith, part of the Coast Plutonic Complex, occurs in the southern part of the study area (Figures 4 and 5). The gold-bearing quartz veins on Pellaire are dominantly hosted within the granodiorite of the Mount McLeod batholith (Figure 4A).

The batholith is a medium- to coarse-grained, hornblende granodiorite. It is equigranular, with crystal sizes ranging from 1 to 10 mm and an average size of about 2–3 mm (Figure 5A). It is composed of about 40% quartz, 30% euhedral plagioclase, 15% subhedral hornblende, 10% euhedral K-feldspar, 3% hematite and magnetite, and 2% subhedral biotite. The quartz crystals appear to occur interstitially to all other minerals, and the feldspars occur interstitially to the mafic minerals. Oxide minerals appear to be a post-crystallization overprint of the host rock. In some areas at Pellaire, the Mount McLeod batholith also contains up to 20% cobble-sized, fine-grained mafic enclaves. Areas of significant clay alteration and oxidation occur sporadically throughout the batholith in the study area. The grain size of the batholith decreases slightly towards its margin. Discrete zones of intense Cu- and Fe-oxide alteration are commonly observed in the Mount McLeod batholith.

The mineralized quartz veins range in texture from isolated massive veins, to stockworks, to brecciated veins cemented by subsequent generations of quartz. The veins vary in thickness from about 20 cm to 2 m and strike west to southwest with dips ranging from 40 to 80 degrees to the north. Faults of similar orientation to the veins are observed in the country rock surrounding the granodiorite. The veins are interpreted to have formed during or after the displacement along these faults, but only precipitated from hydrothermal solution when the circulating fluids interacted with the granodiorite. Subsequent displacement along these faults also occurred after vein emplacement, as evidenced by faulted lower contacts along some veins. The kinematics observed in fault gouge are consistent with thrusting towards the south.

Hydrothermal brecciation occurs at the contact between the Mount McLeod batholith and the Falls River succession on the eastern side of the property (Figure 4B). Clasts of both units are present in the breccia and are cemented by quartz, sericite and minor jarosite and gypsum. Disseminated pyrite is also present in the granodiorite clasts within the breccia. The contact between the granodiorite and quartz-sericite-cemented hydrothermal breccia has subsequently been faulted (Figure 4C), but only minor displacement is observed across the fault, and quartz veins are continuous a short way into the hydrothermal breccia from the granodiorite.

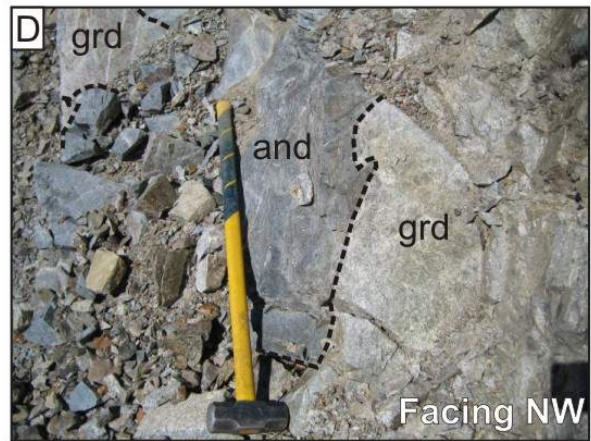
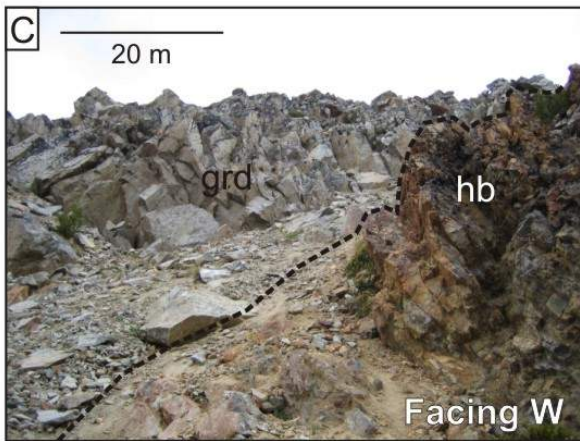
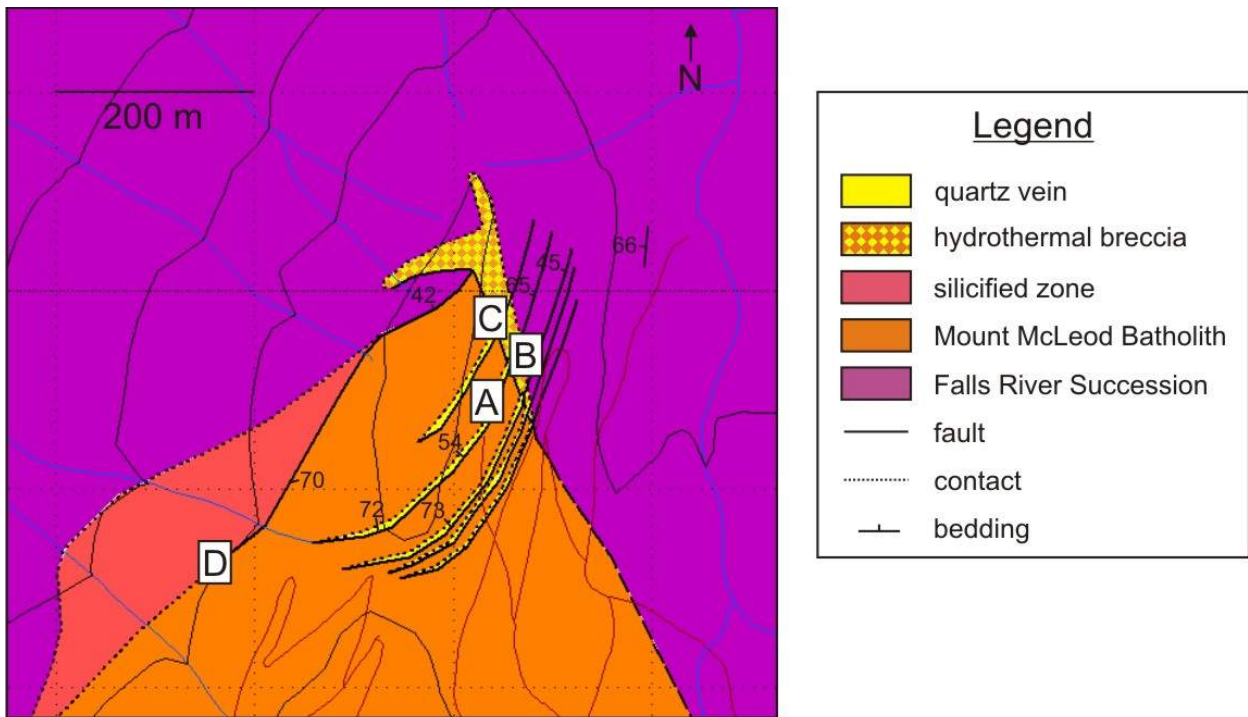


Figure 4. Geologic map of the Pellaire area, showing the locations of photographs: **A**) one of the main quartz-veins (qv) hosted by the Mount McLeod batholith at Pellaire; **B**) part of the hydrothermal breccia at Pellaire, which contains clasts from both the Mount McLeod batholith and the Falls River succession (Ar-Ar date of sericite is pending for the hydrothermal breccia matrix); **C**) a faulted contact separating the Mount McLeod granodiorite (grd) from the hydrothermal breccia unit (hb) and **D**) irregular, intrusive contact between the Mount McLeod granodiorite (grd) and an andesite of the Falls River succession.

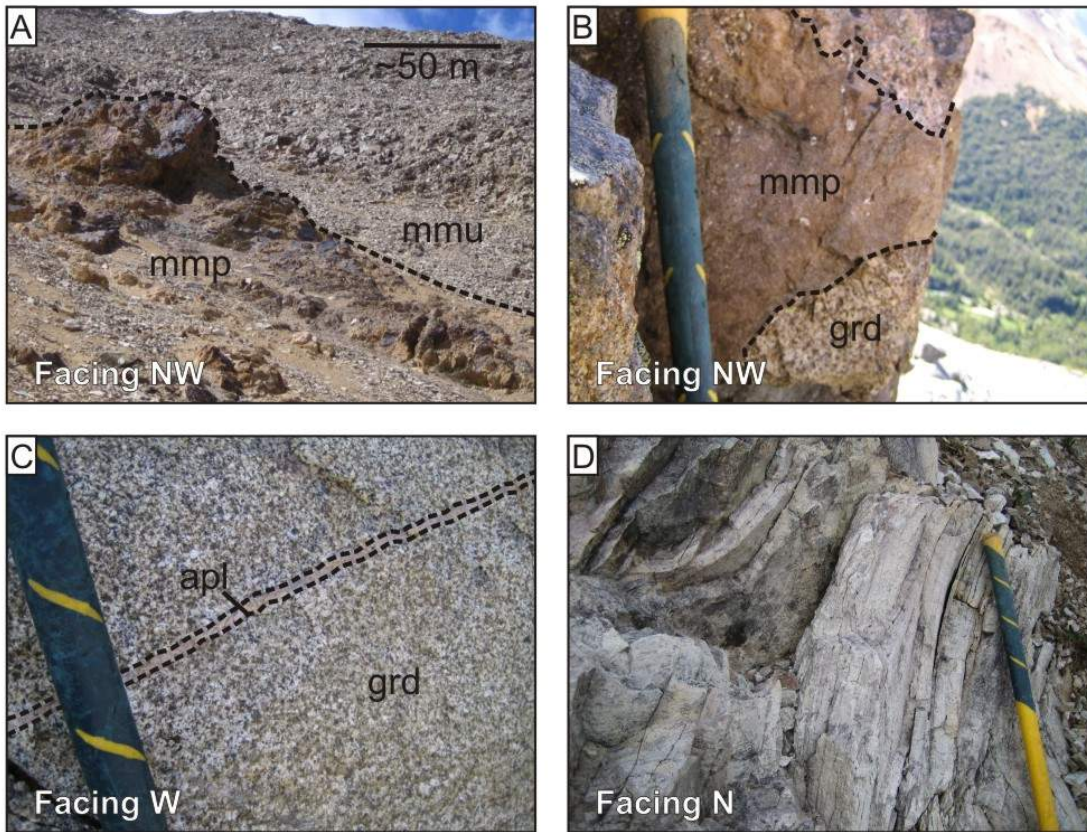
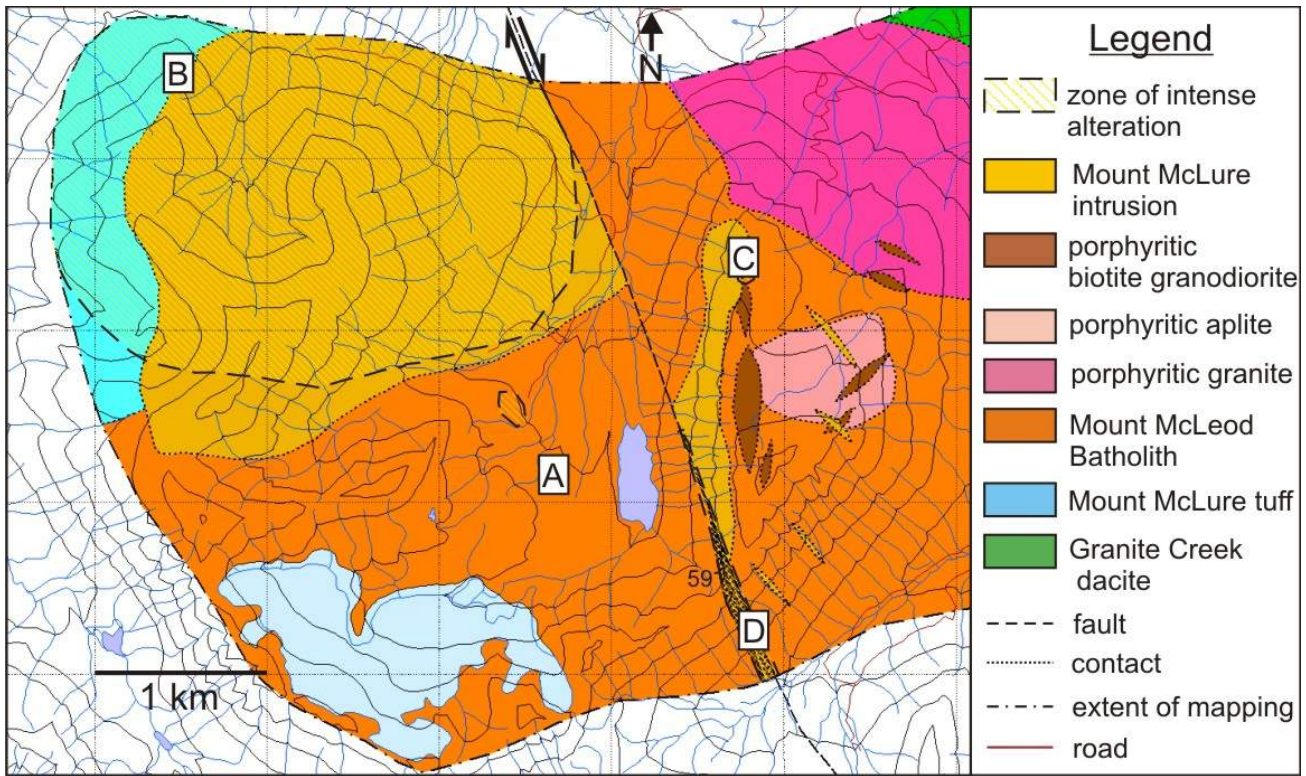


Figure 5. Geologic map of the Mount McLure area showing locations of photographs: **A**) aplite dike (apl) cutting the Mount McLeod granodiorite (grd), **B**) contact between the rusty Mount McLure pluton (mmp) and the grey Mount McLure pluton (mmu), **C**) irregular contact between the Mount McLure pluton (mmp) and the Mount McLeod granodiorite (grd), **D**) silicified fault zone (Ar-Ar date for sericite from the fault zone is pending).

On the western side of the property, the Mount McLeod batholith has an intrusive contact with the Falls River Succession (Figure 4D). The Falls River succession is highly silicified proximal to this contact, but there are no observed signs of brecciation.

Empress Deposit

The Empress deposit is classified as a copper porphyry deposit (Lambert, 1991). Work was undertaken to map in detail the alteration and mineralization in the deposit and to place temperature, depth and age constraints on the conditions of its formation.

The Empress deposit occurs approximately 12 km to the southeast of Upper Taseko Lake, east of Granite Creek, just above its junction with the Taseko River (Figure 3). The altered and mineralized zone extends outwards from the contact with the Coast Plutonic Complex into rocks inferred to be part of the Lower Cretaceous Taylor Creek Group, and is underlain by a porphyritic granite, named the Empress pluton for the purpose of this study. There is no outcrop exposed in the vicinity of the deposit, thus information on it is limited to examination of drill core. The Empress deposit has been interpreted as a porphyry copper deposit; however, much of the reported alteration in the area is also characteristic of high-sulphidization epithermal systems (Osborne, 1999). The Empress deposit contains 10 048 000 tonnes of 0.61 percent copper and 0.79 gram per tonne gold (MINFILE, 2007), with chalcopyrite being the predominant ore mineral.

The only outcrop exposure in the area occurs in the gully around Granite Creek, just beyond the western margin of the deposit. Six drillholes (89-3, 89-6, 90-17, 90-19, 90-22 and 90-30) from the 1989 and 1990 exploration programs on the property by Westpine Metals Ltd. were logged and sampled in detail (Figure 7). In drill core, three intrusive phases were distinguished, including a porphyritic granite and associated dikes, andesitic dikes and aplitic dikes. Five separate alteration types were distinguished: their classification was aided by SWIR analysis. The alteration types include clay-dominated, quartz-chlorite-dominated, quartz-sericite-dominated, quartz-dominated and quartz-magnetite-dominated. Quartz appears to be overprinted by all other alteration minerals, and chlorite appears to overprint magnetite. Up to several percent pyrite and chalcopyrite occur in all alteration phases, but the highest sulphide grades occur within quartz-magnetite alteration.

The Granite Creek unit crops out west of the Empress deposit in the gully surrounding Granite Creek (Figure 5). It is composed of feldspar-phyrlic dacite and associated volcaniclastic rocks and interpreted to be part of the Taylor Creek Group (Jeletzky and Tipper, 1968; McLaren, 1990; Schiarizza et al., 1997). It is inferred to be the host lithology of the Empress deposit.

The Empress pluton underlies the zone of intense alteration and mineralization at the Empress deposit. Proximal to the deposit, the pluton does not crop out at the surface and is only visible in drill core. Similar rock types crop out in Granite Creek southwest of the deposit and on the ridge above it to the southeast, and are interpreted to be part of the same intrusive phase. The pluton is composed of porphyritic hornblende-biotite granite, with quartz and feldspar phenocrysts ranging from 0.5 to 1 cm in size (Figure 7H). Hornblende tends to be variably altered to biotite, which is then in turn variably altered to chlorite. The groundmass of the intrusive rock is also variably altered to K-feldspar. Small dikes of the intrusion are observed in drill core of the overlying rocks and possess similar alteration styles. The Empress pluton is locally a host to mineralization, but further investigation is required to establish whether it has any causative role in mineralization.

A similar porphyritic monzonite occurs in the Empress and Mount McLure areas and is interpreted to be from the same intrusive phase as the pluton that underlies the Empress deposit, although more detailed study is required to confirm this interpretation. It consists of about 40% euhedral feldspar laths ranging from 5 to 10 mm in size, and 15% mafic phenocrysts (biotite and hornblende variably altered to chlorite) in a grey, aphanitic groundmass. It often contains minor amounts (up to 5%) of disseminated magnetite and/or hematite. The porphyritic monzonite cuts the Mount McLeod batholith, but is cut by other porphyritic dikes in the area.

Clay-dominated alteration of the Empress deposit is characterized by blotchy, intermingling layers and patches of paragonite, montmorillonite, halloysite, pyrophyllite, dickite, kaolinite (Figure 7A). These zones typically also consist of significant quartz and Fe-oxide, but are composed of at least ca. 30% clay minerals. Fe-oxide, carbonate and gypsum veinlets, as well as clay fracture coating, are observed in clay-dominated alteration. Clay-dominated alteration tends to host the lowest concentration of pyrite and chalcopyrite out of any alteration type.

Quartz-chlorite-dominated alteration consists of at least 10% chlorite in a quartz-dominated rock (Figure 7B). Chlorite can be patchy, disseminated or grade in as veinlets. Minor amounts of illite are also present in quartz-chlorite alteration. Magnetite and hematite are present in variable proportion with chlorite, and grade into quartz-magnetite-dominated alteration. Gypsum and Fe-oxide veinlets typically cut quartz-chlorite alteration.

Quartz-sericite-dominated alteration is characterized by one or more phases of quartz alteration that appear to have been weakly to moderately overprinted by illite-dominated alteration (Figure 7C). Illite occurs as blebs or patches within the quartz alteration and comprises at least 10% of

the rock. Illite and Fe-oxide veinlets and fracture coating are typically present in quartz-sericite-dominated alteration. Quartz-sericite alteration can also show gradational changes into both clay-dominated and quartz-dominated alteration, and is inferred to be an intermediate alteration style between the two.

Quartz-dominated alteration is characterized by one or more generations of quartz coexisting in the same rock (Figure 7D). These separate quartz phases vary from milky, to clear, to light and dark grey phases. They coexist as either separate zones of blotchy or patchy, uneven alteration, or can occur as brecciation with one or more phases comprising the clasts of the breccia, and the other comprising the matrix. For this study, quartz-dominated alteration is defined to be at least 90% quartz. This alteration phase typically contains small amounts of magnetite, hematite, chlorite or illite. It may also contain small Fe-oxide veinlets and quartz-cemented fractures.

Quartz-magnetite alteration is characterized by at least 10% magnetite overprinting quartz-dominated alteration (Figure 7E). Magnetite has a disseminated or banded occurrence, and also occurs as the matrix of a quartz-magnetite breccia. It can grade in as dense magnetite and hematite veining in quartz-dominated alteration. Intense quartz-magnetite alteration may consist of up to 90% magnetite. This alteration type also tends to host the highest grades of ore (up to 40% disseminated chalcopyrite in discrete zones). Pyrite and chalcopyrite also occur as veinlets cutting quartz-magnetite alteration. Chlorite also appears to variably replace magnetite and hematite and certain zones. This can result in a gradational change in alteration style from quartz-magnetite to quartz-chlorite.

The Empress deposit is cut by at least two generations of post-mineralization dikes. One generation is slightly to moderately chlorite-carbonate-altered, sparsely plagioclase-phyric andesitic dikes (Figure 7F). These dikes tend to host significant carbonate veining. They vary from less than 1 to greater than 10 metres in apparent thickness in drill core, and are interpreted to have been emplaced post-mineralization because of the lack of significant hydrothermal alteration and mineralization observed in them relative to the rocks that they intrude. The other set of dikes are fine-grained, pink, feldspar-dominated, aplitic dikes (similar to those described in the Local Geology section) that contain disseminated Fe-oxide (Figure 7G). No cross-cutting relationships were observed between the two generations of dikes, but the aplite dikes are interpreted to be emplaced late- to post-mineralization and are therefore older than the andesitic dikes. This interpretation is based on the higher Fe-oxide content and higher degree of alteration observed in the aplite dikes.

Taylor-Windfall Deposit

The Taylor-Windfall deposit is classified as a high grade epithermal gold-silver vein deposit (Lane, 1983). The deposit was mapped at scales of 1:5 000 and 1:10 000 with the aim of characterizing the intense alteration zones present in the vicinity of the deposit and to identify any structural controls on the alteration and mineralization. Results from field and laboratory work will provide insights into the conditions of formation of the Taylor-Windfall deposit and possible links with the Empress deposit.

The Taylor-Windfall deposit is a past-producing, vein-hosted gold deposit. It occurs within the Upper Cretaceous Powell Creek Formation (Price, 1986). Production records show that 555 tonnes of ore were mined in 5 years: 14 525 grams of gold and 156 grams of silver were recovered from this ore. The deposit is located in the gully surrounding Battlement Creek just above its junction with the Taseko River; approximately 15 km southeast of Upper Taseko Lake (Figure 3). Hydrothermal alteration of the host rock is dominated by minerals characteristic of advanced argillic alteration (corundum, andalusite, pyrophyllite, alunite, dickite, kaolinite) and silicification (Price, 1986). Known mineralization is largely restricted to two discrete veins: one, sulphide-dominated and one, tourmaline-dominated (Lane, 1983). The occurrence of ore minerals including chalcopyrite, tennantite, enargite, sphalerite, galena and native gold, together with the alteration mineralogy, is suggestive of a high-sulphidation epithermal system.

The underground workings at the Taylor-Windfall deposit were inaccessible during field work. As a result, sampling and mapping were restricted to limited surface exposures, and incorporated logging of drill hole 84-03 from an 1984 exploration program by Westmin Resources. The Powell Creek Formation underlies the region north of the Tchaikazan fault on the north side of Taseko Valley (Figure 6). These rocks were originally assigned to the Powell Creek Formation by McLaren (1990). Maxon (1996) documented ages for the Powell Creek Formation that ranged from 94.6 ± 6.6 Ma and 95.9 Ma at its base to 78.95 ± 4.1 Ma upsection. The base of the formation is intruded by the Dickson-McClure batholith, which has been dated at 92 Ma (Parrish, 1992). The Powell Creek Formation is inferred to host the Taylor-Windfall deposit (Price, 1986). The majority of the rocks exposed at the surface and in drill core are intensely altered, however, and it was not possible during this study to discern the protolith and therefore to confirm the hostrock.

The majority of the alteration observed in the gully around the Taylor-Windfall deposit exhibits some degree of fracture control (Figure 6A). As a result, variations in alteration style and intensity are easily observed, depending on prox-

imity to pervasive fractures at the outcrop scale. Common alteration assemblages observed are vuggy quartz±pyrite (Figure 6B), quartz-sericite-pyrite, and quartz-chlorite-sericite. Illite, paragonite, halloysite, kaolinite and dickite are common clay minerals associated with the quartz-sericite-pyrite and quartz-chlorite-sericite alteration phases. Dissemination and veining of tourmaline is also observed in concentrations up to 10%. Discrete zones of hydrothermal brecciation are also observed in surface exposures (Figure 6C). These zones are less than ca. 2 m thick and are cemented by quartz-illite-palygorskite. On the ridge to the east and above the deposit, significant quartz-alunite alteration is present (Figure 6D). This alteration also appears to be confined to a few tens of metres on either side of a marked fracture or fault zone, and is characteristic of leached cap alteration that commonly overlies epithermal systems.

Mount McLure Area

The contact between the Coast Plutonic Complex and the southeast Coast Belt was studied mainly in the Mount McLure area, between the Empress and Pellaire deposits (Figure 3). This work was done in order to identify the different intrusive phases that occur along the margin of the Coast Plutonic Complex, and to determine any potential relationship among the intrusive phases, alteration zones, and observed mineralization. Separate lithological units, alteration zones and intrusive were identified, mapped and sampled (Figure 5).

Intrusive phases in the Mount McLure area include porphyritic plagioclase-hornblende-pyroxene porphyry (named the Mount McLure pluton for the purposes of this study), aplitic to porphyritic biotite-hornblende granite, porphyritic plagioclase diorite, and the Mount McLeod granodiorite. A zone of intense alteration in the western area of Mount McLure is centred on the Mount McLure pluton. There is a sharp contact in the westernmost part of the area, marked by a sharp change in colour and alteration style (Figure 5A). This contact is inferred to result from primary lithological differences between the units prior to the alteration event. The Mount McLure pluton is observed to intrude the Mount McLeod granodiorite (Figure 5B). Aplite dikes are common within the Mount McLeod batholith (Figure 5C) and at the Empress deposit in the Granite Creek unit. A sub-vertical fault zone trends south-southeast through the centre of the Mount McLure area. The rocks within the fault zone are variably silicified and foliated (Figure 5D). The fault is interpreted to have acted as a conduit for hydrothermal fluids, resulting in intense alteration of the rocks within the zone. Mafic dikes cut the fault zone, and run parallel to the trend of the fault. These dikes are therefore inferred to have intruded after the deformation and silicification events.

Discussion and Future Work

The southeast Coast Belt hosts several prospective and past-producing mineral deposits, including the Bralorne (MINFILE 092JNE 001), Pioneer Mines (MINFILE 092JNE 004), and Prosperity deposits (MINFILE 092O 041). The Bralorne and Pioneer Mines deposits are located approximately 50 km southeast of the Taseko Lakes area, and together represent British Columbia's largest historical gold producers (Bellamy and Arnold, 1985; Figure 2). These deposits and similar ones to the south are vein-hosted mesothermal gold deposits. The Bralorne mining area was in operation from the late 1920s to the early 1970s, during which it produced over 4 million ounces of gold (Sanche, 2004). The Prosperity deposit, formerly known as Fish Lake, is a developed porphyry Cu-Mo-Au prospect. It is situated approximately 30 km north of the Taseko Lakes region and most recent information gives an estimated measured and indicated resource of 491 million tonnes grading 0.43 grams per tonne gold and 0.22 percent copper (Brommeland and Wober, 1999). The Bralorne area is located more or less along strike with the Taseko Lakes area, and has a mineralization age constrained at 85.7 ± 3 Ma by a K-Ar date from hornblende within a syn-post mineralization hornblende porphyry dike (Ash, 2001).

The Empress, Pellaire and Taylor-Windfall deposits all show different styles of mineralization and alteration, but occur in similar geologic settings. The connection, if any, among the deposits remains unclear, but laboratory studies during the winter of 2007–2008 should help to better understand the P-T conditions of formation and the ages of mineralization. If there is a temporal link among the deposits, it is possible that they are in some way genetically linked and may be a part of the same system, with local differences perhaps reflecting local variances in depth of formation in the crust, or relative contributions of magmatic fluids versus buffering due to crustal interactions of fluids.

Laboratory work will also provide more information on lithological compositions and alteration mineralogy, as well as provide insight into age relationships between separate alteration and intrusive phases. Further study of fluid inclusions and thermochronological data will provide insight into temperatures and depths of mineralization for the deposits studied. From these data, it is anticipated that the mineral deposits within the Taseko Lakes region will be placed into a regional geologic context and a model for mineralization of the area can be developed.

Acknowledgments

The authors would like to thank Galore Resources Inc. and Geoscience BC for their support in funding the project. We are grateful to Great Quest Metals Ltd. for permitting access to the Empress property and drill core. The help of M.

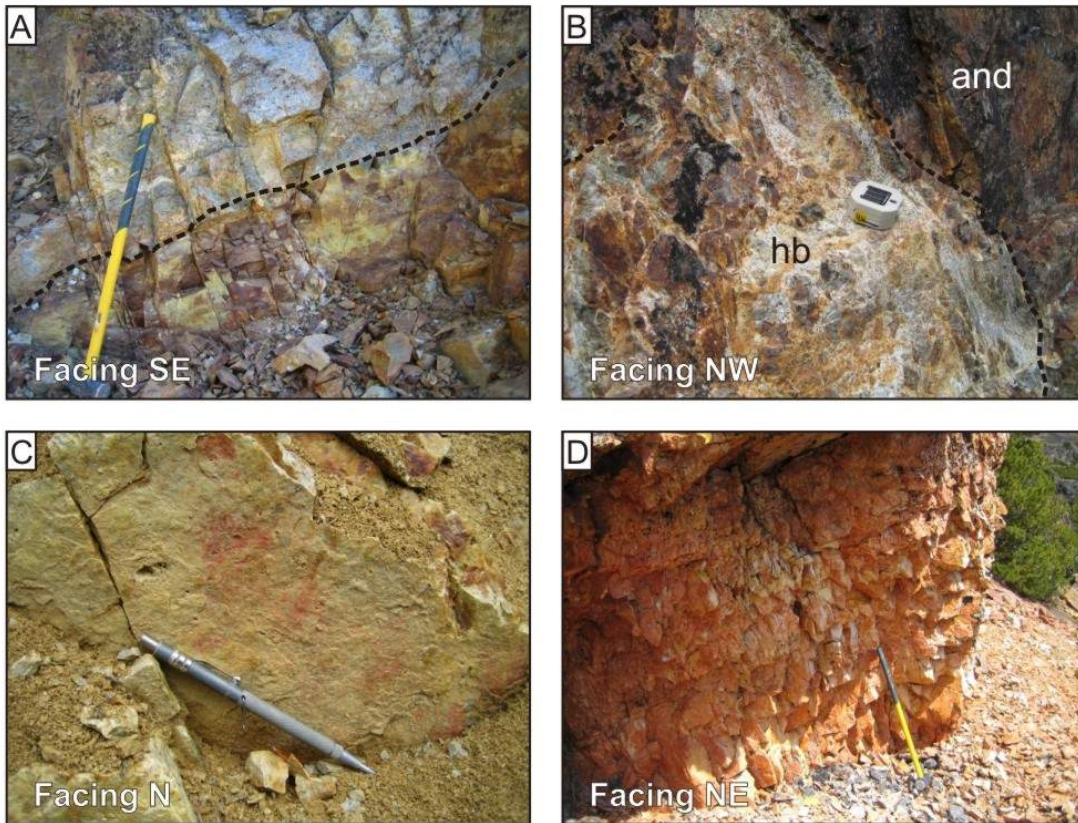
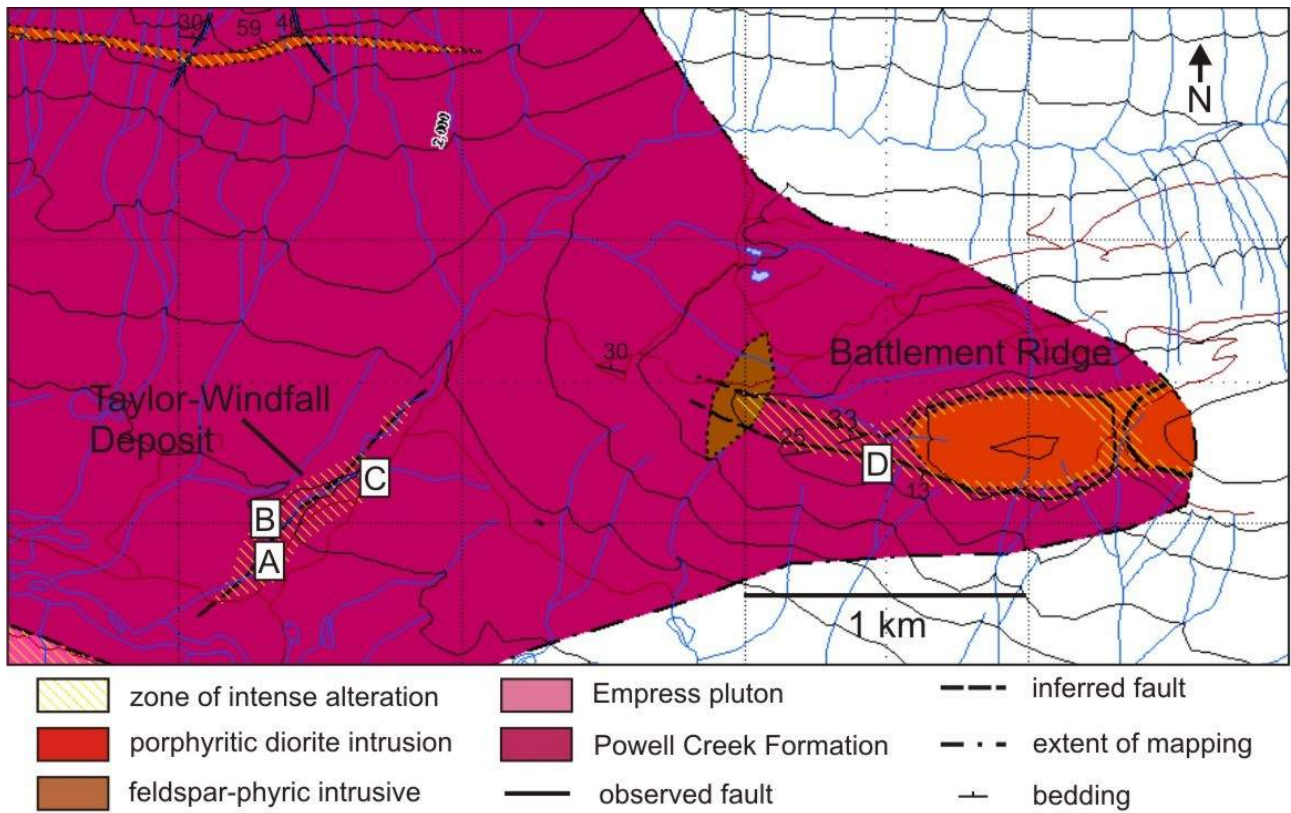


Figure 7. Geology of the Taylor-Windfall and Battlement Ridge areas, showing locations of photographs: **A)** marked changes in alteration intensity inferred to be fracture-controlled; **B)** hydrothermal breccia (hb) cutting andesite of the Powell Creek Formation (an Ar-Ar date of sericite is pending for the hydrothermal breccia); **C)** red staining on fractures in an intensely silicified, vuggy unit; **D)** pervasive, bright orange, intense quartz-allunite alteration proximal to a fault-fracture zone on Battlement Ridge, indicative of leached cap environments.

Cruickshanks and E. Looby during the 2007 field season was greatly appreciated. C. Chamberlain is thanked for reviewing this manuscript.

References

- Ash, C.H. (2001): Relationships between ophiolites and gold-quartz veins in the North American Cordillera; BC Department of Energy, Mines and Petroleum Resources, Bulletin 108, 140 p.
- BC Geological Survey (2006): MapPlace GIS internet mapping system; BC Ministry of Energy, Mines and Petroleum Resources, MapPlace website, URL <<http://www.MapPlace.ca>>; [November 2006].
- Bellamy, J. and Arnold, R. (1985): Bralorne Mine Project: Report on the 1984 exploration work, Bridge River Area, B.C.; unpublished company report, E and B Explorations Inc.
- Brommeland, L.K. and Wober, G. (1999): Prosperity gold-copper project, 1998 diamond drilling assessment report; unpublished company report, Taseko Mines Ltd.
- Friedman, R.M. and Armstrong, R.L. (1995): Jurassic and Cretaceous geochronology of the southern Coast Belt, British Columbia, 49° to 51°N; *in* Jurassic Magmatism and Tectonics of the North American Cordillera: Boulder, Colorado, Miller, D.M. and Busby, C. (ed.), Geological Society of America, Special Paper 299, p 95–139.
- Herrmann, W., Blake, M., Doyle, M., Huston, D., Kamprad, J., Merry, N. and Pontual, S. (2001): Short wavelength infrared (SWIR) spectral analysis of hydrothermal alteration zones associated with base metal sulfide deposits at Rosebery and Western Tharsis, Tasmania, and Highway-Reward, Queensland; *Economic Geology*, v. 96, no. 5, p. 939–955.
- Hollis, L., Blevings, S.K., Chamberlain, C.M., Hickey, K.A. and Kennedy, L.A. (2007): Mineralization, alteration and structure of the Taseko Lakes region (NTS 092O/04), southwestern British Columbia: Preliminary analysis; *in* Geoscience BC, Paper 2007-1, p. 297–307.
- Holtby, M.H. (1988): An assessment report of diamond drilling and underground development on the Lord 1 to 3 and Hi 1 to 4 claims; unpublished company report, Consolidated Silver Standards Limited.
- Israel, S., Schiarizza, P., Kennedy, L.A., Friedman, R.M. and Villeneuve, M.E. (2006): Evidence for Early to Late Cretaceous, sinistral deformation in the Tchaikazan River area, southwestern British Columbia: Implications for the evolution of the southern Coast Belt; *in* Paleogeography of the western North American Cordillera, J. Haggart, R. Enkin and J.W.H. Monger (ed.), Geological Association of Canada, Special Paper 46, p. 331–350.
- Jeletzky, J.A. and Tipper, H.W. (1968): Upper Jurassic and Cretaceous rocks of Taseko Lakes map area and their bearing on the geological history of southwestern British Columbia; Geological Survey of Canada, Paper 67-54, 218 p.
- Lambert, E. (1991): 1990 Diamond drill program of the Taseko property; unpublished company report, Westpine Metals Ltd., Vancouver B.C., 205 p.
- Lane, R. (1983): Geological and geochemical assessment report on the Taseko property (Bluff Claims 1 and 2, Windfall C-G, Windfall #2 C-G, and Province C-G); unpublished company report, Westmin Resources Ltd., Vancouver, B.C., 53 p.
- MacMillan, W.J. (1991): Porphyry Deposits in the Canadian Cordillera; *in* Ore Deposits, Tectonics and Metallogeny in the Canadian Cordillera, BC Ministry of Energy, Mines and Petroleum Resources, Paper 1991-4, p. 252–276.
- MapPlace (2006): Geology and mineral deposits of southwestern British Columbia (NTS 092O/04); British Columbia Geological Survey MapPlace website, BC Ministry of Energy, Mines and Petroleum Resources, URL <<http://webmap.em.gov.bc.ca/mapplace/minpot/bsgs.cfm>> [June 2007].
- Maxson, J.A. (1996): A sedimentary record of Late Cretaceous tectonic restructuring of the North American cordillera: The Tyaughton-Methow basin, southwest British Columbia; M.Sc. thesis, University of Minnesota, 290 p.
- McLaren, G.P. (1990): A mineral resource assessment of the Chilko Lake planning area; BC Ministry of Energy, Mines and Petroleum Resources, Bulletin 81, 117 p.
- MINFILE (2007): MINFILE BC mineral deposits database; BC Ministry of Energy, Mines and Petroleum Resources, URL <<http://www.em.gov.bc.ca/Mining/GeolSurv/Minfile/>> [November 2007].
- Monger, J.H.W. and Journeay, J.M. (1994): Guide to the geology and tectonic evolution of the southern Coast Mountains; Geological Survey of Canada, Open File 2490, 81 p.
- Monger, J.H.W., Price, R.A. and Tempelman-Kluit, D.J. (1982): Tectonic accretion and the origin of the two major metamorphic and plutonic belts in the Canadian Cordillera; *Geology*, v. 10, p 70–75.
- Osborne, W. (1999): Report on the 1998 exploration program of the Taseko Property; unpublished company report, Great Quest Metals Ltd., Vancouver, B.C., 75 p.
- Parrish, R.R. (1992): U-Pb Ages for Cretaceous plutons in the eastern Coast Belt, southern British Columbia; *in* Radiogenic Age and Isotopic Studies, Report 5, Geological Survey of Canada, Paper 91-02, p 109–113.
- Pezzot, E.T. (2005): Assessment report on the Pellaire project; unpublished company report, V. R. Ltd., West Vancouver, B.C., 37 p.
- Price, G. (1986): Geology and Mineralization, Taylor-Windfall Gold Prospect, British Columbia, Canada; M.Sc. Thesis, Oregon State University, 144 p.
- Rusmore, M.E. and Woodsworth, G.J. (1991): Distribution and tectonic significance of Upper Triassic terranes in the eastern Coast Mountains and adjacent Intermontane Belt, British Columbia; *Canadian Journal of Earth Sciences*, v. 28, p. 532–541.
- Rusmore, M.E. and Woodsworth, G.J. (1994): Evolution of the eastern Waddington thrust belt and its relation to mid-Cretaceous Coast Mountains arc, western British Columbia; *Tectonics*, v. 13, p. 1052–1067.
- Sanche, H.A. (2004): Report on the 2003 surface drilling on the Bralorne Pioneer Mine property, Cosmopolitan, Cosmopolitan Fraction and Mauser claims; unpublished company report, Bralorne Pioneer Gold Mines Ltd.
- Schiarizza, P., Gaba, R.G., Glover, J.K., Garver, J.I. and Umhoefer, P.J. (1997): Geology and mineral occurrences of the Taseko–Bridge River Area; BC Ministry of Employment and Investment, Bulletin 100, 292 p.
- Thompson, A.J.B., Hauff, P.L. and Robitaille, A.J. (1999): Alteration mapping in exploration: Application of short-wave infrared (SWIR) spectroscopy; *Society of Economic Geologists Newsletter* no. 39, p. 1, 16–27.

Umhoefer, P.J., Schiarizza, P. and Robinson, M. (2002): Relay Mountain Group, Tyaughton-Methow Basin, southwest British Columbia: A major Middle Jurassic to Early Creta-

ceous terrane overlap assemblage; Canadian Journal of Earth Sciences, v. 39, no. 7, p. 1143–1167.

Layered Intrusions and Regional Geology of the Nootka Sound Area, Vancouver Island, British Columbia (NTS 092E)

K. Fecova, Department of Earth Sciences, Simon Fraser University, Burnaby, BC, kfecova@sfu.ca

D. Marshall, Department of Earth Sciences, Simon Fraser University, Burnaby, BC

R. Staples, Department of Earth Sciences, Simon Fraser University, Burnaby, BC

G. Xue, Department of Earth Sciences, Simon Fraser University, Burnaby, BC

T. Ullrich, Department of Ocean and Earth Sciences, University of British Columbia, Vancouver, BC

S. Close, Department of Earth Sciences, Simon Fraser University, Burnaby, BC

Fecova, K., Marshall, D., Staples, R., Xue, G., Ullrich, T. and Close, S. (2008): Layered intrusions and regional geology of the Nootka Sound area (NTS 092E), Vancouver Island, British Columbia; *in* Geoscience BC Summary of Activities 2007, Geoscience BC, Report 2008-1, p. 35–46.

Introduction

Layered intrusions identified in the Conuma River region of the Nootka Sound area (Marshall et al., 2006) became the subject of a detailed study during 2007. The layered intrusions consist of alternating cyclic ultramafic and mafic units of peridotite and gabbro. Fieldwork also included additional regional geological mapping of the Gold River area (NTS 092E/16). This report contains an updated preliminary geological map of the Nootka Sound region and a cross-section through the region mapped during the summers of 2004–2007. This map also shows localities with new Ar-Ar dates.

Regional Geology

Muller et al. (1981) compiled his work and the work of others identifying the Westcoast Crystalline Complex as consisting of rocks ranging up to amphibolite metamorphic facies. It was described as a “heterogeneous assemblage of amphibolite and basic migmatite with minor metasedimentary and metavolcanic rocks of greenschist metamorphic grade.” Subsequent work (Marshall et al., 2005, 2006) revealed a lack of rocks of amphibolite grade. Instead, it confirmed the occurrence of units that are correlative with units identified in the southern portion of Vancouver Island. The exposed rocks of the Nootka Sound region appear to have a maximum regional metamorphic grade of middle greenschist facies. Contact metamorphic effects are highest near the Jurassic and Eocene intrusive

rocks, where migmatite has been observed (Muller et al., 1981).

Muller et al. (1981) designated a huge portion of the Nootka Sound region as Westcoast Crystalline Complex. Massey et al. (2005) identified the same portion of the region as Paleozoic to early Mesozoic undivided granitic rocks and lower amphibolite–kyanite grade metamorphic rocks. This work modified the earliest maps, which had dividing the region into the Mooyah Formation (Marshall et al., 2006), Mount Mark Formation (Massey, 1991; Yorath et al., 1999) and granodiorite, diorite and gabbro of the Jurassic Island Intrusive Suite. Naming polygons on the map was based on the dominance of a rock type in the area.

The geological map of the Nootka Sound area (Figure 1) compiles data from geological mapping in 2004–2007 (Close, 2006; Marshall et al., 2006). The map also uses data from Muller et al. (1981) and Massey et al. (2005), airphotos, Landsat images and maps with aeromagnetic anomalies (BC Geological Survey, 2007) to infer information on regional geology and structure for inaccessible areas.

Layered Ultramafic and Mafic Rocks

Occurrence and Previous Work

The first mention regarding the occurrence of plutonic rocks of mafic nature in the Nootka Sound region comes from Muller et al. (1981). These were identified as melanosome, described as “plagioclase amphibolites with granoblastic texture and compositions of diorite, gabbro, quartz diorite and quartz gabbro” (Muller et al., 1981, p. 20), and were included as part of the Westcoast Crystalline Complex.

Keywords: *PGE mineralization, Vancouver Island, Nootka, Wrangellia, island arc, ultramafic plutonic rocks, layered intrusions*

This publication is also available, free of charge, as colour digital files in Adobe Acrobat® PDF format from the Geoscience BC website: <http://www.geosciencebc.com/s/DataReleases.asp>.

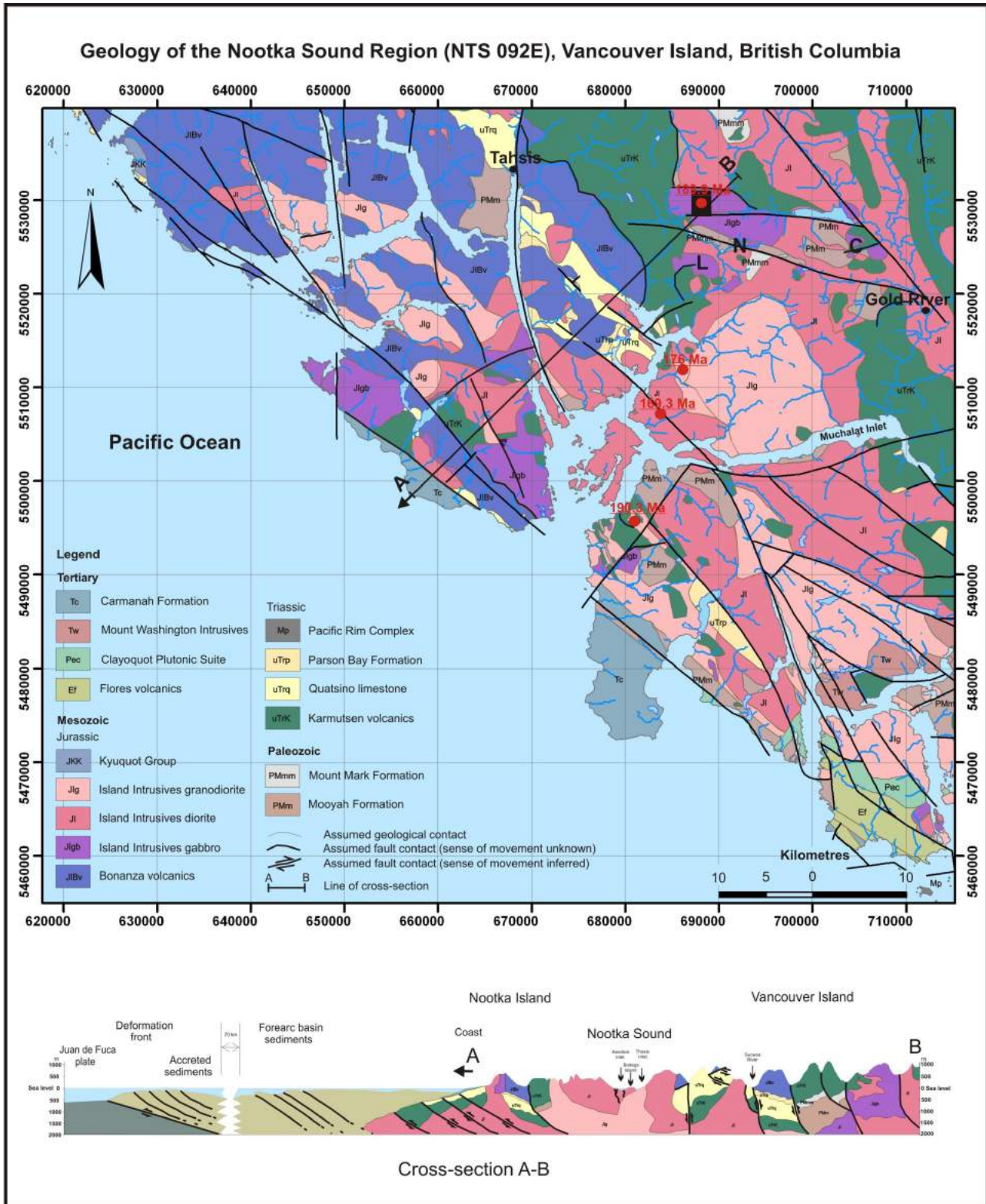


Figure 1. Geology of the Nootka Sound region (*modified after* Muller et al., 1981; Massey et al., 2005; Marshall et al., 2006). The map shows new Ar-Ar dates on plutonic rocks. The black rectangle depicts an area of detailed mapping that is also intersected by the cross-section A-B. Layering in intrusions in cross-section is shown by dashed parallel lines, based on the assumption that more layered intrusions outcrop in the area with similar strike and dip. Some faults were inferred from Landsat images. Abbreviations: C, Cypress Creek; L, Leigh Creek; N, Norgate Creek.

Another brief description of ultramafic and mafic rocks comes from the work of Isachsen (1987), who described the geology of the area around Meares Island. Isachsen (1987) identified outcrops within the Westcoast Crystalline Complex on Meares Island as a unit of early Jurassic or older Westcoast amphibolite. This unit is characterized by “medium to coarse grained granoblastic diorite and uralitized gabbro with granoblastic texture to fine-grained, well lined amphibolite gneiss. In places the amphibolite has a distinctive spotted texture produced by rounded, 1–3 cm diameter hornblende megacrysts in a finer grained amphibolite matrix. In some places megacrysts are aligned like beads on a string, yielding an even more striking texture, reminiscent of a cumulate” (Isachsen, 1987, p. 2049).

Isachsen (1987) also described amphibole as a replacement product after pyroxene, indicating a gabbroic parentage with 5–50% plagioclase of andesine to labradorite composition; biotite is rare and quartz is absent. The sample also shows a relatively high nickel concentration (56–211 ppm), suggesting derivation from mafic igneous rocks.

Isachsen (1987) also identified Early to Middle Jurassic gabbro and peridotite as “isolated dike like masses of uralitized gabbroic rock near the central part of Lemmens Inlet” (Isachsen, 1987, p. 2050). He described this rock type as a “medium to coarse grained unfoliated, granular gabbro-peridotite with 50% poikilitic augite with plagioclase inclusions and fibrous uralitized rims, 25% to 35% of enstatite and olivine replaced by serpentine, 10% of saussuritized bytownite, 3% of hornblende, 2% to 5% of chromite and magnetite and minor chlorite.” Sargent (1941) described similar rocks from a locality near the Bedwell River intruding the Jurassic Bedwell batholith.

The work of DeBari et al. (1999) in the Alberni area and Broken Islands area includes a description of a gabbro-peridotite unit within the Westcoast Crystalline Complex, identified by Muller et al. (1981) and Isachsen (1987). The ultramafic and mafic rocks are grouped into two pyroxene–hornblende gabbro, a pyroxenite and a sheared serpentinite of cumulate nature. Additionally, strongly foliated hornblendite, hornblende gabbro, hornblende diorite, tonalite and rare granodiorite are grouped into the diorite unit of the Westcoast Crystalline Complex. Samples yielded Jurassic ages, implying that these rock units are cogenetic with rocks of the Jurassic Island Intrusive Suite and Bonanza volcanic rocks. They also show similar whole-rock geochemistry. DeBari et al. (1999) also reported an occurrence of ultramafic cumulate near Kennedy Lake with minimal aerial extent and uncertain origin.

Larocque and Canil (2006) published preliminary results from fieldwork in the Port Renfrew area, where they found isolated bodies of ultramafic plutonic rock, which they de-

scribed as peridotite, within the Westcoast Crystalline Complex.

Ultramafic Rocks and Local Geology of the Conuma River Area

Layered intrusions are exposed in the Conuma River area, along the C-50D logging road. The extent of the area in which they outcrop is approximately 70 m by 450 m (Figure 2).

Two types of layered intrusion are present within this area. The first type consists of 20–50 cm thick, very coarse to coarse-grained peridotite layers alternating with 20–30 cm thick, medium-grained gabbro layers (Figures 3 and 4). The second type comprises layers of very coarse grained peridotite. The layers are distinct at outcrop scale, probably due to differential weathering of certain layers. Numerous outcrops of the layered intrusions were found in the area.

The weathered surfaces of the layered intrusions are white and green for medium-grained gabbro and rusty brown for very coarse grained peridotite. At some locations, weathering of very coarse grained peridotite is characterized by a green-brown weathered surface. In other places, these rocks can be identified by typical spheroidal weathering, of which the final product is brown soil. This is consistent with the field observations of Larocque and Canil (2006).

All outcrops of the layered intrusions have an average strike of $040 \pm 20^\circ$ and a dip of $50 \pm 10^\circ$ southeast. Other igneous rock types in the area are fine- to coarse-grained gabbro–hornblende gabbro, fine- to medium-grained diorite, tonalite and plagioclase-phyrlic dacite.

Joint sets and local faults are the major structures in the area. These strike approximately southeast and dip steeply southwest. Local faults are very narrow with slickensided surfaces, with or without fault gouge. They strike west-northwest and southwest and dip steeply north-northeast and northwest, respectively. The trend and plunge of the slickensides implies horizontal movement along these faults, but no offsets were observed. These faults and horizontal movements along them reflect local adjustments of blocks as a response to the current transpressional regime.

In the southernmost portion of the study area, a 20 m wide shear zone with cataclastic-mylonitic fabric trends east. Due to strong deformation along the shear zone, the sheared rock cannot be identified with any confidence. However, the chloritic, green appearance of the shear zone and gradual transition into a very coarse grained peridotite and medium-grained gabbro imply that shear might have occurred preferentially along the ultramafic body. The zone is heavily fractured, veined and chloritized. A portion of sheared gabbro shows plagioclase replaced by epidote and

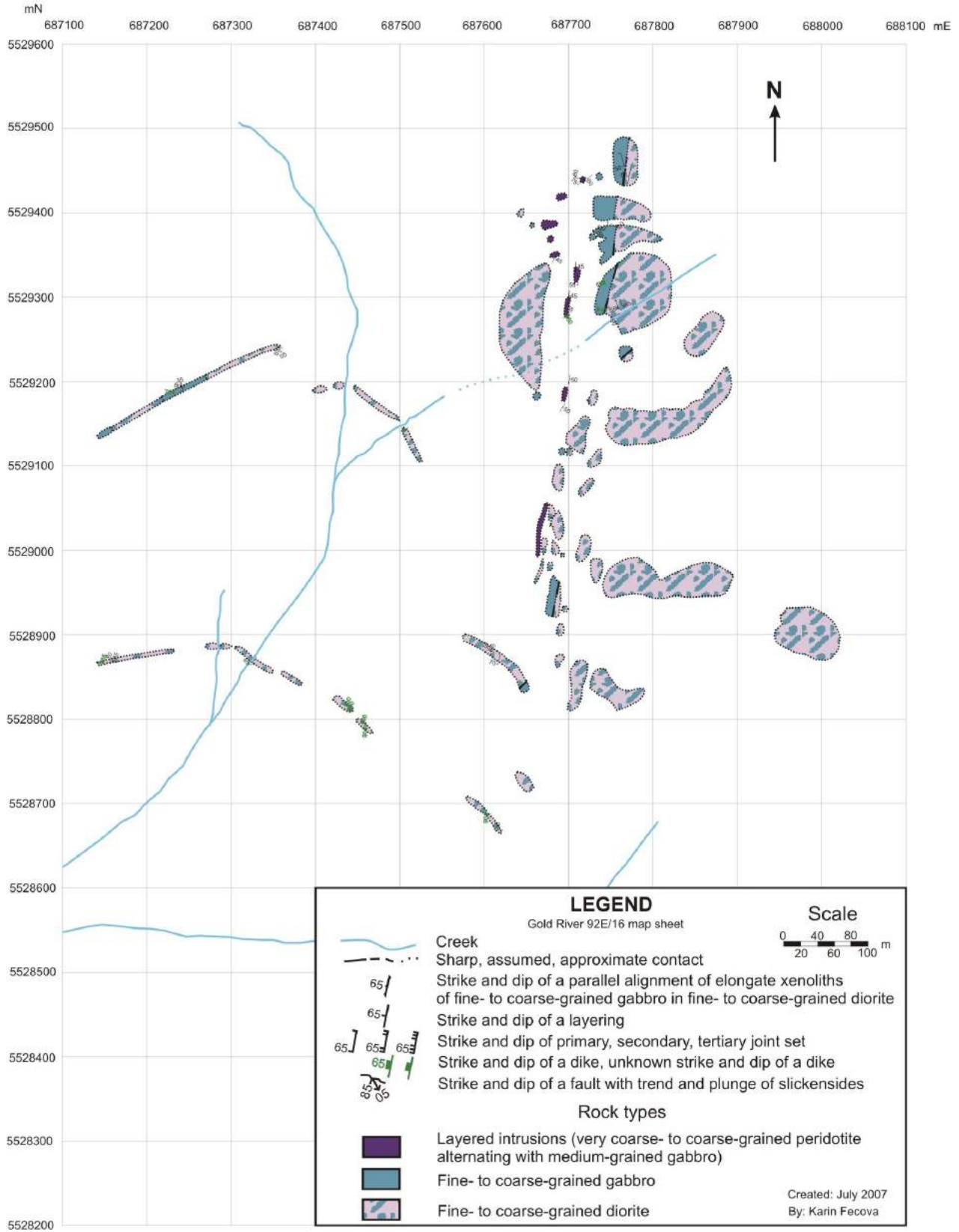


Figure 2. Detailed geology of layered intrusions in the Conuma River area. Location marked by the black rectangle on Figure 1.



Figure 3. Very coarse grained peridotite from the Conuma River area. This unit is distinctive in the field, characterized by the tan colour, strong magnetism and pitted weathered surface with out-lines of pyroxene-hornblende megacrysts.

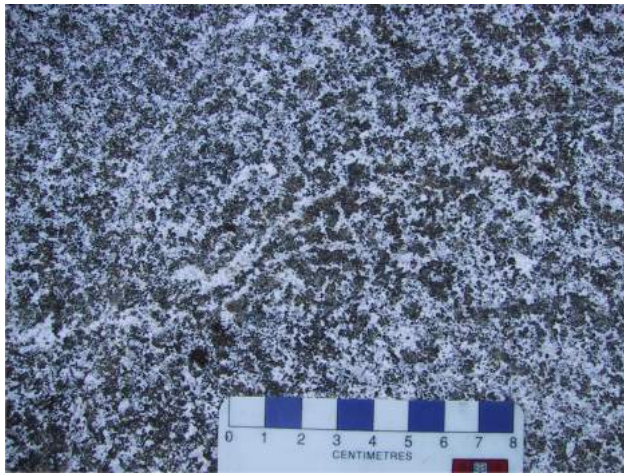


Figure 4. Medium-grained gabbro from the Conuma River area. The unit displays typical white–light grey weathering colour and is associated with both the layered intrusions and the gabbroic units outward from the layered intrusions.

2–4 mm garnet crystals that are likely a product of metasomatism during shearing. A plagioclase-phyric dacite dike, about 50 cm wide, parallels the shear zone and appears to be unaffected by the shear. This type of dike is common in the study area and contains 15% randomly distributed, euhedral plagioclase phenocrysts (2–15 mm) and 5% black hornblende phenocrysts (1–3 mm) in a green-gray dacitic groundmass. The plagioclase phenocrysts were separated and dated by Ar-Ar. The results do not yield a well-defined plateau but favour a Jurassic rather than Eocene age.

Unit Description of Layered Intrusions

The Conuma phase (Marshall et al., 2006) of the Island Intrusive Suite consists of two major rock types, as previously mentioned. These are medium-grained gabbro and

very coarse to coarse-grained peridotite. The peridotite is tan weathering and dark green-black on fresh surfaces, with 40% euhedral, unaltered olivine (millimetre size), enclosed in 45% poikilitic orthopyroxene (20 mm) and 10% poikilitic hornblende (20 mm). Minor constituents are phlogopite, plagioclase and magnetite. The unit is strongly magnetic. Considering hornblende as an alteration product of pyroxene, the original rock type was probably olivine websterite.

The medium-grained gabbro weathers a light brownish green and is dark green-grey on the fresh surface. It is an equigranular holocrystalline rock with 60% euhedral green hornblende (3 mm) and 40% euhedral white plagioclase (3 mm). The unit is weakly magnetic, with sulphide minerals locally ranging up to 5%.

Contact Relationships

Layered intrusions outcrop as isolated blocks that appear discontinuous due to vegetation and Quaternary cover. No tectonic or intrusive contacts between the layered intrusions and country rocks have been observed. Nor has any lateral or vertical continuity been observed between individual outcrops. The layered peridotite unit is observed in a number of outcrops, either exclusively or as cyclic units of very coarse grained peridotite and medium-grained gabbro. Repetition of both units occurs on a scale of approximately 20 cm. The layering is not as obvious at adjacent outcrops, but it is still occasionally present in the coarse- and medium-grained gabbros. This less distinctive layering is probably due to a subtle modal and grain-size change within a single unit. Gabbro with less distinctive layering grades into nonlayered gabbro with variable grain sizes and modal abundances. Where the plagioclase content in nonlayered gabbro increases, it results in hornblende gabbro and hornblende diorite. Patches, pods, lenses, zones and bands of hornblende gabbro and hornblende diorite at the centimetre to metre scale are common in the nonlayered gabbro (Figures 5 and 6). The nonlayered gabbro is in sharp contact with a medium-grained diorite intrusion that intrudes the gabbro. The contact between gabbro and the diorite intrusion was observed in three outcrops and tends to have a general northerly trend that is subparallel to the strike of the layers within the layered intrusions.

Contacts within the layered intrusions and with the nonlayered gabbro are abrupt and are based on differences in grain size and/or phase abundances. Contacts between layers follow a generally planar trend with local irregularities. Contacts between tonalitic dikes and ultramafic/mafic rocks are sharp. Contacts between medium-grained diorite and ultramafic/mafic rocks are dominantly sharp. Contacts between tonalite and medium-grained diorite are also dominantly sharp.

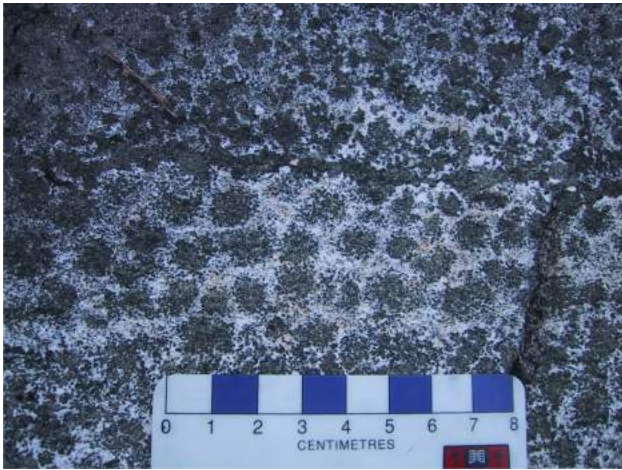


Figure 5. Coarse-grained hornblende gabbro from the Conuma River area. This unit is characterized by well-developed hornblende crystals surrounded by plagioclase, giving the rock a mottled appearance.



Figure 6. Pegmatitic pod, consisting of well-developed hornblende and plagioclase crystals. These pods are very common features in medium-grained gabbro and occur randomly within this unit.

Textural and Structural Features

The cumulate texture in the peridotite is characterized by cumulate olivine crystals in intercumulus crystals of pyroxene and hornblende. Plagioclase, if present, is also intercumulate. Field observations indicate that crystal settling by gravity was one of the depositional mechanisms during formation of the layered intrusions. The presence of magmatic density currents in the magma chamber during crystallization of the ultramafic magma is exhibited by features that resemble soft-sediment deformation and convoluted bedding (Irvine, 1980). Surfaces of the medium-grained gabbro layers with already-settled crystals appear to be disturbed by layers of very coarse grained peridotite similar to scour marks in sedimentary rocks. The disruption of a partially molten gabbro layer can result in partial or

complete separation into a gabbro layer and a dense peridotite crystal mush. These separated or disrupted portions then have the shape of lenses, pods and swirls, which are usually visible at outcrop scale (Figures 7 and 8).

Geochronology

Marshall et al. (2006) published results of Ar-Ar hornblende dating of the very coarse grained peridotite unit. The dating suggests that the ultramafic intrusions are of Jurassic age (189.9 ± 2.1 Ma). Additional ^{40}Ar - ^{39}Ar data obtained from the Jurassic intrusions (Figure 1) are listed in Tables 1 to 4, and the corresponding spectra are shown in Figure 9.



Figure 7. Layered ultramafic intrusions in the Conuma River area, showing soft-sediment-like deformation of the medium-grained gabbro unit.



Figure 8. Detail of the convoluted bedding observed in the medium-grained gabbro and very coarse grained peridotite within layered intrusions of the Conuma River area. According to Irvine (1974), the convoluted layering is a result of deformation of crystal-mush layers during emplacement.

Table 1. ^{40}Ar - ^{39}Ar data from sample DM05-20 (190.3 ± 1.4 Ma), Jurassic Island Intrusive Suite.

Laser power (%)	Isotope Ratios								Age	
	$^{40}\text{Ar}/^{39}\text{Ar}$	$^{38}\text{Ar}/^{39}\text{Ar}$	$^{37}\text{Ar}/^{39}\text{Ar}$	$^{36}\text{Ar}/^{39}\text{Ar}$	Ca/K	Cl/K	% ^{40}Ar atm ⁽¹⁾	f ^{39}Ar ⁽²⁾		$^{40}\text{Ar}^*/^{39}\text{ArK}$
2	783.638 ±0.054	3.629 ±0.075	2.653 ±0.086	2.373 ±0.057	15.34	0.761	81.15	0.13	149.209 ±17.137	1063.77 ±92.30
2.3	192.647 ±0.022	1.334 ±0.031	2.984 ±0.039	0.616 ±0.038	22.82	0.282	84.21	0.47	29.627 ±5.940	267.00 ±49.76
2.6	108.549 ±0.018	0.760 ±0.025	2.679 ±0.039	0.329 ±0.032	21.39	0.159	81.81	1.18	19.321 ±2.662	178.54 ±23.42
2.9	43.037 ±0.009	0.804 ±0.017	2.058 ±0.023	0.105 ±0.029	16.66	0.179	62.91	2.94	15.534 ±0.910	144.90 ±8.16
3.2	31.844 ±0.012	1.415 ±0.016	2.511 ±0.018	0.040 ±0.026	20.37	0.324	28.26	5.86	22.489 ±0.447	206.19 ±3.87
3.5	23.792 ±0.014	1.802 ±0.016	2.681 ±0.018	0.015 ±0.034	21.88	0.415	12.18	20.12	20.843 ±0.349	191.88 ±3.05
3.8	23.020 ±0.013	1.925 ±0.014	2.935 ±0.017	0.013 ±0.027	23.98	0.444	9.19	23.64	20.890 ±0.300	192.29 ±2.62
4.1	22.729 ±0.014	1.917 ±0.017	3.069 ±0.021	0.014 ±0.021	25.06	0.442	9.36	14.75	20.501 ±0.318	188.89 ±2.78
4.4	21.839 ±0.005	1.762 ±0.012	2.520 ±0.014	0.010 ±0.048	20.51	0.405	4.63	11.55	20.610 ±0.183	189.84 ±1.60
5	22.162 ±0.016	1.821 ±0.020	2.821 ±0.021	0.011 ±0.043	23.03	0.419	7.01	19.36	20.546 ±0.364	189.28 ±3.18
Total/avg.	26.380 ±0.003	1.783 ±0.003	12.273 ±0.002	0.023 ±0.006		0.383		100	20.570 ±0.075	

⁽¹⁾ percentage of ^{40}Ar in the analyzed gas fraction

⁽²⁾ percentage of ^{39}Ar released relative to the total amount of ^{39}Ar released from the sample

Flux correction factor (J) = 0.005384 ±0.000006

Volume ^{39}ArK = 157.32

Integrated date = 191.97 ±1.32

Volumes are $1 \times 10^{-13} \text{ cm}^3$ at normal pressure and temperature

Neutron flux monitors: 28.02 Ma FCs (Fish Canyon sanidine; Renne et al., 1998)

Isotope production ratios: ($^{40}\text{Ar}/^{39}\text{Ar}$)K = 0.0302 ±0.00006; ($^{37}\text{Ar}/^{39}\text{Ar}$)Ca = 1416.4 ±0.5; ($^{36}\text{Ar}/^{39}\text{Ar}$)Ca = 0.3952 ±0.0004; Ca/K = 1.83 ±0.01 ($^{37}\text{ArCa}/^{39}\text{ArK}$).

Table 2. ^{40}Ar - ^{39}Ar data from sample DM05-212A (189.9 ± 2.1 Ma), Jurassic Island Intrusive Suite.

Laser power (%)	Isotope Ratios								Age	
	$^{40}\text{Ar}/^{39}\text{Ar}$	$^{38}\text{Ar}/^{39}\text{Ar}$	$^{37}\text{Ar}/^{39}\text{Ar}$	$^{36}\text{Ar}/^{39}\text{Ar}$	Ca/K	Cl/K	% ^{40}Ar atm ⁽¹⁾	f ^{39}Ar ⁽²⁾		$^{40}\text{Ar}^*/^{39}\text{ArK}$
2	3548.409 ±0.168	8.734 ±0.183	8.658 ±0.195	10.238 ±0.171	36.91	2.108	73.58	0.02	1222.646 ±367.349	3653.98 ±470.53
2.4	1575.382 ±0.050	4.205 ±0.067	5.494 ±0.056	4.317 ±0.054	37.95	0.829	75.44	0.13	405.209 ±36.995	2087.36 ±112.92
2.8	612.327 ±0.038	1.705 ±0.051	4.157 ±0.052	1.829 ±0.043	30.21	0.319	81.1	0.27	116.513 ±13.453	878.07 ±80.27
3.2	60.232 ±0.011	0.881 ±0.020	4.046 ±0.021	0.137 ±0.033	32.95	0.196	59.36	3.93	24.210 ±1.389	220.93 ±11.93
3.6	32.541 ±0.015	0.701 ±0.022	3.396 ±0.019	0.041 ±0.035	27.72	0.158	28.54	10.39	23.085 ±0.577	211.24 ±4.98
4	25.486 ±0.013	0.609 ±0.018	2.885 ±0.018	0.021 ±0.031	23.57	0.137	18.05	33.23	20.891 ±0.359	192.19 ±3.13
4.4	23.103 ±0.016	0.575 ±0.019	3.095 ±0.021	0.015 ±0.036	25.29	0.13	11.01	23.81	20.508 ±0.383	188.85 ±3.35
5	23.162 ±0.015	0.727 ±0.018	3.154 ±0.020	0.015 ±0.032	25.78	0.165	11.61	28.21	20.456 ±0.363	188.39 ±3.18
Total/avg.	30.805 ±0.003	0.665 ±0.005	13.766 ±0.003	0.034 ±0.006		0.505		100	20.640 ±0.108	

⁽¹⁾ percentage of ^{40}Ar in the analyzed gas fraction

⁽²⁾ percentage of ^{39}Ar released relative to the total amount of ^{39}Ar released from the sample

Flux correction factor (J) = 0.005381 ±0.000006

Volume ^{39}ArK = 117.79

Integrated date = 202.46 ±1.89

Volumes are $1 \times 10^{-13} \text{ cm}^3$ at normal pressure and temperature

Neutron flux monitors: 28.02 Ma FCs (Fish Canyon sanidine; Renne et al., 1998)

Isotope production ratios: ($^{40}\text{Ar}/^{39}\text{Ar}$)K = 0.0302 ±0.00006; ($^{37}\text{Ar}/^{39}\text{Ar}$)Ca = 1416.4 ±0.5; ($^{36}\text{Ar}/^{39}\text{Ar}$)Ca = 0.3952 ±0.0004; Ca/K = 1.83 ±0.01 ($^{37}\text{ArCa}/^{39}\text{ArK}$).

Table 3. ^{40}Ar - ^{39}Ar data from sample DM05-162 (176.4 ± 1.3 Ma), Jurassic Island Intrusive Suite.

Laser power (%)	Isotope Ratios								Age	
	$^{40}\text{Ar}/^{39}\text{Ar}$	$^{38}\text{Ar}/^{39}\text{Ar}$	$^{37}\text{Ar}/^{39}\text{Ar}$	$^{36}\text{Ar}/^{39}\text{Ar}$	Ca/K	Cl/K	% ^{40}Ar atm ⁽¹⁾	f ^{39}Ar ⁽²⁾		$^{40}\text{Ar}^*/^{39}\text{ArK}$
2	579.288 ±0.038	3.338 ±0.046	1.048 ±0.116	1.465 ±0.057	3.031	0.712	66.19	0.18	189.228 ±20.368	1267.21 ±97.99
2.4	139.154 ±0.018	0.880 ±0.035	0.794 ±0.048	0.355 ±0.041	5.429	0.186	66.87	0.77	44.286 ±3.992	385.74 ±31.31
2.8	45.711 ±0.007	0.572 ±0.022	1.879 ±0.020	0.097 ±0.035	15.93	0.125	54.45	3.23	20.271 ±0.994	186.84 ±8.70
3.2	24.726 ±0.010	1.523 ±0.014	2.317 ±0.016	0.021 ±0.026	20.05	0.349	19.45	31.47	19.902 ±0.260	183.61 ±2.28
3.5	21.336 ±0.006	1.490 ±0.012	2.302 ±0.015	0.012 ±0.021	19.91	0.342	10.48	30.88	19.063 ±0.141	176.24 ±1.24
3.8	21.246 ±0.014	1.656 ±0.014	2.413 ±0.017	0.013 ±0.034	20.86	0.381	10.23	16.69	18.934 ±0.317	175.10 ±2.80
4.1	21.832 ±0.006	1.593 ±0.010	2.456 ±0.014	0.014 ±0.056	21.41	0.366	11.17	15.17	19.240 ±0.262	177.79 ±2.30
4.5	20.999 ±0.013	1.565 ±0.023	3.318 ±0.021	0.044 ±0.079	28.44	0.36	22.89	1.61	14.182 ±1.050	132.72 ±9.48
Total/avg.	24.782 ±0.002	1.514 ±0.003	10.956 ±0.002	0.020 ±0.007		0.353		100	19.240 ±0.066	

⁽¹⁾ percentage of ^{40}Ar in the analyzed gas fraction

⁽²⁾ percentage of ^{39}Ar released relative to the total amount of ^{39}Ar released from the sample

Flux correction factor (J) = 0.005383 ±0.000006

Volume ^{39}ArK = 135.01

Integrated date = 182.89 ±1.17

Volumes are $1 \times 10^{-13} \text{ cm}^3$ at normal pressure and temperature

Neutron flux monitors: 28.02 Ma FCs (Fish Canyon sanidine; Renne et al., 1998)

Isotope production ratios: ($^{40}\text{Ar}/^{39}\text{Ar}$)K = 0.0302 ±0.00006; ($^{37}\text{Ar}/^{39}\text{Ar}$)Ca = 1416.4 ±0.5; ($^{36}\text{Ar}/^{39}\text{Ar}$)Ca = 0.3952 ±0.0004; Ca/K = 1.83 ±0.01 ($^{37}\text{ArCa}/^{39}\text{ArK}$).

Table 4. ^{40}Ar - ^{39}Ar data from sample DM05-121 (169.3 ± 1.2 Ma), Jurassic Island Intrusive Suite.

Laser power (%)	Isotope Ratios							Age		
	$^{40}\text{Ar}/^{39}\text{Ar}$	$^{38}\text{Ar}/^{39}\text{Ar}$	$^{37}\text{Ar}/^{39}\text{Ar}$	$^{36}\text{Ar}/^{39}\text{Ar}$	Ca/K	Cl/K	% ^{40}Ar atm ⁽¹⁾			
2	546.915 ± 0.101	1.222 ± 0.185	1.685 ± 0.169	1.851 ± 0.127	9.494	0.208	78.26	0.06	91.420 ± 53.372	721.32 ± 347.11
2.3	225.262 ± 0.018	0.357 ± 0.144	0.498 ± 0.102	0.721 ± 0.035	4.915	0.048	88.55	0.5	23.603 ± 6.478	215.56 ± 55.76
2.6	102.643 ± 0.014	0.157 ± 0.083	0.444 ± 0.068	0.317 ± 0.042	5.489	0.019	87.19	1.72	12.382 ± 3.715	116.29 ± 33.79
2.9	52.055 ± 0.017	0.123 ± 0.066	0.401 ± 0.082	0.172 ± 0.068	4.696	0.017	86.01	1.24	6.091 ± 3.376	58.14 ± 31.71
3.2	29.102 ± 0.006	0.264 ± 0.026	0.560 ± 0.027	0.067 ± 0.026	7.463	0.055	61.31	6.17	10.594 ± 0.506	99.95 ± 4.65
3.5	20.903 ± 0.007	0.949 ± 0.012	1.422 ± 0.016	0.017 ± 0.028	19.36	0.216	15.65	19.07	17.247 ± 0.182	159.99 ± 1.62
3.8	22.036 ± 0.007	0.774 ± 0.016	1.224 ± 0.031	0.020 ± 0.080	16.52	0.175	10.37	5.18	18.012 ± 0.501	166.78 ± 4.43
4.1	20.470 ± 0.005	1.082 ± 0.011	1.592 ± 0.014	0.012 ± 0.030	21.72	0.248	9.21	28.44	18.350 ± 0.143	169.76 ± 1.26
4.4	19.937 ± 0.005	1.029 ± 0.012	1.538 ± 0.013	0.010 ± 0.042	21.15	0.235	7.12	27.37	18.257 ± 0.156	168.94 ± 1.38
5	19.920 ± 0.008	0.929 ± 0.015	1.455 ± 0.024	0.016 ± 0.035	19.9	0.212	6.51	6.48	17.200 ± 0.229	159.58 ± 2.04
5.5	37.801 ± 0.010	0.737 ± 0.025	1.151 ± 0.024	0.082 ± 0.039	15.6	0.164	55.12	3.78	15.781 ± 0.933	146.94 ± 8.34
Total/avg.	23.659 ± 0.001	0.921 ± 0.003	10.322 ± 0.001	0.025 ± 0.008		0.145		100	18.279 ± 0.064	

⁽¹⁾ percentage of ^{40}Ar in the analyzed gas fraction

⁽²⁾ percentage of ^{39}Ar released relative to the total amount of ^{39}Ar released from the sample

Flux correction factor (J) = 0.005377 ± 0.000006

Volume ^{39}ArK = 94.21

Integrated date = 160.13 ± 1.15

Volumes are $1 \times 10^{-13} \text{ cm}^3$ at normal pressure and temperature

Neutron flux monitors: 28.02 Ma FCs (Fish Canyon sanidine; Renne et al., 1998)

Isotope production ratios: ($^{40}\text{Ar}/^{39}\text{Ar}$)K = 0.0302 ± 0.00006; ($^{37}\text{Ar}/^{39}\text{Ar}$)Ca = 1416.4 ± 0.5; ($^{36}\text{Ar}/^{39}\text{Ar}$)Ca = 0.3952 ± 0.0004, Ca/K = 1.83 ± 0.01 ($^{37}\text{ArCa}/^{39}\text{ArK}$).

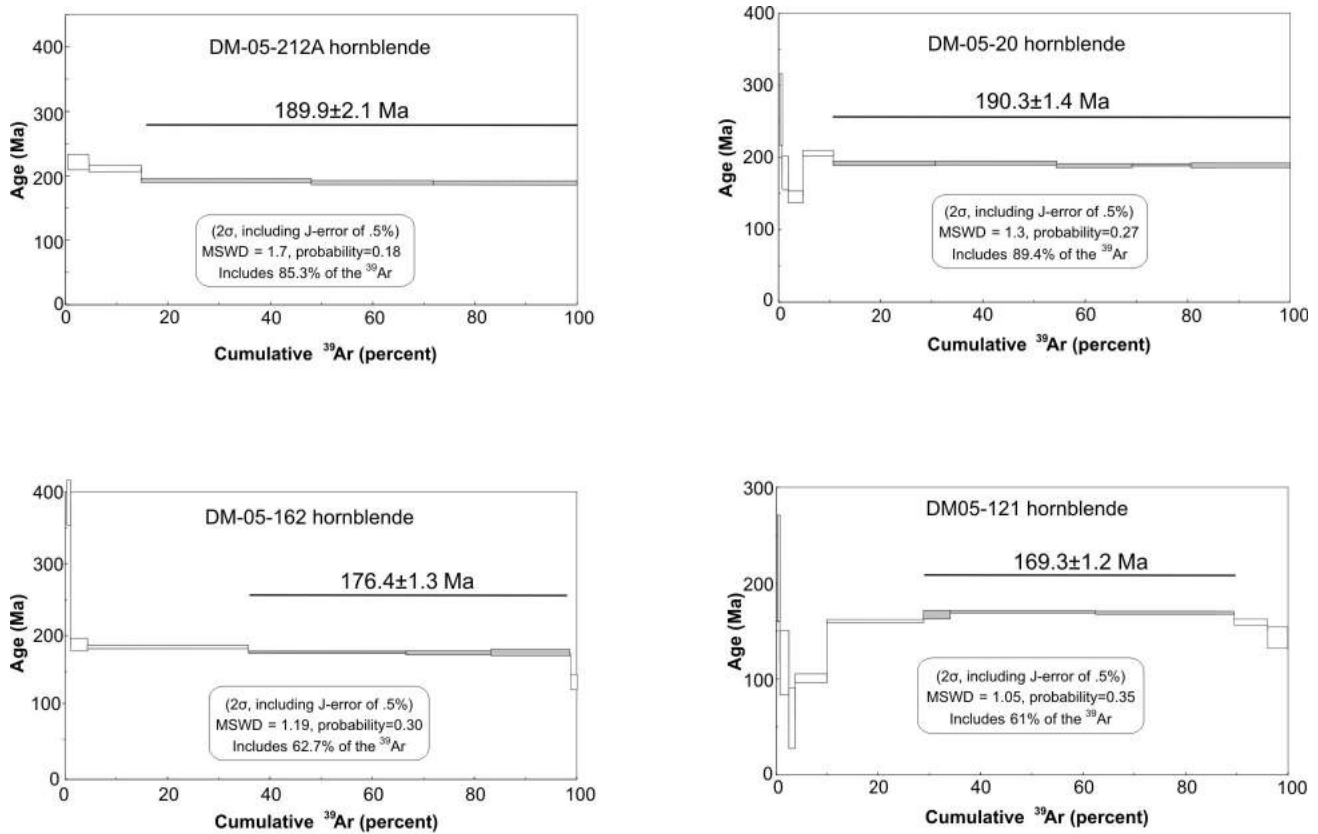


Figure 9. ^{40}Ar - ^{39}Ar gas release spectra of four samples from the Jurassic Island Intrusive Suite, corresponding to the data in Table 1. All samples yield Jurassic plateaus.

Mafic Rocks and Local Geology of the Norgate Creek Area

Mafic intrusions of the Norgate Creek area are continuous outcrops of steep cliffs that can be followed for up to a kilometre. This area shows both horizontally and vertically layered intrusions.

Horizontally layered intrusions exhibit layers at centimetre to millimetre scale and consist of one rock type, a fine- to medium-grained gabbro that consists of approximately 40% plagioclase and 60% pyroxene (\pm hornblende) crystals. Layers are planar, well defined at outcrop scale and probably visible due to differential weathering (Figure 10).

Lateral change along the outcrop cliffs is marked by irregular and abrupt contacts due to changes in modal compositions. No repetition in cyclic units or sedimentary-type structures were observed in these mafic rocks at the outcrop scale. Common rock types are very fine, fine- and medium-grained gabbro and hornblende gabbro. A scanning electron microscope image of well-developed and abundant magnetite grains from a medium-grained hornblende gabbro unit was published by Marshall et al. (2006). Besides the magnetite abundance, interesting replacement textures are also present in this gabbroic unit. The unit weathers dark grey and is black on fresh surfaces and equigranular, consisting of 60% intercumulus hornblende with pyroxene cores, 30% cumulus plagioclase and 10% cumulus olivine that is completely altered to serpentine. The sample in thin section shows a high degree of alteration (Figure 11).

Individual gabbro types can be traced across different outcrops. These gabbro units intrude the Mooyah Formation, which is strongly hornfelsed due to contact metamorphism. The hornfelsed Mooyah Formation contains up to 20% sulphide minerals. No massive diorite intrusions were found in the Norgate Creek area.



Figure 10. Fine layering in the gabbroic rocks from the Norgate Creek area. The layering is best observed on the weathered surface.

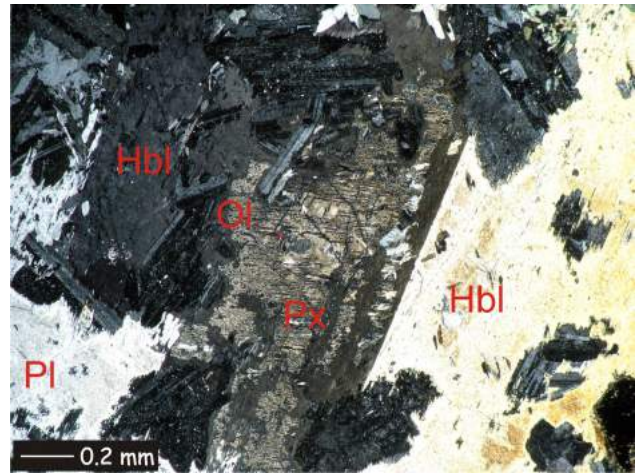


Figure 11. Photomicrograph of medium-grained hornblende gabbro from the Norgate Creek area. Olivine altered to serpentine and saussuritized plagioclase are cumulus crystals within intercumulus zones of serpentinized pyroxene with fresh hornblende rims. Low interference colours (crossed polars) are due to thinning of the thin section at its edge.

Ultramafic and Mafic Rocks, and Local Geology of the Cypress Creek Area

The Cypress Creek area is characterized by isolated ultramafic bodies within mafic phases of medium-grained diorite and by the presence of a very distinctive ultramafic breccia (Figure 12).

The mafic unit is a coarse-grained olivine gabbro. It is black on the weathered surface and greenish black on the fresh surface. It consists of 80% hornblende/pyroxene crystals (5–15 mm) enclosing 10% anhedral olivine crystals (1 mm) and 10% altered plagioclase (5–8 mm). The unit is strongly magnetic.



Figure 12. Ultramafic breccia from the Cypress Creek area shows a very distinctive brecciation of ultramafic rocks into angular clasts. Sulphide-rich mineralized clasts are chloritized peridotite and coarse-grained gabbro enclosed in a leucocratic matrix of quartz and plagioclase.

The outcrop of ultramafic breccia is 150 m long and trends northeast. Medium-grained diorite intrudes Karmutsen volcanic rocks and peridotite at its northeast end. Diorite dikes brecciate peridotite in the central portion of the outcrop and tonalite dikes brecciate peridotite at its southwest end. The ultramafic breccia consists of 10–50 cm, angular to rounded, deformed, fragmented, heavily veined, rusty-weathering and dark green fresh peridotite clasts. Very coarse grained peridotite is composed of 50% intercumulus hornblende or pyroxene (15–20 mm), 45% cumulus olivine crystals (1 mm) and 5% intercumulus plagioclase (2 mm). This unit is magnetic, with up to 15–20% sulphide clusters consisting of crystals of pyrrhotite and other sulphide minerals (up to 10 mm). Sulphide clusters were also found within the dikes.

Medium- to coarse-grained equigranular hornblende diorite intruding ultramafic rocks weathers dark grey and is black and white on the fresh surface, with 50% hornblende crystals (2–3 mm) and 50% plagioclase crystals (2–3 mm).

Ultramafic Rocks and Local Geology of the Leagh Creek Area

Pyroxene-hornblende gabbro is dark grey on fresh and weathered surfaces. It is a medium-grained rock with 40–45% prismatic, euhedral black pyroxene and dark green hornblende crystals (1–2 mm), 55–60% subhedral plagioclase crystals (1–2 mm) and approximately 2% sulphide minerals. This gabbro is magnetic with millimetre- to centimetre-size feldspar-quartz-epidote alteration veins. The gabbro is also intruded by medium-grained hornblende diorite and by north-striking, moderately dipping andesitic dikes. The andesite weathers a medium grey-green and is medium grey on the fresh surface. It is recrystallized in some locations, comprising 1 mm grains of plagioclase, quartz and altered hornblende with occasional phenocrysts of black idiomorphic pyroxene. It contains up to 2% sulphide minerals.

Potential for Platinum-Group-Element Mineralization

Platinum-group-element (PGE) mineralization in layered intrusions associated with continental magmatism has been observed in a number of localities worldwide, such as the Bushveld and Stella in South Africa, the Stillwater in the United States and many other layered intrusions (Prendergast, 2000; Maier et al., 2003). All have a tholeiitic chemical signature and represent two types of layered intrusion with PGE mineralization. The ‘Bushveld type’ is a large intrusion with PGE mineralization at deeper levels, where the PGEs are associated with chromite. The ‘Stella type’ is a small intrusion in which PGE mineralization is found at shallow levels and in association with magnetite (Maier et al., 2003). Although the Conuma layered ultramafic rocks are more likely associated with island-arc

magmatism, they may still be prospective for Stella-type PGE mineralization.

Marshall et al. (2006) published Pt, Pd, Au and Cu analyses from the magnetite-rich sample of the medium-grained hornblende gabbro intrusion from the Norgate Creek area. The values reported were relatively low, compared to a sample of fine-grained, nonmagnetic gabbro from the same area, collected and assayed by prospector E. Specogna. Mr. Specogna released assay results in his open file report, which shows anomalous values for Pt, Pd and Ni (Specogna and Specogna, 2003).

Platinum-group-element mineralization can be correlative with Ni, Au and Cu, and can be also associated with magnetite or chromite (Prendergast, 2000; Maier et al., 2003). Understanding the conditions of crystallization in the magma chamber and considering a presence and/or absence of certain minerals/metals can lead to a reasonable interpretation of PGE precipitation depths within the Conuma River and Norgate Creek intrusions. The elements Os, Ir, Ru and Rh behave as compatible elements and tend to partition into spinel or olivine during early stages of magma crystallization, and thus tend to be concentrated in deeper portions of intrusions. The elements Pt, Pd, Cu and Au can also precipitate during early crystallization of magma and associate with chromite. If the magma is S-undersaturated, these elements behave incompatibly and tend to stay in the melt until the magma reaches S and Fe-oxide saturation. Then they precipitate in association with magnetite with (or without) sulphide minerals during the later stages of magma crystallization at shallow levels (Maier et al., 2003). Additional geochemical studies are underway to further evaluate the PGE potential of these rocks.

The Conuma layered intrusions are magnetite rich, especially the very coarse to coarse-grained peridotite unit, and they may represent shallow levels of an intrusion. It is believed that PGE mineralization at shallow levels favours a contribution from mantle melts, especially mantle plumes and involvement of crustal assimilation. A lack of crustal assimilation can result in early S saturation and PGE precipitation at a deeper level within the intrusion (Maier et al., 2003). The geochronology of the Conuma ultramafic rocks is consistent with the emplacement of the Jurassic Island Intrusive Suite. Thus, there is the possibility that PGE elements could precipitate both at deeper levels within the intrusion (due to arc crust contamination) and at shallow levels (due to association with magnetite-rich layers).

Discussion

Jackson (1971) summarized information on different types of ultramafic intrusions worldwide. The closest analogy to Conuma layered intrusions is ‘Alaskan peridotite’, which also has analogues in the Urals, Russia and in the Tulameen

region of BC. These ultramafic intrusions share similar characteristics, such as

- being restricted to island arcs;
- synorogenic or postorogenic emplacement;
- association with andesitic volcanism or granodioritic intrusions;
- development of a metamorphic aureole;
- cylindrical zonation, with ultramafic rocks in the centre grading outward to mafic and intermediate rocks such as gabbro, tonalite and granodiorite;
- the presence of olivine, clinopyroxene and magnetite;
- magnetite-rich pyroxenite dikes;
- amphibolitized border rocks; and
- PGE enrichment.

According Taylor and Noble (1969) 'Alaskan peridotites' represent cumulates from ultramafic melts, forming in unstable environments with multiple injections of ultramafic crystal mush that mixes prior solidification. The occurrence of ultramafic rocks with gabbros, diorites and granodiorites suggests that these rocks formed from ultramafic melts of alkaline basaltic or andesitic parentage (Jackson, 1971).

Irvine (1967) showed a number of images of folded intrusion layers, soft-sediment-like deformation of intrusion layers, crossbedding and scours in layered intrusions. The deformation and mineralogy of the Conuma ultramafic rocks resembles some of Irvine's images and rock types.

The Tulameen ultramafic-gabbro complex described by Findlay (1969) represents a nonstratiform type of ultramafic intrusion in which ultramafic intrusions intrude each other. This type more closely resembles observations from the Norgate ultramafic intrusions, which record at least four intrusive events.

Larocque and Canil (2006) reported a mica peridotite unit from the Port Renfrew area on Vancouver Island. Lithological and petrographic description, as well as the association of mica peridotite with rocks of the Island Intrusive Suite, implies a similar genesis for the Conuma and Port Renfrew ultramafic rocks. It also implies that there may be many more ultramafic bodies and intrusions between Conuma and Port Renfrew that would be prospective for PGE and Ni mineralization.

Ultramafic and mafic intrusions from the Gold River study area will be examined in detail using data from whole-rock and mineral geochemistry in a manner similar to studies in the Border Ranges of Alaska by Burns (1985) and DeBari and Coleman (1989). Magma-fractionation modelling will be used to find the composition of parent magmas responsible for crystallization of ultramafic rocks and to find any fractionation trends within the layered intrusions and/or a petrological relationship to the Jurassic diorite and

granodiorite. This study will also focus on interpretation of crystallization history, mechanisms responsible for cumulate textures and emplacement of the layered intrusions.

Acknowledgments

The authors are very grateful to Geoscience BC for supporting the project financially and for a student scholarship to the senior author. The authors would also like to thank to E. Specogna and Hard Creek Nickel Corporation for property access. N. Massey from the British Columbia Geological Survey is thanked for comments and improvements to an earlier version of this manuscript.

References

- BC Geological Survey (2007): MapPlace GIS internet mapping system; BC Ministry of Energy, Mines and Petroleum Resources, MapPlace website, URL <<http://www.MapPlace.ca>> [November 2007].
- Burns, L.E. (1985): The Border Ranges ultramafic and mafic complex, south-central Alaska: cumulate fractionates of island-arc volcanics; *Canadian Journal of Earth Sciences*, v. 22, p. 1020–1038.
- Close, S. (2006): Geology and tectonics of the Nootka Island region, British Columbia; M.Sc. thesis, Simon Fraser University, Burnaby, BC, 96 p.
- DeBari, S.M. and Coleman, R.G. (1989): Examination of the deep levels of an island arc: evidence from the Tonsina ultramafic-mafic assemblage, Tonsina, Alaska; *Journal of Geophysical Research*, v. 94, no. B4, p. 4373–4391.
- DeBari, S.M., Anderson, R.G. and Mortensen, J.K. (1999): Correlation among lower to upper crustal components in an island arc: the Jurassic Bonanza arc, Vancouver Island, Canada; *Canadian Journal of Earth Sciences*, v. 36, p. 1371–1413.
- Findlay, D.C. (1969): Origin of the Tulameen ultramafic-gabbro complex, southern British Columbia; *Canadian Journal of Earth Sciences*, v. 6, p. 399–425.
- Irvine, T.N. (1974): Petrology of the Duke Island Ultramafic Complex, southeastern Alaska; *Geological Society of America, Memoir* 138, 240 p.
- Irvine, T.N. (1980): Magmatic density currents and cumulus processes; *American Journal of Science*, v. 280-A, p. 1–58.
- Isachsen, C.E. (1987): Geology, geochemistry, and cooling history of the Westcoast Crystalline Complex and related rocks, Meares Island and vicinity, Vancouver Island, British Columbia; *Canadian Journal of Earth Sciences*, v. 24, p. 2047–2064.
- Jackson, E.D. (1971): The origin of ultramafic rocks by cumulus processes; *Fortschritte der Mineralogie*, v. 48, no. 1, p. 128–174.
- Larocque, J. and Canil, D. (2007): Ultramafic rock occurrences in the Jurassic Bonanza Arc near Port Renfrew (NTS 092C/09, 10, 15, 16), southern Vancouver Island; *in Geological Fieldwork 2006*, BC Ministry of Energy, Mines and Petroleum Resources, Paper 2007-1 and Geoscience BC, Report 2007-1, p. 319–324.
- Maier, W.D., Barnes, S.J., Gartz, V. and Andrews G. (2003): Pt-Pd reefs in magnetites of the Stella layered intrusions, South Africa: a world of new exploration opportunities for plati-

- num group elements; Geological Society of America, v. 31, no. 10, p. 885–888.
- Marshall, D., Lesiczka, M., Xue, G., Close, S. and Fecova, K. (2006): Update on the mineral deposit potential of the Nootka Sound region (NTS 092E), west coast of Vancouver Island, British Columbia; *in* Geological Fieldwork 2005, BC Ministry of Energy, Mines and Petroleum Resources, Paper 2006-1 and Geoscience BC, Report 2006-1, p. 323–330.
- Marshall, D., Street, E., Ullrich, T., Xue, G., Close, S. and Fecova, K. (2006): Geology and mineral potential update for the Muchalat-Hesquiat region, Vancouver Island; *in* Geological Fieldwork 2005, BC Ministry of Energy, Mines and Petroleum Resources, Paper 2006-1 and Geoscience BC, Report 2006-1, p. 355–360.
- Massey, N.W.D. (1991): The geology of the Port Alberni–Nanaimo Lakes area; BC Ministry of Energy Mines and Petroleum Resources, Geoscience Map 1991-1.
- Massey, N.W.D., McIntyre, D.E., Desjardins, P.J. and Cooney, R.T. (2005): Digital geology map of British Columbia; BC Ministry of Energy, Mines and Petroleum Resources, Open File 2005-2.
- Muller, J.E., Cameron, B.E.B and Northcote, K.E. (1981): Geology and mineral deposits of the Nootka Sound map-area, Vancouver Island, British Columbia; Geological Survey of Canada, Paper 80-16, 53 p.
- Prendergast, M.D. (2000): Layering and precious metals mineralization in the Rincón del Tigre Complex, eastern Bolivia; *Economic Geology*, v. 95, p. 113–130.
- Renne, P.R., Swisher, C.C., Deino, A.L., Karner, D.B., Owens, T.L. and De-Paolo, D.J. (1998): Intercalibration of standards, absolute ages and uncertainties in $^{40}\text{Ar}/^{39}\text{Ar}$ dating; *Chemical Geology*, v. 145, p. 117–152.
- Sargent, H. (1941): Supplementary report on Bedwell River area, Vancouver Island, British Columbia; British Columbia Department of Mines, Bulletin 13.
- Specogna, L. and Specogna, E. (2003): Fly One and Two; BC Ministry of Energy, Mines and Petroleum Resources, Assessment Report 27 214, 26 p.
- Taylor, H.P. and Noble, J.A. (1969): Origin of magnetite in the zoned ultramafic complexes of southeastern Alaska; *Economic Geology Monographs*, v. 4, p. 209–230.
- Yorath, C.J., Sutherland Brown, A. and Massey, N.W.D. (1999): LITHOPROBE, southern Vancouver Island, British Columbia; Geological Survey of Canada, Bulletin 498, 145 p.

Gold, Granites, and Geochronology: Timing of Formation of the Bralorne-Pioneer Gold Orebodies and the Bendor Batholith, Southwestern British Columbia (NTS 092J/15)

C.J.R. Hart, Centre for Exploration Targeting (M006), University of Western Australia, Crawley, WA, Australia; craig.hart@uwa.edu.au

R.J. Goldfarb, United States Geological Survey, Denver, CO

T.D. Ullrich, Pacific Centre for Isotopic and Geochemical Research, Department of Earth and Ocean Sciences, University of British Columbia, Vancouver, BC

R. Friedman, Pacific Centre for Isotopic and Geochemical Research, Department of Earth and Ocean Sciences, University of British Columbia, Vancouver, BC

Hart, C.J.R., Goldfarb, R.J., Ullrich, T.D. and Friedman, R. (2008): Gold, granites and geochronology: Timing of formation of the Bralorne-Pioneer gold orebodies and the Bendor batholith, southwestern British Columbia (NTS 092J/15); in Geoscience BC, Summary of Activities 2007, Geoscience BC, Report 2008-1, p. 47–54.

Introduction

The Bridge River mining district in southwestern British Columbia (Figure 1) is the largest historical lode gold producer in the Canadian Cordillera, with more than 128 tonnes (4.1 million ounces) of gold produced between 1897 and 1971 (Church, 1996). Most production came from the Bralorne-Pioneer vein system that yielded (Leitch, 1990) approximately 7 million tonnes of high grade ores averaging 19.1 g/t (0.58 oz/t). Although the district is dominated by Au veins, it also hosts a large number of Sb-dominant and Hg-dominant mineral occurrences, whose distributions form a general easterly zonation (Pearson, 1975; Woodsworth et al., 1977).

A number of geological models have been proposed to account for both the significant gold enrichments near Bralorne and for the regional metallogenic trends throughout the Bridge River district. Determining the most appropriate model is important as it can influence the types and effectiveness of exploration models and programs that are utilized, as well as influencing decisions about regional prospectivity, targeting and investment. Currently, the integrity of existing models for the Bridge River district suffers from a lack of good geochronological constraints.

The absolute timing of formation of gold orebodies at the Bralorne-Pioneer deposit, as well as for most deposits throughout the Bridge River district, is not precisely known. In addition, the timing of some of the numerous and

volumetrically significant plutonic events, such as those responsible for the Coast Plutonic Complex and the Bendor plutonic suite, which may or may not play a significant role in gold formation, is not precisely known. In order to establish temporal, and potentially genetic, associations with regional magmatic, structural, and metamorphic events, and to place constraints on the nature of the geological models responsible for the formation of gold mineralization at Bralorne-Pioneer deposit, new Ar-Ar age determinations on alteration and gangue mineral phases from the gold veins are presented in this paper. Because the Bendor batholith is the nearest, largest, and therefore the most significant magmatic and thermal feature adjacent to the Bralorne-Pioneer gold deposit, conventional U-Pb and SHRIMP U-Pb age determinations on zircons, as well as Ar-Ar determinations, are presented to assess the batholith's crystallization and cooling history. These data allow establishment of new constraints on the various interpretative models for the formation of the Bralorne-Pioneer gold veins.

Regional Geology

The Bridge River district is in the structurally complex region between the southeastern Coast Belt and the adjacent intermontane terranes. In this region, the Mississippian to Middle Jurassic accretionary complexes of oceanic basalt and gabbro and related ultramafic rocks, chert, basalt, shale and argillite of the Bridge River Terrane are juxtaposed with Late Triassic to Early Jurassic island arc volcanic rocks and mostly marine, arc-marginal clastic strata of the Cadwallader Terrane. These assemblages are variably overlain, mostly to the north, by clastic, mostly non-marine successions belonging to the Jurassic-Cretaceous Tyaughton Basin.

Keywords: *Orogenic gold, geochronology, gold deposits, gold deposit models*

This publication is also available, free of charge, as colour digital files in Adobe Acrobat® PDF format from the Geoscience BC website: <http://www.geosciencebc.com/s/DataReleases.asp>.

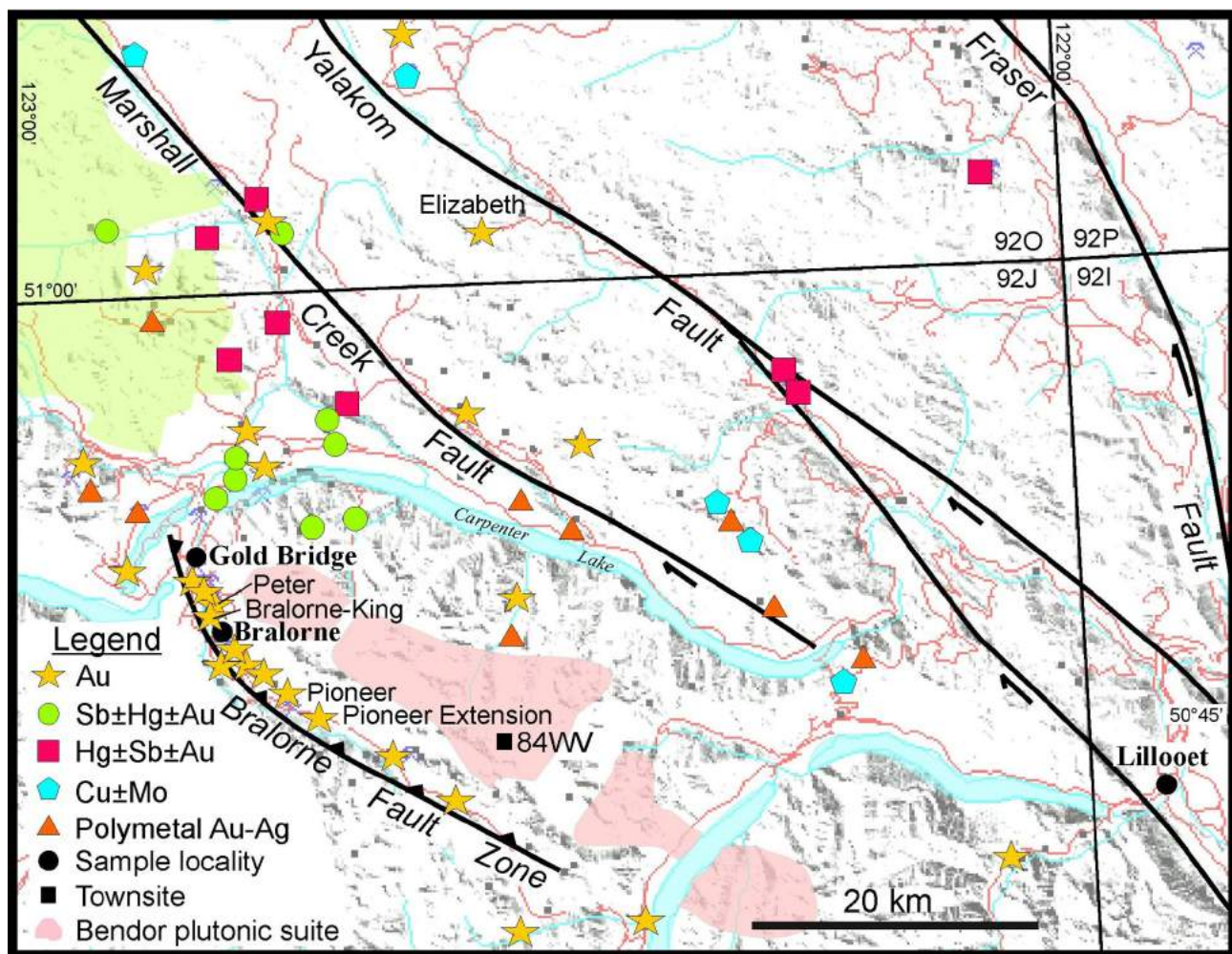


Figure 1. Regional geological setting of the Bridge River camp in southwestern British Columbia showing the major structural features and distribution of mineral deposits. Note the zonation from gold-only to stibnite-dominant, to mercury-dominant deposit types. 84WV is the location of the Bendor Batholith geochronology sample. Shaded area north of Gold Bridge is the Spruce Lake Protected Area.

The region has been intruded and overlain by a wide range of Cretaceous and Tertiary plutonic and volcanic rocks and their hypabyssal equivalents. Most significant among these are the dominantly Cretaceous granitoid bodies that form the Coast Plutonic Complex (CPC), which locally is characterized by the 92 Ma Dickson McClure intrusions (Parrish, 1992) and the large individual bodies of the Late Cretaceous Bendor plutonic suite. The general lack of foliation in all of these igneous rocks indicates their emplacement subsequent to the main regional compressional events along this part of the Cordilleran margin (Armstrong, 1988). Hypabyssal magmatism is reflected by emplacement of porphyritic dikes between 84 and 66 Ma, with the youngest magmatic event being crystallization of 44 Ma lamprophyre dikes (Leitch et al., 1991).

The Bendor plutonic suite consists of a northwest-trending series of plutons that form a belt, perhaps greater than 100 km long from Eldorado mountain in the north to the southeastern Coast Belt towards Hope. These rocks consist

mostly of high-standing, resistant, coarse-grained, hornblende>biotite>pyroxene, magnetite-titanite-bearing granodiorite to quartz diorite. Most pertinent to this study is the >20 km-long, northwest-trending Bendor batholith, the major igneous body nearest to the Bralorne-Pioneer deposit, from which previous age determinations range from 139 to 56 Ma (Church, 1996).

The district has been widely deformed by mid-Cretaceous contractional deformation within the westerly-trending Shulaps thrust belt, and by contractional and oblique-sinistral deformation associated with the Bralorne-Eldorado fault system. The Bridge River and Cadwallader terranes were juxtaposed along this fault system, which in the Bralorne area consists of linear, tectonized, and serpentinized slices of late Paleozoic mafic and ultramafic rocks known as the Bralorne-East Liza Lake thrust belt that forms a 1 to 3 km wide zone bounded by the Cadwallader and Fergusson faults (Scharizza et al., 1997). The timing of this deformation and metamorphism is ca. 130–92 Ma,

with synorogenic sedimentary flysch, as young as mid-Cretaceous, cut by the faults (Garver et al., 1989; Schiarizza et al., 1997). Much of the Bralorne-Pioneer vein system occurs along or within these structures and early Late Cretaceous sinistral movements on the Eldorado fault and the Castle Pass fault system are considered to be coeval with final regional contraction and deposition of most of the Bralorne ores (Schiarizza et al., 1997), and thus also much of the local CPC magmatism.

Younger, northwest-trending dextral displacements reactivated many of the older faults and were dominant in the east, particularly along the Marshall Creek and Yalakom faults, and are considered to have controlled mineralization that is located proximal to the faults in these areas (Schiarizza et al., 1997). Dextral deformation is best estimated as having been initiated at or slightly before 67 Ma (Schiarizza et al., 1997).

Deposit Geology

The Bralorne-Pioneer vein system is hosted in the variably altered mafic and ultramafic rocks that occur as fault-bounded lenses in a structurally complex zone between the Bridge River and Cadwallader terranes. The orebodies occur along an approximate 4.5 km strike length, mostly along, adjacent to, or between the Cadwallader and Ferguson faults. Mineralization was interpreted by Leitch (1990) as synkinematic and structurally controlled by secondary fault sets related to westerly-directed, sinistral transpressional movement along faults bounding the Bralorne ophiolite. Veins are preferentially hosted in the more competent, coarse- to medium-grained gabbroic, dioritic, and trondhjemitic phases; less commonly in metabasalt, and rarely in ultramafic rocks (Cairnes, 1937; Ash, 2001). Several unmined and newly discovered veins, which are the focus of recent exploration, are northeast of the main historically mined orebodies. The Peter vein was considered among the most prospective resource of these recently discovered (1987) veins (MINFILE 092JNE 164; MINFILE, 2007).

Veins form in en echelon arrays, with strike lengths of as much as 1 500 m, between bounding structures. Veins extend to at least 2 000 m in depth, with no significant changes in grade recorded. Ores consist mainly of ribboned fissure veins with septa defined by fine-grained chlorite, sericite, graphite or sulphide minerals. Massive white quartz tension veins also comprise some of the ore, although thinner connecting cross-veins are sub-economic. The fissure veins tend to be larger, thicker, and host the higher gold grades. Quartz is the dominant gangue mineral, with lesser calcite, ankerite and chlorite. The most conspicuous alteration mineral is bright green, chrome-bearing phyllosilicate, which occurs in basaltic and ultramafic host rocks. These bright green blebs occur as disseminated fine-

grained masses composed of fuchsite, mariposite or Crillite. All are referred to herein as fuchsite, irrespective of mineralogy. Notably, this fuchsitic alteration is locally pervasive in some rocks despite being far from the gold-quartz veins. It therefore occurs in response to regional alteration as well as hydrothermal vein formation.

Sulphide volume of the veins is low, consisting of a few percent of pyrite and arsenopyrite with lesser marcasite, pyrrhotite, chalcopyrite, galena, and sphalerite. Gold occurs as free gold, typically in late fractures or along ribbons. The Bralorne-Pioneer gold-bearing veins were deposited from low salinity fluids at 300 to 400°C and 1.25 to 1.75 kbar (Leitch, 1989). The vein style, structure, mineralogy, and alteration are all similar to those defined for orogenic gold deposits (i.e., Groves et al., 1998).

Metallogenic Models

Numerous geological models have been put forth to describe the origin of the metallogenic features observed in the Bridge River district. Most of the models attribute gold deposit formation to result from fault movement, obduction and emplacement of ophiolite rocks, CPC magmatism, or a combination of these events. Some models attempt to directly address the formation of the Bralorne-Pioneer gold ores, whereas others consider the district-wide metallogenic variations and zonation.

Magmatic

Several of the historic and some of the most recent models place a large genetic emphasis on the role of magmatic rocks. Past workers have variably considered the CPC, the Bendor batholith, albitite dikes, or the felsic porphyry bodies as the potential source of fluid, metal, and/or heat for the ores in the district.

Many of the early workers (e.g., Cairnes, 1937) developed models that stressed a direct association with the mafic and ultramafic rocks that now are recognized as forming much of the Bralorne ophiolitic assemblage, in particular the various gabbros, trondhjemitic, and plagiogranites. However, age determinations have conclusively indicated that these rocks are Permian (Leitch, 1989) and therefore quite a bit older than reasonable age estimates of the age of mineralization (see below).

A genetic association of gold with either the Gwyneth Lake stock or Bralorne batholith was proposed by Church (1996), which was suggested to indicate ca. 90 Ma events based upon the best fit the ages on dikes and intrusions presented by Leitch (1989). Church (1996) further considered that the stress caused by intrusion emplacement provided an extensive fracture system, in particular along the reactivated Cadwallader fault zone, with additional heat and the ore fluids provided from the more distal CPC.

Utilizing geochronology from crosscutting relationships in ore zones, Leitch et al. (1991) constrained the timing of mineralization as between 93 and 42 Ma. They emphasized, however, that an altered 86 Ma dike could represent a better minimum age constraint to provide a narrower potential age range of 93 to 86 Ma for formation of the Bralorne-Pioneer deposit, and possibly indicated a direct genetic link with the albitite dikes.

Ophiolite

An ophiolitic association with gold mineralization at the Bralorne-Pioneer deposit, as well as throughout much of the North American Cordillera, has been emphasized by Ash (2001). He suggested that gold formation at Bralorne occurred during regional, mid-Cretaceous tectonic imbrication and stacking of the Paleozoic oceanic lithosphere (e.g., Schiarizza et al., 1997). Ash (2001) also emphasized, however, the important role of “felsic dike rocks” that are coeval with early magmatic phases of the CPC.

Coast Plutonic Complex

Building on the regional metal trends recognized by Pearson (1975), Woodsworth et al. (1977) emphasized a relationship between metal precipitation and the emplacement and cooling of plutons of the CPC. Similarly, an easterly younging of K-Ar ages for mineral occurrences throughout the entire district led Leitch et al. (1991) to suggest the importance of the proximity and cooling of ca. 80 to 59 Ma igneous rocks that form the eastern margin of the CPC. Further dating modified the model, whereby pulses of heat from the CPC resulted in several generations of mineralization, which decrease in age and P-T conditions eastward from the CPC (Leitch et al., 1991).

Fault-Related

Schiarizza et al. (1997) suggested that the metal zonation pattern is the product of different fault systems being active at different times. Specifically, the gold deposits are associated with the Bralorne-Eldorado fault system, the stibnite mineralization is associated with the Castle Pass fault system, and the mercury mineralization is associated with the Marshall Creek and Yalakom-Relay Creek fault systems. Because each of these fault systems is considered to have been active at different times, the logical assumption is that three mineralizing events are necessary to account for the zonation. This conclusion, however, remains based upon limited geochronological data for the mineral deposits in the district.

Geochronology

Three significant orebodies for Ar-Ar geochronological analysis were sampled in this study in order to precisely determine the age of the Bralorne-Pioneer gold deposit. In each case, the relationship between the dated material and

gold ore was clearly evident, in that visible gold was observed in all samples. Appropriate material for isotopic age dating is notoriously difficult to find, which led Leitch et al. (1991) to depend on relationships between crosscutting magmatic phases to constrain the timing of mineralization.

Two analyses were performed at the U.S. Geological Survey's argon geochronology laboratory in Denver. Two argon analyses and the conventional U-Pb analysis were performed at the Pacific Centre for Isotope and Geochemical Research (PCIGR) at the University of British Columbia in Vancouver. Sensitive High-Resolution Ion MicroProbe (SHRIMP) U-Pb analyses were undertaken at the J.D. deLateur Centre at Curtin University in Perth, Australia. All errors are reported to 2σ

The first dated sample (1-BR) was a bright green fuchsite mica collected from the waste dump immediately below the Pioneer mill and is representative of most vein material found in the King vein system, which was a significant part of the Bralorne orebody. A mass of fuchsite mica, 1 cm in diameter, was totally contained within massive fine-grained quartz containing free gold. The initial two low-temperature steps yielded anomalous apparent ages and the subsequent steps 2 through 12 yielded older ages, resulting in a step-shaped spectrum from 65.5 to 69.8 Ma (Figure 2a). The initial $^{40}\text{Ar}/^{36}\text{Ar}$ ratio derived from the isochron was poorly constrained, but suggested the presence of excess argon. As a result, the isochron age of 67.7 ± 0.7 Ma is considered to best represent the timing of mineralization.

A second sample (2-PE) was obtained from the relatively recently discovered Peter vein, and consisted of both fuchsite alteration developed in strongly altered adjacent wallrock and fragments of wallrock that were entrained in the quartz vein. This sample is from a high grade ore zone that also contained pyrite and sphalerite. The analysis yielded a disturbed spectrum with anomalously young apparent ages in the initial low temperature steps: the remaining steps yielded ages between 69.2 and 65.4 Ma (Figure 2b). As with the sample from the King vein, the isochron indicated the presence of excess argon for steps 2–15 so the isochron age of 66.8 ± 0.5 Ma is preferred.

The third sample (P-EXT), collected from the Pioneer Extension adit dump, is of coarse-grained, shiny white muscovite from a small vug in a fine-grained, white quartz vein with carbonaceous and pyrite ribbons. An analysis on multiple muscovite grains yielded an excellent plateau at 64.0 ± 0.4 Ma comprising nine steps representing 98.5% of the ^{39}Ar (Figure 2c). Unlike the other two samples, there is no indication of excess argon, and the inverse isochron age of 64.2 ± 0.6 Ma is in agreement with the plateau age. Dating of a single muscovite grain also yielded a plateau age at 64.2 ± 0.4 Ma comprising eight steps representing 98.3% of

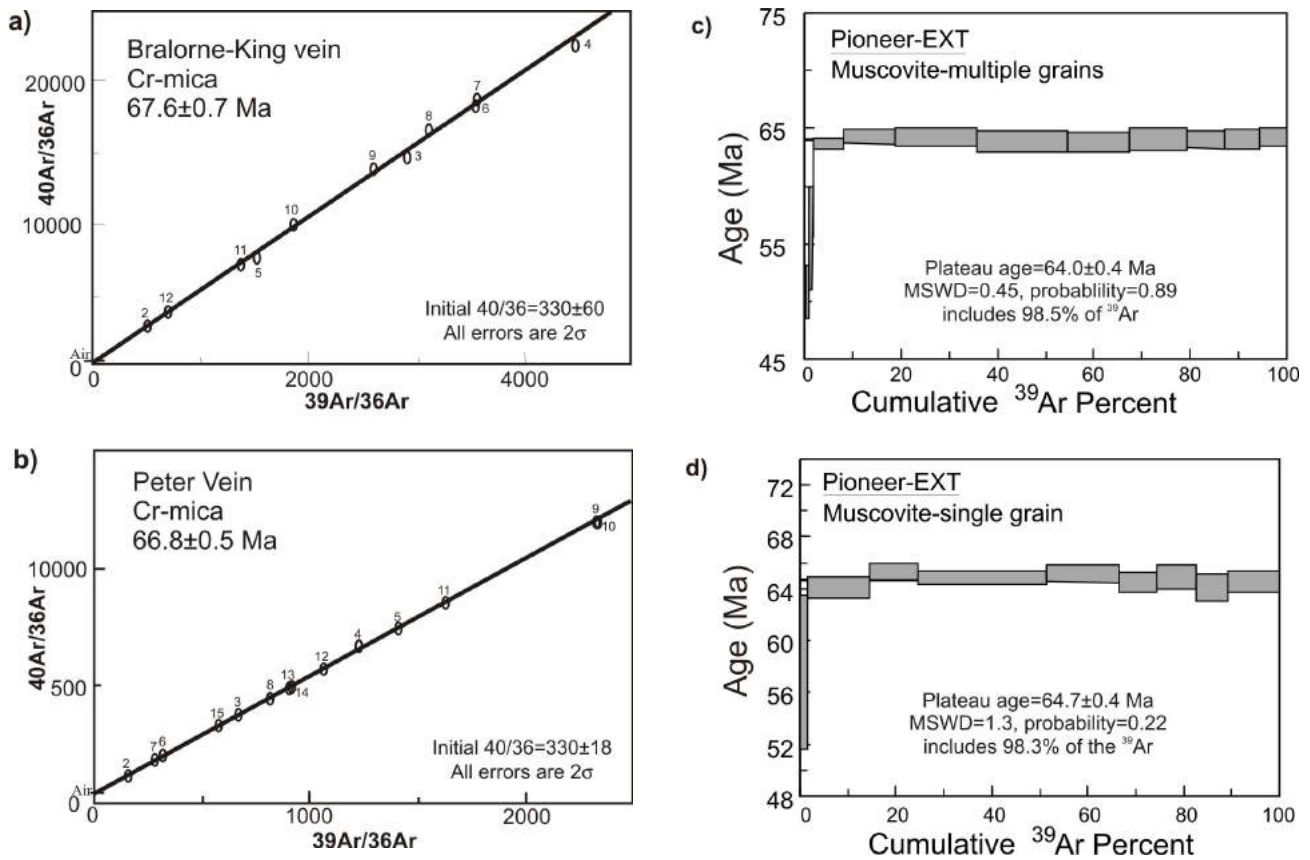


Figure 2. Ar-Ar gas release spectra and isochron plots from the **a)** King (Bralorne), **b)** Peter, **c)** and **d)** Pioneer-Extension veins. All analyses include J-error. MSWD = mean square of weighted deviates.

³⁹Ar released with a matching inverse isochron age of 64.9 ± 0.6 Ma.

The age determinations, despite being from three district Bralorne-Pioneer orebodies located more than 10 km apart, yield very similar results that, despite minor analytical complications, confirm that a latest Cretaceous gold deposition event at the Bralorne-Pioneer gold deposit occurred ca. 68–64 Ma.

To establish a precise age of the nearest major intrusive event to the gold ores, a new date for crystallization of the Bendor batholith was also obtained, using a sample (84WV) collected by G.J. Woodsworth of the Geological Survey of Canada in 1984 from approximately 10 km east of the Pioneer deposit.

Conventional U-Pb dating of zircon from the Bendor pluton indicates an age of ca. 65 Ma. Seven analyses include four from Friedman and Armstrong (1995) and three from this study (Figure 3a). The original four fractions are large (1.1–1.7 mg) and give relatively precise data that are difficult to interpret because they lie parallel to, and just off, concordia. The older two of these analyses were abraded and relatively coarse, suggesting that dispersion of the data

is due to minor Pb loss. In an attempt to confirm the previous data, three new fractions of 1 to 23 strongly abraded grains (20–35 μg) were analyzed. Although less precise, overlap with the original data and a similar style of dispersion confirm Pb loss and a Cretaceous-Tertiary boundary age. The best estimate for the age is based on the oldest fraction (G), with a ²⁰⁶Pb/²³⁸U date of 65.0 ± 0.2 Ma.

Eighteen different zircon grains from the sample used for the conventional TIMS U-Pb analysis were analyzed utilizing a SHRIMP. All determinations were on locations of well-zoned magmatic zircon that lacked inherited cores or radiation damaged regions. A weighted mean of 65.2 ± 0.8 Ma was generated from the eighteen ²⁰⁶Pb/²³⁸U determinations (Figure 3b). The integrity of the data is supported by a sound MSWD of 0.79 and the good correlation with the TIMS determination.

An Ar-Ar determination on well-formed, unaltered, coarse-grained biotite from the same sample yields an excellent plateau from 10 steps at 64.6 ± 0.6 Ma that represent 99% of the total gas (Figure 4). The initial ⁴⁰Ar/³⁶Ar ratio indicated by the isochron was within error of the accepted value and the inverse isochron age was in good agreement with the plateau age.

The geochronological data are summarized in Table 1.

Discussion

The new determinations of the age of mineralization for the Bralorne-Pioneer camp presented above differ significantly from previously reported estimates. Dating of cross-cutting dikes from the eighth level of the Bralorne mine by Leitch et al. (1991) broadly constrained the age of mineralization, with a date of 91.4 ± 1.4 Ma (U-Pb zircon) on a pre-ore, strongly-altered albitite dike, and a date of 43.5 ± 1.5 Ma (K-Ar biotite) on a post-ore lamprophyre. A K-Ar date of 85.7 ± 3 Ma on green hornblende, however, was interpreted by Leitch et al. (1991) as possibly late, intra- to post-ore, and thus perhaps more narrowly constraining the timing of mineralization between 93 and 83 Ma (within the limits of errors). Alternatively, the hornblende date may simply reflect argon loss from ca. 91 Ma, as the hornblende dikes are likely transitional and essentially coeval with the albitite (Leitch et al., 1991). Although the mid-Cretaceous range was favoured by these workers, the uncertainty did not preclude a Late Cretaceous or Tertiary age for gold mineralization.

An Ar-Ar determination on fuchsite from “quartz veined and carbonate altered” metabasalt from the Pioneer orebody dump (Ash, 2001) gave ambiguous results. A sin-

gle step representing 75% of the total gas gave a date of 87 Ma which, when mixed with higher temperature steps that yielded 60–50 Ma ages, returns a total gas age of 79 ± 4 Ma. This latter date was interpreted to represent a lower limit for the age for mineralization (Ash, 2001), although the recognition that the material was from a fine-grained, impure sample that likely endured recoil effects during radiation suggests that the determination cannot be meaningfully interpreted. Two samples of Cr-rich illite, collected from the Cosmopolitan and North veins in the Bralorne-Pioneer deposit, in an area of “sheared, clay-altered zones marginal to pervasively hydrothermally altered felsic dikes along the mineralized quartz-vein structure” (Ash, 2001), yielded a similar spectrum with their ages increasing from ~71 Ma up to 77 Ma. These dates were interpreted to indicate the age of faulting and post-ore hydrothermal alteration. In summary, Ash (2001) interprets the age of Bralorne gold mineralization to be ~86 Ma, presumably in accord with determinations of Leitch et al. (1991), and also interprets the Ar-Ar determinations to represent younger events.

Two age determinations were done in this study on zircons from the Bendor batholith, utilizing different methods. Both methods yielded ages with a high degree of precision, and the similarity of the results indicates a high degree of accuracy with crystallization at ca. 65 Ma. The only slightly younger Ar-Ar age of 64.4 Ma on biotite indicates that the batholith cooled rapidly through ~300° (biotite closure temperature, McDougall and Harrison, 1999).

The Ar-Ar dates of 68 to 64 Ma determined in this study are 20 to 30 Ma younger than previous absolute age estimates for gold mineralization at the Bralorne-Pioneer deposit. These data indicate that the Bralorne-Pioneer mineralizing event is significantly younger than juxtaposition of the Cadwallader and Bridge River terranes, and, most specifi-

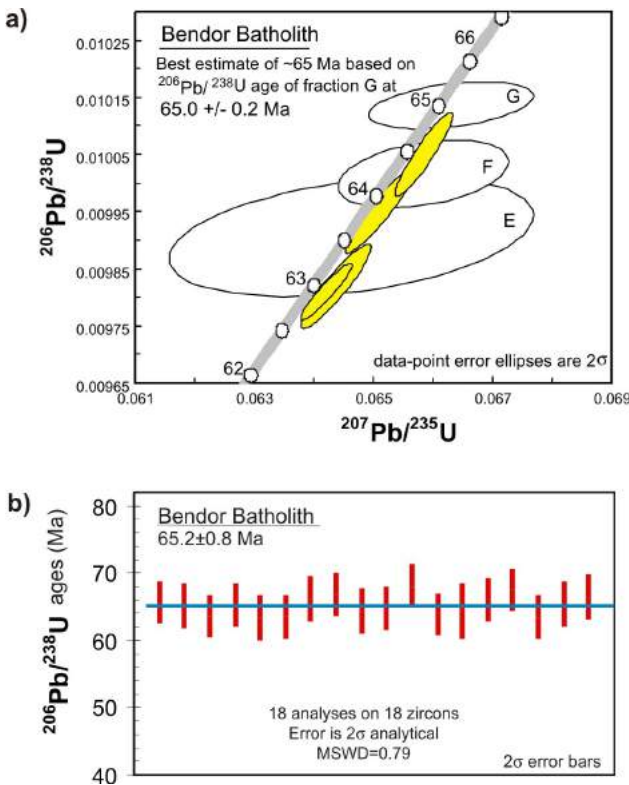


Figure 3. U-Pb plots for Bendor batholith zircon analysis: a) conventional TIMS, b) SHRIMP. MSWD = mean square of weighted deviates.

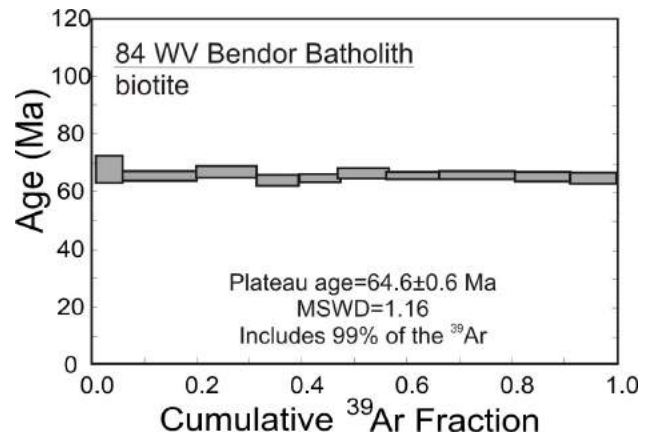


Figure 4. Ar-Ar gas release spectra for Bendor batholith biotite. Plateau steps are filled, rejected steps are open. Box heights are 2σ errors. Error includes J-error of 0.32%. MSWD = mean square of weighted deviates.

Table 1. Compilation of new geochronology for the Bralorne-Pioneer district.

Sample number and source	Sample location	Geochronological technique and sample material	Analyzing laboratory	Date obtained	Interpretation of age
1-BR, King vein (Bralorne)	50.778°N, 122.8208°W	Ar-Ar, fuchsite	United States Geological Survey	67.6 ±0.7 Ma	Age of mineralization
1-PE, Peter vein	50.8621°N, 122.8311°W	Ar-Ar, fuchsite	United States Geological Survey	66.8 ±0.5 Ma	Age of mineralization
P-EXT, Pioneer Extension, vein	50.7542°N, 122.7533°W	Ar-Ar, muscovite, multiple grains	University of British Columbia	64.0 ±0.4 Ma	Age of mineralization
P-EXT, Pioneer Extension, vein	50.7542°N, 122.7533°W	Ar-Ar, muscovite, single grain	University of British Columbia	64.7 ±0.4 Ma	Age of mineralization
84 WV, Bendor batholith	50.7422°N, 122.6166°W	U-Pb TIMS, zircon	University of British Columbia	65.0 ±0.2 Ma	Age of Bendor batholith
84 WV, Bendor batholith	50.7422°N, 122.6166°W	U-Pb SHRIMP, zircon	University of Western Australia	65.2 ±0.8 Ma	Age of Bendor batholith
84 WV, Bendor batholith	50.7422°N, 122.6166°W	Ar-Ar, biotite	University of British Columbia	64.9 ±0.6 Ma	Cooling of Bendor batholith

cally, significantly younger than thrusting and obduction of the ophiolitic rocks. In addition, mineralization is not synchronous with the major contractional and sinistral motion along the Eldorado Fault zone, nor is it coeval with emplacement of the plutons of the CPC.

The new geochronology does indicate temporal association of gold with other events in the district. First, mineralization is synchronous with the emplacement of the Bendor batholith, based upon the new, high-precision dating of the igneous body. Second, the gold event does overlap initiation of dextral strike-slip on the regional fault systems in this part of British Columbia. Finally, given existing K-Ar dates of 69 to 67 Ma for mineralized dikes at the Minto and Congress Sb-Au deposits (Harrop and Sinclair, 1986), and Ar-Ar dates of ca. 70 Ma for the gold-hosting Blue Creek porphyry at the Elizabeth Au deposit (Schiarrizza et al., 1977), the possibility now exists that all mineralization in the Bridge River district may reflect a single, latest Cretaceous hydrothermal event. More detailed absolute dating will be needed to confirm this possibility.

Several points indicate that the 68 to 64 Ma dates for mineralization presented here most likely represent the age of gold mineralization at the Bralorne-Pioneer deposit and are not recording any thermal effects from emplacement of the Bendor batholith. First, the analyses for the three new ore-related samples are the best presented to date, and the materials are also the best quality analyzed to date. In particular, the coarse-grained crystalline muscovite from the Pioneer Extension will retain radiogenic argon to temperatures higher than 350°C, and rocks of the batholith may have been cooler than the biotite closure temperature 300°C (McDougall and Harrison, 1999) when the muscovite formed. Second, none of the argon spectra determined in this study are continuously stepped from an older date to a younger, thus reset, date, which would indicate partial resetting by an overprinting thermal event. Lastly, and most

importantly, other Ar-Ar and K-Ar determinations in the district give dates that are older than 70 Ma, and thus were not reset by intrusion of the Bendor batholith.

In conclusion, the main gold-forming event in the Bridge River district took place at ca. 68 to 64 Ma at the Bralorne-Pioneer deposit, and other mineralization in the district may also have formed during this same event. The onset of dextral strike-slip in this part of the Cordillera facilitated widespread fluid flow along the reactivated fault systems, as is supported by the abundance of Au, Sb and Hg deposits and occurrences along the various main structures in the district. Geochronological constraints suggest the Bendor batholith was unlikely to have been the source of these ore-forming fluids. The spatial association of the most significant known ore system with a shear zone near the batholith margin, however, suggests that a structurally favourable dilational zone existed adjacent to the recently emplacement igneous body during the onset of latest Cretaceous hydrothermal activity.

Acknowledgments

Funding from this project comes from Geoscience BC, with support from the University of Western Australia and the United States Geological Survey. Conversations with N. Church and P. Schiarizza of the BC Geological Survey about rocks and mineralization in the Bridge River district are appreciated. Information and advice from A. Pettipas of Bralorne Gold Mines Ltd., and T. Illidge of Gold Bridge, BC, are also appreciated. Members of the staff at the Gold Bridge Hotel are thanked for their hospitality.

References

- Armstrong, R.L. (1988): Mesozoic and Early Cenozoic magmatic evolution of the Canadian Cordillera; *in* Processes in continental lithospheric deformation, S.P. Clark, B.C. Burchfield and J. Suppe, J. (ed), Geological Society of America, Special Paper 218, p. 55–91.

- Ash, C.H. (2001): Ophiolite-related gold quartz veins in the North American Cordillera; BC Ministry of Energy, Mines and Petroleum Resources, Bulletin 108, 140 p.
- Cairnes, C.E. (1937): Geology and mineral deposits of Bridge River mining camp, BC; Geological Survey of Canada, Memoir 213, 140 p.
- Church, B.N. (1996): Geology and mineral deposits of the Bridge River mining camp; BC Ministry of Energy, Mines and Petroleum Resources, Paper 1995-3, 160 p.
- Friedman, R.M. and Armstrong, R. L. (1995): Jurassic and Cretaceous U-Pb Geochronometry of the southern Coast Belt, British Columbia, 49°-51°N; *in* Jurassic Magmatism and Tectonics of the North American Cordillera; D.M. Miller and C. Busby (ed), Geological Society of America, Special Paper 299, p. 95–139.
- Garver J.I., Schiarizza, P. and Gaba, R.G. (1989): Stratigraphy and structure of the Eldorado Mountain area, Chilcotin ranges, southwestern British Columbia (92O/2;92J/15); Geological Fieldwork 1988, BC Ministry of Energy, Mines and Petroleum Resources, Paper 1989-1, p. 131-143.
- Groves, D.I., Goldfarb, R.J., Gebre-Mariam, M., Hagemann, S.G. and Robert, F. (1998): Orogenic gold deposits: a proposed classification in the context of their crustal distribution and relationship to other gold deposit types; *Ore Geology Reviews*, v. 13, p. 7–27.
- Harrop, J.C. and Sinclair, A.J. (1986): A re-evaluation of production data Bridge River–Bralorne Camp (92J); Geological Fieldwork, 1985, BC Ministry of Energy, Mines and Petroleum Resources, Paper 1986-1, p. 303–310.
- Leitch, C.H.B. (1989): Geology, wallrock alteration and characteristics of the ore fluid at the Bralorne mesothermal gold vein deposit, southwestern British Columbia; Ph.D. thesis, University of British Columbia, Vancouver, 483 p.
- Leitch, C.H.B. (1990): Bralorne: a mesothermal, shield-type vein gold deposit of Cretaceous age in southwestern British Columbia; Canadian Institute of Mining, Metallurgy, and Petroleum, Bulletin, v. 83, no. 941, p. 53–80.
- Leitch, C.H.B., van der Heyden, P., Godwin, C.I., Armstrong, R.L. and Harakal, J.E. (1991): Geochronometry of the Bridge River mining camp, southwestern British Columbia; Canadian Journal of Earth Sciences, v. 28, no. 2, p. 195–208.
- McDougall, I. and Harrison, T.M. (1999): Geochronology and Thermochronology by the $^{40}\text{Ar}/^{39}\text{Ar}$ Method, 2nd Edition, Oxford University Press (USA), 288 p.
- MINFILE (2007): MINFILE BC mineral deposits database; BC Ministry of Energy, Mines and Petroleum Resources, URL <<http://www.em.gov.bc.ca/Mining/Geolsurv/Minfile/>>.
- Parrish R.R. (1992): U-Pb ages for Cretaceous plutons in the eastern Coast Belt, southern British Columbia; *in* Radiogenic age and Isotopic Studies; Report 5; Geological Survey of Canada, Paper 91-02, p. 109–113.
- Pearson, D.E. (1975): Bridge River map-area (92J/15); Geological Fieldwork, 1974; BC Ministry of Energy, Mines and Petroleum Resources, Paper 1975-2, p. 35–39.
- Schiarizza, P., Gaba, R.G., Glover, J.K., Garver, J.I. and Umhoefer, P.J. (1997): Geology and mineral occurrences of the Taseko–Bridge River area; BC Ministry of Energy, Mines and Petroleum Resources, Bulletin 100, 291 p.
- Woodsworth, G.J., Pearson D.E. and Sinclair, A.J. (1977): Metal distribution patterns across the eastern flank of the Coast Plutonic Complex, south-central British Columbia; *Economic Geology*, v. 72, no. 2, p. 170–183.

Mineralization and Alteration Associated with an Hypothesized Copper (Molybdenum) Porphyry System in the Taseko Lakes Area, Southwestern British Columbia (NTS 092O/04)

L. Hollis, Department of Earth and Ocean Sciences, University of British Columbia, Vancouver, BC, lhollis@eos.ubc.ca

K. Hickey, Department of Earth and Ocean Sciences, University of British Columbia, Vancouver, BC

L.A. Kennedy, Department of Earth and Ocean Sciences, University of British Columbia, Vancouver, BC

Hollis, L., Hickey, K. and Kennedy, L.A. (2008): Mineralization and alteration associated with an hypothesized copper (molybdenum) porphyry system in the Taseko Lakes area, southwestern British Columbia (NTS 092O/04); in Geoscience BC Summary of Activities, Geoscience BC, Report 2008-1, p. 55–66.

Introduction

Porphyry copper deposits are one of the world's primary sources of Cu, Mo and, to a lesser degree, Au (Lowell and Guilbert, 1970; Sillitoe, 1979). They are typified by large regions of hydrothermally altered rock that extend outward from a causative intrusion (Lowell and Guilbert, 1970; Dilles et al., 2000; Seedorf et al., 2005; Cannell et al., 2005). Alteration zone patterns are commonly complex owing to multiple pulses of hydrothermal flow that result in multiple, overprinting, alteration events and/or complex fluid flow paths. Being able to recognize the distal hydrothermal footprint of a porphyry system and understand its spatial and temporal relationships to the mineralized core is fundamental to understanding the development of, and exploring for, such systems.

The Taseko Lakes area of British Columbia is located near the eastern limit of the Coast Plutonic Complex, and it is along this boundary that many important subalkaline Cu-(Mo-Au) porphyry deposits are located. Examples of porphyry deposits include the Prosperity deposit, formerly known as Fish Lake, and the Taseko Empress and Chita showings (Figure 1). This study focuses on a porphyritic intrusion, informally named the Hub, exposed along the Tchaikazan River near Fishem Lake (Figure 2). The mountains immediately north of this exposure are characterized by large expanses of largely propylitically altered Cretaceous andesitic and marine sedimentary rocks. Small copper mineral showings are known within this expanse of altered rock. Three of these showings — the Hub, Charlie and Northwest Copper — have been examined as part of this study. The Charlie and Northwest Copper showings were

named by International Jaguar Equities Inc. (MINFILE 092O 043; MINFILE, 2007).

The main objectives of this study, which has been undertaken as an M.Sc. project by the senior author, are to develop a framework for the evolution and development of the showings and assess their relationships to conceptual models of porphyry mineralization within a magmatic-hydrothermal system. To attain these objectives, detailed maps of geology, alteration and mineralization of selected areas will be produced. Petrographic analysis is key in order to recognize subtle variations in mineral assemblages and textures. Fluid inclusions will be used to determine the physical conditions of mineralization. Geochronology will be used as a tool to determine the age of mineralization by isotopic dating of intrusions, country rocks and alteration assemblages. The current paper is a summary of the second season of field work.

Integration of detailed geological and alteration mapping, geochronological and geochemical information is essential to fully understand the magmatic-hydrothermal system within the Taseko Lakes region.

Regional Geological Setting

The Taseko Lakes area of British Columbia is located near the eastern limit of the Coast Plutonic Complex, and it is along this boundary that many important subalkaline Cu-(Mo-Au) porphyry deposits are located, including the Prosperity and Taseko Empress deposits and the Chita showing.

The study area straddles the boundary between the southwest and southeast Coast Belt. The southwest Coast Belt consists of Middle Jurassic to mid-Cretaceous plutonic rocks and Early Cretaceous volcanic rocks (McLaren, 1990). The southeast Coast Belt includes rocks of the Bridge River accretionary complex, the Cadwallader arc terrane and overlying clastic rocks of the Tyaughton-

Keywords: Porphyry Cu-Mo, Taseko Lakes, andesite, veins

This publication is also available, free of charge, as colour digital files in Adobe Acrobat® PDF format from the Geoscience BC website: <http://www.geosciencebc.com/s/DataReleases.asp>.

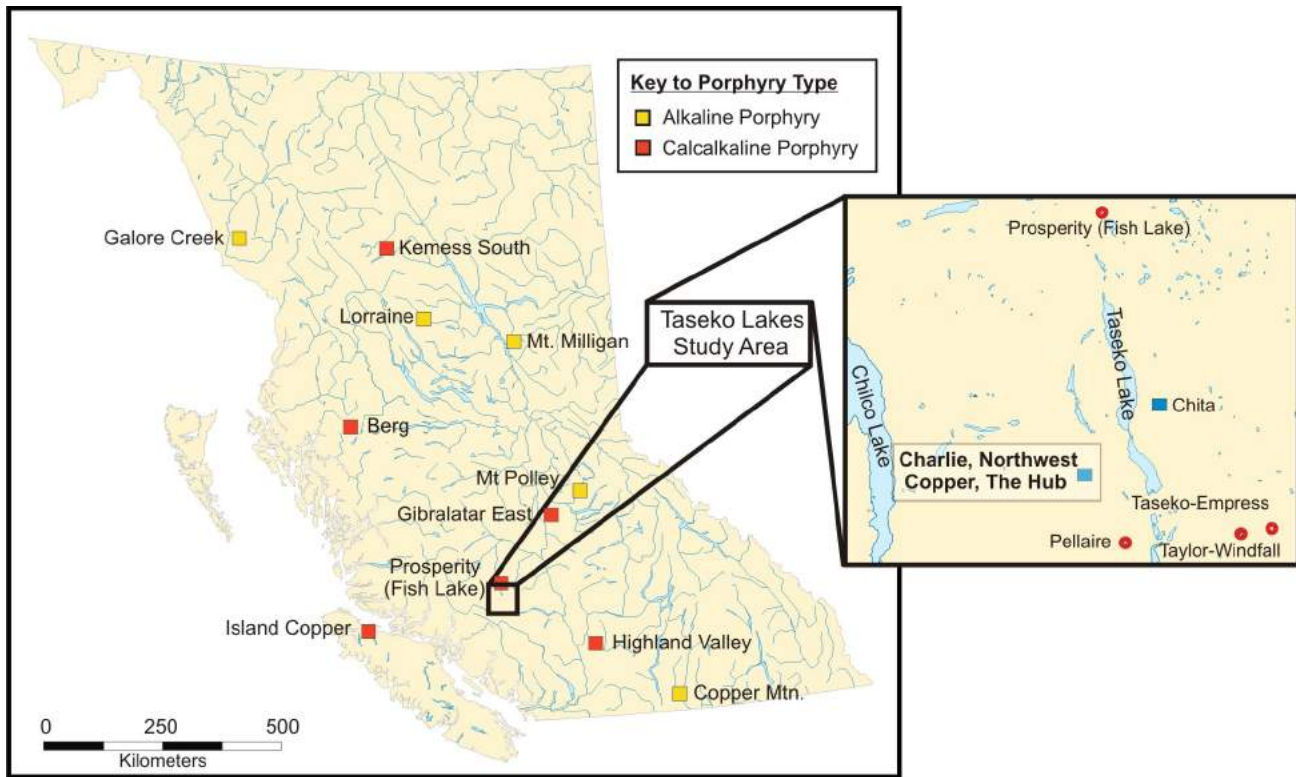


Figure 1. Locations of major alkaline and calkalkaline porphyry copper deposits in British Columbia. The inset map shows the location of major deposits within the Taseko Lakes study area.

Methow Basin (Schiarizza et al., 1997; Monger and Journeay, 1994).

The field area was mapped by Tipper (1969) at a scale of 1:1 000 000 as part of a regional mapping project. More recently, McLaren (1990) and Israel (2001) have mapped parts of the area. A short study of alteration assemblages in the vicinity of the Northwest Copper showing was done as part of an undergraduate honours thesis at the University of British Columbia (Bruce, 2000). The study area is located approximately 10 km south of the well-defined Prosperity Cu-Mo porphyry deposit and 50 km south of Williams Lake (Figure 1). Several past-producing deposits, including the Pellaire (Au) and Taseko Empress (Cu-Au) mines, are located within the district, in a zone that has been explored for potential economic targets for over a century.

Geological Setting of the Study Area

Introduction

The study area is underlain by several rock units of Cretaceous age. These include volcanic and volcano-sedimentary rocks of the Early Cretaceous Tchaikazan River succession and Late Cretaceous Powell Creek Formation (McLaren, 1990; Israel, 2001). The three mineral showings that are the focus of this study are hosted by these Cretaceous rocks. In this report, the Charlie and Northwest Cop-

per mineral prospects are described together, separately from the description of the Hub showing. This separation is based upon differences in rock types, mineralization and alteration observed at the three showings. Hub is the informal name given to a series of geological trenches that parallel the Tchaikazan River (Figure 2). Rocks present in these trenches are an altered porphyritic granodiorite, a diorite, a magnetite±biotite-cemented igneous breccia, and a late-stage, altered quartz-feldspar (QF) porphyry dike that cuts the granodiorite and the breccia. Copper-molybdenum mineralization at the Hub showing is disseminated within all three of these rock types. The Charlie and Northwest Copper prospects are located approximately 300 m topographically above the Hub showing. Copper-molybdenum mineralization at these showings occurs in veins that are typically within the volcanic facies of both the Tchaikazan River succession and the Powell Creek Formation.

Hostrocks

Powell Creek Formation

The Powell Creek Formation was previously described by Hollis et al. (2007). Simply, it is an extensive package of interbedded, nonmarine volcanic and volcanoclastic rocks of Late Cretaceous age (Schiarizza et al., 1997). Hostrocks to the Northwest Copper prospect are massive, maroon andesite flows; volcanic breccias; and resedimented volcanic

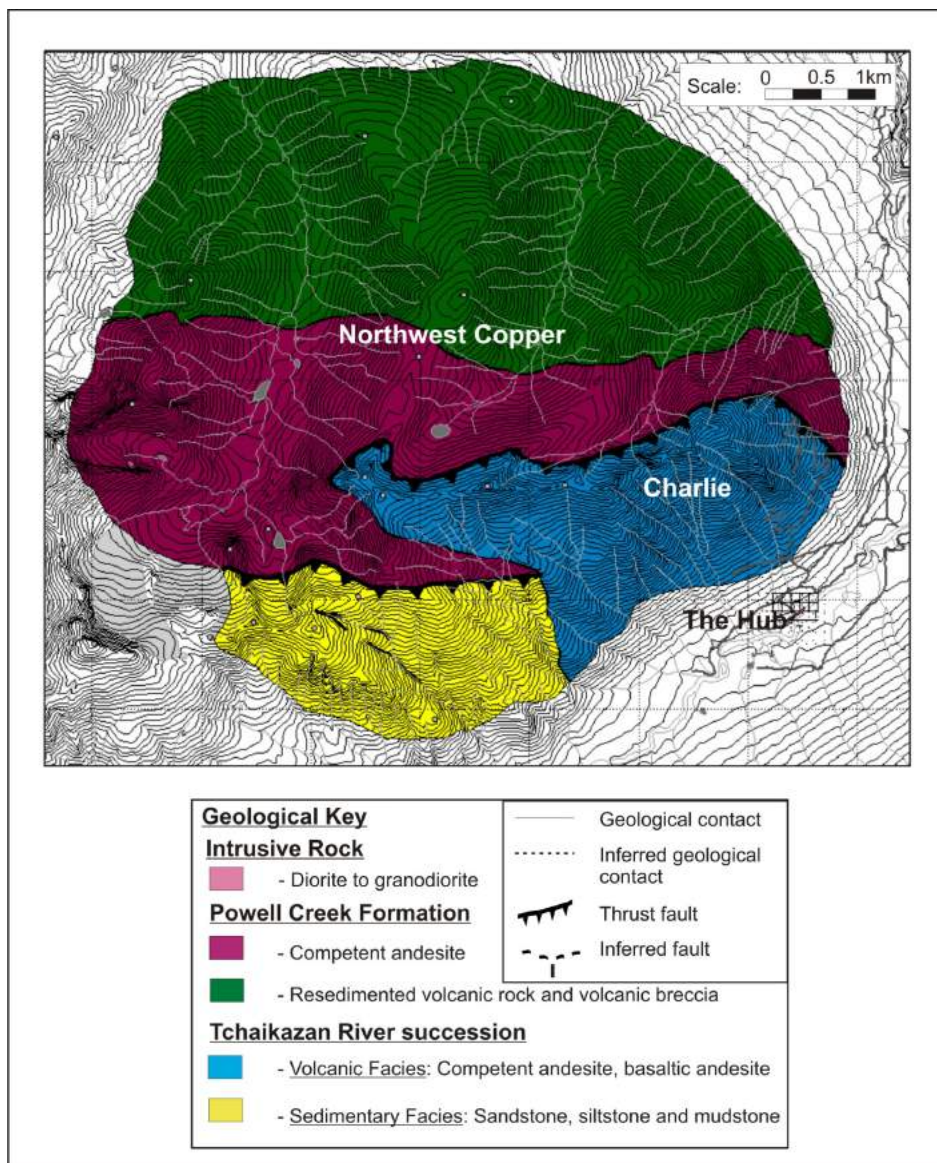


Figure 2. Geology of the Taseko Lakes study area.

flow units. The massive facies consists of large packages of volcanic rocks characterized by porphyritic or aphyric textures. Andesite is the dominant rock type in the massive facies. Plagioclase and hornblende are the dominant phenocryst components in the andesite and are typically altered to chlorite. The age of the Powell Creek Formation is interpreted to be Cenomanian (Schiarizza et al., 1997). Intrusive rocks are present throughout Northwest Copper prospect; these are typically feldspar-hornblende porphyry dikes and diorite intrusions. The age of the intrusive rocks is as yet unknown but they may be as young as Eocene. The base of the Powell Creek Formation is intruded by the 92 Ma Dickson-McClure batholith and Schiarizza et al. (1997) noted that the formation overlies Albian-Cenomanian rocks. The base of the Powell River Forma-

tion must therefore be Turonian (93.5 ± 0.8 to 89.3 ± 1 Ma) in age.

Volcanic Facies of the Tchaikazan River Succession

The volcanic facies of the Tchaikazan River succession is dominated by the intercalation of subaqueous to subaerial volcanic rocks, typically andesite in composition (Israel, 2001), with minor, shallow marine, clastic sedimentary rocks. The volcanic facies stratigraphically overlies the sedimentary rocks of the Tchaikazan River succession. Massive andesite flows, some greater than 50 m thick, dominate the upper part of the volcanic facies (Figure 3a). Peperitic contacts (Figure 3e) with the sedimentary rocks are also present at higher elevations, particularly near the Charlie showing. Since peperite textures form as a result of

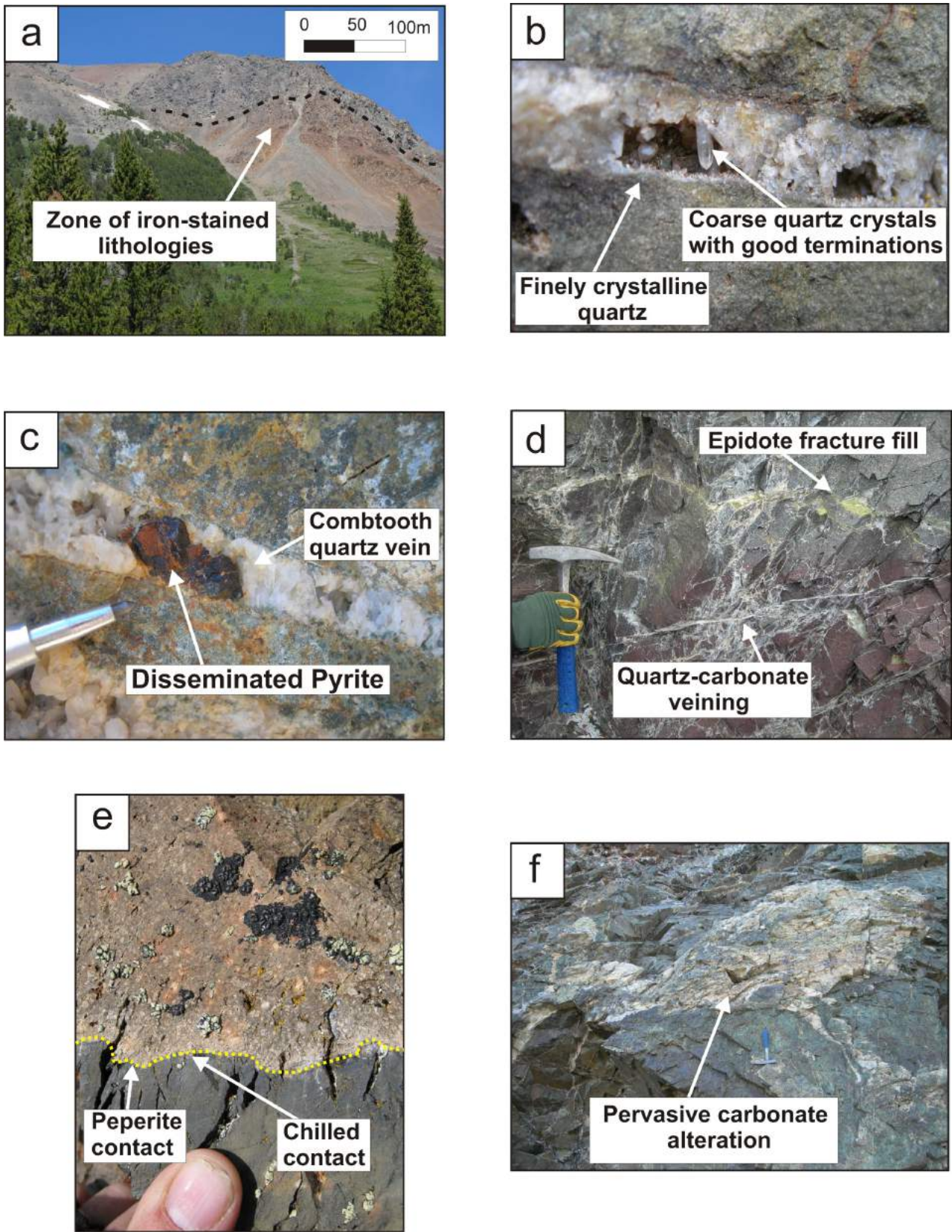


Figure 3. Photographs of the Charlie showing: **a**) view of the Charlie showing, taken from the Hub showing; the rusty red outcrops are phyllic altered rocks, contrasting with the propylitic altered andesite; **b**) comb tooth quartz vein in andesite hostrock; **c**) comb tooth quartz vein with centre fill of coarse, disseminated chalcopyrite centre fill; **d**) epidote and quartz-carbonate stock work veining; **e**) peperite contact between sediments and an andesite; and **f**) area of pervasive carbonate alteration in propylitic altered andesite of the Tchaikazan River Succession.

the intrusion and subsequent mingling of magma with unconsolidated or poorly consolidated, typically wet, sediments (White et al., 2000), their occurrence in the study area indicates the close relationship between subaqueous and volcanic environments in the Early Cretaceous rocks.

Sedimentary Facies of the Tchaikazan River Succession

The sedimentary facies of the Tchaikazan River succession is highly variable in grain size, bed thickness, sedimentary structure and rock type. Common rock types include medium- to coarse-grained, well-sorted sandstone, conglomerate, siltstone and mudstone. Soft sediment deformation is common, particularly in interbedded sequences of mudstone and medium- to coarse-grained sandstone. Bedding is often planar and sometimes undulating, but contacts are generally sharp. Black mudstone dominates and is often found in association with lenses of fine sandstone. Rocks of the sedimentary facies are often intercalated with minor volcanic rocks of the Tchaikazan River succession, especially toward the inferred upper parts of the sedimentary facies.

Many parts of this sedimentary sequence have been interpreted in this study as parts of a Bouma Sequence. In theory, a Bouma Sequence comprises clastic sediments deposited in response to a waning turbidite flow. A complete Bouma Sequence, from base to top, consists of laminated siltstone and fine pelagic mudstone, crosslaminated sandstone with ripple mark, parallel-laminated sandstone, massive sandstone and a highly erosive base with tool mark (Shanmugam, 1997). The sedimentary facies of the Tchaikazan Succession consists of coarse, chaotic clastic sedimentary rocks, often overlain by successively finer grained, well-bedded sandstone and mudstone. The B, C and E facies of a Bouma Sequence were frequently observed in the sedimentary facies of the Tchaikazan River succession. The B facies was the most common, forming well-bedded, parallel-laminated sandstone. Fossil material was observed within the sedimentary rocks, typically consisting of crinoids, bivalves and brachiopods, together with abundant trace fossils. Bioturbation occurs in finer grained units.

Areally extensive packages of sediment-dominated facies and a volcanic-dominated facies of the Tchaikazan River succession dominate the Charlie and Northwest Copper showings, forming the hostrocks to porphyry-style mineralization and alteration. Fossil evidence from these units suggests an age as old as 140 Ma (Berrasian), whereas U-Pb dates from abraded zircon fractions from a crosscutting intrusion (McLaren, 1990; Israel et al., 2006) suggest an age older than 102 ± 2 Ma, which is consistent with fossil evidence.

Showings Studied

Hub Showing

The Hub mineral showing is a prospect that is exposed in geological trenches along the Tchaikazan River. Several igneous rock types, including a porphyritic granodiorite (Figure 4), a diorite, and a quartz-feldspar porphyry dike (QF porphyry) account for greater than 90 % of all exposure.

Intrusive Rocks

The intrusive rocks exposed at the Hub showing are granodiorite to diorite in composition. Several intrusive phases have been recognized:

- 1) The main phase is coarsely crystalline granodiorite with a strong porphyritic texture. The granodiorite is composed of zoned plagioclase (~50%), quartz (~20%), biotite (10–25%) and hornblende (5%) phenocrysts in an aphanitic, plagioclase-quartz-dominated groundmass (Figure 4a).
- 2) A diorite intrusion appears to crosscut the main phase granodiorite. The diorite is identifiable by changes in mineralogy that are in contrast to the granodiorite. The rock is darker than the granodiorite and appears to contain a greater percentage of biotite and hornblende.
- 3) Quartz-feldspar (QF) porphyry differs from other intrusive rocks in that it is clearly a linear intrusion, likely a dike, that trends approximately northwest and is approximately 3 m thick. The dike is highly altered. It has a strongly porphyritic texture with plagioclase (~35%) and hornblende phenocrysts (15–20%), with chlorite replacing primary hornblende. The groundmass is aphanitic and appears to be largely dominated by altered feldspar. The QF porphyry is younger than the other intrusive phases as it cuts across them and displays chilled margins.

The Hub granodiorite has a cooling age (Ar-Ar, biotite) of 80.53 ± 0.42 Ma. The diorite yielded a cooling age (Ar-Ar, biotite) of 79.56 ± 0.42 Ma (T. Ullrich, pers. comm., 2006). The late QF porphyry dike is unmineralized and crosscuts both these igneous phases, and is therefore younger and post-mineralization. A whole rock age of 77.2 ± 2.8 Ma (T. Ullrich, pers. comm., 2006) was obtained for the Prosperity deposit by J.E. Harakal at the University of British Columbia. This is considered to be the age of mineralization at the Prosperity deposit and is similar to that inferred for mineralization at the Hub showing.

Hydrothermal Alteration

The granodiorite at the Hub showing is moderately to strongly altered. Primary plagioclase is typically silicified and may be replaced by secondary sericite (Figure 4b) and quartz-magnetite±K-feldspar alteration is extensive. This

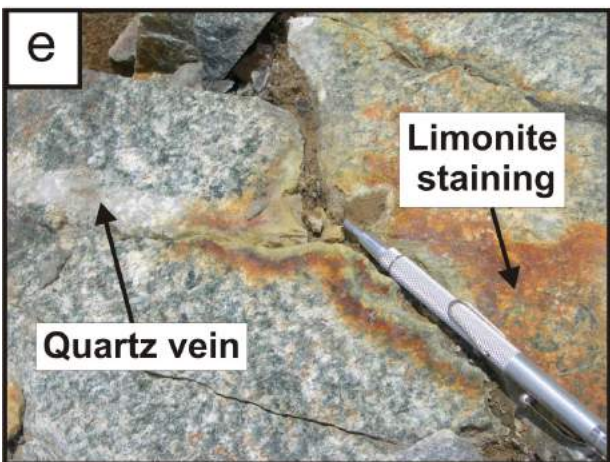
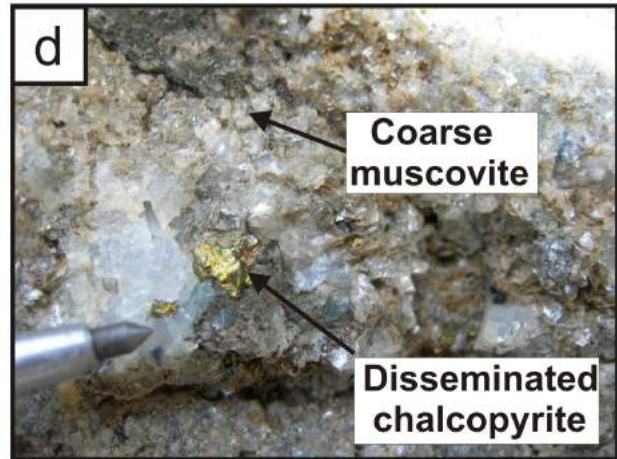
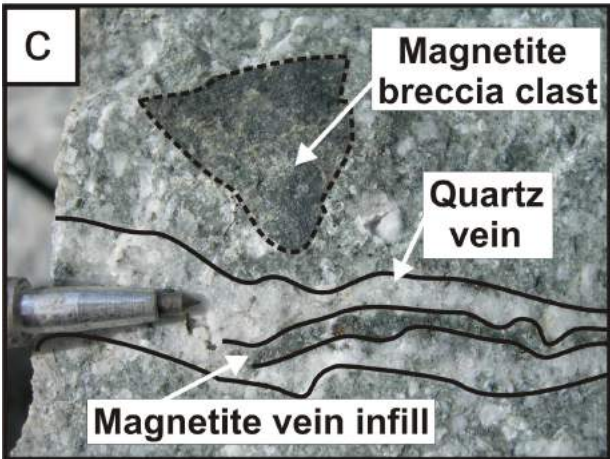
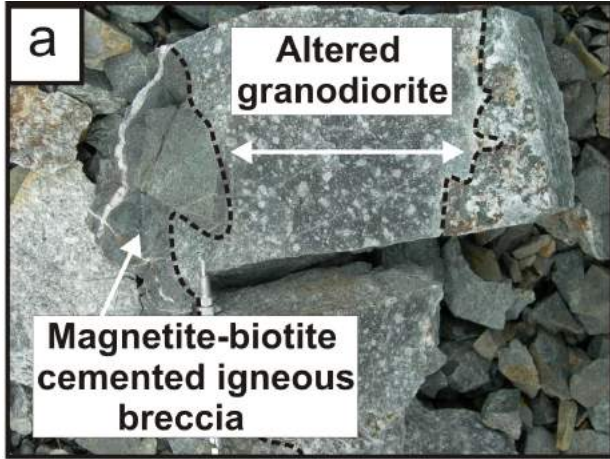


Figure 4. Photographs from the Hub showing: **a)** altered magnetite-biotite granodiorite in contact with magnetite-biotite–cemented igneous breccia; **b)** silicified reaction front with highly altered granodiorite and magnetite-biotite–cemented breccia; **c)** angular magnetite-altered clast in partially altered granodiorite; **d)** coarse disseminated chalcopyrite in centre of quartz-magnetite vein; and **e)** crosscutting quartz veins with secondary Fe-staining, probably a result of supergene weathering of pyrite.

alteration grades into hydrothermal biotite, K-feldspar, and magnetite alteration (Figure 4c) which extensively developed in the granodiorite, diorite and breccia with clasts showing pervasive quartz-biotite. K-feldspar crystals in this zone exhibit regular concentric zoning. Subeconomic quartz-pyrite±chalcopyrite±molybdenite veins with chlorite selvages are present in this altered zone (Figure 4d, e). Magnetite flooding appears to have affected the granodiorite along most of the trench exposures. The magnetite appears to be paragenetically associated with the K-feldspar, quartz, pyrite, chalcopyrite and molybdenite. The granodiorite shows moderate to weak potassic alteration containing the growth of secondary K-feldspar and biotite in the groundmass (Figure 3a).

The altered QF porphyry cuts the granodiorite, diorite, and magnetite±biotite-cemented breccia. The granodiorite, diorite and breccia are associated with porphyry style, stock work quartz veining, potassic alteration, silicification and disseminated Cu-Au mineralization.

Hydrothermal Breccia

A magnetite±biotite-cemented breccia is volumetrically the most abundant alteration facies. It is, however, poorly exposed and its geological architecture and extent are therefore ambiguous. The breccia is poorly sorted, containing up to 30% clasts (whose composition appears to be mostly intensely magnetite-flooded granodiorite) and is matrix-supported. Clasts are generally angular to subangular (Figure 4c) and appear to be highly altered (magnetite-biotite) granodiorite. The hydrothermal cement consists of fine-grained magnetite, biotite, quartz and sulphides. The magnetite±biotite-cemented breccia is characterized by a sometimes intensely brecciated or clastic texture. Parts of the granodiorite appear to be variously altered with infilling of biotite±magnetite in the groundmass. The original igneous texture of the granodiorite is still visible, although in places it has been obscured by pervasive and texturally-destructive biotite-magnetite-quartz alteration. The hydrothermal breccia cuts across the granodiorite and diorite.

Magnetite is abundant in both clasts and cement. The cement contains up to 40% crystalline quartz. In these zones, strong silicification and secondary magnetite are observed in the cement at what appear to be intrusive contacts with the granodiorite (Figure 4b).

Charlie and Northwest Copper Showings

Hostrocks to mineralization and alteration in the area of the Charlie and Northwest Copper showings are typically massive andesite, forming either part of the volcanic facies of the Tchaikazan River succession or the massive andesite of the Powell Creek Formation. These rocks overlie the granodiorite and other intrusive rock types observed at the Hub showing. Resedimented volcanic rocks, which form a

large part of the Powell Creek Formation, have also been hydrothermally altered and host sulphide-bearing veins. Rocks of the sedimentary facies of the Tchaikazan River succession are characterized by packages of well-bedded, often fining upwards, clastic sedimentary rocks.

Intrusive Rocks

An intrusion, named here the Northwest Copper intrusion, crops out on the western fringe of the Northwest Copper showing (Figure 5a, b). It is granitic in composition, containing approximately 40% quartz, 30% plagioclase and 30% other minerals, including biotite and hornblende. The intrusion is complex with several compositional variations. The granite intrudes rocks of the Powell Creek Formation and therefore must be younger. The granite contains numerous round xenoliths of the Powell Creek Formation (Figure 5d).

Diorite dikes emanate from the main intrusion and intrude into the overlying rocks of the Powell Creek Formation (Figure 5c, e). These dikes appear to be unaltered and are composed of 25–30% plagioclase feldspar, 10–15% hornblende, and minor biotite, quartz and pyroxene (Figure 5c).

Aplite dikes are abundant and crosscut the granite and the diorite. These dikes are very fine grained and white, with quartz and feldspar being the major minerals. They are likely to have some affinity to the main intrusive body and to be the last part of the magma to crystallize.

A syenite first identified in the 2006 field season (S.K. Blevings, pers. comm., 2006) was also found in the vicinity of the Northwest Copper showings. It is a pink to grey, coarsely crystalline, and K-feldspar-rich with accessory phenocrystic hornblende. It is only exposed in a limited area at the surface (Figure 2) on the central ridge of the Northwest Copper showing. The contact relationship with surrounding rocks of the Powell Creek Formation is unclear. The syenite has yet to be dated, but is unmineralized, and therefore may be a pre- or post-mineralization intrusion.

Mineralization

Mineralization and alteration are similar at the Charlie and Northwest Copper showings and will be described together. Mineralization is typically vein hosted. Veinlets of native copper are hosted by quartz and carbonate composite veins. Copper typically forms veinlets less than 2 mm thick that are identified in the field as a result of the close association of the native copper with bright green malachite (Figure 6e).

Mineralization consists of chalcopyrite-bearing quartz veins. Chalcopyrite, pyrite and galena are the readily identified sulphides in comb-textured quartz veins. Sulphides are characteristically associated with magnetite and biotite.

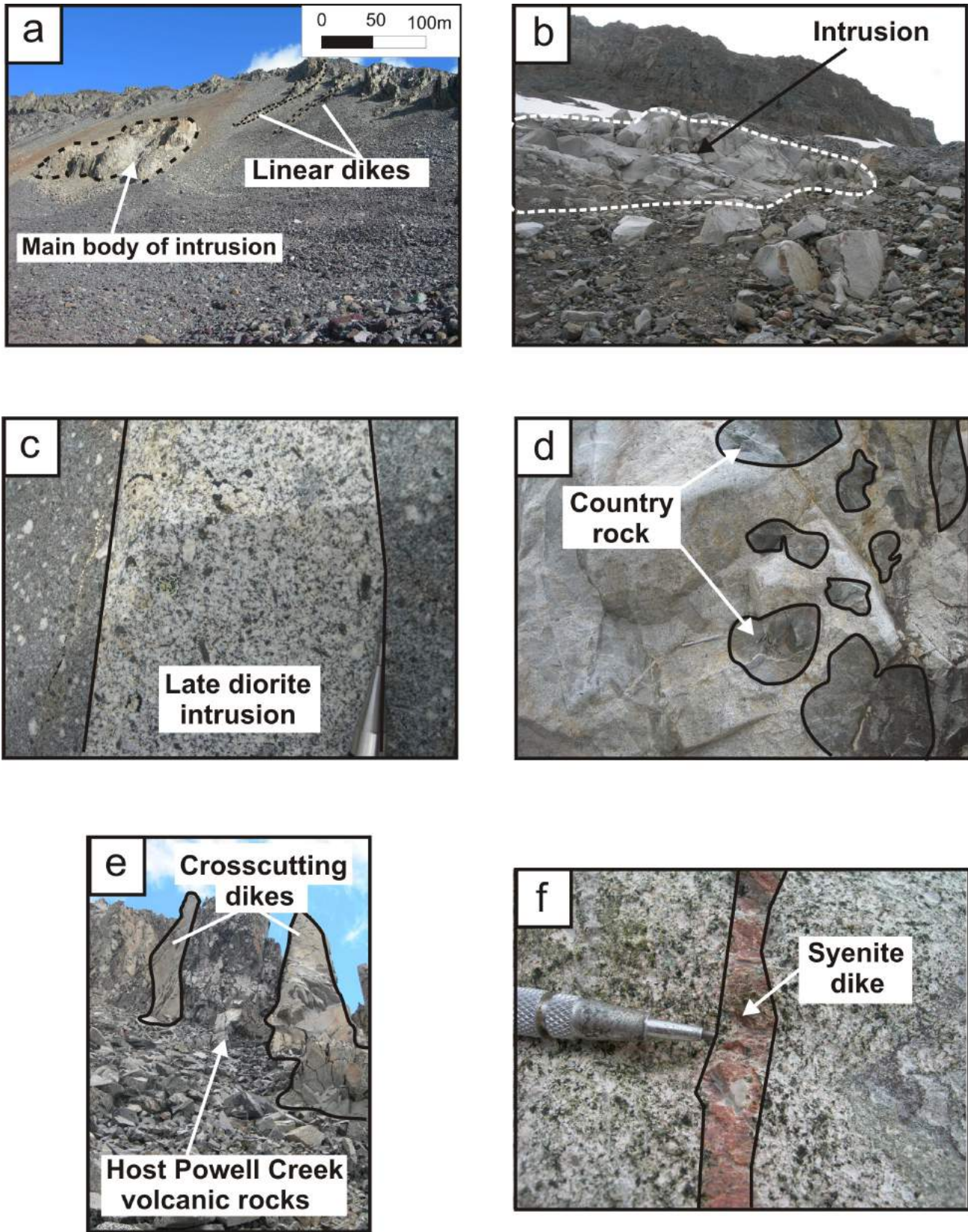


Figure 5. Photographs of the Northwest Copper showing: **a)** view facing north of the Northwest Copper intrusion and associated diorite dikes, **b)** view of the southern part of the intrusion, **c)** planar intrusive contact of diorite dike within host granodiorite intrusion, **d)** round xenoliths of wallrock within the intrusion, **e)** diorite dikes intruding the overlying resedimented volcanic rocks of the Powell Creek Formation, and **f)** syenite dike at the Northwest Copper showing.

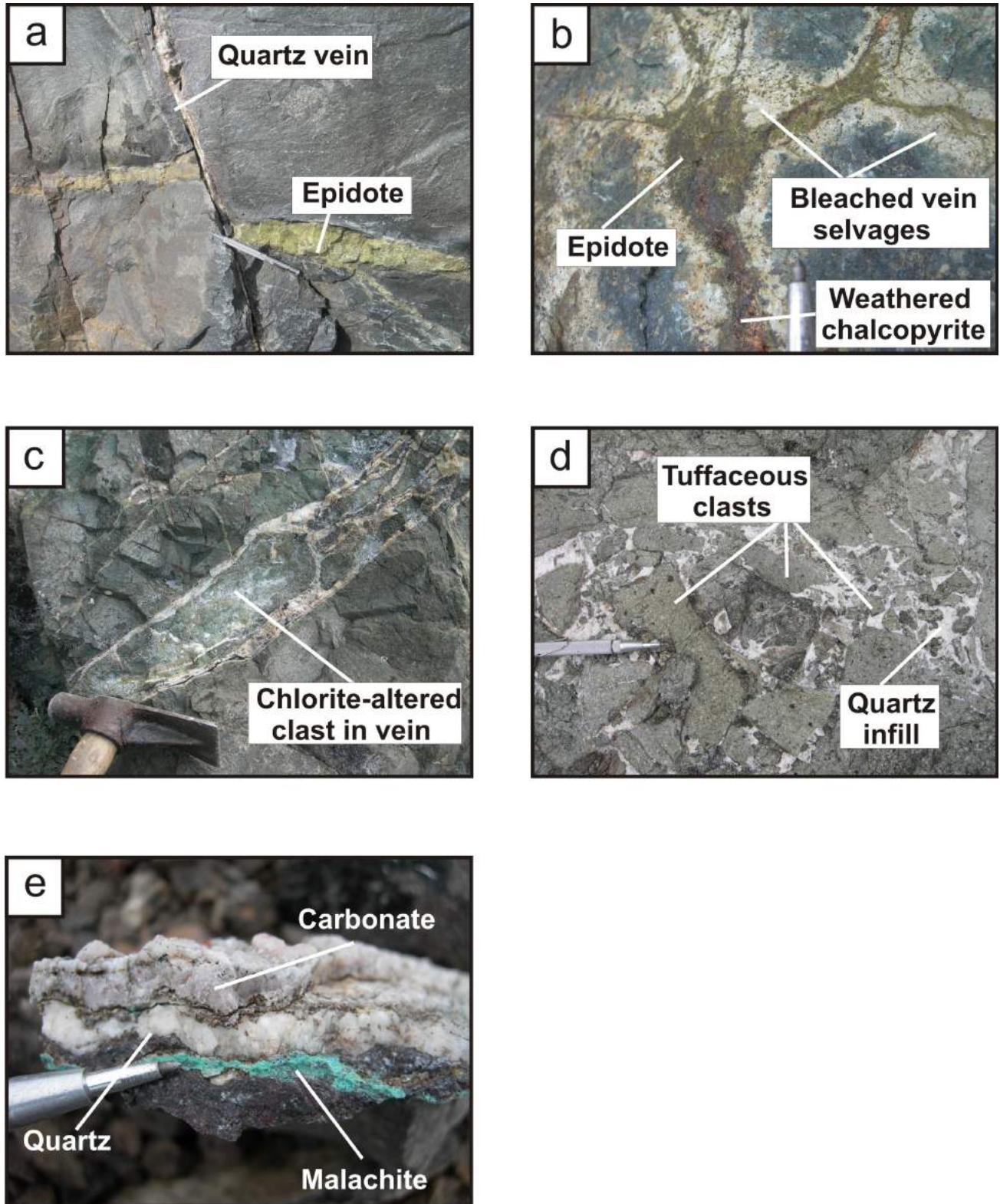


Figure 6. Features of mineralization and alteration at the Charlie and Northwest Copper showings: a) late-stage quartz vein offsetting massive epidote vein, b) well-developed alteration selvages associated with sulphide-bearing epidote veins, c) large clast within vein, d) hydrothermal quartz infill between tuffaceous clastic rocks, and e) quartz-carbonate vein with secondary malachite.

Pyrite occurs as a secondary mineral disseminated in most of the intrusive phases as well as an alteration product in some of the Fe-bearing sedimentary rocks and propylitically altered andesite. Veins are typically up to 10 cm thick and are usually continuous for several metres. Several are laterally continuous for up to 30 m, but these are barren quartz veins, typically associated with large fault zones. Vein compositions include quartz-only and quartz-carbonate (Figure 4b). Quartz-carbonate is a late stage infill, filling voids between comb quartz crystals. Quartz veins with chlorite selvages (usually millimetre scale) are common.

Hydrothermal Alteration

The alteration mineral assemblages of the Charlie and Northwest Copper showings are dominated by propylitically altered andesite of both the Tchaikazan River succession and the Powell Creek Formation. Phyllic alteration, silicification and advanced argillic alteration are also present.

Chlorite-Epidote±Calcite (Propylitic)

Volcanic rocks are pervasively altered to propylitic mineral assemblages of chlorite-epidote-pyrite, calcite, sericite and magnetite. Hydrothermal minerals such as chlorite, epidote, actinolite, sericite and quartz commonly replace primary phases such as hornblende, biotite and plagioclase. An abundance of chlorite gives the andesite a distinctive dark green colour. Plagioclase crystals are replaced by aggregates of sericite, chlorite and calcite. Chlorite appears to be widespread as a dominant mineral phase but is typically extensively developed in the exterior parts of veins and as zones between veins. Areas adjacent to veins are often propylitically altered, in particular showing the development of chlorite vein haloes, predominantly associated with quartz-only veins. Epidote is commonly associated with chlorite-altered rocks, particularly along fractures (Figure 4d) and often related to quartz veining. Calcite alteration accompanies the propylitic mineral assemblage and areas of pervasive calcite alteration are found at high elevations at the Charlie and Northwest Copper showings (Figure 4g).

Quartz-Sericite-Pyrite (Phyllic)

The alteration assemblage of quartz-sericite-pyrite is manifest in rusty red outcrops of the lower parts of the volcanic facies of the Tchaikazan River succession (Figure 5), where it is pervasive. The porphyritic texture of the rock is often still visible, although sericite-quartz-pyrite mineral assemblages replace the primary components of the groundmass. The alteration is characterized by the substitution of plagioclase by sericite and the mafic components by quartz.

Veins

The northwestern portion of the area of the Charlie and Northwest Copper showings exhibits the highest density of

veins in the study area. It also exhibits the widest variety of vein compositions, textures and forms. There are three main vein types: 1) quartz-only, 2) quartz-carbonate and 3) epidote veins. All three vein types may contain sulphides.

- 1) Quartz-only veins are rare at the Northwest Copper showing. The quartz is often massive (Figure 6a), and there are typically several crosscutting vein generations, with wallrock trapped between generations (Figure 6c). Quartz-only veins are locally common in areas of silicification and are typically associated with secondary malachite and, less commonly, azurite. These veins are altered along their margins, with chlorite selvages that sometimes extend several centimetres into the surrounding hostrocks. Quartz generally forms an hydrothermal fill to brecciated volcanic material. Quartz infill between clasts of a tuff (Figure 6d) is widespread near the Northwest Copper showing, indicating fluid flow throughout the area.
- 2) Quartz-carbonate veins are common in the area of the Charlie and Northwest Copper showings. They are several centimetres thick, continue for no more than a few metres and are hosted within the volcanic facies of both the Powell Creek Formation and the Tchaikazan River succession. They typically are not mineralized.
- 3) Epidote veins are locally abundant, particularly in the altered andesite surrounding the Northwest Copper intrusion (Figure 6b). The epidote is fine-grained and massive and is often associated with minor quartz and disseminated chalcopryrite and pyrite. These veins exhibit well-developed alteration haloes, giving the surrounding, magnetite-rich andesite a bleached appearance that is possibly a result of the introduction of secondary sericite.

Interpretation and Discussion

The Taseko Lakes area is endowed with numerous metallic mineral showings that have yet to be fully described. The objective of this study is to classify three of these showings.

The Hub showing is intrusion-related, porphyry Cu±Mo-style mineralization in a granodiorite stock and a stockwork of quartz+chalcopryrite±pyrite veins. The Hub granodiorite has a cooling age (Ar-Ar, biotite) of 80.53 ±0.42 Ma (T. Ullrich, pers. comm., 2006). The Hub diorite yielded a cooling age (Ar-Ar, biotite) of 79.56 ±0.42 Ma (T. Ullrich, pers. comm., 2006). The QF porphyry dike is unmineralized and crosscuts both the granodiorite and the diorite and is therefore younger and post-mineralization. A whole rock age of 77.2 ±2.8 Ma was obtained for the Prosperity deposit by J.E. Harakal at the University of British Columbia (MINFILE 0920 041; MINFILE, 2007), who considered this radiometric age to be the age of mineralization at the Prosperity deposit, and is similar to that deter-

mined for mineralization at the Hub showing. The mineralization and alteration style exhibited by the Hub showing shows several characteristics of classic porphyry-style mineralization. These include copper minerals disseminated throughout the intrusion and associated Cu-bearing quartz stockwork veins and the hydrothermal magnetite±biotite-cemented breccia that crosscuts the granodiorite and diorite. Sulphide mineralization, in particular chalcopyrite and molybdenite, is disseminated in the granodiorite and magnetite±biotite breccia and in quartz veins in these rocks. The magnetite±biotite breccia is exposed at the surface at the Hub showing, indicating that breccia emplacement may have been relatively shallow (<3 km). The diorite intrusion can be interpreted as a compositional variation of the granodiorite as a result of differentiation.

The Charlie and Northwest Copper showings are vein-hosted, with typical metallic minerals, including chalcopyrite, pyrite, galena and native copper. Alteration assemblages are different from those at the Hub showing. Propylitic mineral assemblages dominant in the Charlie and Northwest showings, with discrete areas of silicification and phyllic alteration also observed. This is in contrast to the potassic alteration and silicification observed at the Hub showing. These alteration assemblages are interpreted to be early alteration in the central parts of the mineralization at the Hub showing. An intrusion in the area of the Charlie and Northwest Copper showings has yet to be dated, but must be younger than the Powell Creek Formation since it intrudes these upper Cretaceous rocks.

The question remains whether the study area displays evidence for a single hydrothermal event or multiple events. Based on the alteration sequences, crosscutting veins and geochronology, alteration and mineralization appear to have formed as overlapping episodes during the evolution of an hydrothermal system. Mineralization is hosted by the main Hub granodiorite and the magnetite±biotite-cemented breccia, and vein-hosted sulphides are present in overlying andesite and basaltic andesite rocks of the Tchaikazan River Succession and Powell Creek Formation at the Charlie and Northwest Copper showings. The hydrothermal mineralization and alteration events consist of two spatially overlapping and overprinting stages: 1) potassic, propylitic and phyllic alteration with associated Cu-Mo mineralization, and 2) quartz-sulphide veins with associated magnetite alteration. Potassic alteration is represented by relicts of K-feldspar, magnetite and biotite, and appears to pass outwards into propylitic mineral assemblages of chlorite-epidote-calcite. Most of the copper mineralization occurs as disseminated chalcopyrite, accompanied by pyrite and magnetite, replacing mafic minerals in potassic-altered hostrock.

In conclusion, the rock types and alteration assemblages present at the Hub, Charlie and Northwest Copper prospects show evidence of porphyry-related mineralization and hydrothermal alteration. The question remains whether these showings are related to the same hydrothermal system at depth or whether they represent part of a proximal to distal facies of a large-scale, widespread porphyry system in which the rocks in the vicinity of the Charlie and Northwest Copper showings were altered in response to a large-scale system at depth.

Future Work

Much of what is known about the physical-chemical evolution of magmatic hydrothermal fluids between the plutonic regime of porphyritic granitoid bodies and the meteoric regime is based upon fluid inclusions in veins from porphyry-hosted ore deposits (Dilles et al., 2000). Following detailed petrographic study of fluid inclusions using transmitted light, further work in this study will be focused upon an in-depth study of the fluid inclusions themselves and what they can reveal about the conditions of formation of the veins in the region. Defining the hydrothermal features and related altered rock types of these showings will be of value for exploration in the Taseko Lakes region, especially given recent work on the advanced Prosperity deposit.

The further application of geochronological methods to date the Northwest Copper intrusion is of importance in relating this intrusion to those already identified in the study area and to those within the broader porphyry environment of southwestern British Columbia.

Acknowledgments

Galore Resources Inc., in particular U. Schmidt, is thanked for logistical support while field work was being done, and for financial assistance for laboratory analysis. M. Cruickshanks and E. Looby are thanked for their help during the 2007 field season and C. Chamberlain is thanked for reviewing this paper prior to its submission. Finally, Galore Resources Inc. and Geoscience BC are thanked for their financial support for the project.

References

- Bruce, J.O. (2000): Alteration and mineralogy associated with the Northwest Copper prospect, Taseko Lakes region, south-central, British Columbia; undergraduate thesis, University of British Columbia.
- Cannell, J., Cooke, D.R., Walshe, J.L. and Stein, H. (2005): Geology, mineralization, and structure of the El Teniente porphyry Cu-Mo deposit; *Economic Geology*, v. 100, p. 979–1003.
- Dilles, J.H., Einaudi, M.T., Proffett, J and Barton, M.D. (2000): Overview of the Yerington Porphyry Copper District; magmatic to nonmagmatic sources of hydrothermal fluids; their flow paths and alteration effects on rocks and Cu-Mo-Fe-Au

- ores; Society of Economic Geologists, Guidebook Series, v. 32, p. 55–66.
- Garver, J.L. (1992): Provenance of Albian–Cenomanian rocks of the Methow-Tyughton basin, southern British Columbia; a mid-Cretaceous link between North America and the Insular Superterrane; *Canadian Journal of Earth Sciences*, v. 29, p. 1274–1295.
- Hollis, L., Blevings, S.K., Chamberlain, C.M., Hickey, K.A. and Kennedy, L.A. (2007): Mineralization, alteration and structure of the Taseko Lakes region (NTS 0920/04), southwestern British Columbia: preliminary analysis; *in* Geological Fieldwork 2006, BC Ministry of Energy, Mines and Petroleum Resources, Paper 2007-1 and Geoscience BC, Report 2007-1, p. 297–306.
- Israel, S. (2001): Structural and stratigraphic relationships within the Tchaikazan River area, southwestern British Columbia: implications for the tectonic evolution of the southern Coast Belt; M.Sc. thesis, University of British Columbia, 129 p.
- Israel, S., Schiarizza, P., Kennedy, L.A., Friedman, R.M. and Villeneuve, M.E. (2006): Evidence for Early to Late Cretaceous, sinistral deformation in the Tchaikazan River area, southwestern British Columbia: Implications for the evolution of the southern Coast Belt; *in* Paleogeography of the western North American Cordillera, J. Haggart, R. Enkin and J.W.H. Monger (ed.), Geological Association of Canada, Special Paper 46, p. 331–350.
- Lowell, J.D and Guilbert, J.M. (1970): Lateral and vertical alteration-mineralization zoning in porphyry ore deposits; *Economic Geology*, v. 65, no. 4, p. 373–408.
- McLaren, G.P. (1990): A mineral resource assessment of the Chilko Lake planning area; BC Ministry of Energy, Mines and Petroleum Resources, Bulletin 81, 117 p.
- MINFILE (2007): MINFILE BC mineral deposits database; BC Ministry of Energy, Mines and Petroleum Resources, URL <<http://www.em.gov.bc.ca/Mining/Geosurv/Minfile/>>.
- Monger, J.H.W. and Journeay, J.M. (1994): Guide to the geology and tectonic evolution of the southern Coast Mountains; Geological Survey of Canada, Open File 2490, 81 p.
- Schiarizza, P., Gaba, R.G., Glover, J.K., Garver, J.I. and Umhoefer, P.J. (1997): Geology and mineral occurrences of the Taseko–Bridge River area; BC Ministry of Energy, Mines and Petroleum Resources, Bulletin 100, 291 p.
- Schanmugam, G. (1997): The Bouma sequence and the turbidite mind set; *Earth Science Reviews*, v. 42, no. 4, p. 201–229.
- Seedorf, E., Dilles, J.H., Jr., Einaudi, M.R., Zurcher, L., Stavast, W.J.A., Johnson, D.A. and Barton, M.D. (2005): Porphyry copper deposits: characteristics and origin of hypogene features; *Economic Geology*, 100th Anniversary Volume, J.W. Hedenquist, J.F.H. Thompson, R.J. Goldfarb and J.P. Richards (ed.), p. 485–522.
- Sillitoe, R.H. (1979): Some thoughts on gold-rich porphyry copper deposits; *Mineralium Deposita*, v. 14, no. 2, p. 161–174.
- Tipper, H.W. (1969): Mesozoic and Cenozoic geology of the northeast part of Mount Waddington map-area (92N), Coast District, British Columbia; Geological Survey of Canada, Paper 68-33, 103 p.
- White, J.D.L. (2000): Subaqueous eruption-fed density currents and their deposits; *Precambrian Research*, v. 101, no. 2, p. 87–109.

Hyperspectral Imagery Demonstration Project, British Columbia

W.E. Kilby, Cal Data Ltd., Kelowna, BC, wkilby@telus.net

C.E. Kilby, Cal Data Ltd., Kelowna, BC

Kilby, W.E. and Kilby, C.E. (2008): Hyperspectral imagery demonstration project, British Columbia; *in* Geoscience BC Summary of Activities 2007, Geoscience BC, Report 2008-1, p. 67–76.

Introduction

Remote sensing has become a successful tool in mineral exploration in many parts of the world. Early use of Landsat imagery and other multispectral instruments has allowed regional exploration to move swiftly to areas of interest. More recently, the use of hyperspectral tools, with up to 250 discrete readings per spectrum collected at each discrete sample area on the ground, has been able to further assist exploration and mapping of geology and mineral alteration at various scales down to detailed deposit scale.

In British Columbia, the use of remote sensing in mineral exploration has lagged behind other mineral provinces due to the extensive cover of forests. However, the newer instruments allow collection of data at discrete points of a few metres and can collect useful spectra wherever outcrops can be discerned, along forestry roads, in areas of dry brush and above the treeline. A variety of images from within BC has been acquired over the last several years from a number of multi- and hyperspectral instruments over mines and other areas with potentially interesting geology. These images have been processed and placed on the MapPlace website, along with a number of basic tools to enable explorationists to evaluate the usefulness of this type of information in the search for new mineral deposits.

This project is the first by Geoscience BC to acquire remote images by selectively flying areas of high interest with a hyperspectral instrument in order to obtain images for on-line analysis by the exploration community.

Background

The Hyperspectral Imagery Demonstration Project, sponsored by Geoscience BC, provides examples of airborne hyperspectral images taken at high spectral and spatial resolution over typical exploration and mining sites in BC. This new imagery is available through the MapPlace website of the BC Ministry of Energy, Mines and Petro-

leum Resources (BC Geological Survey, 2007). Ten flight lines of hyperspectral data covering six sites have been added to the 68 Landsat 7, 239 ASTER (Advanced Spaceborne Thermal Emission and Reflection Radiometer), 1 Hyperion and 1 AVIRIS (Airborne Visible/Infrared Imaging Spectrometer) images already available for online analysis through MapPlace's Image Analysis Toolbox (IAT; Kilby et al., 2004; Kilby, 2005; Kilby and Kilby, 2006a, b, 2007). Enhancements have been made to the IAT to provide additional analysis capabilities. A spectrum viewer provides the ability to examine the image spectrum at any image pixel. A reference library of mineral spectra has been added to the Spectral Angle Mapper (SAM) tool to allow SAM mapping of images using the United States Geological Survey (USGS) Spectral Library (Clark et al., 2007) spectra or image-obtained spectra.

Following a request for proposals, SpecTIR LLC (SpecTIR, 2007) was selected to provide the hyperspectral imagery. The imaging spectrometers utilized in the collection were the AISA (Airborne Imaging Spectrometer for Applications) Eagle, sampling the visible and near infrared (VNIR), and Hawk, sampling the shortwave infrared (SWIR), the sensors being combined in the AISA DUAL sensor package (Specim, 2007). The imagery was collected on August 1, 2007.

ITRES Research Limited (ITRES, 2007) offered to collect some imagery as part of a field test of their constructed sensors. Two sites were selected in the Rocky Mountains near Golden, BC. The collection was performed on July 12, 2007 utilizing their SASI 600, sampling the SWIR, and TASI 600, sampling the Thermal Infrared (TIR). The SASI 600 shortwave infrared (SWIR) data from this collection will be provided to this project at some future date.

Survey sites were selected to provide realistic examples of conditions likely to be encountered during exploration in BC (Figure 1). The six sites collected by SpecTIR included two sites with active surface mines with good bedrock exposure of known alteration characteristics (Gibraltar and Mount Polley). One flight line sampled an underground past producer, Blackdome, that has moderate exposure and well-known geology. Another flight line covers an area of known alteration above the treeline, the Limonite occurrence in the Taseko Lakes area. The Prosperity deposit was

Keywords: remote sensing, hyperspectral imagery, online analysis, data download, MapPlace

This publication is also available, free of charge, as colour digital files in Adobe Acrobat® PDF format from the Geoscience BC website: <http://www.geosciencebc.com/s/DataReleases.asp>.

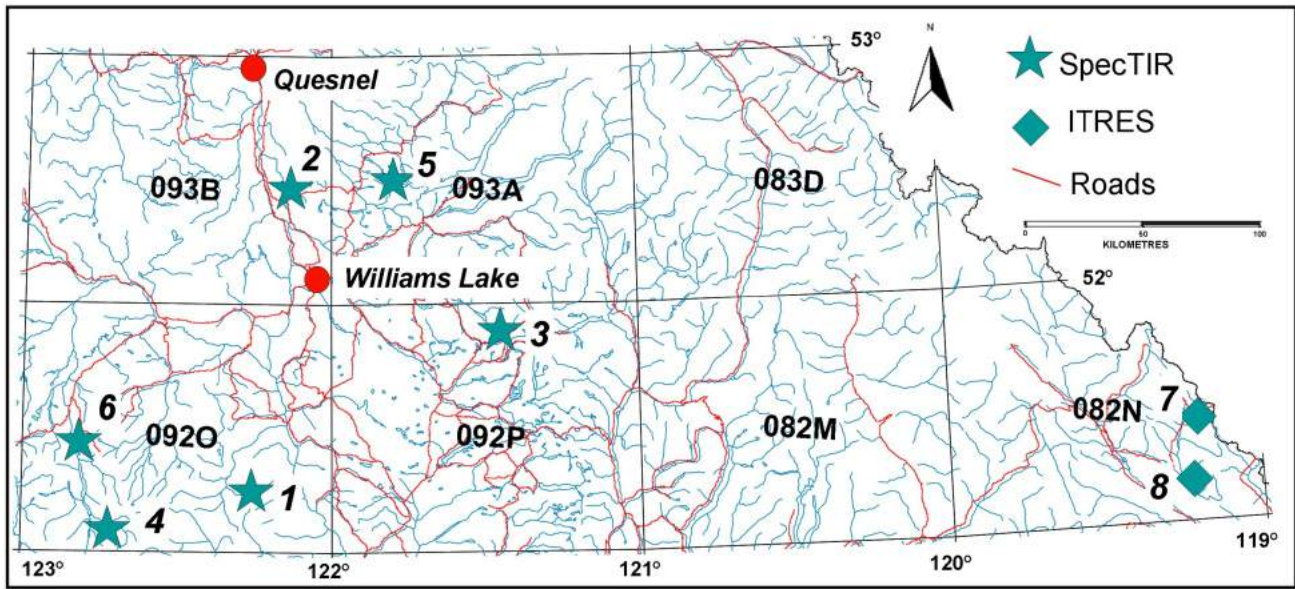


Figure 1. Locations of the eight demonstration sites: 1) Blackdome, 2) Gibraltar, 3) Lang Lake, 4) Limonite, 5) Mount Polley, 6) Prosperity, 7) Kicking Horse, and 8) Ice River.

sampled with another line to provide an example of an area with active exploration and limited exposure. The sixth flight line sampled a heavily vegetated area in the Lang Lake region. The combination of sites provides a variety of surface exposure conditions, geology and deposit types.

The two sites flown by ITRES during their instrument testing flight included past producers and prospects at Kicking Horse Pass and Ice River. The Kicking Horse site includes carbonate rocks that hosted Mississippi Valley–type deposits, and the Ice River site includes carbonatite and skarn deposits of the Ice River complex.

In the IAT, the hyperspectral imagery is orthorectified and atmospherically corrected. This allows any analysis to be immediately integrated with the existing geological information contained in MapPlace, such as geological maps and mineral occurrence, geophysical and geochemical data. The original image data can also be downloaded for offline processing in image-analysis software. The information is available in radiance and reflectance values, and is provided in BIL format.

Hyperspectral Imagery

Field spectrometers are now in common use during exploration programs where the identification of alteration mineralogy is essential to the unraveling of the mineralization process. Hyperspectral imagery is simply an extension of this technique to the generation of imagery with an imaging spectrometer. Hyperspectral imagery has been defined as “the acquisition of images in hundreds of regis-

tered, contiguous spectral bands such that for each picture element it is possible to derive a complete reflectance spectrum” (Goetz, 2002). Imaging spectrometers have been mounted on a wide variety of platforms, such as spacecraft, aircraft, motor vehicles and workbenches. Spatial sample spacing commonly ranges from a couple of millimetres (core loggers) to tens of metres (Hyperion).

The SpecTIR sensors sample the electromagnetic spectrum in a continuous manner with 178 bands (VNIR and SWIR). The ITRES sensor collects 100 continuous bands in the

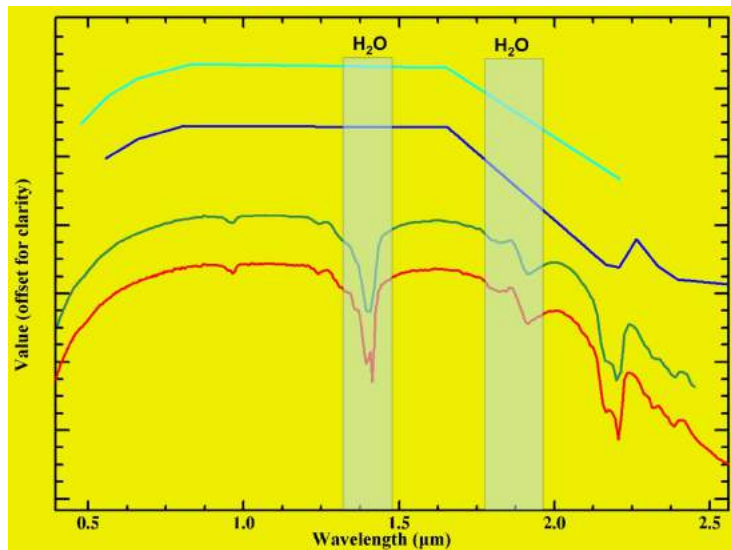


Figure 2. Comparative spectral plot of spectra obtained from three sensors: SpecTIR (green), ASTER (blue) and Landsat (cyan). The library spectrum for kaolinite is shown in red. The inflexion points on the Landsat and ASTER spectra mark the locations of their bands. Note the distinctive absorption feature at ~2.2 µm. Shaded ‘H₂O’ areas indicate regions of the electromagnetic spectrum blocked by atmospheric water.

SWIR portion of the spectrum. The other major image types included in the IAT, Landsat and ASTER, are multispectral imagers that sample only a limited number of bands, 6 and 9 respectively (within the VNIR and SWIR). Figure 2 illustrates the spectrum that would be obtained by these three sensors. It is obvious that only the SpecTIR hyperspectral sensor provides enough readings to accurately define the complete reflectance spectrum of the mineral being examined.

SpecTIR Imagery

The hyperspectral imagery obtained for this project by SpecTIR LLC was collected on August 1, 2007 from a fixed-wing aircraft flying approximately 1155 m above the ground surface. A sun elevation angle of about 56° was available on this date at the latitude of the sites. The resulting imagery has a pixel size and ground sample distance (GSD) of about 1.5 m. The images are 296 samples (pixels) wide. The full width at half maximum (FWHM; i.e., bandwidths) for the 178 bands ranges from 9.1 to 12.6 nm. Individual flight lines ranged from 4.2 to 18.7 km in length, requiring between 2 800 and 12 500 scan lines respectively. This sample density results in about 21 million individual spectra being collected during this project. The imagery is provided in radiance and reflectance values. The atmospheric correction used to convert the data from radiance to reflectance was performed by SpecTIR using the ATCOR4 commercial software that employs the MOTRAN4 radiative transfer code. The raw reflectance output spectra were then modified and polished to remove any model- or sen-

sor-related artifacts with proprietary SpecTIR techniques. Orthorectification solutions for the imagery were also provided using information obtained from the onboard GPS/INS sensor.

The AISADUAL sensor package of imaging spectrometers was used to collect the image data from two adjacent ranges of the electromagnetic spectrum. The AISA Eagle was used to collect 59 bands of information from the VNIR range of the spectrum (0.4–0.95 μm), and the AISA Hawk was used to collect 119 bands from the SWIR range (0.967–2.45 μm). A full description of this instrument package is available from the manufacturer, Spectral Imaging Ltd.

ITRES Imagery

The hyperspectral imagery obtained for this project by ITRES Research was collected on July 12, 2007. The details of this collection and subsequent processing are not yet available, but the sensor used was the SASI 600, which collects 100 bands between wavelengths of 0.95 and 2.45 μm, with a bandwidth of about 15 nm.

Survey Sites

Six sites were selected for inclusion as hyperspectral demonstration locations. The sites were located in the interior region of the province and include a variety of surface exposure conditions and geological environments (Figure 1). The IAT contains Landsat and ASTER coverage for all these sites and the ability to compare capabilities between the different image types. Most of the sites have detailed

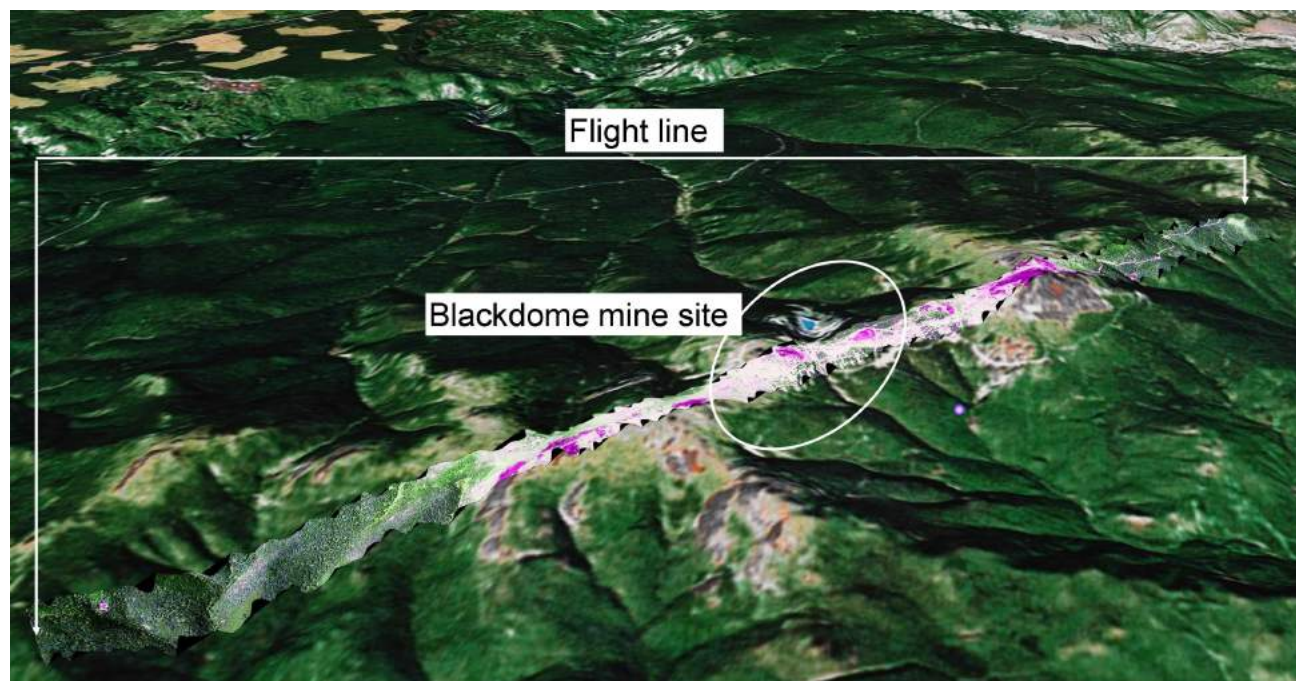


Figure 3. Blackdome hyperspectral false-colour image draped over Google™ Earth terrain. Ellipse marks the area of the mine's surface disturbance. Image is about 11 km wide.

exploration information available in the form of BC Mineral Assessment Reports, and all have regional geology, geochemistry and geophysical information available for reference in MapPlace.

Blackdome

The Blackdome site is centred on the mine site at 51.314°N, 122.50°W. The one flight line collected for this site is 11 km long, about 400 m wide (Figure 3) and has a bearing of about 200°. The site includes the Blackdome past-producing epithermal Au-Ag vein deposit and the Midas epithermal Au-Ag showing, MINFILE 092O 053 (MINFILE, 2007). The flight line includes the transition from heavily forested to alpine vegetation. Surface topography ranges from 1700 to 2220 m. South of the mine site, the flight line covers terrain that is undisturbed; north of the mine site, it parallels the main mine access road. The geology covered by the flight line includes Early–Middle Tertiary volcanic and associated volcanoclastic sedimentary rocks cut by small intermediate to mafic dikes. A significant fault is also present in the southern portion of the flight line. The varied exposure types and presence of a significant epithermal system should prove to be a very interesting site for hyperspectral analysis in the BC context.

Gibraltar

The Gibraltar site is centred on the producing Cu-Mo porphyry open pit mine at 52.514°N, 122.273°W, MINFILE 093B 012 (MINFILE, 2007). Three overlapping flight lines

were collected at this site to provide coverage over an area measuring 9.6 km long by about 1 km wide. In addition to the active mine site with its good rock exposure, the flight lines include areas of typical logging and mineral exploration features (Figure 4). The lines are oriented north-south to take full advantage of the solar illumination. The flight line is underlain by the Early Jurassic Granite Mountain batholith. All three phases of this batholith are imaged by these flight lines: the Southern Border phase; the Mine phase tonalite and Northern Border phase; and the Granite Mountain phase. The surface topography is relatively subdued, with the average elevation being about 1200 m. This site offers the opportunity to examine very good exposures of this deposit, with its well described alteration minerals and structures.

Lang Lake

The Lang Lake site is a single flight line centred at 51.93°N, 120.9°W. The line is oriented approximately north-south and is 18.7 km long and about 400 m wide (Figure 5). There are five known showings and one prospect within 1 km of the flight line. There are a number of very interesting copper, molybdenum and gold Regional Geochemical Survey (RGS) stream sediment values in the area of the flight line. The northern portion of the line is underlain by Triassic–Jurassic plutonic rocks of the Takomkane and Thuya batholiths. The southern portion is underlain by Late Triassic basalt flows. A number of faults crosscut the flight line. The recently released Bonaparte East multiparameter geophysical survey (Miles et al., 2007) provides detailed infor-



Figure 4. Gibraltar hyperspectral false-colour image draped over Google™ Earth terrain. The hyperspectral image is a mosaic constructed from the three individual lines flown over this site.

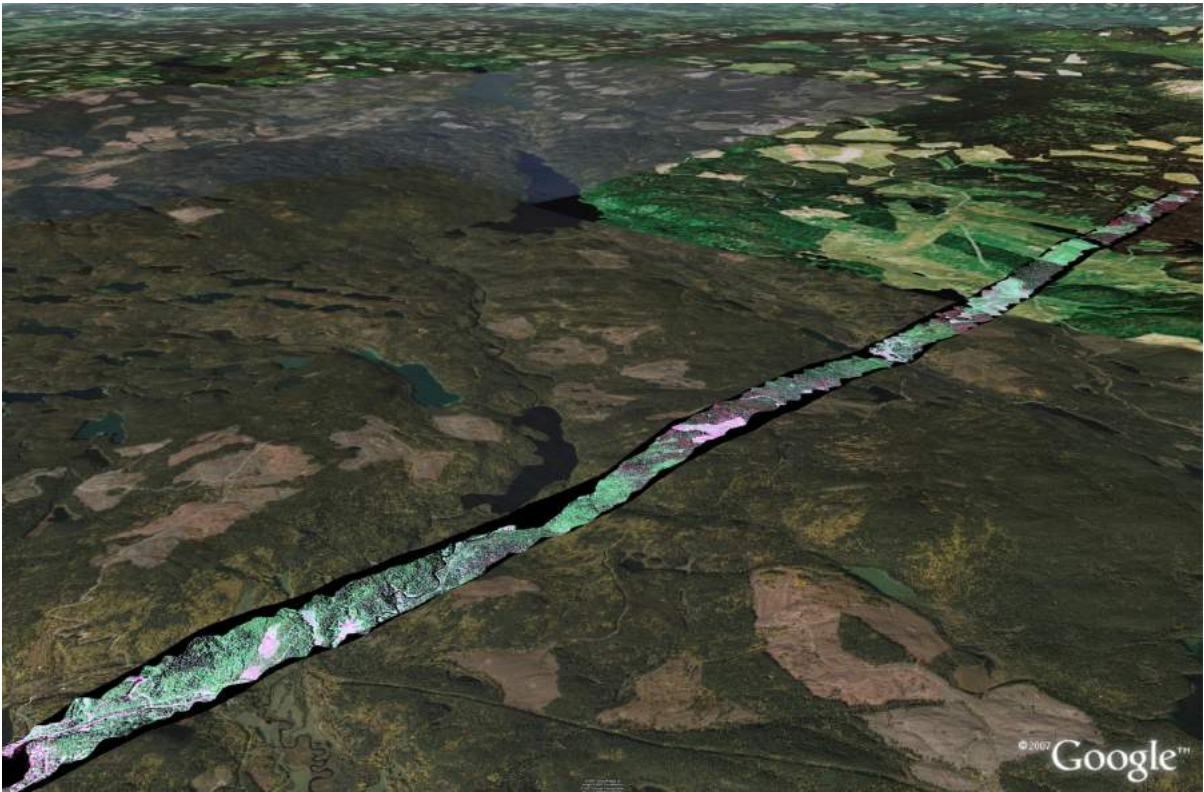


Figure 5. Lang Lake hyperspectral false-colour image draped over Google™ Earth terrain. The image is about 12 km wide. The high-resolution Google Earth background image in the lower part of this figure is not properly registered (about 300 m too far west). Google Earth is used here to show the topographic relief.

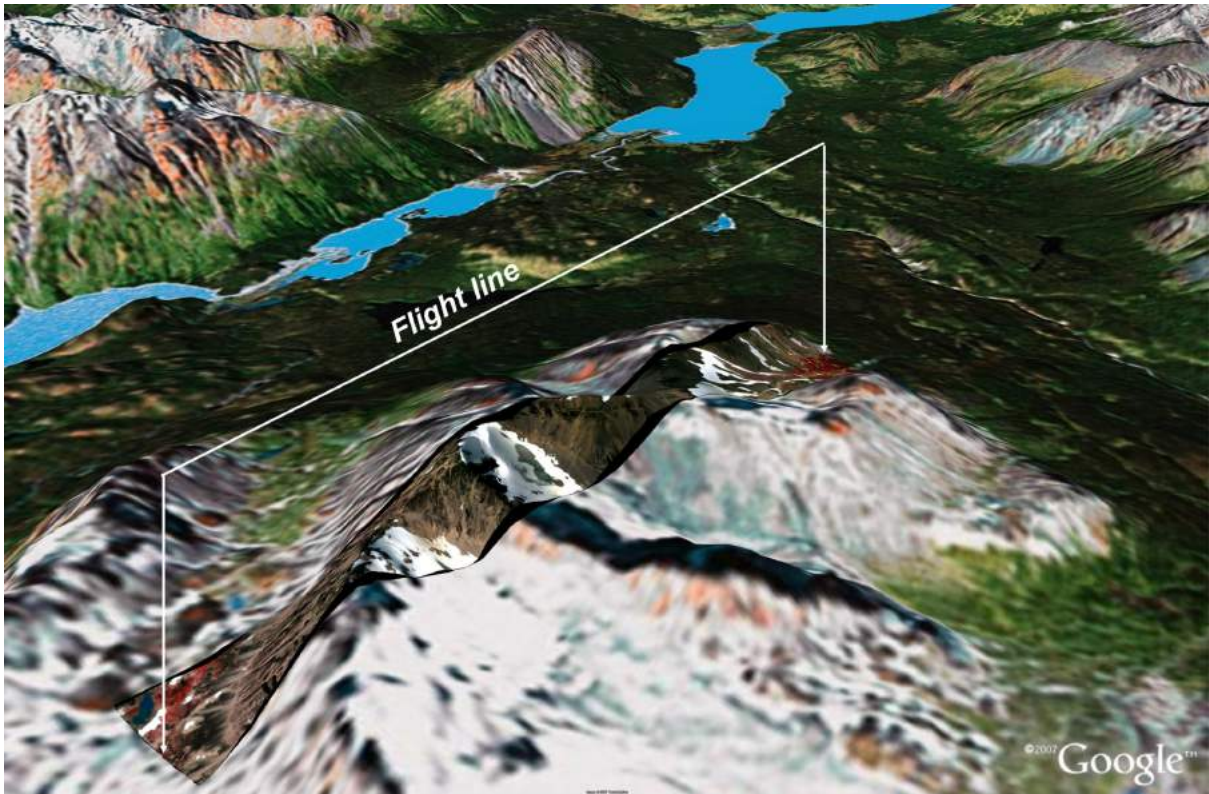


Figure 6. Limonite site hyperspectral false-colour image draped over Google™ Earth terrain. Taseko Lakes can be seen in the upper portion of the image. The red in the hyperspectral image represents chlorophyll-bearing vegetation.

mation for the entire flight line. This site was selected as an example of typical poorly exposed terrain in the interior portion of the province. The area has been partially logged and heavily infested with mountain pine beetle. Rock exposures are limited to man-made surface disturbances associated with logging and along water features. The combination of interesting geochemistry, good geophysics and poor surface exposure at this site will provide a good test of the capabilities of hyperspectral imagery.

Limonite

The Limonite site is a single flight line centred at 51.086°N, 123.4756°W, MINFILE 0920 010 (MINFILE, 2007). The line is oriented north-south and is 4.2 km long and about 500 m wide (Figure 6). The line samples typical alpine exposures of variably altered rock types. Elevation along the flight line ranges from 2000 to 2670 m. Significant copper and gold RGS stream sediment values are present in streams draining the area of the flight line, and known porphyry mineralization has been discovered in the area. This site is the only one to include small glaciers and snow fields. The northern portion of the line covers Late Cretaceous volcanoclastic strata of the Powell Creek Formation and the southern portion is underlain by Late Cretaceous granodioritic intrusive rocks of the Coast Plutonic Complex. The central portion of the line is underlain by a Late Cretaceous–Early Tertiary feldspar porphyry. This site provides an excellent example of typical alpine terrain to be found in the province. It also samples the contact of the Coast Plutonic Complex and contains obvious visible alteration minerals.

Mount Polley

The Mount Polley site, MINFILE 093A 008, was sampled with three overlapping flight lines centred on the Mount Polley producing alkalic porphyry Cu-Au open pit mine at 52.55°N, 121.6345°W (Figure 7; MINFILE, 2007). The lines are oriented north-south, and are about 12 km long and cover a width of about 1.0 km. They cover areas of the Early Jurassic Nicola Group volcanoclastic rocks and the deposit-hosting felsic Jurassic–Triassic Polley stock. Propylitic and potassic alteration are present around the mineralization, and a zone of garnet-epidote alteration has been noted between these two zones. Beyond the mine workings, the surface is well vegetated. Various ages of logging and mineral exploration roads and drill sites provide ground exposures in these vegetated areas. Information from a recent, high-resolution, helicopter-borne, multiparameter geophysical survey is available for the area covered by the flight lines (Shives et al. 2004). This site will provide a good example of alteration mineralization associated with alkalic porphyry deposits, as well as including areas at various stages of reforestation and some mineral exploration features.

Prosperity

The Prosperity site is a single north-south flight line centred on the Prosperity Cu-Mo porphyry deposit at 51.466°N, 123.630°W, MINFILE 0920 041 (MINFILE, 2007). The line is 6.3 km long and about 500 m wide (Figure 8). The area sampled by this flight line is an example of very poor exposure, with the northern portion being covered with Pleistocene–Holocene alluvium and till, while the southern portion is covered with Miocene–Pleistocene Chilcotin

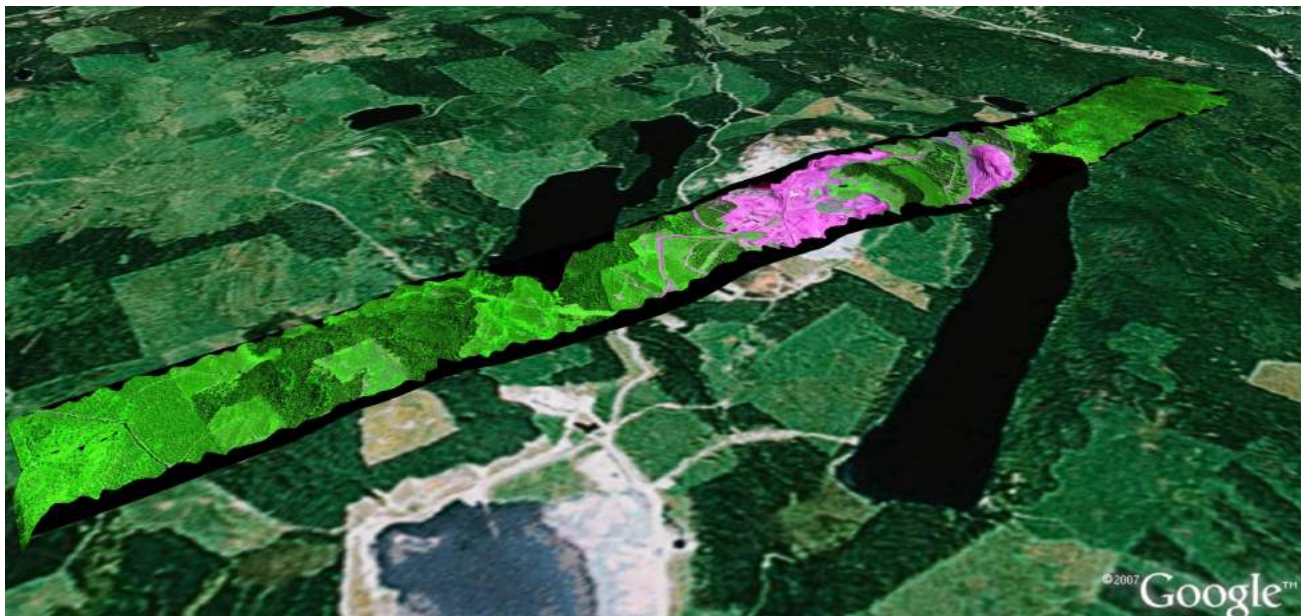


Figure 7. Mount Polley hyperspectral false-colour image mosaic draped over Google™ Earth terrain. The hyperspectral mosaic is constructed from the three individual images collected over this site. Bare rock exposure appears pink in this false-colour image.

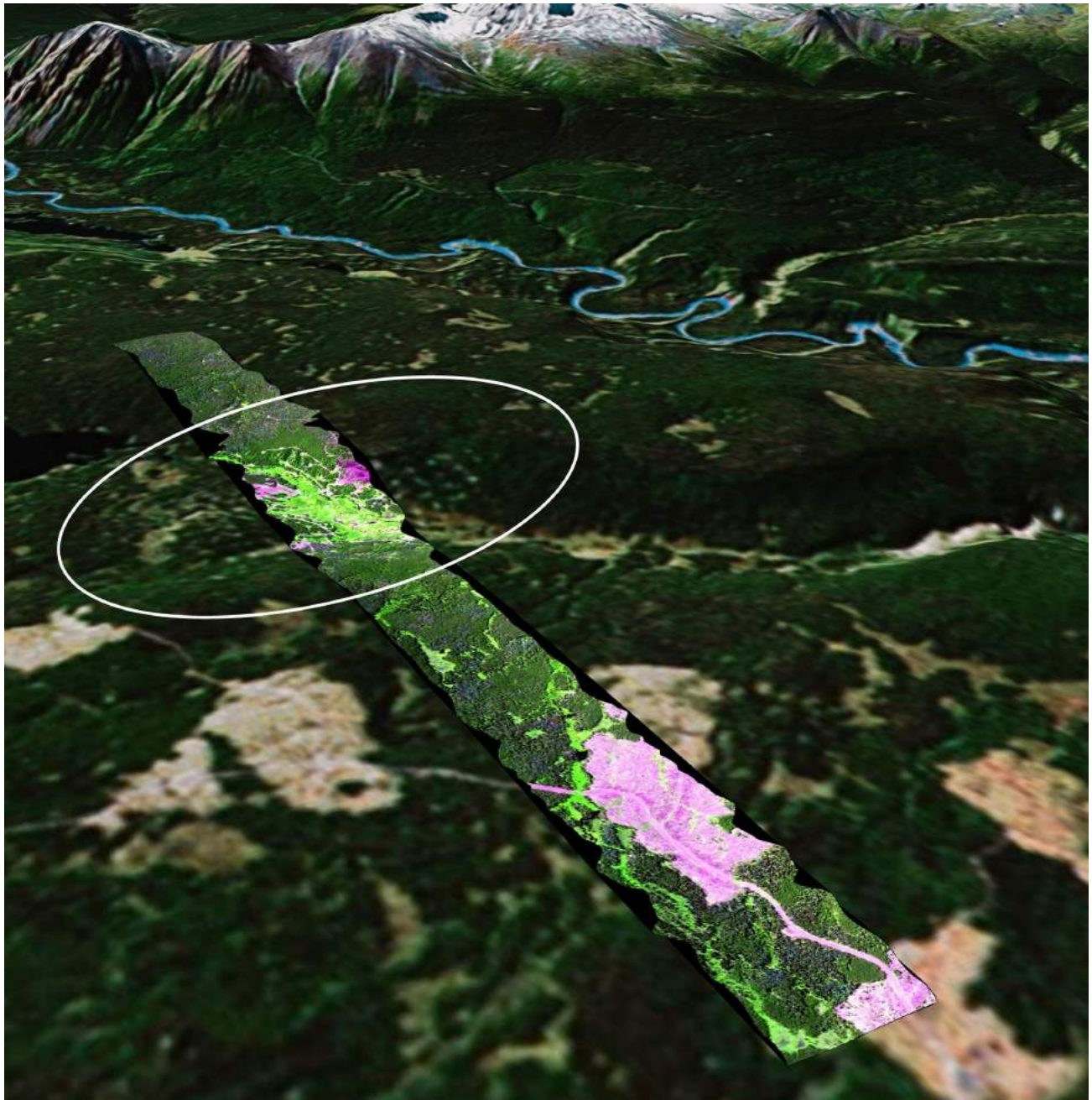


Figure 8. Prosperity hyperspectral false-colour image draped over Google™ Earth terrain. The ellipse marks the area underlain by the deposit. The regular pattern of exploration drill sites can be easily seen on the background Landsat imagery, as well as in the hyperspectral image.

Group alkaline volcanic rocks. Some ground exposure is available in the form of logging and exploration roads, and drill sites. There are several excellent copper and gold RGS stream sediment values in drainages crossing the area of the flight line. The site has been well documented and there is a recent (1995), high-resolution, multiparameter geophysical survey available (Shives et al., 2005). This site was selected to investigate the potential of hyperspectral imagery to provide additional information in an area with thick cover.

Kicking Horse

The Kicking Horse site is centred on the Kicking Horse past-producing Pb-Zn mine at 51.424°N, 116.445°W, MINFILE 082N 020 (MINFILE, 2007). The deposit is located within a thick succession of massive to thin-bedded limestone and dolomite of the Middle Cambrian Cathedral Formation. The site falls within Yoho National Park but provides a good example of a carbonate-hosted deposit that could be found elsewhere in the province.

Ice River

The Ice River site is located west of the Ice River in Yoho National Park, centred about 57.17°N, 116.46°W. The site samples the ultrabasic Ice River intrusive complex and associated skarn deposits. Carbonatite is present within the imaged area. The site is above the treeline and should provide an example of some very interesting mineral assemblages.

Image Analysis Toolbox Enhancements

New Imagery

The SpecTIR hyperspectral image data can be interactively analyzed in the same manner as the previously existing Landsat, ASTER, AVIRIS and Hyperion data. The images are named S1 through S10 and their footprints can be toggled on and off with the 'SpecTIR' button on the initial IAT tool panel. Access to the downloadable SpecTIR hyperspectral data is through the 'SpecTIR Download' button (Figure 9). A new download button for the ITRES imagery will be added when the imagery becomes available.

The downloadable SpecTIR data will be available in radiance and reflectance values. The image data will be in Band Interleaved by Line (BIL) format. The images will be divided into data cubes that can be readily downloaded. The cubes will be 296 pixels wide and contain 178 bands. The number of scan lines in each data cube will be decided fol-

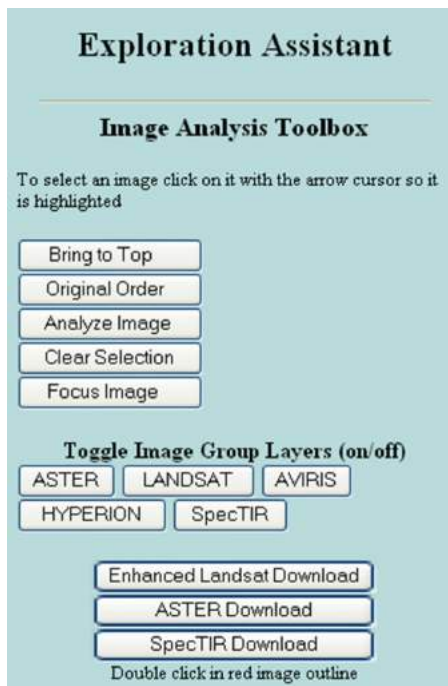


Figure 9. Introductory IAT panel in the Exploration Assistant map on MapPlace. The new SpecTIR hyperspectral imagery can be accessed for online analysis or downloaded through the two new buttons on this panel.

lowing analysis of download speeds obtained through the final server configuration. The orthorectification solution will be provided in ENVI's (Environment for Visualizing Images) Input Geometry (IGM) format that provides the co-ordinates (UTM Zone 10, WGS-84) for each image pixel resulting from the orthorectification process.

SpecTIR hyperspectral imagery available for online analysis is orthorectified and atmospherically corrected. In the IAT, it is essential that the imagery is orthorectified so it can be integrated with all the supporting GIS data available in MapPlace. The downloadable image cubes are available in the raw form with accompanying files to enable orthorectification.

New Tools

Two new capabilities have been added to the IAT to enhance its analysis capabilities. These new capabilities can be used with the Landsat, ASTER, ITRES and SpecTIR datasets.

Spectrum Viewer

The ability to view the spectrum from a specific image pixel or a sample from the included USGS Mineral Spectral Library has been added to the Spectral Angle Mapper (SAM)

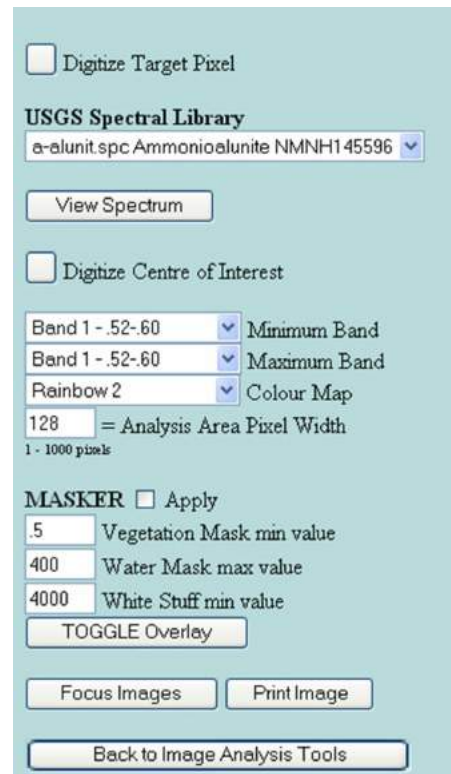


Figure 10. New layout of the 'Spectral Angle Mapper' panel. The 420 entries in the USGS Mineral Spectral Library are available through the pull-down selection box. The 'View Spectrum' button produces a spectrum plot of the selected spectrum.

tool. Once a target pixel has been digitized from the image being analyzed, or one of the library spectra has been selected, the 'View Spectrum' button can be clicked to present a display of the spectrum (Figure 10). The 'Minimum Band' and 'Maximum Band' selection boxes can be used to select the range of contiguous bands to be displayed in the spectrum plot. The selected spectrum, from the image or spectra library, can also be used to perform a SAM analysis on the image simply by clicking on the 'Digitize Centre of Interest' button and then clicking on a point on the image. The ability to view image spectra is a very powerful capability in the interactive investigation of an image (Figure 11).

Spectral Library Reference

The USGS Mineral Spectral Library has been added to the IAT to provide known reference spectra for comparison with spectra from images contained in the IAT. The detailed spectra contained within this library have been resampled to correspond to Landsat, ASTER and SpecTIR bandwidths. The appropriate resampled library is loaded when any of these three image types is being analyzed. The USGS Spectral Library contains laboratory-obtained spectra from 420 minerals. The spectra span the range from 0.3951 to 2.56 μm . As a result of the library spectra only sampling the VNIR and SWIR range of the electromagnetic spectrum, the TIR (Thermal Infrared) bands of ASTER and Landsat are not represented and are not dealt with when comparing to the USGS Spectral Library. The spectra obtained from the spectral library are in reflectance values. Both the ASTER and SpecTIR imagery have been converted to reflectance or relative reflectance values and, as such, the spectral shapes are comparable.

Summary

Eight sites in southern BC have been sampled with high spatial and spectral resolution hyperspectral sensors. The resulting hyperspectral imagery is available for online analysis and integration with other mineral exploration data in MapPlace or downloading for offline analysis. The

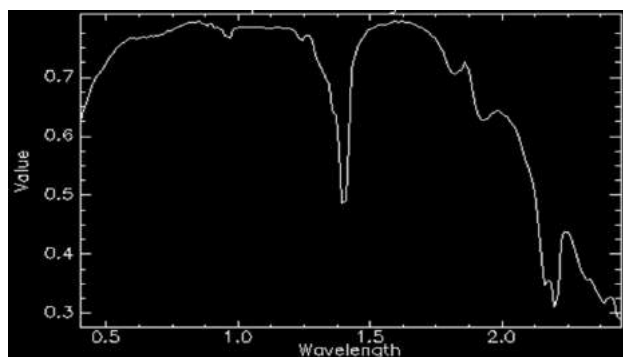


Figure 11. Spectrum plot for kaolinite (kaolin1.spc Kaolinite CM9) from the USGS Spectral Library. This spectrum has been resampled to match the SpecTIR band positions and widths.

purpose of the project was to provide examples within British Columbia of high-quality hyperspectral imagery to allow the exploration community to assess its value in a number of varied situations. As such, the selected target sites include a range of surface and geological characteristics common in BC.

Modifications were made to the IAT to enhance the analysis capabilities of this online toolbox.

This progress report was prepared just as the final data products from SpecTIR were received and ITRES imagery was expected. Additional analysis of the imagery will be performed during the life of this project to highlight the capabilities of this exploration tool.

Acknowledgments

This project was made possible by a grant from Geoscience BC. The BC Ministry of Energy, Mines and Petroleum Resources provided support in the form of Internet hosting of the project products and enabling software on their MapPlace website.

The authors would like to thank J. Zamudio and G. Kirkham for their thorough review of this paper and useful suggestions regarding hyperspectral imagery and analysis.

References

- BC Geological Survey (2007): MapPlace GIS internet mapping system; BC Ministry of Energy, Mines and Petroleum Resources, MapPlace website, URL <<http://www.MapPlace.ca>> [October 2007].
- Clark, R.N., Swayze, G.A., Wise, R., Livo, E., Hoefen, T., Kokaly, R. and Sutley, S.J. (2007): USGS digital spectral library splib06a; United States Geological Survey, Digital Data Series 231, URL <<http://speclab.cr.usgs.gov/spectral.lib06>> [October 2007].
- Goetz, A.F.H. (2007): Hyperspectral imaging and data analysis; Centre for the Study of Earth from Space, University of Colorado, Short Course Notes, 628 p.
- ITRES (2007): SASI 600; ITRES Research, URL <<http://www.itres.com>> [October 2007].
- Kilby, W.E., Kliparchuk, K. and McIntosh, A. (2004): Image analysis toolbox and enhanced satellite imagery integrated into the MapPlace; *in* Geological Fieldwork 2003, BC Ministry of Energy, Mines and Petroleum Resources, Paper 2004-1, pages 209–215.
- Kilby, W.E. (2005): MapPlace.ca image analysis toolbox — phase 2; *in* Geological Fieldwork 2004, BC Ministry of Energy, Mines and Petroleum Resources, Paper 2005-1, pages 231–235.
- Kilby, W.E. and Kilby, C.E. (2006): ASTER imagery for BC — an online exploration resource; *in* Geological Fieldwork 2005, BC Ministry of Energy, Mines and Petroleum Resources, Paper 2006-1 and Geoscience BC, Report 2006-1, pages 287–294.
- Kilby, W.E. and Kilby, C.E. (2006): Examining ASTER imagery with the MapPlace image analysis toolbox — a tutorial manual; BC Ministry of Energy, Mines and Petroleum Resources, Report 2006-1, pages 287–294.

- sources, GeoFile 2006-8 and Geoscience BC, Report 2006-3, 41 p.
- Kilby, W.E. and Kilby, C.E. (2007): ASTER multispectral satellite imagery and product coverage, BC — phase 2; *in* Geological Fieldwork 2006, BC Ministry of Energy, Mines and Petroleum Resources, Paper 2007-1 and Geoscience BC, Report 2007-1, pages 315–318.
- Miles, W.F., Shives, R.B.K., Carson, J., Buckle, J., Dumont, R. and Coyle, M. (2007): Airborne gamma-ray spectrometric and magnetic surveys over the Bonaparte Lake area (NTS 092P), south-central British Columbia; *in* Geological Fieldwork 2006, British Columbia Ministry of Energy, Mines and Petroleum Resources, Paper 2007-1 and Geoscience BC, Report 2007-1, pages 373–374.
- MINFILE (2007): MINFILE BC mineral deposit database; BC Ministry of Energy, Mines and Petroleum Resources, URL <<http://www.em.gov.bc.ca/Mining/Geolsurv/Minfile/>> [October 2007].
- Shives, R.B.K., Carson, J.M., Ford, K.L., Holman, P.B. and Cathro, M. (2004): Helicopter-borne gamma ray spectrometric and magnetic total field geophysical survey, Imperial Metals Corporation's Mount Polley mine area, British Columbia (part of NTS 93A/12); Geological Survey of Canada, Open File 4619 and BC Ministry of Energy, Mines and Petroleum Resources, Open File 2005-10.
- Shives, R.B.K., Holman, P.B. and Rebolledo, L. (2005): Airborne geophysical survey, Fish Lake area, British Columbia (parts of NTS 92O/05NE; 90O/12SE; 92O/12NE; 92O/13SE); Geological Survey of Canada, Open File 2800 and BC Ministry of Energy, Mines and Petroleum Resources, Open File 2005-10, 82 p. and 12 maps.
- Specim (2007): AISADUAL hyperspectral sensor; Spectral Imaging Ltd., information sheet, URL <<http://www.specim.fi>> [October 2007].
- SpecTIR (2007): Airborne hyperspectral imagery; SpecTIR LLC, URL <<http://www.SpecTIR.com>> [October 2007].

Geological Setting of Volcanogenic Massive Sulphide Occurrences in the Middle Paleozoic Sicker Group of the Cowichan Lake Uplift, Port Alberni Area, Southern Vancouver Island, British Columbia (NTS 092F/02, /07)

T. Ruks, Mineral Deposit Research Unit, Department of Earth and Ocean Sciences, University of British Columbia, Vancouver BC, tyler_ruks@hotmail.com

J.K. Mortensen, Mineral Deposit Research Unit, Department of Earth and Ocean Sciences, University of British Columbia, Vancouver BC

Ruks, T. and Mortensen, J.K. (2008): Geological setting of volcanogenic massive sulphide occurrences in the Middle Paleozoic Sicker Group of the Cowichan Lake uplift, Port Alberni area (NTS 092F/02, /07), southern Vancouver Island, British Columbia; *in* Geoscience BC Summary of Activities 2007, Geoscience BC, Report 2008-1, p. 77–92.

Introduction

Volcanogenic strata of the mid-Paleozoic Sicker Group on Vancouver Island (Figure 1) occur in several distinct basement highs (referred to as ‘uplifts’ herein). These rocks host the world-class Myra Falls volcanogenic massive sulphide (VMS) deposit (combined production and proven and probable reserves in excess of 30 million tonnes of Zn-Cu-(Au-Ag) ore), as well as numerous other VMS deposits and occurrences, especially in the Big Sicker Mountain area in the southeastern part of the Cowichan Lake uplift (Figure 1). Three of these deposits, the Lenora, Tye and Richard III (MINFILE occurrences 092B 001, 002, 003) have seen limited historical production, and the Lara deposit (MINFILE occurrence 092B 129), farther to the northwest, also contains a significant drill-indicated resource. Geological mapping (Massey and Friday, 1987; Mortensen, 2005; Ruks and Mortensen, 2006) suggests that the geology of the Mount Sicker area consists mainly of deformed mafic to felsic volcanic and volcanoclastic rocks of the Nitinat and McLaughlin Ridge formations, and high-level intrusions of the Saltspring intrusive suite, as well as abundant gabbroic dikes and sills of the Triassic Mount Hall gabbro.

Geological mapping in the Cowichan Lake uplift of the Port Alberni area (Massey and Friday, 1989) indicates that this area is largely underlain by basalt to basaltic-andesite volcanic rocks of the Duck Lake and Nitinat formations, respectively, in addition to felsic tuffaceous volcanoclastic rocks belonging to the McLaughlin Ridge Formation. The nature of the McLaughlin Ridge Formation rocks in the Port Alberni area is interpreted to represent deposition distal from a volcanic centre, which is thought to be repre-

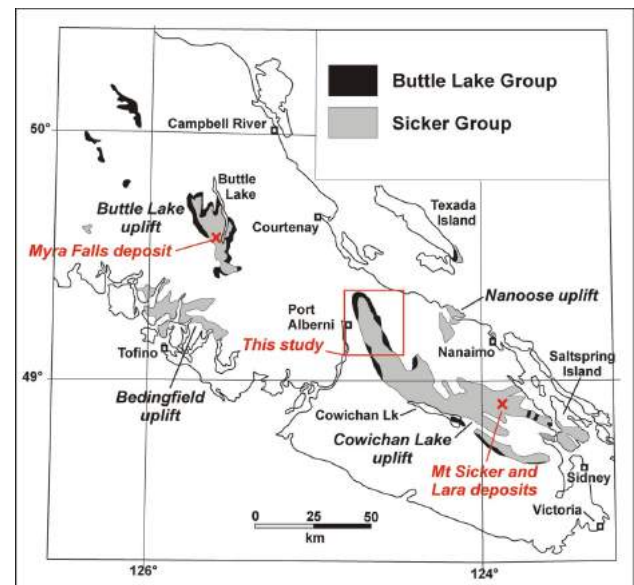


Figure 1. Distribution of Paleozoic strata of the Sicker and Buttle Lake groups on Vancouver Island and the Gulf Islands.

sented in the Saltspring Island–Cowichan Lake area by felsic intrusive rocks of the Saltspring intrusive suite (Massey and Friday, 1989).

The Debbie 3 VMS occurrence is hosted by Sicker Group rocks of the Port Alberni area (MINFILE occurrence 092F 445) but, unlike the majority of VMS occurrences in the Sicker Group, is not associated with felsic volcanic rocks of the McLaughlin Ridge Formation. Instead, the occurrence is interpreted to be hosted by mafic volcanic rocks of the underlying Duck Lake and Nitinat formations and may therefore represent the oldest known VMS mineralization in the Sicker Group.

Abundant iron formations that may be exhalative in origin are also present in Sicker Group rocks of the Port Alberni area (e.g., the Lacy Lake and Esary Lake showings; MINFILE occurrences 092F 245 and 244, respectively). These iron formations are similar to those occurring in

Keywords: Sicker Group, Paleozoic, Vancouver Island, Cowichan Lake uplift, VMS deposit, stratigraphy, U-Pb zircon geochronology, litho geochemistry

This publication is also available, free of charge, as colour digital files in Adobe Acrobat® PDF format from the Geoscience BC website: <http://www.geosciencebc.com/s/DataReleases.asp>.

rocks that are stratigraphically above VMS mineralization at the Myra Falls, Lara, Lenora, Tyee and Richard III occurrences, and are believed to represent oxide-facies iron mineralization related to hydrothermal mineralizing systems similar to those that formed the underlying VMS deposits. As with the Debbie 3 VMS occurrence, however, the iron formations of the Port Alberni area are underlain by mafic volcanic rocks of the Duck Lake or Nitinat formations.

If the Debbie 3 VMS occurrence is indeed the same age as the potential VMS-related exhalative iron formations in the same general area, this makes the Port Alberni area, specifically where it is underlain by rocks of the Nitinat and Duck Lake formations, significantly more prospective for VMS mineralization than was previously appreciated. Logging activity in the area over the past decade has provided abundant new outcrops and greatly improved access, and has prompted a re-examination of the geological setting of VMS mineralization and of the potential for new discoveries in this area.

Both reconnaissance and detailed geological mapping, together with sampling for litho geochemistry, U-Pb zircon dating, and Nd, Hf and Pb isotopic studies, were conducted over a 20-day period in the Port Alberni area in October 2007. This work was concentrated in the vicinity of the Debbie 3 VMS occurrence and the area of potentially correlative exhalative iron formations to the west. This report presents a preliminary version of revised geological mapping in this area, with emphasis on understanding the geology in the vicinity of the Debbie 3 VMS occurrence and the potentially correlative Lacy and Esary Lake exhalative iron formations.

Regional Geology of the Sicker Group

The mid-Paleozoic Sicker Group on southern and central Vancouver Island represents the stratigraphically lowest portion of the Wrangellia Terrane. Equivalents of the Sicker Group are not present in Wrangellia in northwestern British Columbia, southwestern Yukon and southern Alaska, where the oldest rock units are the Skolai Group, which is no older than Pennsylvanian (e.g., Katvala, 2006). This, and other differences between the Wrangellian stratigraphy on Vancouver Island and that in more northerly exposures, emphasizes the lack of understanding regarding much of Wrangellia (e.g., Katvala, 2006) and the need for further studies. The Cowichan Lake uplift on Vancouver Island and adjacent portions of the Gulf Islands, which is the main focus of this study, is the largest of four uplifts that expose the Sicker and overlying late Paleozoic Buttle Lake groups (Figure 1).

Previous detailed studies of the Sicker Group have focused mainly on the stratigraphic setting of VMS mineralization at the Myra Falls deposits in the Buttle Lake uplift (Figure 1; e.g., Juras, 1987; Barrett and Sherlock, 1996). Re-

gional mapping of the Cowichan Lake uplift by Massey and Friday (1987, 1989) and Yorath et al. (1999) led to an interpreted stratigraphic framework that may be applicable to the entire Sicker Group (Figure 2). This stratigraphic framework, however, is based on mapping in only one of the four main uplifts of Sicker Group rocks, and is supported by a very limited amount of biostratigraphic and isotopic age data (e.g., Brandon et al., 1986). Major along- and across-strike facies changes and geochemical variations are to be expected in submarine volcanic sequences such as the one that forms the Sicker Group; hence, the regional applicability of the proposed stratigraphic framework of Yorath et al. (1999) must be tested with detailed mapping and subsequent litho geochemical and U-Pb dating studies. This is critical for regional exploration for VMS deposits within the Sicker Group. For example, the questions of whether VMS deposits and occurrences in the Cowichan Lake uplift are all of the same age, and whether their hostrocks are directly correlative with those that host the Myra Falls deposit, are of obvious importance.

The Sicker Group within the Cowichan Lake uplift is presently interpreted to represent three distinct and regionally mappable volcanic and volcanoclastic assemblages that together are thought to record the evolution of an oceanic magmatic arc (Massey, 1995; Yorath et al., 1999). The lowermost Duck Lake Formation yields mainly normal mid-ocean-ridge basalt (N-MORB) geochemical signatures (Massey, 1995) and is interpreted to represent the oceanic crust basement on which the Sicker arc was built. The upper portions of the Duck Lake Formation yield tholeiitic to calcalkaline compositions and may represent primitive arc rocks. The Duck Lake Formation is overlain by the Nitinat Formation, which comprises mafic, submarine, volcanic and volcanoclastic rocks with dominantly calcalkaline compositions and trace-element signatures typical of volcanic arc settings. These rocks are interpreted as an early stage of arc development. The andesitic to mainly dacitic and rhyolitic McLaughlin Ridge Formation that overlies the

Muller, 1977 (Vancouver Island)		Juras, 1987 (Buttle Lake Uplift)		Yorath et al., 1999 (Alberni area)	
Sicker Gp	X	Buttle Lake Gp	Henshaw Fm	Buttle Lake Gp	St. Mary Lk Fm
	Buttle Lk Fm		Mt Mark Fm		Mt Mark Fm
	Sediment Sill Unit				Fourth Lk Fm
	Myra Fm	Sicker Gp	Flower Ridge Fm	Sicker Gp	McLaughlin Ridge Fm
	Nitinat Fm		Thelwood Fm		Nitinat Fm
		Myra Fm		Duck Lk Fm	
		Price Fm			

Figure 2. Stratigraphic nomenclature for the Sicker and Buttle Lake groups on Vancouver Island (Yorath et al., 1999).

Nitinat and hosts the Myra Falls deposit reflects a more evolved stage of arc activity. Eruption of Nitinat volcanic and volcanoclastic rocks appears to have occurred from several widely scattered centres, whereas the McLaughlin Ridge Formation within the Cowichan Lake uplift is thought to represent eruption from one or more major volcanic edifices. The abundance of proximal felsic volcanoclastic rocks and the presence of voluminous comagmatic felsic intrusions (Saltspring intrusions) in the Saltspring Island and Duncan areas (Figure 1) indicates that one of these major volcanic centres was located in this area. Plant material and trace fossils indicate that at least a minor amount of the McLaughlin Ridge volcanism occurred in a subaerial setting. In the Port Alberni area, the McLaughlin Ridge Formation comprises felsic, fine-grained tuffaceous volcanoclastic and epiclastic rocks, indicating deposition distal from a volcanic centre. Deposition of sedimentary and volcano-sedimentary rocks of the overlying Fourth Lake Formation of the Buttle Lake Group followed the cessation of Sicker arc magmatism, and scarce mafic volcanic rocks contained within the Fourth Lake Formation yield enriched tholeiitic rather than the calcalkaline compositions that characterize the McLaughlin Ridge. Massey (1995) speculated that the Buttle Lake Group may represent a marginal-basin assemblage that developed on top of the Sicker arc.

Studies of the Sicker and Buttle Lake groups on southern Saltspring Island at the southeastern end of the Cowichan Lake uplift by Sluggett (2003) and Sluggett and Mortensen (2003) provided new U-Pb zircon age constraints on both felsic volcanic rocks of the McLaughlin Ridge Formation and several bodies of Saltspring intrusions. This work demonstrates that two distinct episodes of felsic magmatism occurred in this portion of the Cowichan Lake uplift. One sample of felsic volcanic rocks from the McLaughlin Ridge Formation and three samples of Saltspring intrusions yielded U-Pb ages in the range 359.1–356.5 Ma. A somewhat older U-Pb age of 369.7 Ma was obtained from a separate body of the Saltspring intrusions at Burgoyne Bay on the southwest side of Saltspring Island, indicating that magmatism represented by the McLaughlin Ridge Formation and associated Saltspring intrusions occurred over a time span of at least 15 million years. There is insufficient age control available at this point to determine whether the magmatism was continuous or episodic during this time period.

Results of New Mapping in the Port Alberni Area

Mapping of Sicker Group bedrock geology and sampling for lithochemistry, U-Pb zircon and Ar-Ar hornblende geochronology, and Pb, Nd and Hf isotope tracer studies was conducted in the Port Alberni area (Figure 3). This work was concentrated in three main areas: 1) in the vicin-

ity of the Lacy Lake and Esary Lake iron formations, located between Lacy and Horne lakes; 2) in the vicinity of a previously mapped dacite unit to the north of the Port Alberni highway; and 3), in the vicinity of the Debbie 3 VMS occurrence, located to the south of the Port Alberni highway (Figure 3). Mapping was conducted using ESRI's Arcpad™ 7 on an HP IPaq HX4700 Pocket PC hardwired to a Garmin 76CS GPS. The British Columbia Geological Survey's regional geology compilation for UTM zone 10, southwestern British Columbia was used (Massey et al., 2005). Bedrock outcrop in both areas is moderate, with the best exposures contained in logging-road cuts. Off-road exposures are typically covered with thick layers of moss and organic detritus, often in forested, low-light conditions.

Lacy Lake–Horne Lake Area

Stratified Rocks

The oldest rocks in the Lacy Lake–Horne Lake area are assigned to the Duck Lake Formation (Figure 4; Massey and Friday, 1989). These consist largely of massive, dominantly aphyric to weakly plagioclase-phyric, variably hematite-altered basalt flows, flow breccias, lapilli tuffs, and tuff breccias (Figure 5). In the vicinity of the Lacy Lake iron formation, weakly to strongly hematite-altered, commonly highly vesicular basalt flow autobreccias, lapilli tuffs, and tuff breccias are abundant (Figure 5a). Carbonate alteration is locally abundant in these volcanic rocks as pink ankerite veins up to 7 cm wide, and as carbonate amygdules up to 3 mm in size (Figure 5b). Ankerite veining is most prevalent in basaltic rocks with the strongest hematite alteration. Duck Lake Formation lapilli and tuff breccias in this area are commonly rich in strongly hematite-altered, vesicular, variably carbonate amygdule-bearing basalt clasts (Figure 5c).

Jasperoid iron formation of the Lacy Lake showing (MINFILE 092F 245) is interbedded with green- to cream-coloured chert and is in very sharp contact with underlying hematite- and carbonate-altered autobreccia assigned to the Duck Lake Formation (Figures 5a and 6). The iron formation itself is dark red and silica rich. The Lacy Lake iron formation showing is approximately 21 m thick and passes gradationally upwards into a package of interbedded green chert- and silica-rich mudstone and siltstone. Farther upsection, interbedded green chert- and silica-rich mudstone grade into a package of moderately to well-sorted, green-grey, intermediate volcanic crystal tuff, sandstone and siltstone. These units display excellent normal graded bedding, indicating they are upright (Figure 7). Still farther upsection, a dominantly matrix-supported, hematitic heterolithic breccia to boulder conglomerate becomes prevalent. This unit is strongly heterolithic and varies from matrix to clast supported, with clasts up to boulder size consisting of angular, intermediate volcanic sand-

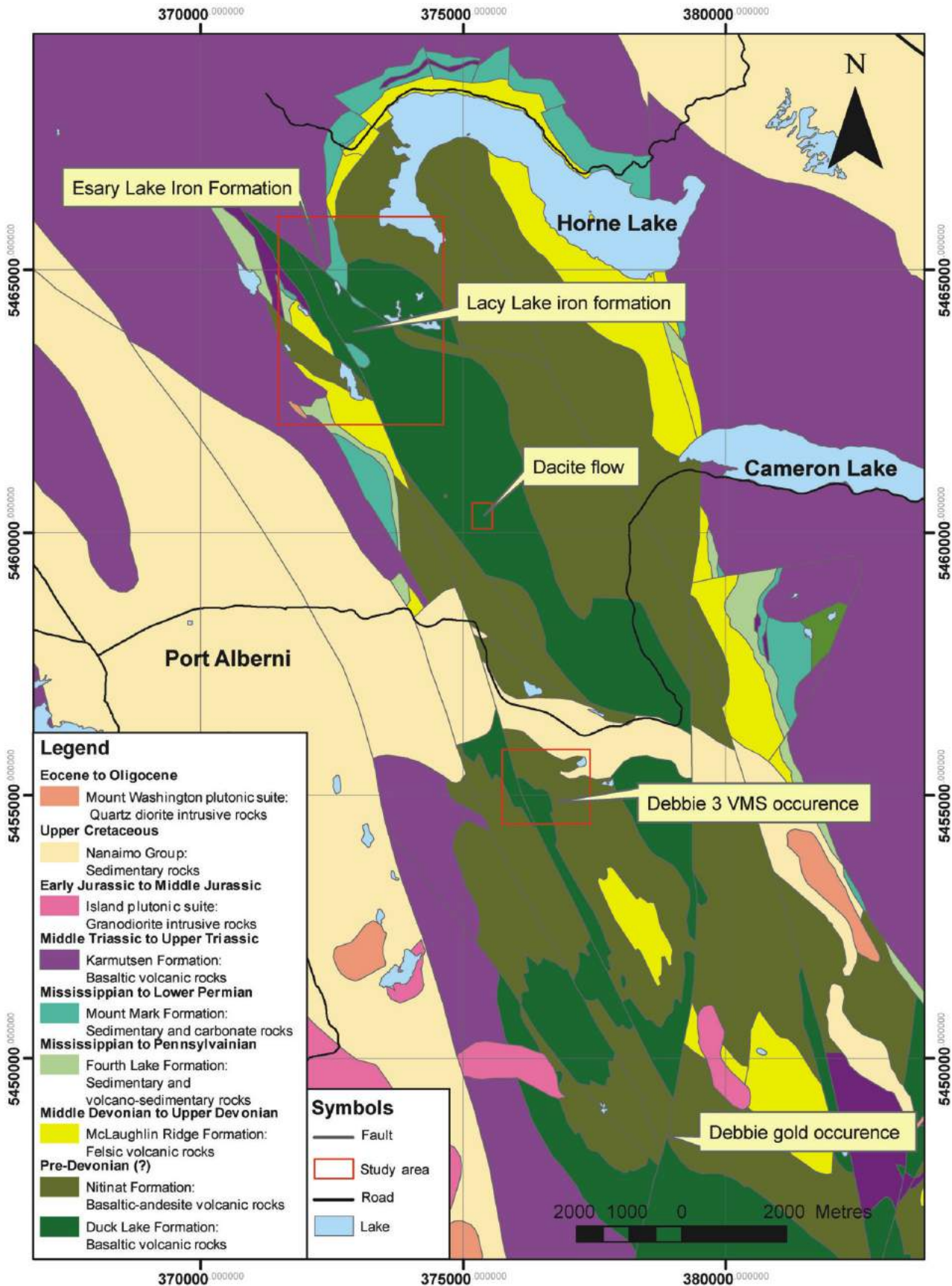


Figure 3. Regional geology (after Massey et al., 2005) of the Port Alberni area, with areas of study outlined in red.

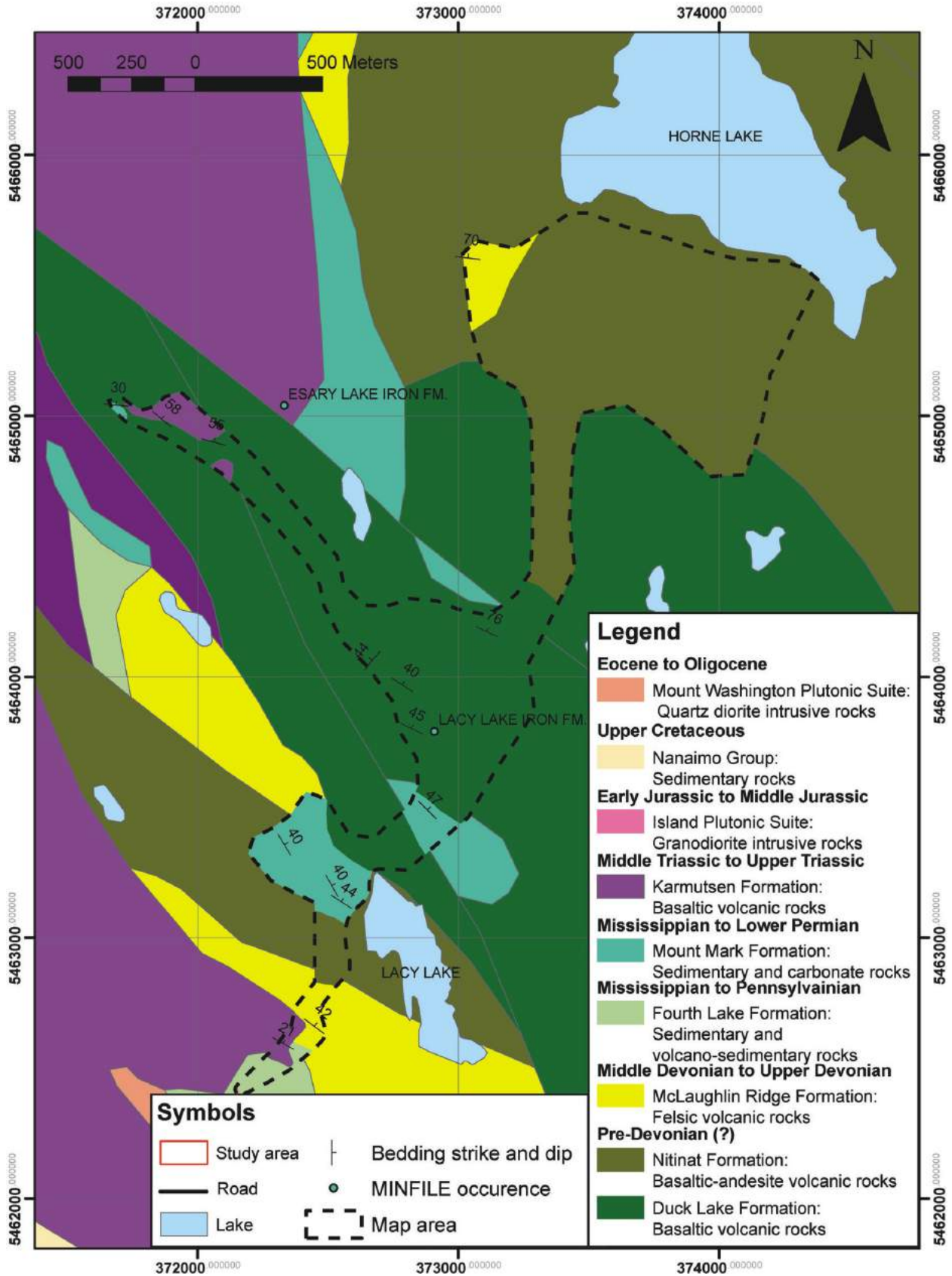


Figure 4. New geological mapping in the Lacy Lake–Horne Lake area, Port Alberni area. Regional geology *after* Massey et al. (2005).

stone; dark red, angular, jasperoid iron formation clasts; dark green, vesicular basalt clasts; and cream to white, subangular to rounded, variably crinoidal limestone boulders (Figure 8).

In a second outcrop, approximately 450 m to the northwest of the Lacy Lake iron formation showing, jasperoid iron

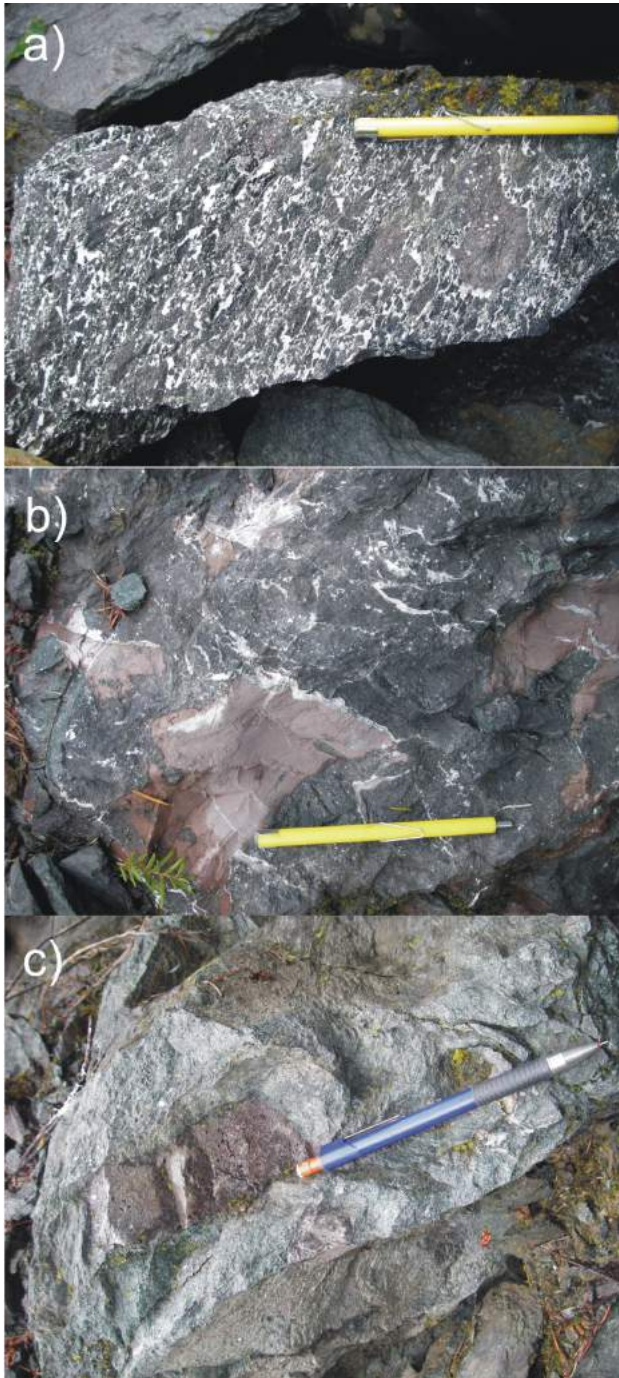


Figure 5. Basaltic volcanic rocks of the Duck Lake Formation in the Lacy Lake–Horne Lake area: **a)** hematite-altered basalt autobreccia with carbonate matrix; **b)** carbonate amygdule-bearing basalt with pink carbonate (ankerite) veins; **c)** basalt tuff-breccia containing vesicular, hematite-altered clasts.

formation with increasing elevation grades into hematite-bearing, intermediate volcanic sandstone, which becomes progressively more clast rich and coarse grained until it ul-

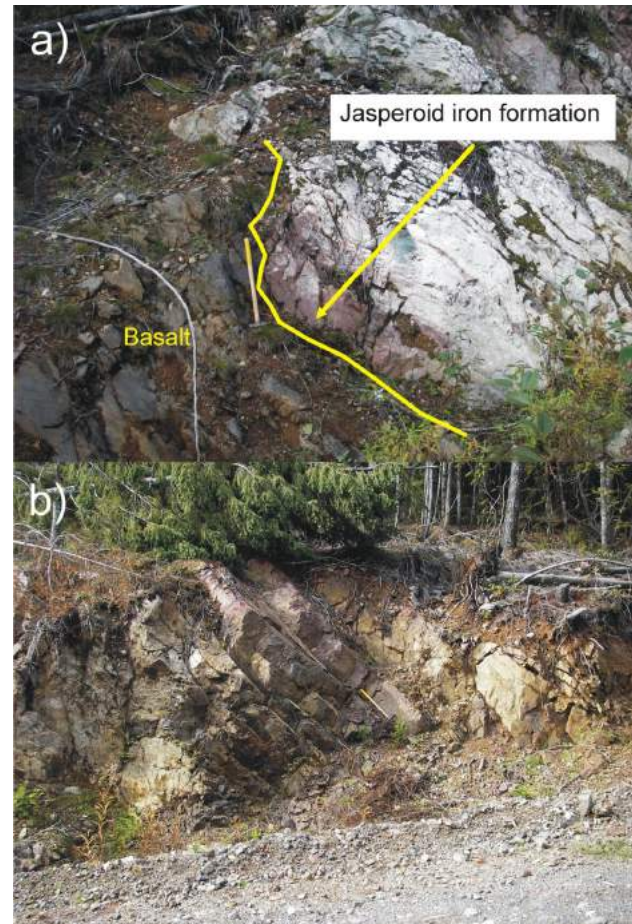


Figure 6. **a)** Sharp contact between underlying basalt and jasperoid iron formation and green chert of the Lacy Lake occurrence (MINFILE 092F 245). **b)** Jasperoid iron formation of the Lacy Lake MINFILE occurrence is approximately 21 m in thickness.



Figure 7. Moderately to well-sorted, green-grey, intermediate volcanic crystal tuff, sandstone and siltstone exhibiting normal grading.

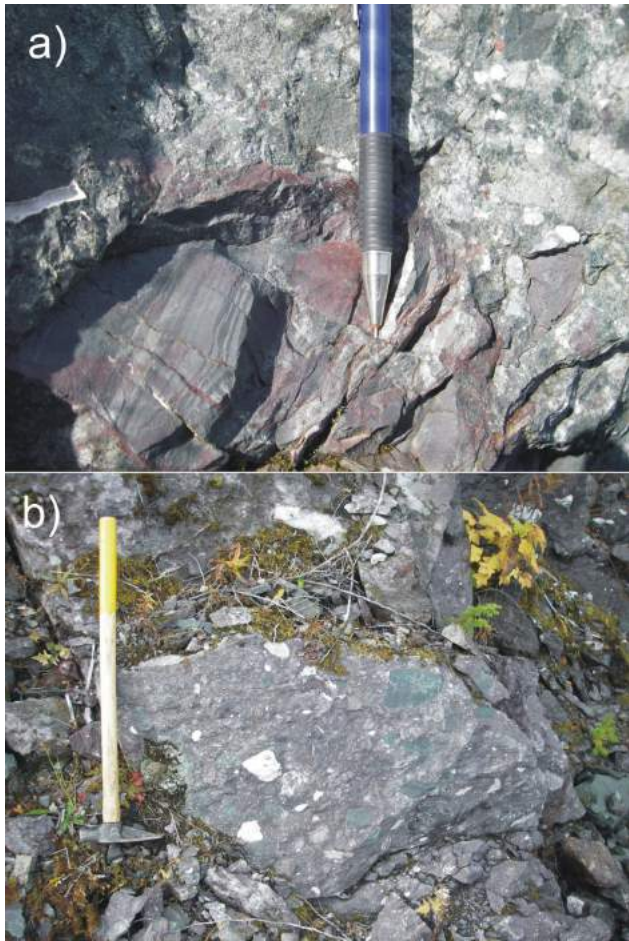


Figure 8. a) and b) Matrix- to clast-supported heterolithic breccia, with clasts up to boulder size consisting of angular, intermediate volcanic sandstone; dark red, angular, jasperoid iron formation clasts; dark green, vesicular basalt clasts; and cream to white, subangular to rounded, variably crinoidal limestone boulders.



Figure 9. Interbedded jasperoid iron formation and chloritic siltstone, approximately 450 m northwest of the Lacy Lake occurrence (MINFILE 092F 245).

timately becomes hematitic crinoidal limestone-bearing heterolithic breccia (Figures 9 and 10). The presence of crinoidal limestone as clasts within the heterolithic breccia that sits apparently conformably above the Lacy Lake iron formation suggests that these iron formations and the accompanying sedimentary rocks may not be part of the Duck Lake Formation, as previously interpreted, but instead may be part of the Fourth Lake Formation, which is believed to be, in part, temporally equivalent to crinoid-bearing limestone of the Mt. Mark Formation (Buttle Lake Group; Yorath et al., 1999). Float boulders of dacite tuff-breccia were also observed proximal to an outcrop of crinoidal limestone-bearing heterolithic breccia (Figure 11a). These boulders are highly angular in shape, suggesting local sourcing, and contain abundant feldspar-phyric dacite clasts, with minor, rounded, hematite-altered basaltic-andesite clasts, (Figure 11b). In addition, a small roadbed outcrop of grey-green, pebble to boulder conglomerate with abundant subrounded pebble- to boulder-size quartz-feldspar-phyric rhyolite clasts is present near the contact between rocks assigned to the Duck Lake Formation and those assigned to the Nitinat Formation, to the north (Figure 12).

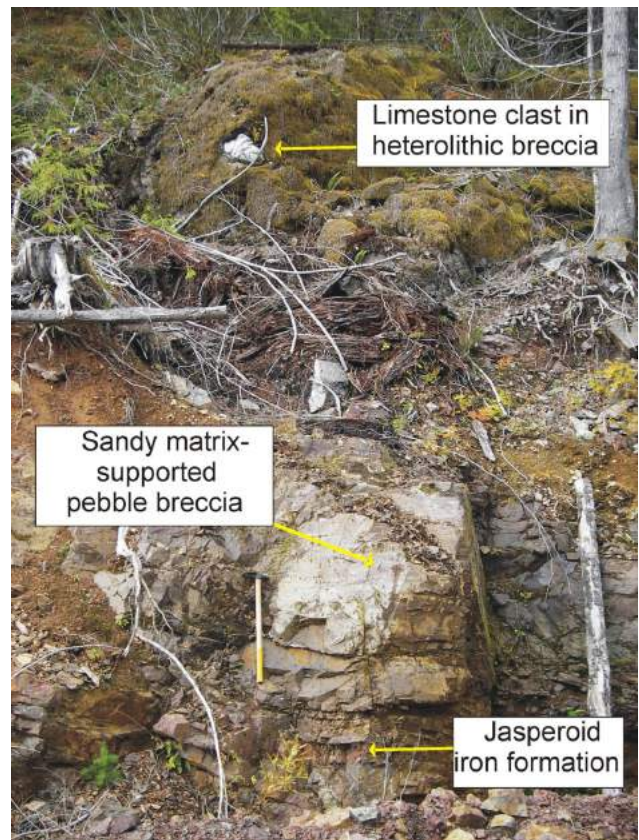


Figure 10. Jasperoid iron formation with increasing elevation grades into hematite-bearing, intermediate volcanic sandstone, which becomes progressively more clast rich and coarse grained until it ultimately becomes hematitic crinoidal limestone-bearing heterolithic breccia.

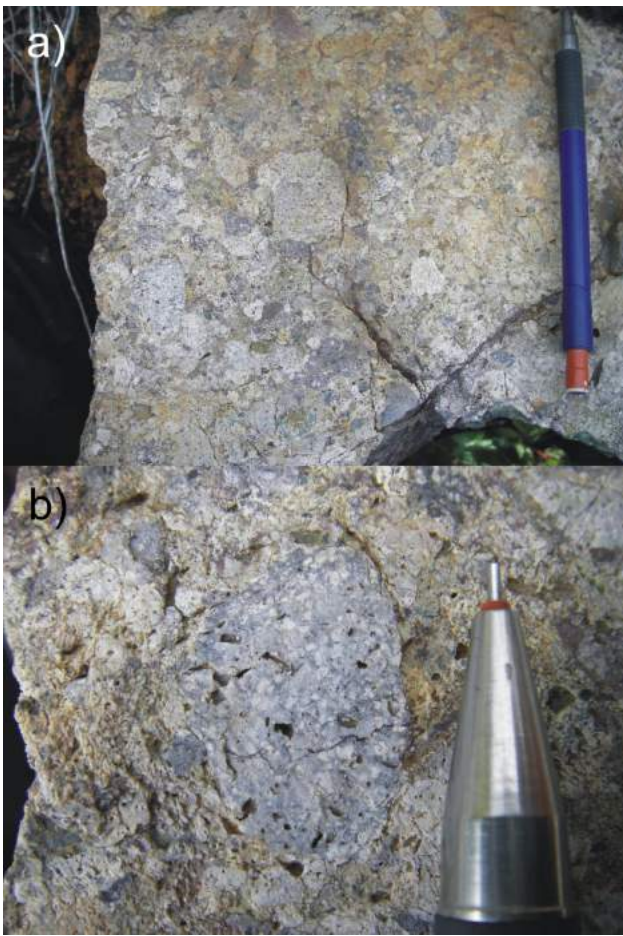


Figure 11. a) Float boulders of dacite tuff-breccia located proximal to an outcrop of crinoidal limestone-bearing heterolithic breccia. b) Close-up of dacite tuff-breccia boulders that shows them to be highly angular, suggesting local sourcing, and to contain abundant subangular to subrounded feldspar-phyric dacite clasts, with minor, rounded, hematite-altered basaltic-andesite clasts.



Figure 12. Clasts of pebble- to boulder-size quartz-feldspar-phyric rhyolite clasts are found in a small roadbed outcrop of grey-green, pebble to boulder conglomerate near the contact between rocks assigned to the Duck Lake Formation and those assigned to the Nitinat Formation, to the north.

The presence of felsic volcano-sedimentary rocks suggests that the sedimentary rocks in this area are part of the McLaughlin Ridge Formation or possibly the Fourth Lake Formation. Furthermore, if the Lacy Lake iron formations are indeed hosted by the Fourth Lake or uppermost McLaughlin Ridge Formation, this suggests that underlying mafic volcanic rocks in this area, which are in sharp contact with the iron formations, may represent a component of mafic volcanism belonging to the McLaughlin Ridge or Nitinat Formation. Exhalitive iron formations are abundant elsewhere in the Sicker Group, hosted in rocks assigned to the Fourth Lake and Thelwood formations of similar age, which stratigraphically overlie VMS mineralization hosted by the McLaughlin Ridge Formation in the eastern Cowichan Lake and Buttle Lake areas, respectively. To constrain the age of the Lacy Lake iron formations, abundant samples of iron formation and associated chert were taken for possible radiolarian biostratigraphic studies.

Rocks assigned to the Nitinat Formation were observed in two main areas. First, strongly pyroxene-phyric basaltic-andesite agglomerate was observed on the south side of



Figure 13. a) Pyroxene-phyric basaltic-andesite agglomerate of the Nitinat Formation. b) Pyroxene phenocrysts in basaltic-andesite clast; in places, the pyroxene phenocrysts can reach 1 cm in size.

Lacy Lake, with the best examples found directly beneath a power line (Figure 13a). Here, euhedral, green pyroxene phenocrysts constitute up to 5% of the rock and reach up to 1 cm in size (Figure 13b). Nitinat Formation volcanic rocks in this location appear to be in fault contact along their northern margin on the west side of Lacy Lake with a belt of Mt. Mark Formation crinoidal limestone. The southern margin of this outcrop of Nitinat Formation volcanic rocks appears to be in contact with felsic tuffaceous rocks belonging to the McLaughlin Ridge Formation.

The second main area of Nitinat Formation observed in this study occurs along the southern shore of Horne Lake and extends approximately 1500 m to the south, where it is in contact with mafic volcanic rocks of the Duck Lake Formation. Nitinat Formation along the southern edge of Horne Lake comprises mostly pyroxene-phyric agglomerate, tuff breccia and lesser lapilli tuff. Mapping during this study has identified a zone of Nitinat Formation basaltic-andesitic volcanic rocks extending well into an area previously mapped as Duck Lake Formation basalt. To accommodate this new zone, the contact between the Nitinat and Duck Lake formations south of Horne Lake has been extended an additional 600 m to the south (Figure 4).

Felsic volcanic rocks assigned to the McLaughlin Ridge Formation in this study were encountered in two areas (Figure 4). The southernmost exposure of this formation in the study area is located south of Lacy Lake. It comprises mainly light green-grey, dacitic ash tuff with small feldspar crystals; medium-grained, dacitic volcanic sandstone; and heterolithic, dacitic lapilli tuff, consisting of chert clasts up to 4 mm in size, dark green, highly chlorite-altered andesite clasts up to 4 mm in size, and medium to light green, strongly sericite-altered dacite clasts up to 5 mm in size set in a matrix that may contain fine-grained feldspar and quartz crystals (Figure 14a). The northernmost exposure of McLaughlin Ridge Formation in the study area comprises largely well-sorted, medium-grained arkosic sandstone, and thinly bedded to laminated mudstone, siltstone and buff- to creamy-weathering chert, with potential felsic ash tuff components (Figure 14b, c). Finer grained McLaughlin Ridge sedimentary rocks in this area exhibit normal graded bedding, indicating an upright orientation (Figure 14a).

Rocks belonging to the Fourth Lake Formation (Yorath et al., 1999) were recognized to the south of Lacy Lake. This small exposure, heavily inundated with basaltic dikes belonging to the Karmutsen Formation, consists of thinly bedded, cream-coloured chert; black mudstone; grey siltstone; and grey to buff, well-sorted, fine-grained sandstone (Figure 15).

A significant zone of crinoidal limestone and associated sedimentary rocks belonging to the Mt. Mark Formation of the Buttle Lake Group has been recognized along the west-

ern shore of Lacy Lake, in areas previously mapped as Nitinat and McLaughlin Ridge formations. These carbonate rocks are typically medium grey to buff, medium-grained, sandy-textured crinoidal packstone with up to 4% by volume of crinoid ossicles up to 4 mm in diameter (Figure 16a). Lesser amounts of darker grey wackstone and



Figure 14. Felsic volcano-sedimentary rocks of the McLaughlin Ridge Formation: **a)** dacitic heterolithic lapilli tuff; **b)** well-sorted, medium-grained arkosic sandstone, siltstone and thinly bedded to laminated mudstone; **c)** white-weathering, laminated chert or cherty tuff.

white-weathering radiolarian chert are also present (Figure 16b). The western limits of this zone were not determined during this study. This package of Mt. Mark Formation carbonate and sedimentary rocks was traced approximately 500 m to the northwest of Lacy Lake.

Intrusive Rocks

Basaltic to diabasic volcanic rocks belonging to the Karmutsen Formation are abundant in the field area, typically occurring as large dikes (Figure 17a). They are typically dark green to black, moderately magnetic and dominantly equigranular, with acicular hornblende and plagioclase phenocrysts averaging 1 mm in length.

Hornblende granodiorite intrusions assigned to the Mount Washington intrusive suite are present in the field area, but are less abundant than basaltic dikes of the Karmutsen Formation. These rocks are typically porphyritic, with up to 30% medium-grained feldspar phenocrysts and 1–2% hornblende phenocrysts. In places, hornblende phenocrysts can be up to 2 cm in length. These rocks tend to form dikes and small intrusions ranging from 10 to 500 m in

length, often with excellent chilled margins at their contacts (Figure 17b).

Structural Geology of the Lacy Lake–Horne Lake Area

Bedding of sedimentary and volcano-sedimentary rocks in the Lacy Lake–Horne Lake area is dominantly northwest striking, with moderate dips to the northeast (Figure 4). Rare disruptions to this fabric were observed approximately 350 m northwest of the Lacy Lake iron formation, and may indicate the hinge area of a localized, tight, parasitic, isoclinal antiformal structure related to regional F_1 folding.

Felsic Volcanic Rocks of the Duck Lake Formation

A minor amount of geological mapping and sampling was focused in the immediate vicinity of a quartz-feldspar-phryic dacite flow-dome hosted in Duck Lake Formation basaltic volcanic rocks to the south of the BC Tel microwave tower, north of the Port Alberni highway (Figure 3).



Figure 15. Sedimentary rocks of the Fourth Lake Formation: **a)** thinly bedded chert, siltstone and mudstone; **b)** laminated chert and mudstone.



Figure 16. Carbonate and sedimentary rocks of the Mt. Mark Formation: **a)** grey to buff, medium-grained, sandy-textured crinoidal packstone with up to 4% crinoid ossicles up to 4 mm in diameter; **b)** white-weathering radiolarian chert.

The goal of this mapping was to elucidate whether or not this unit was an intrusion of McLaughlin Ridge Formation age or a previously unrecognized felsic volcanic component of the dominantly basaltic Duck Lake Formation that would be datable by U-Pb zircon geochronology.

Previous workers have interpreted this quartz-feldspar-phyric dacite as a flow, and have traced it for approximately 1.5 km along strike (Laanela et al., 1987). During the course of this study, both massive dacite porphyry and dacite breccia were observed in roadcut outcrops. Massive dacite porphyry in this area is characterized by large, buff-to creamy-weathering outcrops with 0.5% feldspar and quartz phenocrysts up to 1 mm in size (Figure 18a). Feldspar is the dominant phenocryst phase, with quartz phenocrysts rare to absent in hand sample. Fresh surfaces are grey-green in colour. Chlorite-altered phenocrysts (possibly biotite) that form 0.25–0.5% of the rock are also present. Weak to moderate sericite alteration is present locally, as are carbonate veinlets and rare disseminated pyrite. Rare chalcopyrite is also locally present. Dacite breccia was rec-

ognized approximately 150 m to the northwest of the main dacite body, and consists of abundant, variably feldspar-phyric, variably silica-altered, angular dacite clasts up to 10 cm in size, commonly with autobrecciated margins (Fig-

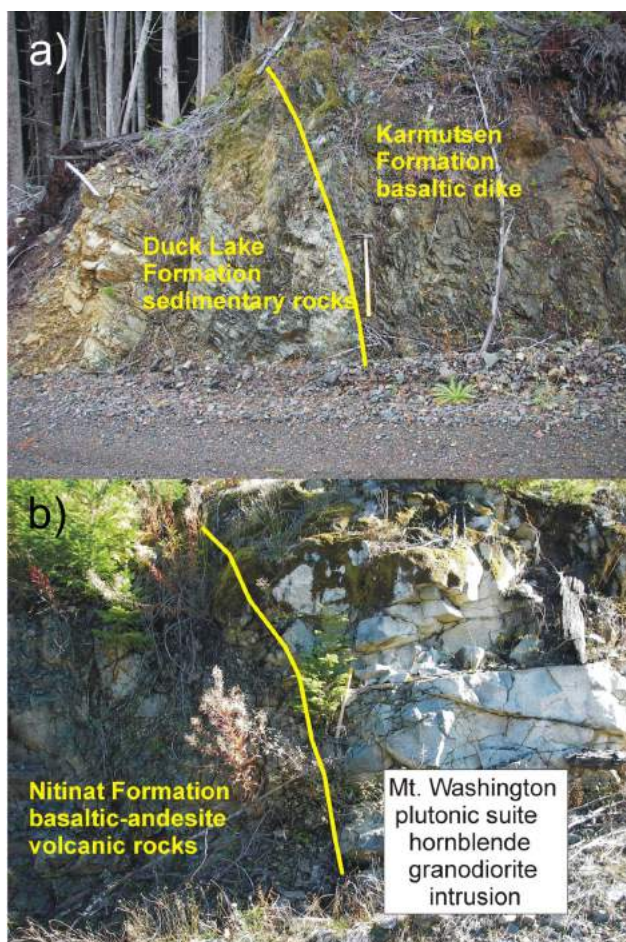


Figure 17. a) Karmutsen Formation basaltic dike cuts sedimentary rocks assigned to the Duck Lake Formation. b) Intrusion of hornblende granodiorite cuts basaltic-andesite rocks of the Nitinat Formation.



Figure 18. a) Massive feldspar+quartz-phyric dacite flow in basalt assigned to the Duck Lake Formation. b) Dacite breccia with strongly silica+sericite-altered clasts, often containing sulphide mineralization; crosscutting quartz-carbonate veinlets contain trace chalcopyrite and bornite. c) Autobrecciated dacite clast margins and intensely silica+sericite-altered clasts with pyrite±chalcopyrite mineralization.

ure 18b). The most intensely silica-altered clasts commonly contain fine-grained disseminated sulphide (pyrite±chalcopyrite) mineralization (Figure 18c). Sulphide blebs and possible sulphide clasts up to 4 cm in size are also present in the breccia. The dacite breccia is crosscut by quartz-carbonate veinlets, some of which contain trace chalcopyrite and bornite.

Debbie 3 Volcanogenic Massive Sulphide Occurrence

The Debbie 3 volcanogenic massive sulphide occurrence (MINFILE occurrence 092F 445), currently owned by Bitterroot Resources Ltd., occurs in mafic volcanic and volcano-sedimentary rocks assigned to the Duck Lake and Nitinat formations, and is located along the Cameron Main logging road, close to the intersection with the Mt. Arrowsmith ski road. The showing consists of four stratiform lenses of banded massive sphalerite, with minor chalcopyrite and galena, each band ranging between 5 and 20 cm in thickness. The best grade obtained from sampling of this mineralization by previous workers includes 14.1% Zn, 0.87% Pb and 0.12% Cu over a 20 cm thickness (MINFILE, 2007). The mineralization is hosted in fine-grained chloritic schist with variable carbonate, sericite and silica alteration.

Mapping of the Debbie 3 area has identified alternating zones of massive basaltic and basaltic-andesite volcanic rocks, with variably chlorite-, sericite- and silica-altered mafic schist (Figure 19). Mafic volcanic rocks in this area tend to occur as robust, massive outcrops with little to no foliation. In the northern portion of the map area, these outcrops comprise dominantly massive, grey-green, pyroxene-phyric basalt flows and agglomerate. Pyroxene phenocrysts can reach abundances of 0.5–1.5% and sizes up to 3–4 mm. Feldspar-phyric basalt flows with abundant chlorite amygdules become more abundant towards the west. Here, variably epidote-altered plagioclase phenocrysts with diffuse margins average 1.5 mm size, and chlorite amygdules reach abundances up to 3.5% and sizes up to 1–2 mm. Epidote alteration patches up to 5–10 cm in width are also present. In the southern portion of the map area, massive, largely unfoliated mafic volcanic rocks comprise mainly chlorite amygdule-bearing basalt flows, pyroxene-phyric basaltic-andesite agglomerate and mafic lapilli tuff with abundant flattened, chlorite-altered pumice clasts. Mafic schist in both the northern and southern portions of the map area comprises strongly foliated, strongly chlorite-altered mafic tuff with variable carbonate, sericite and silica alteration (Figure 20a). Mineralization is observed in this mafic schist only in the southern part of the area, and is present as stratiform bands of massive sphalerite with minor chalcopyrite and galena that reach up to 20 cm in thickness (Figure 20b). Strong carbonate and sericite alteration of the mafic schist is present in the immediate vicinity of sulphide mineralization. Approximately

320 m west of the showing, a zone of intensely silica+sericite+carbonate-altered mafic schist is associated with quartz-carbonate and blue-green gypsum veins (Figure 21). In this zone, quartz-carbonate veins carry blebs of chalcopyrite. The presence of this stockwork-style sulphide mineralization to the west of the stratiform sulphide mineralization of the Debbie 3 VMS occurrence suggests that rocks to the west of the main showing may reflect deeper stratigraphic levels, and the stratigraphic package may young to the east.

Debbie 3 Structural Geology

Structures in the area are best observed in fine-grained mafic volcanic rocks in the vicinity of the Debbie 3 occurrence (Figure 19). These rocks, typically chloritic schist, display a prominent northwest strike, with moderate to steep dips to the northeast. Folding of this fabric was observed only in two areas. In the northwestern part of the map area, chloritic schist was observed to strike northeast for a limited extent, with weak dips to the southeast. This may represent F₂ kink folding. Additional kink folding was observed in chloritic schist approximately 415 m west of the Debbie 3 occurrence. Here, warping of the main fabric is represented by small, outcrop-scale, F₂ kink folds with hinges plunging steeply towards the northeast.

New Sulphide Mineralization and Implications for VMS Exploration in the Alberni Area

Two new occurrences of significant sulphide mineralization were discovered during the course of this mapping. The first, along the power line overlooking the south side of Lacy Lake (Figure 4), occurs near the contact between pyroxene-phyric basaltic-andesite agglomerate of the Nitinat Formation and overlying felsic tuffaceous rocks belonging to the McLaughlin Ridge Formation. Here, a 20 m long float train consists of bleached, highly sericite-, silica- and fuchsite-altered subangular boulders up to 40–50 cm in size that contain up to 4% pyrite, occurring as disseminations, stringers and blebs up to 2 cm in size (Figure 22). This float train was traced into a small exposure of hematite+chlorite-altered basalt. Trenching of this outcrop exposed bleached, strongly sericite+silica-altered, pyrite-mineralized rock similar to that observed in the nearby mineralized float. This sulphide occurrence is significant in that it occurs at the contact between mafic to intermediate volcanic rocks of the Nitinat Formation and overlying felsic tuffaceous volcanic rocks of the McLaughlin Ridge Formation. In the Buttle Lake uplift, this contact is associated with the giant HW deposit, which has a pre-mining inventory of 16.5 million tonnes of ore with an average grade of 2.2 g/t Au, 39.6 g/t Ag, 1.7% Cu, 0.4% Pb and 4.3% Zn (Robinson, 1992). In the Port Alberni area, this contact may be especially significant, as the lack of overlying felsic volcanic rocks intimately associated with high-energy eruptive activity (i.e., rhyolite flows, felsic tuff-breccia, etc.)

would provide ample time for the accumulation of VMS mineralization.

The second significant new sulphide occurrence discovered during the course of this mapping is associated with the dacite flow-dome within basalt assigned to the Duck

Lake Formation that was described above (Figure 3; Massey and Friday, 1989). Here, disseminated to bleb-sized pyrite±chalcopyrite mineralization is associated with strongly silica-altered clasts in a dacite breccia occurring along the flanks of a massive, feldspar+quartz-phyric dacite dome (Figure 18c). In addition, both the massive

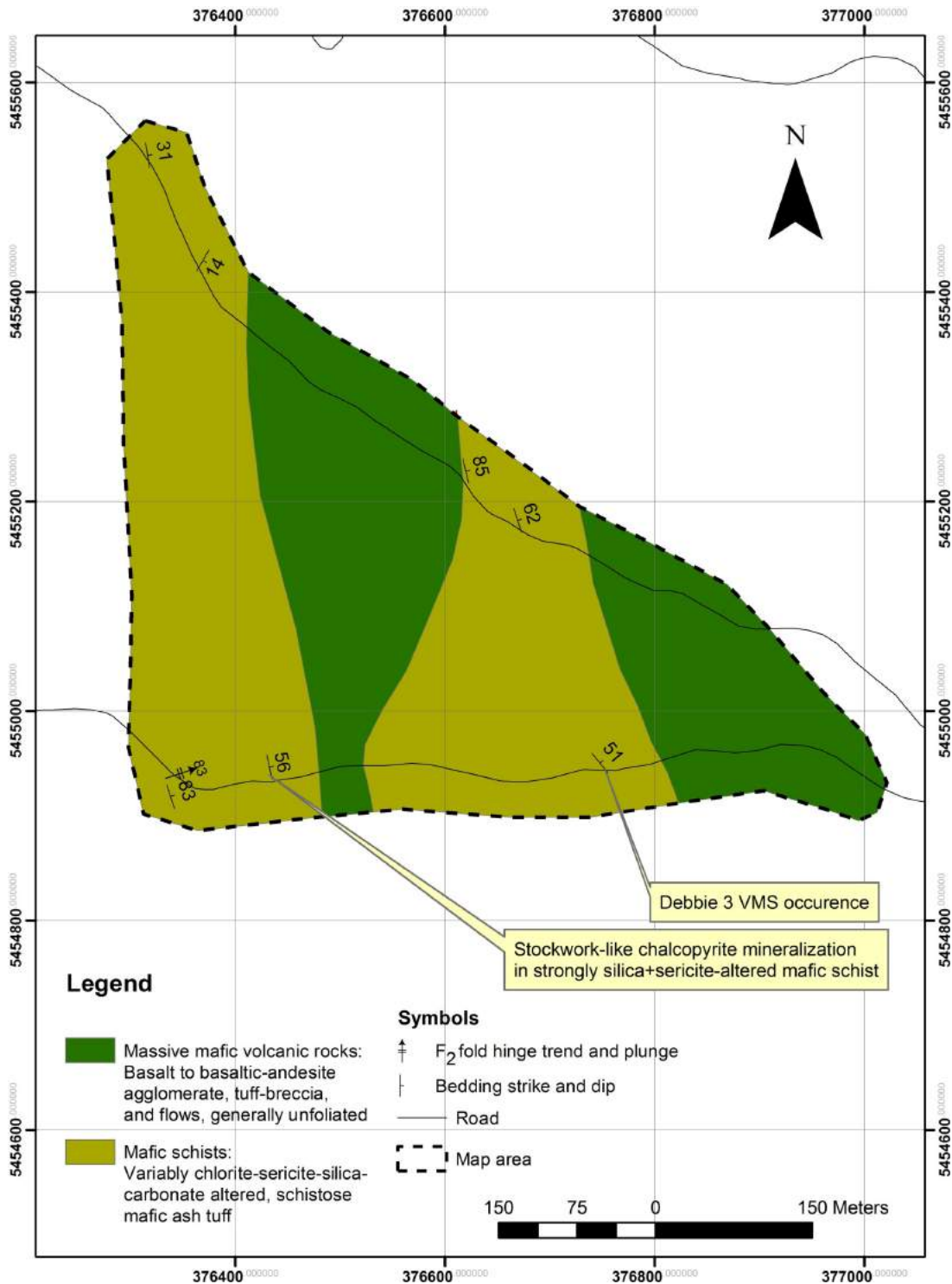


Figure 19. Geology of the Debbie 3 VMS occurrence, Port Alberni area.



Figure 20. a) Strongly foliated mafic tuff with variable chlorite, carbonate, sericite and silica alteration. **b)** Stratiform bands of massive sphalerite with minor chalcopyrite and galena, hosted in strongly foliated, sericite+chlorite+carbonate-altered mafic ash tuff.



Figure 21. Intensely silica+sericite+carbonate-altered mafic schist with quartz-carbonate and blue-green gypsum veins; in places, quartz-carbonate veins contain blebs of chalcopyrite.

dacite and the dacite breccia are crosscut by quartz-carbonate veins containing trace chalcopyrite and bornite mineralization. This dacite unit may represent a locus of hydrothermal activity related to potential volcanogenic massive sulphide mineralization in the area.

Lastly, the association of polymetallic massive sulphide mineralization of the Debbie 3 occurrence with fine-grained, chloritic mafic tuff assigned to either the Nitinat or the Duck Lake Formation indicates that significant hiatuses in mafic volcanism exist in the formations where VMS mineralization could develop. This suggests that further VMS exploration in mafic volcanic rocks belonging to the Duck Lake and Nitinat formations is warranted. This work should concentrate on identifying zones of significant interflow sedimentation, similar to that hosting VMS mineralization of the Debbie 3 occurrence.

Future Work

Fieldwork planned for the winter of 2007 will include logging and sampling of recent drillcore from the Debbie property (Bitterroot Resources Ltd.). This work has several goals, including identifying and sampling marker horizons within mafic volcanic rocks of the Duck Lake and Nitinat formations, with the ultimate goal of constraining the age of these formations, which are currently understood to be the oldest rocks in the Wrangellia Terrane. It will aid in determining the age and stratigraphic position of VMS-prospective horizons within the Nitinat and Duck Lake formations, and will assist in constraining relative motions along fault systems, which are host to significant epithermal gold mineralization at the Debbie occurrence (MINFILE occurrence 092F 079). In addition, sampling of sulphide mineralization from the Debbie property for Pb-isotope studies will provide a framework through which epigenetic sulphide occurrences associated with gold mineralization on the



Figure 22. Bleached, highly sericite+silica+fuchsite-altered mafic volcanic rock with up to 4% pyrite mineralization as disseminations, stringers and blebs up to 2 cm in size.

property (e.g., the Debbie occurrence) can be distinguished from those associated with VMS mineralization (e.g., the Debbie 3 VMS occurrence).

Fieldwork planned for 2008 will be concentrated in the Cowichan and Port Alberni areas, with additional work in potential outcrops of Sicker Group rocks in the Bedingfield Bay and Muchalat Inlet areas. In the Cowichan area, continued work will focus on understanding the stratigraphic and volcanological setting of VMS occurrences hosted by the Sicker Group, particularly those of the Lara/Coronation, Randy and Anita zones, north and west of Big Sicker Mountain (MINFILE occurrences 092B 129, 128 and 037, respectively), and other potential VMS occurrences in the immediate vicinity and west of Cowichan Lake. Additional regional work in the Alberni area will focus on identifying stratigraphic marker horizons within the Sicker Group that can be used to constrain the age of lithological units in the area, particularly those belonging to the Duck Lake and Nitinat formations.

In the Bedingfield Bay and Muchalat Inlet areas, similar regional and focused outcrop-scale mapping and sampling will be conducted to understand the stratigraphy and volcanological setting of potential Sicker Group rocks and VMS occurrences, most notably in the vicinity of the Rant Point and Dragon (Paget Resources Corp.) VMS occurrences (MINFILE occurrences 092F 494 and 092E 072, respectively). In parallel with the geological mapping and synthesis work, the authors will also carry out additional U-Pb dating, lithochemical, and Nd, Hf and Pb isotopic studies in order to constrain the age and magmatic evolution of Sicker Group volcanic rocks, and to develop a framework through which VMS occurrences hosted by the Sicker Group can be distinguished from younger, epigenetic sulphide occurrences.

Acknowledgments

This project is jointly funded by a Geoscience BC grant, Bitterroot Resources Ltd., Paget Resources Corp. and a Natural Sciences and Engineering Research Council of Canada (NSERC) Discovery Grant to Mortensen. The authors thank N. Massey for discussions and insights into the geology of the Sicker Group, and K. Hickey for having provided a critical review of this manuscript. They also thank several prospectors, consultants and explorationists working on Vancouver Island, especially M. Becherer of Mineral Creek Ventures Inc., M. Carr of Bitterroot Resources Ltd., J. Bradford of Paget Resources Corp., E. Specogna of Specogna Minerals Corp., A. Francis, J. Houle, H. McMaster and S. Tresierra, for sharing their time and knowledge of Sicker Group geology and mineralization.

References

- Barrett, T.J. and Sherlock, R.L. (1996): Volcanic stratigraphy, lithochemistry and seafloor setting of the H-W massive sulfide deposit, Myra Falls, Vancouver Island, British Columbia; *Exploration and Mining Geology*, v. 5, p. 421–458.
- Brandon, M.T., Orchard, M.J., Parrish, R.R., Sutherland Brown, A. and Yorath, C.J. (1986): Fossil ages and isotopic dates from the Paleozoic Sicker Group and associated intrusive rocks, Vancouver Island, British Columbia; *in* Current Research, Part A, Geological Survey of Canada, Paper 86-1A, p. 683–696.
- Juras, S.J. (1987): Geology of the polymetallic volcanogenic Buttle Lake Camp, with emphasis on the Price Hillside, central Vancouver Island, British Columbia, Canada; Ph.D. thesis, University of British Columbia, Vancouver, BC, 279 p.
- Katvala, E.C. (2006): Reexamining the stratigraphic and paleontologic definition of Wrangellia; *Geological Society of America, Abstracts with Program*, v. 38, p. 24.
- Laanela, H. (1987): Assessment report on geological, geochemical, and geophysical surveys on the Lacy and Stokes claim groups in the Alberni and Nanaimo mining divisions, BC; BC Ministry of Energy, Mines and Petroleum Resources, Assessment Report 16138, 93 p.
- Massey, N.W.D. (1995): Geology and mineral resources of the Duncan sheet, Vancouver Island, 92B/13; BC Ministry of Energy, Mines and Petroleum Resources, Paper 1992-4.
- Massey, N.W.D. and Friday, S.J. (1987): Geology of the Chemainus River–Duncan area, Vancouver Island (92C/16; 92B/13); BC Ministry of Energy, Mines and Petroleum Resources, Paper 1988-1, p. 81–91.
- Massey, N.W.D. and Friday, S.J. (1989): Geology of the Alberni–Nanaimo Lakes area, Vancouver Island (92F/1W, 92F/2E and part of 92F/7); BC Ministry of Energy, Mines and Petroleum Resources, Open File 1987-2.
- Massey, N.W.D., MacIntyre, D.G., Desjardins, P.J., and Cooney, R.T., (2005): Digital map of British Columbia: Tile NM10 Southwest BC; BC Ministry of Energy, Mines and Petroleum Resources, GeoFile 2005-3.
- MINFILE (2007): MINFILE BC mineral deposits database; BC Ministry of Energy, Mines and Petroleum Resources, URL <<http://www.em.gov.bc.ca/Mining/Geosurv/Minfile/>> [November 2007].
- Mortensen, J.K. (2005): Stratigraphic and paleotectonic studies of the Middle Paleozoic Sicker Group and contained VMS occurrences, Vancouver Island, British Columbia; *in* Geological Fieldwork 2005, BC Ministry of Energy, Mines and Petroleum Resources, Paper 2006-1, p. 331–336.
- Robinson, M. (1992): Geology, mineralization and alteration of the Battle zone, Buttle Lake camp, central Vancouver Island, southwestern British Columbia; M.Sc. thesis, University of British Columbia, Vancouver, BC, 268 pages.
- Ruks, T.R. and Mortensen, J.K. (2006): Geological setting of volcanogenic massive sulphide occurrences in the Middle Paleozoic Sicker Group of the southeastern Cowichan Lake uplift (NTS 092B/13), southern Vancouver Island; *in* Geological Fieldwork 2006, BC Ministry of Energy, Mines and Petroleum Resources, Paper 2007-1, p. 381–394.
- Sluggett, C.L. (2003): Uranium-lead age and geochemical constraints on Paleozoic and Early Mesozoic magmatism in Wrangellia Terrane, Saltspring Island, British Columbia;

- B.Sc. thesis, University of British Columbia, Vancouver, BC, 56 p.
- Sluggett, C.L. and Mortensen, J.K. (2003): U-Pb age and geochemical constraints on the paleotectonic evolution of the Paleozoic Sicker Group on Saltspring Island, southwestern British Columbia; Geological Association of Canada–Mineralogical Association of Canada, Joint Annual Meeting, Program with Abstracts, v. 28.
- Yorath, C.J., Sutherland Brown, A. and Massey, N.W.D. (1999): LITHOPROBE, southern Vancouver Island, British Columbia: geology; Geological Survey of Canada, Bulletin 498, 145 p.

New Models for Mineral Exploration in British Columbia: Is There a Continuum between Porphyry Molybdenum Deposits and Intrusion-Hosted Gold Deposits?

J.L. Smith, Department of Geology, University of Nevada, Reno, Nevada, smith264@unr.nevada.edu

G.B. Arehart, Department of Geology, University of Nevada, Reno, Nevada

R. Pinsent, Adanac Molybdenum Corporation, White Rock, BC

Smith, J.L., Arehart, G.B. and Pinsent, R. (2008): New models for mineral exploration in British Columbia: is there a continuum between porphyry molybdenum deposits and intrusion-hosted gold deposits?; in Geoscience BC Summary of Activities 2007, Geoscience BC, Report 2008-1, p. 93–104.

Introduction

There has been little research into, or exploration for, Mo deposits in Canada or elsewhere since the early 1980s, but that is likely to change, particularly if the price of Mo stays at or anything near current levels. There are numerous poorly understood, relatively underexplored Mo deposits and occurrences in the Canadian Cordillera that are likely to be explored over the next several years, and it would be of great benefit to the exploration community if more was known about Mo deposits of high- (climax-type) and low- (quartz-monzonite-type) fluorine type in the province.

In addition, there are geochemical similarities between porphyry Mo deposits and ‘intrusion-hosted’ Au deposits (e.g., Tombstone Belt; Figure 1), suggesting a possible genetic link. The Adanac Mo deposit belongs to an important class of mineral occurrences within the Atlin gold camp. The Adanac deposit contains no Au itself, but placer gold is still being mined on the lower reaches of Ruby Creek below the deposit. Historically, it has always been assumed that the Mo deposit postdates Au mineralization, which occurs in quartz-carbonate shears in Cache Creek Group volcanic strata and as placer gold. Isotope work by Mihalynuk et al. (1992), however, suggests that some of the placer gold in the Atlin area may have been derived from the Surprise Lake batholith. This is consistent with the presence of Au- and W-bearing quartz veins in drainage areas immediately south of the Adanac Mo deposit, because, in general, wolframite is commonly associated with porphyry Mo deposits, peripheral to the molybdenite zone (Wallace et al., 1968). Thus, the presence of Au in those wolframite veins raises the question of a potential linkage between Au-depleted Mo and Au-bearing W ‘intrusion-related’ deposits. Understanding the association, or lack thereof, is an important

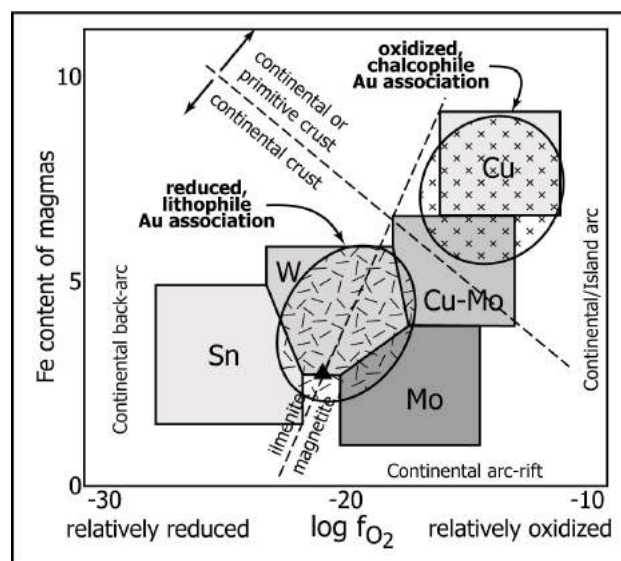


Figure 1. Plot of Fe content vs. oxidation state for plutons and associated ‘porphyry’ mineral deposits (fields from Thompson et al., 1999); note that Au is found in both oxidized (porphyry Cu) and reduced (porphyry Sn-W-Mo) environments; Surprise Lake batholith plots approximately at the solid triangle.

step toward focusing further exploration in the province for both of these deposit types.

Geological Background

The Adanac Mo deposit is located in the northwestern corner of British Columbia, near the town of Atlin (Figure 2). The geology of the Atlin area was mapped by Aitken (1959), and the regional setting of the deposit was discussed by Christopher and Pinsent (1982). The Atlin area (Figure 3) is underlain by deformed and weakly metamorphosed ophiolitic rocks of the Pennsylvanian and/or Permian Cache Creek Group (Monger, 1975). These rocks, which include serpentinite and basalt, as well as limestone, chert and shale, have long been thought to be the source of much of the placer gold found in the Atlin area. The sedimentary and volcanic rocks are cut by two younger batholiths: a Jurassic granodiorite to diorite intrusion

Keywords: porphyry, molybdenum, isotope geochemistry, whole-rock geochemistry, Atlin

This publication is also available, free of charge, as colour digital files in Adobe Acrobat® PDF format from the Geoscience BC website: <http://www.geosciencebc.com/s/DataReleases.asp>.

(Fourth of July batholith) north of Pine Creek and a Cretaceous granite to quartz monzonite intrusion (Surprise Lake batholith) north and south of Surprise Lake. The rocks are locally strongly faulted and the Adanac deposit is located near the intersection of two major syn- to post-mineralization fault systems.

The deposit area was described by Sutherland Brown (1970), White et al. (1976), Christopher and Pinsent (1982) and Pinsent and Christopher (1995). The Adanac Mo deposit underlies the valley floor near the head of Ruby Creek. It is largely buried and has very little surface expression. There is little outcrop in the lower part of the valley and molybdenite is only rarely found in float and/or veins in outcrop in the bed of the creek. The geology underlying the valley floor is largely derived from drill data (Figure 4). Although the geology of the Adanac deposit is moderately well understood, it has had almost no detailed research. It was reported to resemble a quartz-monzonite-type low-fluorine stockwork deposit (Westra and Keith, 1981) with a single flat-lying to steeply dipping shell of mineralization over a main porphyry intrusion, as described by White et al. (1976) and Pinsent and Christopher (1995).

The deposit is near the western margin of the Surprise Lake batholith, a composite, highly evolved, U-rich granite. The deposit occurs in the Mount Leonard stock, a satellite body of the batholith. The deposit is entirely within plutonic rock. There are three stages of intrusion: an early, generally coarse-grained stage that was deformed prior to the intrusion of second-stage ‘porphyry domes’, and a late, fine-grained phase that was injected into the first two phases at about the same time as mineralization. The deposit itself is a disrupted, blanket-shaped deposit that formed late in the development of the plutonic suite. The deposit is partially controlled and offset by the Adera fault system, which trends approximately northeast and defines much of the southern boundary of the pre-ore Fourth of July batholith. The approximately north-trending Boulder Creek fault system appears to have localized emplacement of the late, third-stage porphyritic and aplitic plutonic rocks.

Figure 5 shows most of the main rock types in the deposit. They are listed, with hand-sample photographs, in order from oldest to youngest. Coarse-grained quartz monzonite (CGQM) is the main unit in the deposit. Most other rock types cut this unit or are a textural variation of it. Mafic quartz-monzonite porphyry (MQMP) is an intrusion that postdates CGQM and occurs to the east and south of the deposit. The contact between the two units is a roughly north-trending fault. Coarse-grained quartz monzonite is interpreted to grade into transitional and hybrid varieties (CGQM-T and CGQM-H), which both represent increasing matrix content. These units occur as dikes, and also as mappable phases on the southwestern end of the deposit and in the north section of the deposit. The north section of

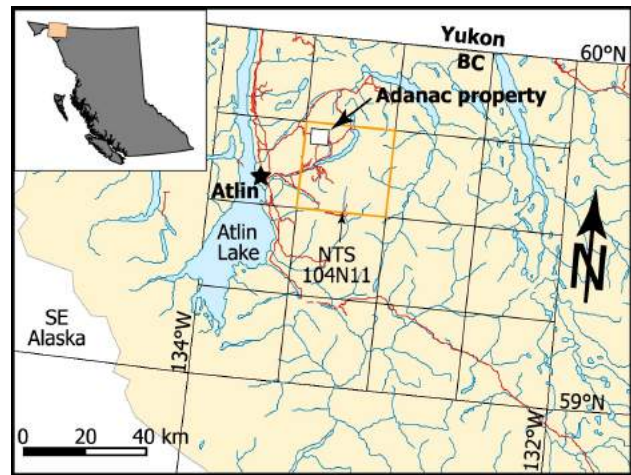


Figure 2. Location of the Adanac Mo deposit; white box is the approximate location of Figure 3.

the deposit is the ‘cap’ of the system that has been dropped down and separated from the rest of the deposit by the Adera fault, a northeast-trending normal fault. This area also contains crowded and sparse quartz-feldspar porphyry (CQFP and SQFP), which represent the temporal end-members of the CGQM evolution. The series CGQM, CGQM-T, CGQM-H, CQFP and SQFP coarsens inward, with SQFP being at the top of the stock and having the greatest matrix content, and CGQM being at the deepest parts and having a coarse-grained texture. Intruding the CGQM is the crowded and sparse quartz-monzonite porphyry (CQMP and SQMP) on the east end of the deposit, in the central pit area. This intrusion disappears to the southwest; whether this is the result of a fault or simply a steep contact is not known. On the southwest end, there is a younger intrusion of medium-grained equigranular quartz monzonite (MEQM). Also occurring at this end of the de-

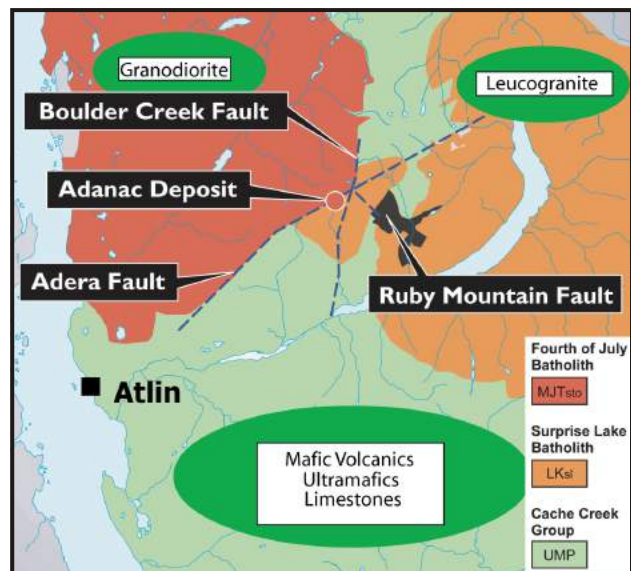


Figure 3. General geology of the Adanac deposit area (modified from Aitken, 1959).

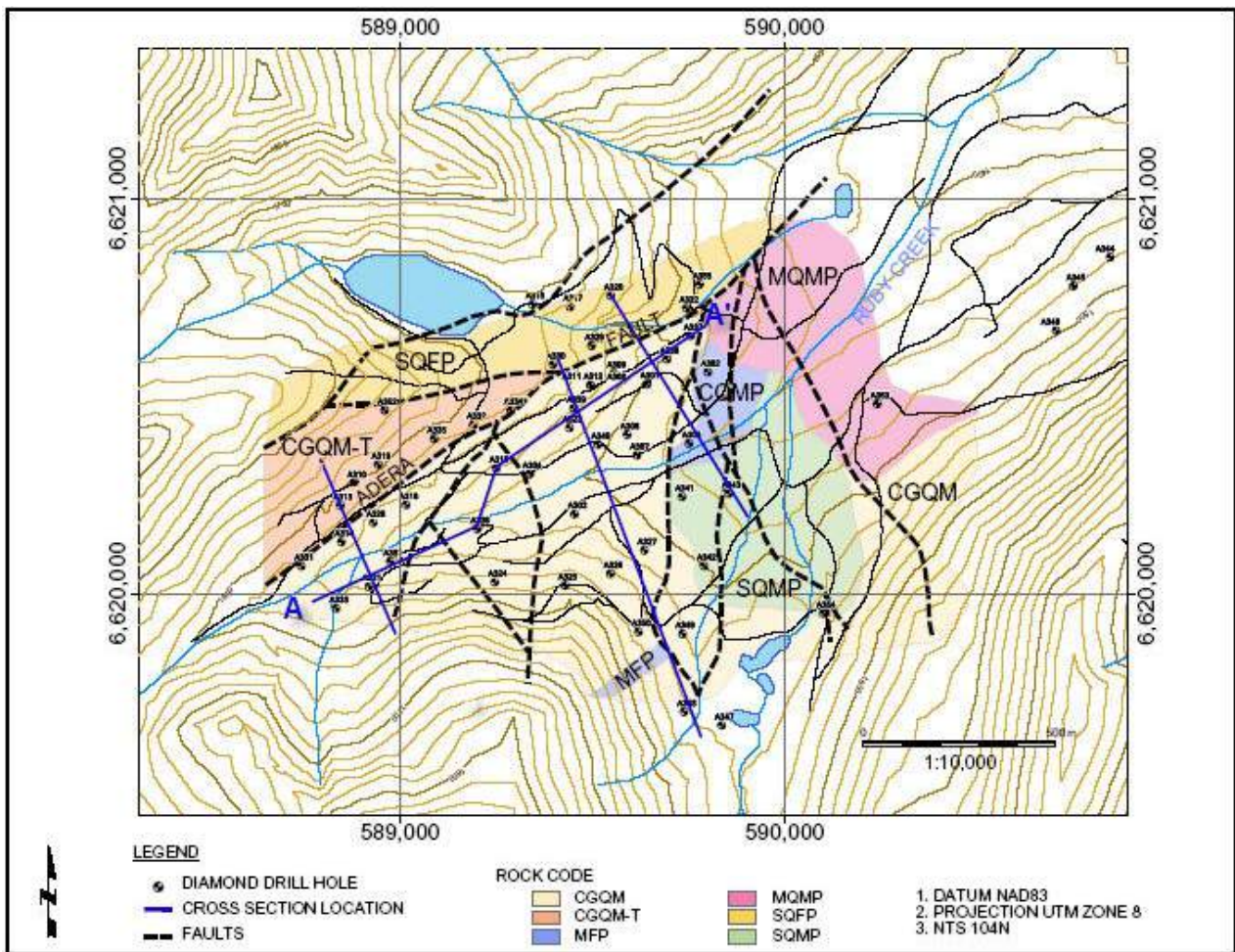


Figure 4. Surface geology of the Adanac Mo deposit (modified from unpublished company reports), showing a cross section of diamond-drill holes from which samples were collected for geochemical analysis.

posit in the form of a dike is megacrystic feldspar porphyry (MFP). Throughout the deposit, there are numerous fine-grained dikes (FGQM) that cut all other rock types.

Molybdenite mineralization postdates all rock types and appears in drillcore to postdate hydrothermal alteration. Mineralization is in the form of quartz-vein stockwork. Based on visual estimates in drillcore and confirmed by a downhole geophysical study done by Aurora Geophysical Consultants in Whitehorse, Yukon, most veins are subhorizontal, and there is a second set of veins that is subvertical and trending east. There appears to be multiple mineralization events. A broad generalization can be made that ductile (sheared, interpreted as forming at high temperatures within hostrock), smoky quartz veins are early, and that subhorizontal, lower grade, white quartz veins with brittle, sharp contacts with the hostrock are relatively late. There are also some rare veins that contain other minerals such as pyrite, galena, huebnerite and chalcopyrite. Without precise dates for each event, it is difficult to determine how many mineralization events occurred and whether or not there was a significant, if any, time lapse between them.

Alteration is not pervasive or incredibly strong in the deposit, at least relative to climax-type molybdenite deposits. Early primary hydrothermal alteration exists in the form of silicified zones and K-feldspar envelopes around veins, K-feldspar floods and secondary biotite, which is characterized by large (3–5 cm) biotite crystals. Early primary alteration is more pronounced at the southwest end of the deposit. Late primary alteration in the deposit is mainly seen as clay alteration and late 1 mm veins or fractures containing small amounts of pyrite and commonly coated with calcite and/or stilbite. Most clay alteration appears to be green to black chlorite, judging from hand sample, and is prominent in faults. There is also sometimes an apple-green sericite alteration that occurs as rims on feldspars or pervasively alters feldspars. This usually occurs for a few tens of feet above and below faults, and reflects fault focusing of fluids. A pyrite-rich halo does not occur in the area of the proposed central pit, but it can be seen in higher elevations that surround the deposit, still within the CGQM-T, or the cap of the system. Conveniently for mining, glaciation has removed this halo from directly above the deposit and the proposed pit area.

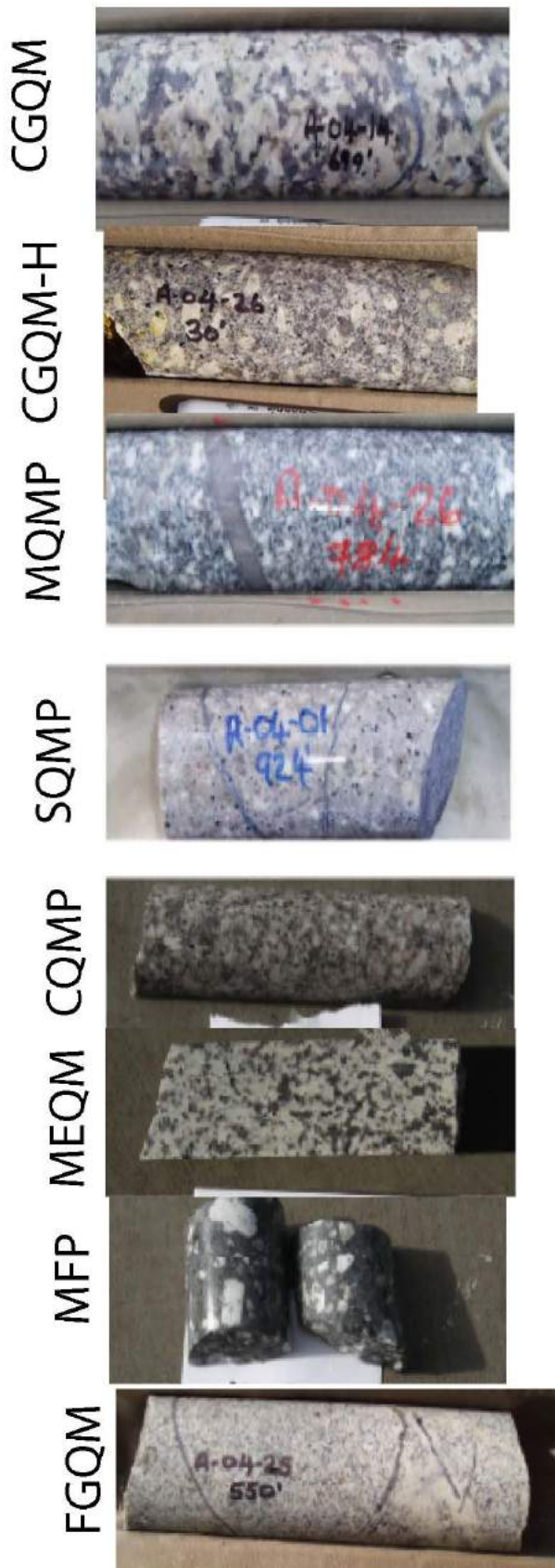


Figure 5. Photographs of rock types from drillcore, in order from oldest (at the top) to youngest (at the bottom).

Research Objectives

The goal of this research is twofold. The first goal is to determine the place of the Adanac deposit within the spectrum of molybdenite deposits (i.e., a climax type or quartz-monzonite type, or a transitional type between these two end members) based on new drillhole and geochemical information acquired in the last five years. Part of this goal has been obtained by studying the trace-element and whole-rock geochemistry at Adanac. Additional work to further this goal, such as an alteration study and a study of various aspects of geochronology at Adanac, is planned for the academic year of 2007–2008. The second goal of the research is to compare the Adanac Mo deposit to intrusion-hosted Au deposits in the North American Cordillera and to determine whether there are geochemical similarities between Adanac and these deposits.

Results of Work Completed in 2006–2007

Rock Descriptions

Each rock type in the deposit was described according to hand sample and thin section analyses. These analyses were done in order to complement the whole-rock geochemical data and for comparison to other molybdenite deposits. Rock types are roughly listed in order from oldest to youngest, based on crosscutting relationships. Because crosscutting relationships are absent between a few rock types, some relationships are uncertain.

Coarse-grained quartz monzonite (CGQM) is the oldest and most common rock in the Mount Leonard stock (Figure 3). It is a weakly to moderately deformed pink or grey, equigranular, coarse-grained (0.5–3.0 cm) granite to quartz monzonite. It contains roughly equal amounts of K-feldspar, plagioclase and quartz. Minor biotite is present. Two samples of fresh CGQM were selected for thin section examination. Quartz is the dominant mineral in both sections, at 45–50%, with K-feldspar and plagioclase having roughly equal amounts at about 20–25% each. Biotite comprises 3–10% of the rock. Other minerals noted (secondary) were chlorite replacing biotite, sericite and kaolinite replacing feldspars, euhedral topaz (less than 0.1 mm), euhedral pyrite replacing or overprinting chlorite, cogenetic pyrrhotite and magnetite replacing chlorite, and the presence of calcite. Total secondary minerals comprise from 1 to 5% of the rock. Minor myrmekitic textures were noted of quartz and feldspar (0.2 mm). Feldspar commonly has perthitic texture.

Transitional and hybrid coarse-grained quartz monzonite (CGQM-T and CGQM-H) are varieties of CGQM that contains increased groundmass, 25% in transitional and 50% in the hybrid type. The groundmass is 2–4 mm in size. This phase occurs at contacts where CGQM grades into FGQM. It is presumed to be a volatile-rich residual phase preparing

for the release of hydrothermal fluids, as this rock type has some features that are not clearly magmatic or hydrothermal, such as graphic intergrowths and myrmekitic textures. This phase sometimes occurs as early dikes that are cut by mineralized quartz veins. The composition is the same as CGQM. Thin section examination showed that CGQM-H is 50% quartz, and 20% each of alkali feldspar and plagioclase. Also noted were calcite, biotite (fresh and altered), pyrite, magnetite, sericite and chlorite (alteration product of biotite). Pyrite and calcite are associated and occur in the groundmass as 5–6 mm crystals. Pyrite also occurs replacing chlorite along cleavage planes and replacing magnetite. Magnetite occurs in close proximity to biotite and replacing chlorite. Sericite occurs as fine crystals on feldspars. In one sample, a 1 mm fluorite grain was noted alongside calcite inside a plagioclase crystal. Calcite was noted to postdate pyrite and magnetite.

Mafic quartz-monzonite porphyry (MQMP) is a grey rock unit characterized by an increase in biotite. This unit cuts CGQM, but is cut by the two main porphyry units (listed next). The MQMP unit contains fine biotite crystals (1 mm), plagioclase crystals (phenocrysts and groundmass) that are chalky white in colour and 5–7 mm in size, and quartz phenocrysts are 6–10 mm in diameter, on average smaller than plagioclase crystals. The matrix comprises a mixture of biotite, quartz and feldspar. From thin section analysis, this rock was noted to have slightly more feldspar content than CGQM. Quartz comprises 40% of the rock, while plagioclase and alkali feldspar makes up 50%, with slightly more plagioclase than alkali feldspar. Biotite makes up the other 10% of the rock, with secondary minerals and zircon all making up less than 1%. Pyrite and magnetite are both present replacing biotite and chlorite, while chlorite exclusively replaces biotite. Pyrite is more euhedral than magnetite, and both are about 0.4 mm in size. Kaolinite and sericite were noted as fine dustings on feldspars. Anhydrous calcite was noted near the pyrite- and magnetite-altered biotite. Graphic intergrowth texture was noted in one 0.5 mm sized area. Texture appears to be made up of feldspar and quartz ‘liquid like’ streaks.

Sparse and crowded quartz-monzonite porphyry (SQMP and CQMP) are younger than CGQM and MQMP. They both consist of white plagioclase, pink orthoclase, quartz and biotite phenocrysts that are 2–6 mm in size, in a light brownish to pinkish aphanitic matrix. In the sparse variety, phenocrysts make up 10–30% of the rock and in the crowded variety, about 60–80%. The SQMP may be slightly younger, as it is seen to sometimes cut the crowded version. The thin section analysis determined that quartz makes up about 45% of the rock with plagioclase and alkali feldspar at about 25% each. Biotite is about 4% in some of the samples, and opaque minerals such as pyrite, magnetite and molybdenite comprise the rest. One zircon crystal was noted, with a brownish to orange damage halo at about

0.5 mm in size. Chlorite is commonly seen to replace biotite, and feldspars have dustings of clays (which appear to be kaolinite and sericite) clustered in the centres of crystals. In two samples, it was noted that molybdenite does not occur in veins but in cleavage planes of altered biotite (to chlorite). Molybdenite crystals are large (1 mm) and euhedral. Clustering around the molybdenite and appearing to postdate it are small amounts of subhedral, 0.3 mm sized sphalerite and galena grains. Some larger, subhedral, 1 mm sized pyrite crystals were noted, and nearby in the same field of view, small magnetite crystals (0.2 mm, euhedral) with a chalcopyrite grain (0.1 mm, euhedral) were noted next to the magnetite. These sulphides were not in veins but occurred near chlorite. In one sample, galena was clearly seen to be replacing pyrite. One small area (0.3 mm) exhibited graphic intergrowth textures, as mentioned above.

Medium-grained equigranular quartz monzonite (MEQM) is a rock type that is not widespread in the deposit. It is possibly a transition between CGQM and FGQM, but may also be a separate intrusion at the southwest end of the deposit. It has a mosaic texture that is equigranular, and consists of equal amounts of quartz, plagioclase and alkali feldspar grains that are about 1–2 cm. Biotite is present as well, with crystals about half this size. In thin section, it was noted that biotite is more abundant than in CGQM or FGQM. Biotite makes up 15% of the rock. Quartz, plagioclase and alkali feldspar comprise roughly equal amounts at 25% each. Other minerals are zircon, clay dustings on feldspars, calcite, chlorite, pyrite and magnetite. Pyrite is replacing feldspar and magnetite is replacing chlorite.

Megacrystic feldspar porphyry (MFP) is noticeably different from other rock types in the deposit. It consists of a dark blue matrix, is very fine grained and contains small biotite crystals (1 mm). Phenocrysts are rounded, 6 mm smoky quartz eyes, and larger, 1–4 cm plagioclase and alkali feldspar crystals that are euhedral. It is not widespread and usually occurs as dikes or sills (cutting CGQM and MQMP) on the southwest end of the deposit. The rock sometimes exhibits mylonitic texture. In thin section, quartz is 40% of the rock, biotite is 15% and plagioclase and alkali feldspar are 20% each, roughly. The matrix is mostly extremely microcrystalline quartz and feldspar (<1/30 mm) with intergrown biotite. Feldspars are moderately to strongly altered to kaolinite and/or sericite. Feldspars sometimes exhibit poikilitic textures, with plagioclase (1 mm) inside larger alkali feldspar. The rock has an increased amount of opaque minerals, mostly pyrite and magnetite with minor chalcopyrite and pyrrhotite, comprising up to 7% of the rock. Opaque minerals occur with ‘veins’ of microcrystalline quartz that are not visible to the naked eye and may be flow textures. Magnetite replaces chlorite.

Fine-grained quartz monzonite (FGQM) is probably the youngest rock type in the deposit, as it is seen to cut all other units. This unit occurs as both dikes and sills throughout the deposit. It is also noted in drillcore to postdate hydrothermal alteration such as silicification. It is a brownish to pinkish rock type that is equigranular and appears to be a mixture of white and pink feldspar, quartz and trace biotite. The grain size ranges from less than 1 mm to about 3 mm. In thin section, FGQM is noted to contain roughly equal amounts of quartz, plagioclase and alkali feldspar, usually at about 90% of the rock. Biotite makes up 5–10%, with secondary minerals comprising the rest. The secondary minerals include chlorite replacing biotite, clays and calcite replacing feldspars, and small grains (0.2 mm) of pyrite or magnetite, euhedral to subhedral, either in the matrix or replacing biotite or chlorite. There is an elevated amount of graphic intergrowth textures (quartz and feldspar) in one thin section where FGQM is a dike cutting CGQM. Where this small dike (1–2 cm) comes into contact with CGQM, CGQM has increased clay alteration of feldspars. In one thin section, there appears to be two mixing phases of FGQM, one with very fine grains (less than 0.1 mm) and another with grain sizes of about 0.2 mm. In one sample where FGQM is completely ‘by itself’ (i.e., not in contact with other phases or quartz veins), the rock is noticeably fresh (no clay).

Whole-Rock Geochemistry

Major element geochemistry was determined for 10 samples of fresh rock, one from each major rock type in the deposit. The analyses were done at ACME Analytical Laboratories Ltd. in Vancouver, BC, using inductively coupled plasma–emission spectroscopy. The rock types include CGQM and its transitional varieties (CGQM-T and CGQM-H), the feldspar porphyries (CQFP and SQFP), which represent the cap of the system, MQMP, the two porphyry intrusions (SQMP and CQMP), MFP and MEQM. Normative mineral amounts were calculated using the CIPW (Cross et al., 1903) method. According to the International Union of Geological Sciences (IUGS) system of classification (Streckeisen, 1973), all rocks in the suite are granite. The rocks have an average of 35% normative quartz. Alkali/total feldspar ratios in each rock type were about 50. An alkali-lime index at 50 wt% SiO₂ was calculated, meaning the rocks are further classified as alkaline. It was also determined that the suite is peraluminous, and a series of Harker diagrams was also made. With increasing silica, Al₂O₃, Fe₂O₃, MgO, CaO, TiO₂, P₂O₅, MnO, Ba, Sr and Zr decrease; Rb, Na₂O and Cr₂O₃ remain constant; and K₂O increases.

Published literature on porphyry Mo deposits broadly outlines two basic types of deposits: the granite and quartz-monzonite types (Sutherland Brown, 1969; White et al., 1981; Wallace, 1995). Westra and Keith (1981) recognized

that these two basic types can be separated based on the K₂O value at 57.5 SiO₂ wt%. A natural dividing line occurs between those deposits with a K₂O value of less than 2.5% and those with values above that. If the value is less than 2.5%, the Mo deposits are classified as the ‘calcalkaline’ quartz-monzonite type with low F values. These deposits typically have lower molybdenite grades, little Sn, and W is present as scheelite. Source plutons have between 100 and 350 ppm Rb, and between 100 and 800 ppm Sr (Figure 6). Those deposits with values above 2.5% are broadly referred to as the climax type of Mo deposit. These deposits are associated with alkali-calcic to alkalic granite, and are enriched in F and Sn. Rubidium content of the source plutons is typically 200–800 ppm, with less than 125 ppm Sr (Figure 6). The molybdenum grades are typically higher and W is present as wolframite. Using the Westra and Keith (1981) classification scheme of porphyry Mo deposits, the K₂O value at 57.5 wt% SiO₂ (K₂O_{57.5}) was calculated at >2.5% for the rocks of Adanac. All of the rocks at Adanac contain between 70 and 76% silica, so the K₂O value had to be extrapolated considerably. Figure 6 illustrates how the K₂O_{57.5} value is consistent with the Rb vs. Sr data in dividing porphyry molybdenite deposits based on geochemistry. Since granite and quartz-monzonite Mo deposits have these different and predictable geochemical characteristics, they should be useful in delineating the nature of the system at Adanac. Fresh rock types at Adanac group well with other climax-type deposits based on Rb and Sr ratios, as well as on the basis of the K₂O_{57.5} value.

Trace Element Zonation

A series of cross sections in the deposit were completed in order to show trace-element zonation in comparison with deposit geology. Four examples of the main (A–A’, refer to Figure 4 for cross-section location) cross sections are shown in Figures 7–10. Figure 7 shows Mo values contoured against a black-and-white background of geology. High Mo values (670–1430 ppm) occur as a blanket over the main porphyry intrusion and the blanket steeply dips off to the west, where it is above the apex of another intrusion, the MEQM. High F values (Figure 8, 1000–3300 ppm) occur geographically above and peripheral to the Mo highs. Transitional phases of CGQM (CGQM-T, CGQM-H and the feldspar porphyries) typically have higher F values, while CGQM itself has relatively lower values. In drillholes 333 and 321 (at the southwest end of the section, Figure 8), the CGQM exhibits increased matrix content (CGQM-T) and has high F values. The Adera fault is parallel and north of the cross section of Figures 7–10. This fault has dropped the cap of the system, and the SQFP and CQFP are in the hangingwall. The highest F values in the deposit occur here in the SQFP and CQFP.

The average background values of W, Pb and Zn in an alkaline granite are 16 ppm, 15 ppm and 108 ppm, respectively

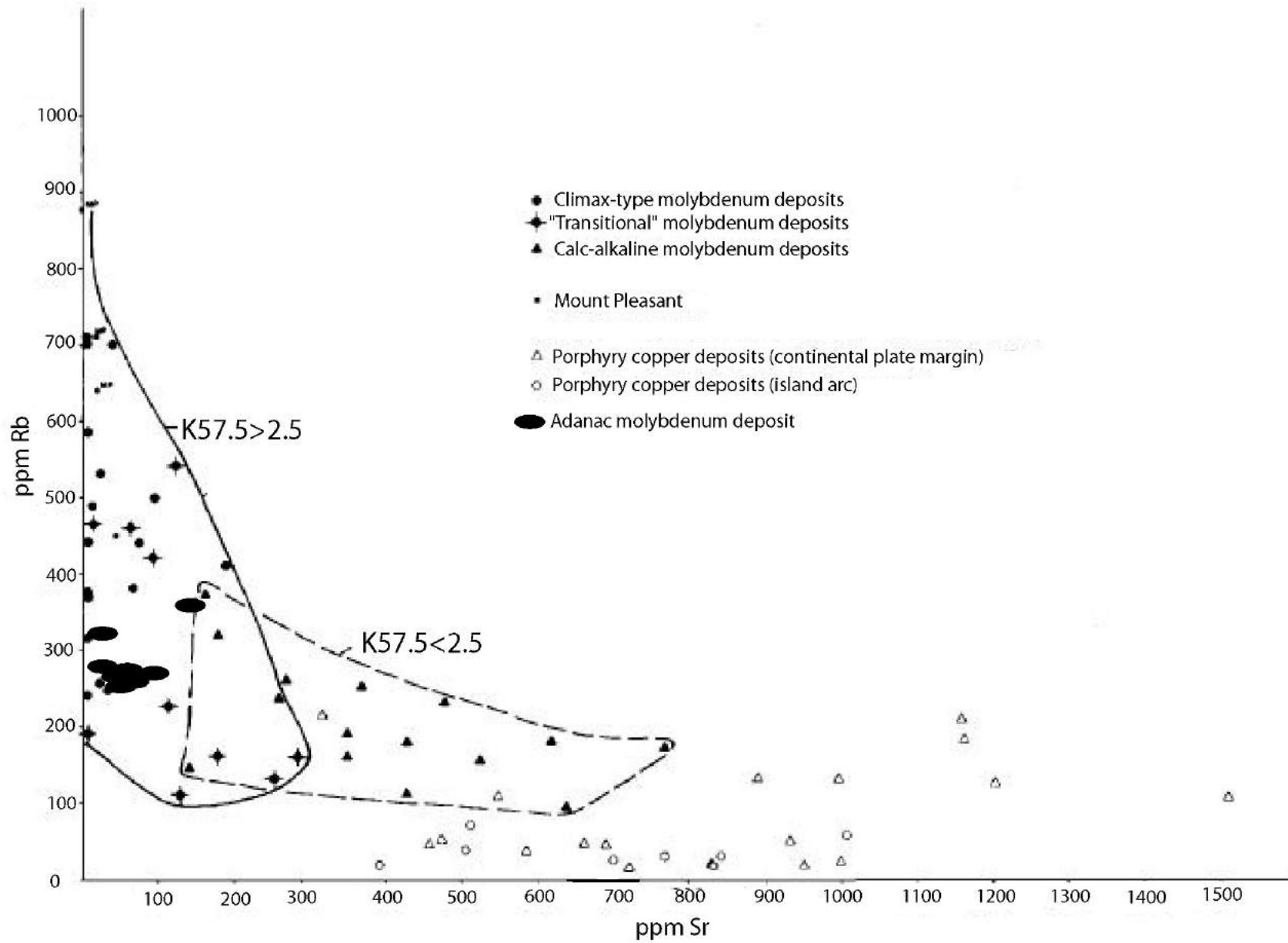
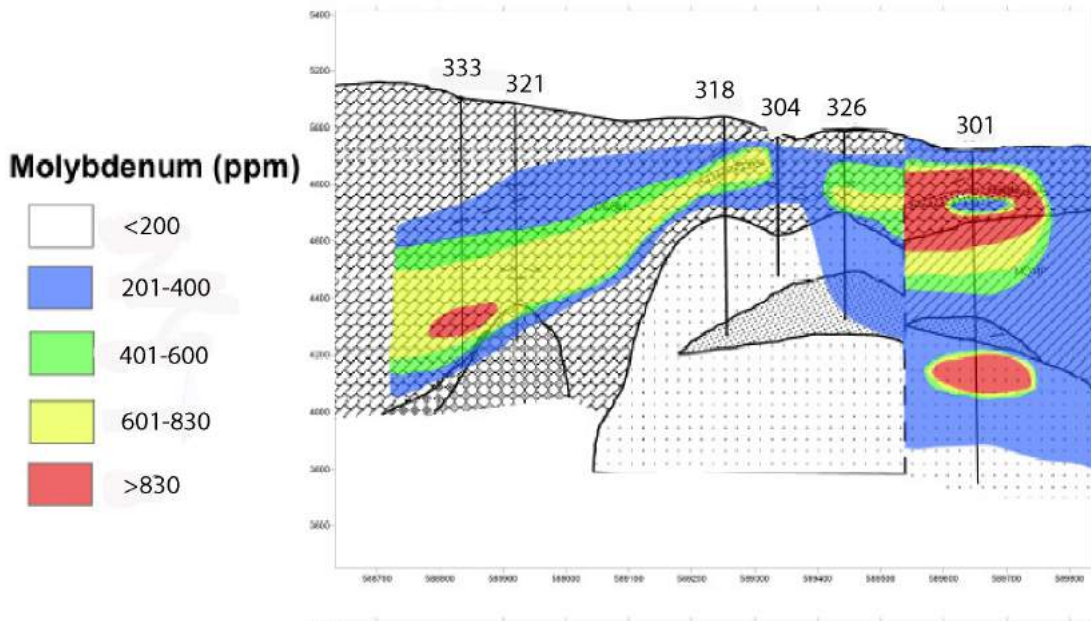


Figure 6. Graph showing Rb and Sr values for various types of porphyry deposits, including Cu porphyry and a W-Mo porphyry (Mt. Pleasant). The $K_2O_{57.5}$ value fields are superimposed on the graph. As their $K_2O_{57.5}$ value would indicate, rocks at Adanac fall within the field of climax-type deposits.



(Robb, 2005). Both W and Pb are elevated (100–200 ppm) in the central pit area (Figures 9–10). While the higher values for Zn in the central pit area (also around 100–200 ppm) are not anomalous for an alkaline granite, they are elevated relative to the pervasive low values (~10 ppm) elsewhere in the deposit. Tungsten highs occur as thin blankets coincident with the high-Mo zones. Elevated Pb and Zn occur only near faults within the molybdenite zone. Copper and Sn have values of 10 ppm or less in the central pit. Outside of the central pit area (and thus outside of the main molybdenite mineralization zone), higher values of Cu, Pb and Zn (200–1000 ppm) may be present at faults and in silicification zones. There is less than 0.1 ppm Au throughout the deposit.

A correlation matrix was calculated for a suite of 41 trace metals plus F. Molybdenum correlates with no other element in the deposit. Zinc correlates with Cu, Pb, Ag, Sn and Cd. These correlation coefficients are near 0.5 for all except Cd, which is 0.8. Copper correlates with Sn and Mn (correlation coefficient ~0.5). Lead correlates with Ag, Mn, Cd and Sb (coefficient ~0.5). Arsenic also correlates with Sb (0.7). Tungsten does not correlate with any other element. Tin correlates with Cd (0.6). Fluorine correlates with Th (0.5), Y (0.6) and Zr and Hf (0.7). The implications of these correlations are still being considered.

2007 Summer Field Season and Future Work

The 2007 summer field season was spent logging core and preparing various current deposit maps as required. Maps were prepared showing updated drillhole locations, including the 2007 drill program. Also updated were fault locations, various structures such as joints, and the current un-

GEOLOGY KEY:

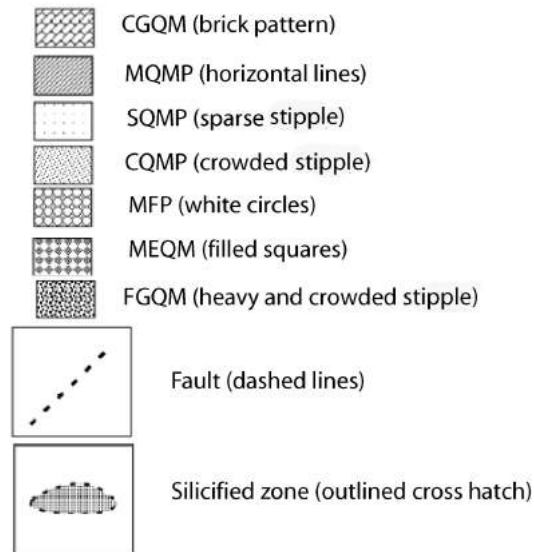


Figure 7. Cross section A-A', showing geology (rock type occurrences, faults and some silicification zones) in black and white, and Mo (in ppm) contoured against the black-and-white background.

derstanding of surface rock type. Another main focus of the summer was sampling and preparation for the 2007–2008 academic year goals. The goals for the coming academic year are outlined below. An accompanying schematic diagram (Figure 11) illustrates some important sample locations.

Alteration Study

The first aspect of the alteration study is the creation of a series of cross sections of the deposit with a focus on megascopic alteration patterns. Because of the lack of surface exposure, the distribution of alteration types has been

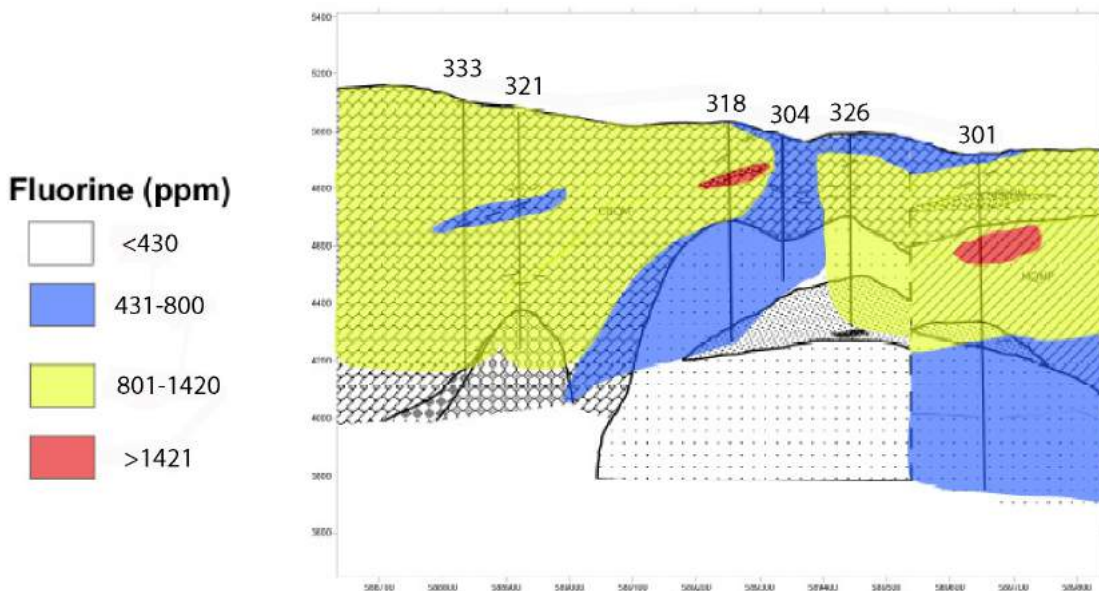


Figure 8. Cross section A-A', showing geology (rock type occurrences, faults and some silicification zones) in black and white, and F (in ppm) contoured against the black-and-white background; key as in Figure 7.

determined based primarily on drill logs. All the holes from which the cross sections were created were relogged over the summer with a focus on alteration. These data are being plotted on the same cross sections as the trace-element data and will be utilized to outline the locations of early primary hydrothermal alteration, such as silicification and K-feldspar flooding, and some late primary alteration, such as zeolite and calcite veins (propylitic).

An x-ray diffraction (XRD) study of the distribution of clay types in the deposit will be undertaken to further refine the alteration zoning. Samples of clay alteration were taken

from strategic areas of the deposit to provide three-dimensional spatial coverage. Based on drillcore observations, most clay alteration occurs at faults; however, within the faults, there may be zoning patterns outward from high-grade areas and feeder zones, presumably representing variations in fluid chemistry and temperature. In addition, because different faults display different characteristics, such as dark green gouge, or recemented white sheared faults, some paragenetic information may also be gleaned from these clay studies. These data will be utilized to compare patterns between Adanac and other molybdenite deposits worldwide.

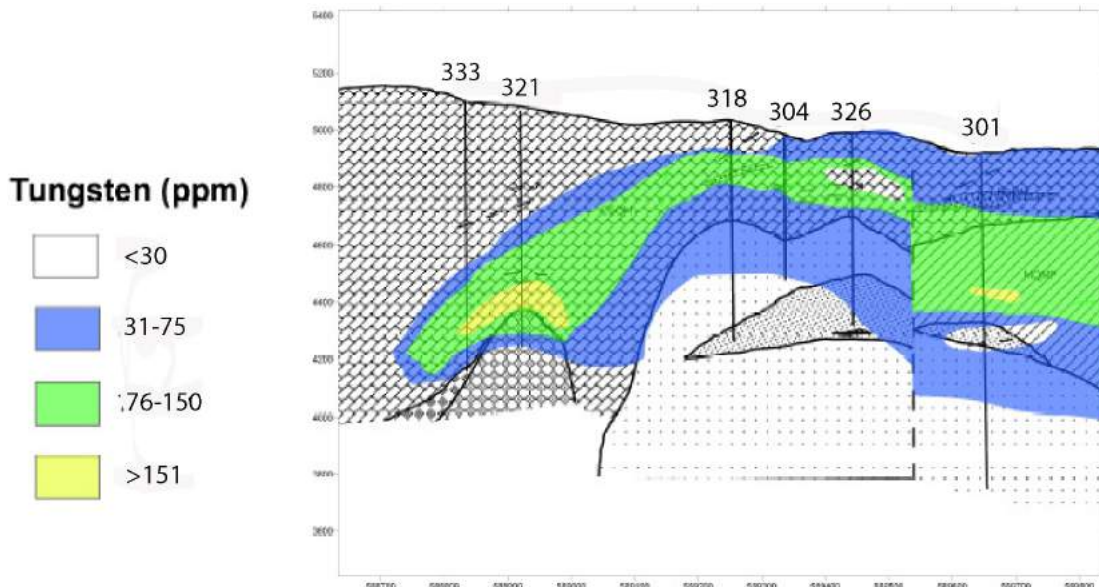


Figure 9. Cross section A-A', showing geology (rock type occurrences, faults and some silicification zones) in black and white, and W (in ppm) contoured against the black-and-white background; key as in Figure 7.

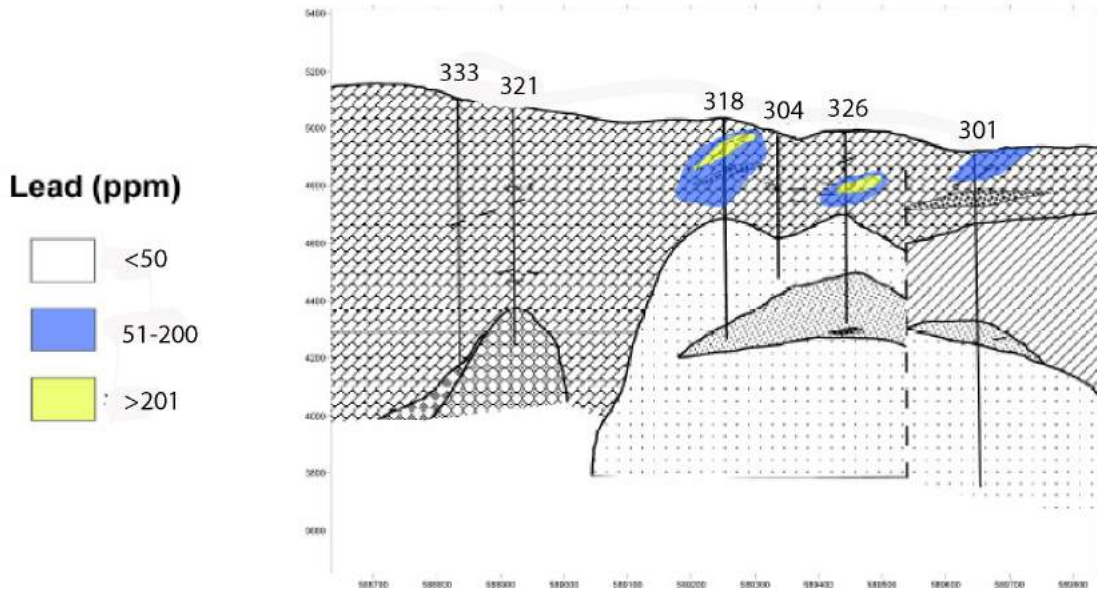


Figure 10. Cross section A-A', showing geology (rock type occurrences, faults and some silicification zones) in black and white, and Pb (in ppm) contoured against the black-and-white background; key as in Figure 7.

In conjunction with the XRD work, representative thin-section petrography of each alteration type in the deposit is planned. Forty-five thin sections are currently being made. These sections will be utilized to assess the relationship(s) between various clay species and their precursors, thus allowing a better understanding of water-rock interaction during mineralization.

Geochronology

The sampling completed over the 2007 summer field season was designed to allow us to determine precise ages for mineralization; to determine if there are multiple stages of

mineralization; and to compare and possibly correlate mineralizing events with magmatic events. This geochronological study also aims to determine the duration of the mineralizing event or events that occurred at Adanac.

The first aspect of the geochronological study is the dating of mineralization events using Re-Os isotopes in molybdenite from various samples, as shown schematically in Figure 6. Twenty samples have been collected for possible analysis. The sample locations are based on hypothesized centres of mineralization and observed paragenesis as described below:

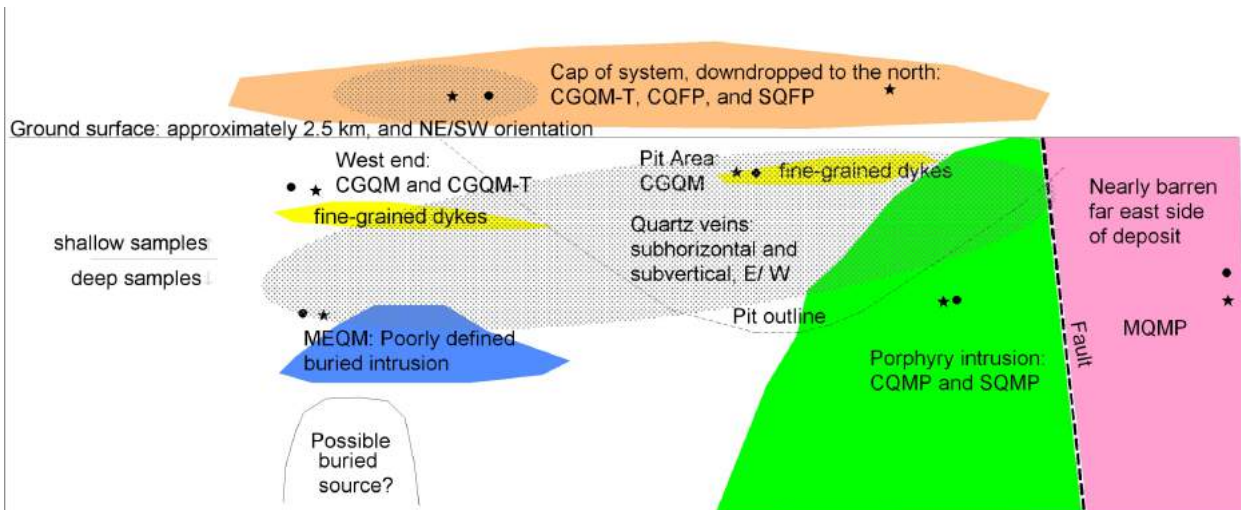


Figure 11. Schematic diagram representing sample locations throughout the deposit. The cross section follows the same orientation as A-A'. Biotite samples (black circles) are for microprobe analysis, in order to determine changes in trace-element content in early fluids. Molybdenite samples (black stars) are for Re-Os isotope geochronology and for an x-ray diffraction (XRD) determination of polytype. A sample of fresh rock for U-Pb zircon age dating was taken within 30.5 m (100 ft) of each molybdenite sample. An attempt was made to collect samples from distinctive areas in the deposit, e.g., feeder zones, lateral distance from feeder zones and the 'cap' of the system. These areas are labelled on the map, along with their associated rock types. Shaded areas represent high-grade zones.

- Feeder zone: the southwest portion of the system, as presently understood, displays an increased amount of early primary hydrothermal alteration. It also contains the most myrmekitic and unidirectional solidification textures, suggesting a volatile-rich area of the deposit. This area is where the proposed earliest stage of mineralization is located.
- Proximal to the feeder zone: samples from the main pit area and the southern and far eastern ends of the deposit are believed to be late-stage mineralization, based on the large lateral distance from the feeder zone.
- Cap areas and upper portions of drillholes: the analysis of samples from larger vertical, as well as lateral, distances away from the feeder zones may be later stages of mineralization, or may represent an evolution from the fluids passing through the feeder zone.
- Samples included different types of molybdenite veins: in addition to spatial variation, there are clearly two types of molybdenite veins, namely 'fine molybdenite in ductile veins' and 'coarse molybdenite in brittle veins' (i.e., veins have a sharp contact with host). Based on crosscutting relationships observed in drillcore, the molybdenite veins that are 'ductile' and contain fine molybdenite are older. A precise date will indicate the time lapse between these two mineralization events.
- Vein paragenesis: samples included molybdenite from veins with different associated minerals. There is molybdenite in veins by itself, in veins with pyrite and also in veins with other sulphides (chalcopyrite, galena). Unfortunately, these different types of veins are seen so rarely that temporal relationships between them cannot be determined. Therefore, geochronological analyses may yield insights into the paragenetic sequence of vein types.

In conjunction with the dating of mineralization, the timing of magmatic events will be determined using U-Pb isotope ratios in zircons. Samples of each rock type in the deposit were taken for age comparison. These included certain transitional phases present of each rock type, such as the transitional variety of the coarse-grained quartz monzonite, and aplite dikes, which are typically associated with a main rock type, such as CGQM. Ages of intrusion based on the zircon data will be compared to the timing of mineralization based on the Re-Os. Sampling locations for zircon are primarily based on locations of molybdenite Re-Os samples, i.e., a sample for each rock type was taken in proximity (within 30.5 m, or 100 ft) of a molybdenite sample. In addition, there was an extra sample taken of FGQM near the west end of the property, as opposed to the central pit area, to see if there is an age difference that may reflect local thermal variations. It is hypothesized that that deeper rock types on the southwest end (MEQM) will yield ages closest to mineralization, and thus may indicate a genetic relationship.

Two other types of studies will be carried out in parallel with the geochronological work. The first of these is a microprobe study of biotites to determine trace-element content, particularly F, S and Se. Understanding the temporal evolution of volatiles in the magmatic system, as reflected in biotite, may provide insights into molybdenite mineralization in the context of the evolution of the magmatic system. Primary magmatic biotite samples were collected from feeder zones of the deposit and laterally in various rock units. Secondary biotite from feldspar flood zones was collected as well, moving laterally from the feeder zone and into the central pit, and out to the far south and east ends of the deposit.

The second ancillary study comprises an x-ray diffraction study of molybdenite to determine polytype. The same samples used for Re-Os geochronology are a good representation of each type of mineralization from each distinct area of the deposit and will be used for the polytype study. There are two polytypes of molybdenite: the hexagonal 2H and the rhombohedral 3R. The 2H type is far more common than the exotic 3R, with the formation of the latter largely dependent upon impurities (commonly Re) in the molybdenite crystal (Newberry, 1979). Virtually nothing is known about the polytype or trace-element content of the molybdenite at Adanac. If there is a variation in polytype, it may be correlated with age, vein type or location, and thus may be indicative of an evolving system.

Regional Exploration Model

A much broader study of other Mo deposits by comparison of datasets, such as whole-rock geochemistry, is necessary to update and refine the exploration model for these deposits. In particular, preliminary work indicates that the geochemistry of plutons associated with molybdenite deposits and intrusion-hosted Au deposits is similar (e.g., redox state of the associated plutons; trace- and major-element chemistry of associated plutons; mineral and elemental assemblages such as high Be, Te and W, and low and peripheral Cu, Pb and Zn). Additional work is required to determine just how similar the geochemistry is, and whether there is a genetic link between these deposit types. This will proceed on two fronts, which are described below.

We will continue to compile and compare data from molybdenite and intrusion-related Au deposits in the western Cordillera of North America. In particular, we expect to both compile and generate some new data, such as isotopic data, that can be utilized in conjunction with more traditional geochemical data to help delineate similarities and differences among systems in the Cordillera.

At a more local scale, exploration of the connection between the Adanac Mo deposit and local placer gold deposits may yield insights into possible links between Mo and Au. To do this, the initial Os isotope signature of local

placer gold will be compared with the initial Os isotope signature of the Adanac hydrothermal system. Samples of magnetite in the same vein with molybdenite have been collected and (if sufficient Os is present for analysis) will be analyzed for initial Os isotope ratios. These data should be similar to the calculated initial Os isotope ratio from the molybdenite. The data from the Adanac deposit will then be compared with the initial Os isotope signature of placer gold samples from the lower reaches of Ruby Creek, just downstream from Adanac. If the signatures are similar, it may be postulated that a hydrothermal system(s) of the same age in the same area are responsible for both Au and molybdenite mineralization. Thus the two systems may have a genetic link. This has obvious ramifications for both molybdenite and Au deposits at a large scale in terms of both genesis and exploration.

Conclusions

The Adanac Mo porphyry deposit falls into the category of a climax-type deposit on the basis of geochemistry of Rb, Sr and $K_2O_{57.5}$. The host rock and mineralizing pluton is a peraluminous, alkalic granite. Trace-element distributions indicate a central blanket of Mo with coincident, but sporadic W. Highest F values occur peripheral to the main Mo zone, and other metals show an ambiguous zoning pattern. Hydrothermal alteration is similar to, but considerably less intense than, typical climax-type systems.

Further refinement of the alteration and trace-metal zonation patterns is underway. Geochronological measurements over the coming year will more clearly elucidate the timing and duration of both magmatic and hydrothermal mineralization events. Broader comparison of Adanac to other molybdenite deposits, as well as to intrusion-hosted Au deposits, will allow us to further refine our genetic and tectonic models for both deposit types in the Canadian Cordillera.

Acknowledgments

Adanac Molybdenum Corporation and Geoscience BC are thanked for financial and logistical support. J. Chesley from University of Arizona is thanked for a summer 2007 visit to aid in molybdenite sampling for the Re-Os isotopic aspects of this project. We appreciate constructive and anonymous reviews by the staff of Geoscience BC.

References

Aitken, J.D. (1959): Atlin map area, British Columbia; Geological Survey of Canada, Memoir 307, 89 p.
 Christopher, P.A. and Pinsent, R.H. (1982): Geology of the Ruby Creek–Boulder Creek area (Adanac molybdenum deposit);

BC Ministry of Energy, Mines and Petroleum Resources, Preliminary Map 52, scale 1:12 000.
 Cross, W., Iddings, J.P., Pirsson, L.V. and Washington H.S. (1903): Quantitative Classification of Igneous Rocks Based on Chemical and Mineral Characters, with a Systematic Nomenclature. University of Chicago Press, Chicago, IL, 63p.
 Mihalyuk, M.G., Smith, M.T., Gabites, J.E. and Runkle, D. (1992): Age of emplacement and basement character of the Cache Creek terrane as constrained by new isotopic and geochemical data; Canadian Journal of Earth Sciences, v. 29, p. 2463–2477.
 Monger, J.W.H. (1975): Upper Paleozoic rocks of the Atlin terrane; Geological Survey of Canada, Paper 74-47, 63 p.
 Newberry, R.J. (1979): Polytypism in molybdenite (I): a non-equilibrium impurity-induced phenomenon; American Mineralogist, v. 64, p. 758–767.
 Pinsent, R.H. and Christopher, P.A. (1995): Adanac (Ruby Creek) molybdenum deposit, northwest British Columbia; Canadian Institute of Mining and Metallurgy, Special Volume 46, p. 712–717.
 Robb, L. (2005): Introduction to Ore Forming Processes. Blackwell Publishing, Malden, MA, 373 p.
 Sutherland Brown, A. (1969): Mineralization in British Columbia and the copper and molybdenum deposits; Canadian Mining and Metallurgy Bulletin, v. 62, p. 26–40.
 Sutherland Brown, A. (1970): Adera; in Geology, Exploration and Mining in British Columbia in 1969; BC Ministry of Energy, Mines and Petroleum Resources, p. 29–35.
 Streckeisen, A.L. (1973): Plutonic rocks, classification and nomenclature recommended by the IUGS subcommission on the systematics of igneous rocks; Geotimes, v. 18, p. 26–30.
 Thompson, J.F.H., Sillitoe, R.H., Baker, T., Lang, J.R. and Mortensen, J.K. (1999): Intrusion related gold deposits associated with tungsten-tin provinces; Mineralium Deposita, v. 34, p. 323–334.
 Wallace, S.R., Muncaster, N.K., Jonson, D.C., Mackenzie, W.B., Bookstrom, A.A. and Surface, V.E. (1968): Multiple intrusion and mineralization at Climax, Colorado; in Ore Deposits of the United States, 1933–1967, American Institution of Mining, Metallurgical and Petroleum Engineers, p. 605–641.
 Wallace, S.R. (1995): The climax-type molybdenite deposits: what they are, where they are, and why they are; Economic Geology, v. 90, p. 1359–1380.
 Westra, G. and Keith, S.B. (1981): Classification and genesis of stockwork molybdenum deposits; Economic Geology, v. 76, p. 844–873.
 White, W.H., Stewart, D.R. and Ganster, M.W. (1976): Adanac (Ruby Creek) porphyry molybdenum deposits of the calc-alkaline suite; Canadian Institute of Mining and Metallurgy, Special Volume 15, p. 476–483.
 White, W.H., Bookstrom, R.J., Kamilli, M.W., Ganster, R.P., Smith, D.E. and Steininger, R.C. (1981): Character and origin of climax-type molybdenum deposits; Economic Geology, 75th Anniversary Volume, p. 270–316.

Hydrothermal Breccia in the Mount Polley Alkalic Porphyry Copper-Gold Deposit, British Columbia (NTS 093A/12)

R.M. Tosdal, Mineral Deposit Research Unit, University of British Columbia, Vancouver, BC, rtosdal@eos.ubc.ca

M. Jackson, Mineral Deposit Research Unit, University of British Columbia, Vancouver, BC

H.E. Pass, Australian Research Council Centre for Excellence in Ore Deposit Research, University of Tasmania, Hobart, Tasmania, Australia

C. Rees, Imperial Metals Corporation, Vancouver, BC

K.A. Simpson, Mineral Deposit Research Unit, University of British Columbia, Vancouver, BC and Australian Research Council Centre for Excellence in Ore Deposit Research, University of Tasmania, Hobart, Tasmania, Australia

D.R. Cooke, Australian Research Council Centre for Excellence in Ore Deposit Research, University of Tasmania, Hobart, Tasmania, Australia

C.M. Chamberlain, Mineral Deposit Research Unit, University of British Columbia, Vancouver, BC and Teck Cominco Limited, Vancouver, BC

L. Ferreira, Imperial Metals Corporation, Vancouver, BC

Tosdal, R.M., Jackson, M., Pass, H.E., Rees, C., Simpson, K.A., Cooke, D.R., Chamberlain, C.M. and Ferreira, L. (2008): Hydrothermal breccia in the Mount Polley alkalic porphyry copper-gold deposit, British Columbia; *in* Geoscience BC Summary of Activities 2007, Geoscience BC, Report 2008-1, p. 105–114.

Introduction

Hydrothermal and magmatic-hydrothermal breccias are common in porphyry Cu deposits. Depending on their timing relative to mineralization and the nature and genesis of the breccias, they can provide either preferential sites for sulphide mineral deposition, leading to high-grade ore zones, or they can provide fluid barriers that retard fluid movement, causing the ponding of mineralizing fluids adjacent to low-grade or barren zones (Burnham, 1985; Sillitoe, 1985; Zweng and Clark, 1985; Bushnell, 1988; Serrano et al., 1996). Late breccia formation can also dilute ore by mixing fragments of variably mineralized rock, or by erupting, thereby venting potentially mineralizing fluids to the atmosphere and diluting the grade of the rock mass (e.g., Zweng and Clark, 1985; Cannell et al., 2005). Establishing those relations is therefore important, as breccias can have strong influences on distribution of metals and the economics of the deposit.

Lang et al. (1995b) noted that hydrothermal breccia is present in the silica-saturated and silica-undersaturated alkalic

porphyry deposits of British Columbia. In the silica-saturated deposits, the breccia formed during the main-stage mineralization, whereas, in the silica undersaturated deposits, it is interpreted to have formed pre-, syn-, and post-main stage mineralization. At Mount Polley, the breccia is a major host to ore grade Cu and Au (Fraser et al., 1995; Lang et al., 1995b).

Mount Polley is one of a series of silica-undersaturated alkalic Cu-Au porphyry deposits in British Columbia that formed in the Triassic to Early Jurassic Quesnel and Stikine terranes (Figure 1; Barr et al., 1976; Lang et al., 1995a; Logan and Mihalynuk, 2005). The Mount Polley deposit, owned and operated by Imperial Metals Corporation, is composed of several porphyry Cu-Au(-Ag) centres (Figure 2), most of which are breccia hosted (Hodgson et al., 1976; Fraser, 1994a, b; Fraser et al., 1995; Rees et al., 2005, 2006; Logan and Mihalynuk, 2005). The Cariboo, Bell and Springer deposits (Core zone) are hosted in part by hydrothermally brecciated intrusive rocks, with veins extending into surrounding monzonite and diorite (Fraser, 1994a, b; Fraser et al., 1995; Imperial Metals Corporation, 2007). In contrast, the Northeast zone, currently being mined in the Wight pit, is predominantly hosted by a polyolithic hydrothermal breccia body (Deyell, 2005; Deyell and Tosdal, 2005; Jackson et al., 2007; Pass et al., 2007; Imperial Metals Corporation, 2007).

Keywords: *alkalic, porphyry, hydrothermal breccia, Mount Polley*

This publication is also available, free of charge, as colour digital files in Adobe Acrobat® PDF format from the Geoscience BC website: <http://www.geosciencebc.com/s/DataReleases.asp>.

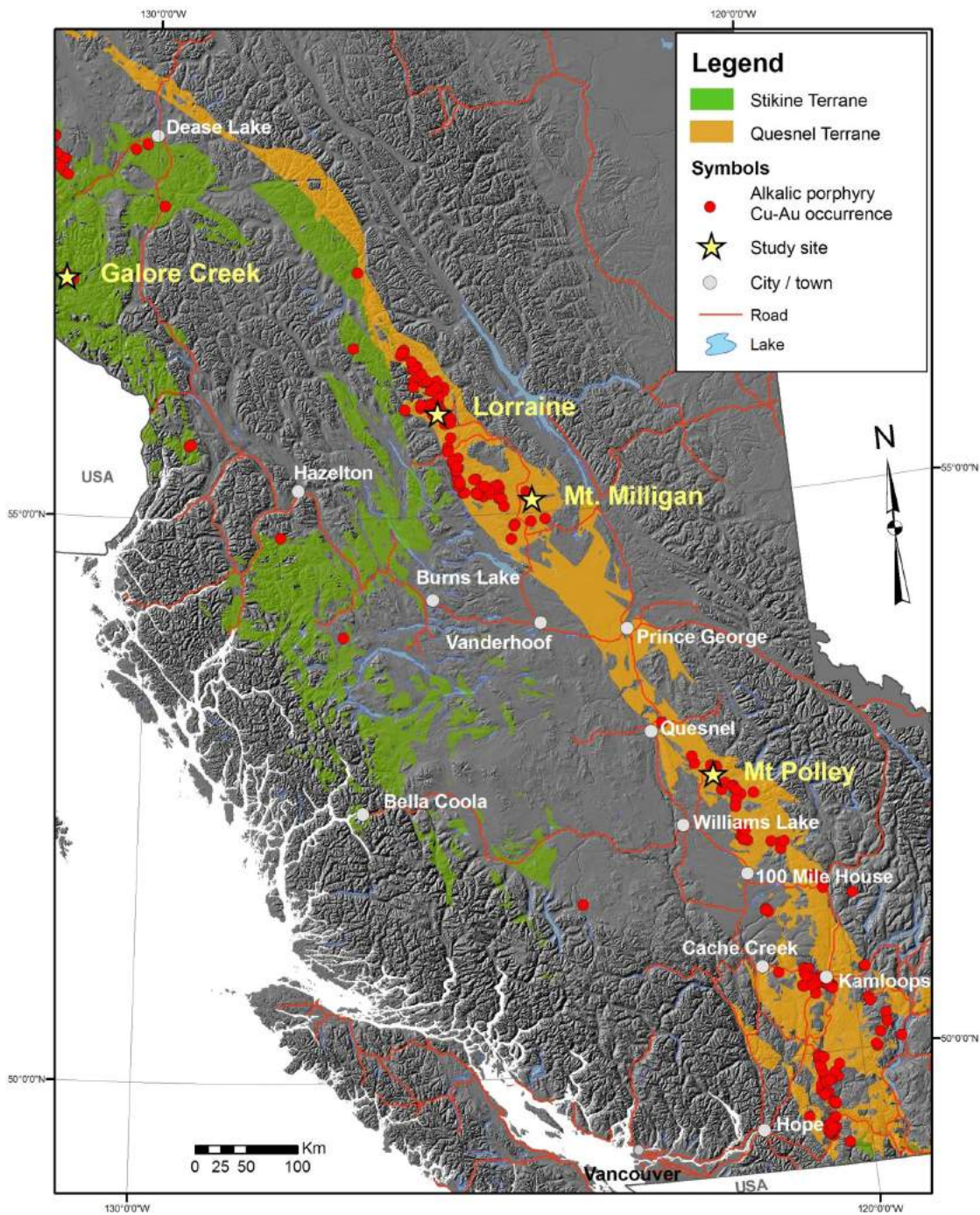


Figure 1. Location of alkalic porphyry Cu deposits in British Columbia, showing location of Mount Polley with respect to the other deposits and to the Triassic and Early Jurassic Quesnel and Stikine terranes.

Geological Framework of the Mount Polley District

The Mount Polley alkalic porphyry Cu-Au deposit lies along the eastern margin of the Intermontane Belt, close to the boundary with the Omineca Belt. Upper Paleozoic to Lower Mesozoic volcanic, plutonic and sedimentary rocks of the Quesnel Terrane are the principal rocks underlying the region (Panteleyev et al., 1996; Logan and Mihalynuk,

2005). The Quesnel Terrane consists primarily of Late Triassic to Early Jurassic magmatic-arc complexes formed above an east-dipping subduction zone (Mortimer, 1987). Mount Polley is one of a chain of alkalic intrusion-related porphyry Cu-Au deposits that developed at intervals along the arc (Barr et al., 1976; Lang et al., 1995a).

The Mount Polley deposit is hosted by a multiphase alkalic intrusive complex (Figure 2). The intrusive complex is a

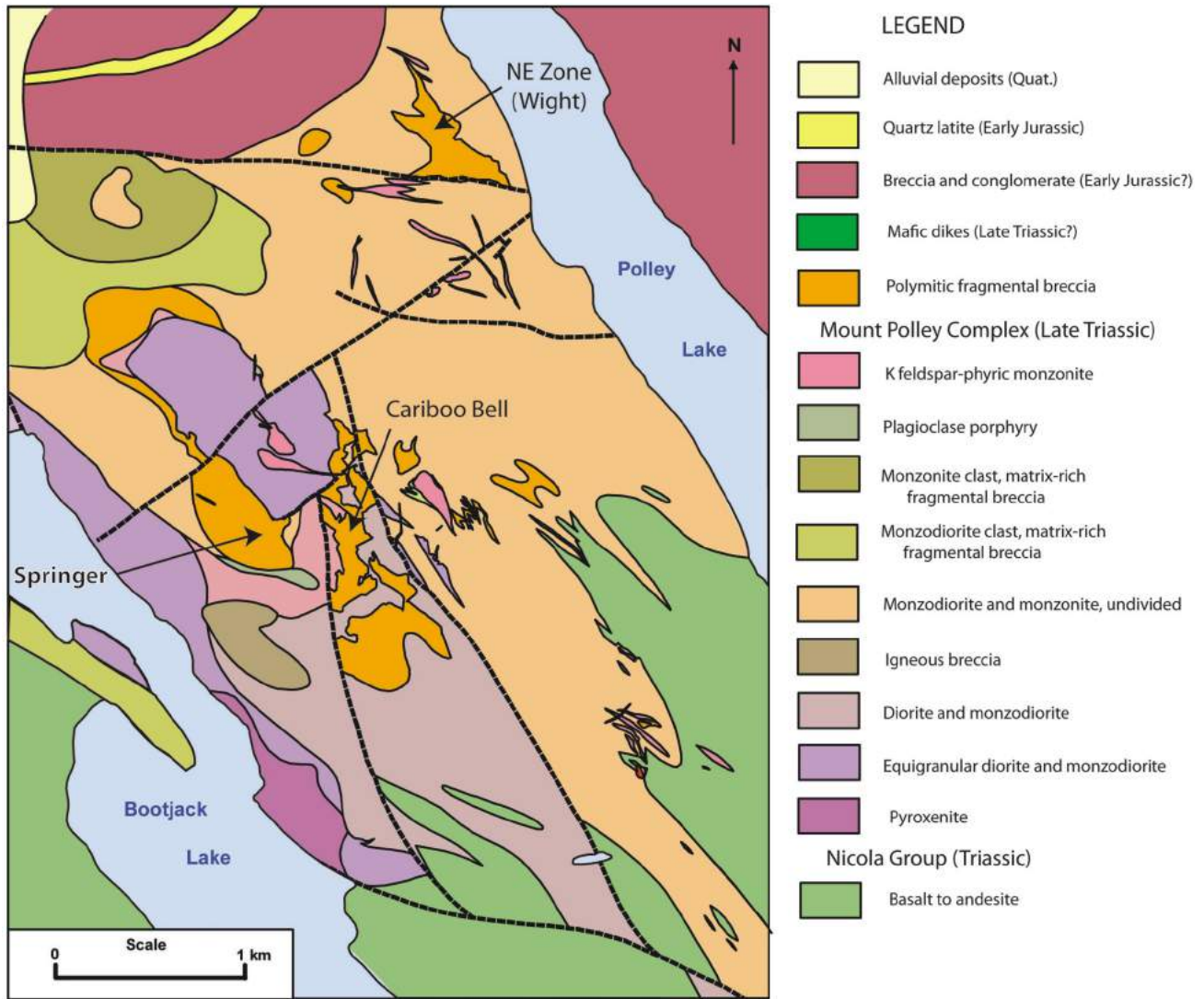


Figure 2. Generalized geology of the Mount Polley region, showing location of mineralized centres in the deposit (*adapted from Logan and Mihalynuk, 2005; Rees et al., 2005*).

north- to northwest-trending body composed primarily of equigranular to porphyritic diorite, monzodiorite and monzonite intruded by syenite dikes. Uranium-lead and ^{40}Ar - ^{39}Ar ages from several of the intrusive phases in the complex give dates between 201 and 205 Ma, indicating a Late Triassic age (Bailey and Archibald, 1990; Mortensen et al., 1995; Logan et al., 2007).

Diorite and monzodiorite are the oldest intrusive rocks in the complex (Logan and Mihalynuk, 2005; Rees et al., 2005, 2006) and consist largely of augite and plagioclase with minor K-feldspar in the monzodiorite. Monzonite, the most abundant rock type, consists of augite and lesser biotite, and subequal amounts of plagioclase and K-feldspar. Monzonite can be equigranular or porphyritic and is commonly reddish due to pervasive fine-grained hematite along grain boundaries. The hematite forms a halo around the orebody, and is an alteration common to many alkalic

porphyry systems (e.g., Wilson et al., 2003; Holliday and Cooke, 2007). Equigranular monzonite is the principal hostrock to breccia in the Northeast zone and is the most common clast type in that breccia. A distinctive, megacrystic, K-feldspar–phyric monzonite is present as clasts within breccia and also forms dikes or small elongate intrusive bodies outside the breccia bodies where they are spatially associated with most of the mineralized centres (Fraser, 1994b; Fraser et al., 1995; Logan and Mihalynuk, 2005; Logan et al., 2007). The megacrystic K-feldspar–phyric monzonite intrusions are thought to be associated with the hydrothermal system (Logan et al., 2007).

Core Zone (Springer-Bell-Cariboo Deposits)

The Mount Polley mine opened in 1997, with initial mining in the Cariboo and Bell orebodies (Fraser, 1994b; Fraser et al., 1995; Imperial Metals Corporation, 2007). Early work

on these mineralized zones identified concentrically zoned alteration assemblages, a central potassic zone, surrounded successively by garnet-epidote and a distal propylitic fringe (Hodgson et al., 1976; Bailey and Hodgson, 1979). Fraser et al. (1995) subsequently showed that the garnet-epidote was spatially restricted and did not form a concentric zone. Within the potassic zone, Cu-Fe sulphides are hosted in hydrothermal breccia and lesser veins (Fraser, 1994a, b; Fraser et al., 1995). Diorite, monzodiorite, and monzonite of the Mount Polley complex are the country rock to the breccia (Figure 3). Megacrystic K-feldspar-porphphyry dikes and small elliptical stocks are present in the area (Fraser et al., 1995; Rees et al., 2005).

The Cariboo deposit (Central zone *in* Fraser, 1994a, b) is developed in pink, potassically altered, fractured or brecciated diorite. Calcite, epidote, actinolite and microcline occur as breccia cement, within minor veins and as a replacement style of alteration. This alteration assemblage is more intense in more strongly mineralized rock. Magnetite as a breccia cement and veins is spatially highly variable (Fraser et al., 1995) but correlates with Cu and Au grade (Imperial Metals Corporation, 2007). Chalcopyrite is predominantly disseminated as a cement to the breccia, and less commonly as disseminations or in veinlets that cut the country rock and breccia.

The Bell deposit (Central zone *in* Fraser, 1994a, b), essentially a northward extension of the Cariboo deposit (Figures 2 and 3), is developed in K-feldspar-altered, brecciated monzodiorite and monzonite. Chalcopyrite is present as breccia cement, as well as disseminated and infill to veins. Hypogene bornite, chalcocite, covellite and digenite are also present, indicating that the hydrothermal fluid evolved toward high-sulphidization mineral assemblages (Einaudi et al., 2003). The Cariboo is characterized by a greater abundance of pyrite than the adjoining Cariboo (Imperial Metals Corporation, 2007).

The Springer deposit (West zone *in* Fraser, 1994a, b) is developed in strongly K-feldspar- and albite-altered breccias (Fraser et al., 1995; Imperial Metals Corporation, 2007). Rocks are frequently reddish due to the ubiquitous fine-grained hematite. Chalcopyrite is present as breccia cement, as well as disseminated and infill to veins. Minor bornite and trace quantities of covellite, chalcocite and digenite are also present. Albite veins present outside the breccia cut older K-feldspar and actinolite veins, indicating a late alteration stage.

Hydrothermal breccia in each zone is heterolithic, composed of clasts of diorite and monzonite with minor altered mafic rocks (Fraser, 1994a, b; Fraser et al., 1995). Using the terminology of Davies (2002; Davies et al., 2003), clast organization in the breccias ranges from jigsaw fit with angular clasts (indicative of *in situ* fragmentation and little to no

transport) to a chaotic organization with rounded clasts (interpreted to indicate significant transport and milling of clasts). Clast margins locally are partially replaced by actinolite, biotite or albite. Silicate alteration minerals and Cu-Fe sulphide minerals cement the clasts. Actinolite with minor chalcopyrite veins cut the breccia (Fraser, 1994b).

Fraser (1994a, b; Fraser et al., 1995) divided the hydrothermal breccias in the Cariboo-Bell and Springer deposits into four types, based on dominant silicate cement mineralogy: biotite, actinolite, albite and magnetite. Albite-cemented breccia in the Springer is characterized by the presence of tabular albite and lesser biotite, magnetite and sulphides as breccia cement. Clast boundaries are diffuse and albite has extensively replaced the clasts. Biotite- and actinolite-cemented breccia characterize the Cariboo and Bell. The actinolite-cemented breccia dominates the Bell, whereas the biotite-cemented breccia dominates the Cariboo (Figure 3). Fraser et al. (1995) reported that the transition between the two breccia cements is gradational. Actinolite or biotite forms the dominant breccia cement and contains Cu-Fe sulphide minerals in varying amounts. In the actinolite breccia, K-feldspar replaces breccia clast margins and also forms alteration selvages around actinolite-sulphide veins that cut the country rock and breccia. In the biotite-cemented breccia, the clasts are moderately to completely replaced by K-feldspar (Fraser, 1994b). Albite-cemented breccia overprints actinolite-cemented breccia in the northern part of the Bell pit.

Magnetite-cemented breccias are uncommon (Fraser, 1994b). Where present, however, they are commonly associated with elevated Cu concentrations (Imperial Metals Corporation, 2007). Clasts in these breccias are also partially replaced by K-feldspar. Sulphide and sparse pyroxene are also present as breccia cement.

Northeast Zone (Wight Pit)

The Northeast zone (Wight pit) is distinctly higher grade than other Mount Polley deposits and consists of coarser grained Cu-Fe sulphides than the Cariboo, Bell or Springer ores. The average Cu grade in this zone is 0.8–1.0%, which is approximately three times higher than the other zones (Imperial Metals Corporation, 2007).

Copper-iron sulphides in the Wight pit are confined to a dominantly polyolithic breccia body (Figure 4) hosted in a distinctly hematite-dusted monzonite (Jackson et al., 2007; Logan et al., 2007; Pass et al., 2007; Imperial Metals Corporation, 2007). The breccia body is irregular in shape and intruded by multiple generations of post-mineral, petrologically related dikes and cut by post-mineral faults. The breccia appears to be divisible into two segments (Figure 4). A northern segment appears to narrow with depth (Pass et al., 2007), where it is extensively intruded by post-breccia barren dikes. A southern segment is fault bounded,

forming a discordant wedge between the Green Giant fault, the Brown Wall fault and potentially a fault that cuts the breccia obliquely, separating the southern from the northern end (Figure 4). The breccia consists of jigsaw-fit, rotated and chaotic facies, which reflect increasing degrees of transport during brecciation. Approximately 90% of breccia clasts are equigranular, augite-bearing, monzonite

country rock. The breccia also contains clasts of mafic rock and strongly altered material.

Locally, a significant percentage (up to 10% overall but locally greater than 50%) of the breccia is composed of K-feldspar megacrystic monzonite porphyry clasts, many of which have fine-grained margins and globular shapes, im-

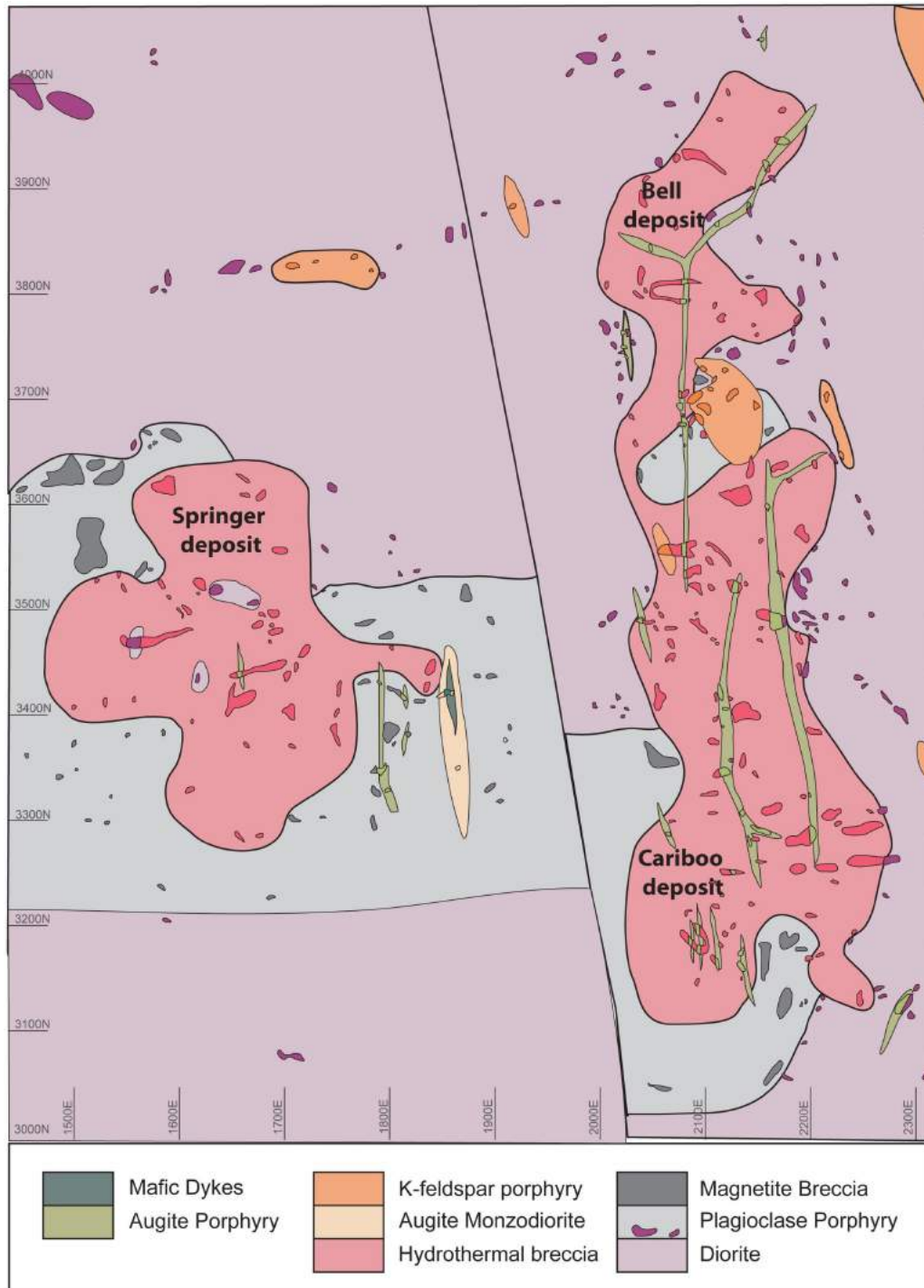


Figure 3. Pre-mining surface geological map of the 'Central and West' zones, now referred to as the Core zone (modified from Fraser et al., 1995).

plying they were still hot and able to plastically deform at the time of brecciation (Rees et al., 2006; Jackson et al., 2007). Equigranular to plagioclase-phyric monzonite is the most volumetrically significant intrusive phase of the Mount Polley complex, and is the dominant clast type in the breccia.

Alteration is characterized by reddish K-feldspar, calcite and a marginal zone marked by fine-grained andraditic garnet. Significant hydrothermal magnetite is not present, in contrast to the Cariboo-Bell and Springer zones (Imperial Metals Corporation, 2007). Chalcopyrite occurs as a cement in both jigsaw-fit breccia and in matrix-poor, clast-supported, polyolithic chaotic breccia. Bornite accompanies chalcopyrite in the high-grade core of the orebody (Deyell, 2005; Deyell and Tosdal, 2005; Pass et al., 2007), where it commonly rims and locally replaces chalcopyrite, becoming the dominant Cu-Fe sulphide. Pyrite is sparse to absent in the high-grade core but increases towards the outer parts

(Imperial Metals Corporation, 2007). A second generation of volumetrically minor Cu-Fe sulphide-bearing veinlets followed intrusion of post-breccia, equigranular, augite-bearing monzonite dikes.

The bulk of sulphide mineral deposition is accompanied by biotite cement and alteration of clasts, with the highest Cu grades found near the contact between biotite-dominant and K-feldspar-dominant assemblages (Jackson et al., 2007; Pass et al., 2007). Magnetite is present at depth beneath the Cu-Fe sulphide minerals but is not associated with higher Cu grades, in contrast to the situation in the Cariboo and Bell pits (Imperial Metals Corporation, 2007). The magnetite at depth is overprinted by a late albite-epidote assemblage. Hematite dusting and carbonate blebs are ubiquitous throughout and around the ore zone. Late quartz-sericite-pyrite and carbonate-pyrite assemblages are localized along fractures, faults and veins (Pass et al., 2007).

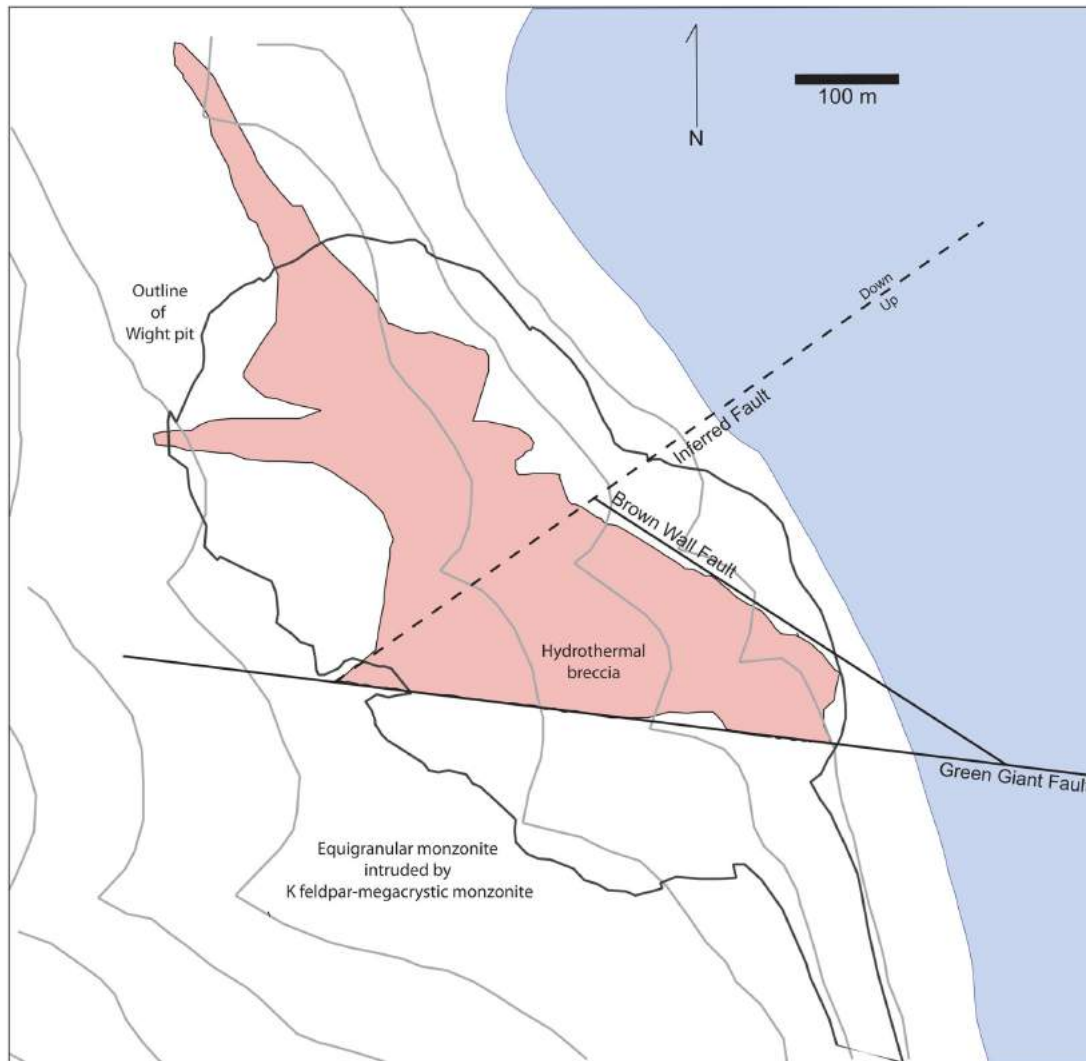


Figure 4. Surface map of Northeast Zone breccia being developed in the Wight pit.

Most of the breccia margins are truncated by post-breccia faults or are exploited by post-breccia dikes, leading to a highly irregular map pattern (Figure 4). Where breccia margins are preserved, there is a gradation from coherent country rock to jigsaw-fit breccia to rotated and chaotic breccias. Preserved breccia margins are rare, so the original volume and geometry of the breccia body is poorly constrained.

Hydrothermal Breccia in Alkalic Porphyry Systems

It is evident that, in the orebodies that have been mined or are being mined at Mount Polley, there is a close relationship between hydrothermal breccia and economic Cu-Fe sulphide minerals (Lang et al., 1995b; Imperial Metals Corporation, 2007). Furthermore, there is also an association between Cu grade and the apparent intensity of brecciation, as the Core zone (Cariboo-Bell-Springer) contains both breccia- and vein-hosted Cu, whereas the higher grade Northeast zone is entirely hosted in breccia (Fraser et al., 1995; Lang et al., 1995; Imperial Metals Corporation, 2007).

Despite the differences in grade and brecciation style, there are similarities between the orebodies at Mount Polley. They all have a high-temperature core consisting of potassic alteration minerals (K-feldspar and biotite) that are typical of most porphyry Cu deposits regardless of composition (Seedorff et al., 2005). Actinolite associated with Cu-Fe sulphide minerals is also common in all the Core zone deposits, although it is rare in the Northeast zone. The presence of actinolite indicates a calcipotassic assemblage in the high-temperature portions of the deposits, a characteristic found in most alkalic porphyry systems worldwide (Lang et al., 1995b; Wilson et al., 2003; Holliday and Cooke, 2007).

The widespread presence of hydrothermal breccia in the ore zones of Mount Polley distinguish this alkalic system from many of the other alkalic porphyry systems in British Columbia. Hydrothermal breccias are reported to be common at Galore Creek (Enns et al., 1995), where they in part host Cu-Au ore but can also lack any significant Cu and Au values (Lang et al., 1995b). Of the many deposits around the Iron Mask batholith, only the DM and Crescent deposits are hosted in significant hydrothermal breccia (Lang et al., 1995b). Hydrothermal breccias are present but reportedly insignificant at Copper Mountain and Mount Milligan (Lang et al., 1995b; Sketchley et al., 1995). It is interesting that, although the tonnage of the various deposits varies considerably, grade correlates with the presence of significant breccia, with Mount Polley and Galore Creek both having generally higher grades than do systems lacking significant breccia (*see* Table 1 *in* Lang et al., 1995b).

Hydrothermal breccia forms where the ambient fluid pressure exceeds the lithostatic load of the overlying rock column coupled with the tensile strength of the surrounding rock (Burnham, 1985). Thus, breccia should form more easily in shallow upper-crustal environments. As such, it is tempting to suggest that Mount Polley represents one of the shallower alkalic porphyry deposits in BC. As an analogy, Zweng and Clark (1995) used fluid inclusions from the breccia-hosted Toquepala porphyry Cu-Mo system (>800 million tonnes) in southern Peru to suggest that it formed at much shallower depths than the nearby vein-dominated Cuajone porphyry Cu-Mo deposit (>1200 million tonnes). Unfortunately, most alkalic porphyry systems in British Columbia lack the appropriate minerals from which depth of formation can be determined, and geological constraints on the scale of post-mineral erosion and deformation of the Triassic and Early Jurassic deposits are limited. These two factors have, to date, precluded the establishment of any independent constraints on the depth of formation of these systems (Lang et al., 1995b).

Acknowledgments

Support for the porphyry component of the project derives from the following companies and organizations, and their financial and logistical support is gratefully acknowledged: Geoscience BC, Natural Sciences and Engineering Research Council of Canada (NSERC), AngloGold Ashanti Limited, Amarc Resources Ltd., Barrick Gold Corporation, Imperial Metals Corporation, Lysander Minerals Corporation, Newcrest Mining Limited, Newmont Mining Corporation, NovaGold Resources Inc. and Teck Cominco Limited. The authors are particularly indebted to Imperial Metals Corporation for their logistic support and scientific collaboration.

References

- Bailey, D.G. and Archibald, D.A. (1990): Age of the Bootjack stock, Quesnel Terrane, south-central British Columbia (93A); *in* Geological Fieldwork 1989, BC Ministry of Energy, Mines and Petroleum Resources, Paper 1990-1, p. 79–82.
- Bailey, D.G. and Hodgson, C.J. (1979): Transported altered wall rock in laharic breccias at the Cariboo-Bell Cu-Au porphyry deposit, British Columbia; *Economic Geology*, v. 74, p. 125–153.
- Barr, D.A., Fox, P.E., Northcote, K.E. and Preto, V.A. (1976): The alkaline suite porphyry deposits: a summary; *in* Porphyry Deposits of the Canadian Cordillera, A. Sutherland Brown (ed.), Canadian Institute of Mining and Metallurgy, Special Volume 15, p. 359–367.
- Burnham, C.W. (1985): Energy release in subvolcanic environments: implications for breccia formation; *Economic Geology*, v. 80, p. 1515–1522.
- Bushnell, S.E. (1988): Mineralization at Cananea, Sonora, and the paragenesis and zoning of breccia pipes in quartzofeldspathic rock; *Economic Geology*, v. 83, p. 1760–1781.

- Cannell, J., Cooke, D.R., Walshe, J.L. and Stein, H. (2005): Geology, mineralization, alteration, and structural evolution of El Teniente porphyry Cu-Mo deposit; *Economic Geology*, v. 100, p. 979–1004.
- Davies, A.G.S. (2002): Geology and genesis of the Kelian gold deposit, East Kalimantan, Indonesia; Ph.D. thesis, University of Tasmania, Hobart, Tasmania, Australia, 404 p.
- Davies, A.G.S., Cooke, D.R. and Gemmell, J.B. (2003): The Kelian breccia complex: a giant epithermal gold-silver deposit in Kalimantan, Indonesia; *Society for Geology Applied to Mineral Deposits (SGA), 7th Biennial Meeting, Proceedings*, p. 465–468.
- Deyell, C.L. (2005): Sulfur isotope zonation at the Mt. Polley alkalic porphyry Cu-Au deposit, British Columbia (Canada); *Society for Geology Applied to Mineral Deposits, 8th Biennial Meeting, Proceedings*, p. 373–376.
- Deyell, C.L. and Tosdal, R.M. (2005): Alkalic Cu-Au deposits of British Columbia: sulfur isotope zonation as a guide to mineral exploration; *British Columbia Ministry of Energy, Mines, and Petroleum Resources, Paper 2005-1*, p. 191–208.
- Einaudi, M.T., Hedenquist, J.W. and Inan, E.E. (2003): Sulfidation state of fluids in active and extinct hydrothermal systems: transitions from porphyry to epithermal environments; *Society of Economic Geologists, Special Publication 10*, p. 285–313.
- Enns, S.G., Thompson, J.F.H., Stanley, C.R., and Yarrow, E.W. (1995): The Galore Creek porphyry copper-gold deposits, northwestern British Columbia; *in Porphyry Deposits of the Northwestern Cordillera of North America*, T.G. Schroeter (ed.), Canadian Institute of Mining and Metallurgy, Special Volume 46, p. 630–644.
- Fraser, T.M. (1994a): Geology, alteration and origin of hydrothermal breccias at the Mount Polley alkalic porphyry copper-gold deposit, south-central British Columbia; M.Sc. thesis, University of British Columbia, Vancouver, BC, 261 p.
- Fraser, T.M. (1994b): Hydrothermal breccias and associated alteration of the Mount Polley copper-gold deposit (93A/12); *in Geological Fieldwork 1993*, BC Ministry of Energy and Mines and Petroleum Resources, Paper 1994-1, p. 259–267.
- Fraser, T.M., Stanley, C.R., Nikic, Z.T., Pesalj, R. and Gorc, D. (1995): The Mount Polley alkalic porphyry copper-gold deposit, south-central British Columbia; *in Porphyry Deposits of the Northwestern Cordillera of North America*, T.G. Schroeter, T.G. (ed.), Canadian Institute of Mining and Metallurgy, Special Volume 46, p. 609–622.
- Hodgson, C.J., Bailes, R.J. and Verzosa, R.S. (1976): Cariboo-Bell; *in Porphyry Copper Deposits of the Canadian Cordillera*, A. Sutherland Brown (ed.), Canadian Institute of Mining and Metallurgy, Special Volume 15, p. 388–396.
- Holliday, J.R. and Cooke, D.R. (2007): Advances in geological models and exploration methods for copper ± gold porphyry deposits; *Proceedings of Exploration 07, Fifth Decennial International Conference on Mineral Exploration*, p. 791–809.
- Imperial Metals Corporation (2007) Imperial Metals Annual Information Form; Imperial Metals Corporation, 47 p.
- Jackson, M.L., Tosdal, R.M., Chamberlain, C.M., Simpson, K. and McAndless, P. (2007): Breccia architecture as a control on ore distribution, Mount Polley mine, British Columbia; *in Breccias (abstract volume)*, Economic Geology Research Unit (EGRU), School of Earth Sciences, James Cook University, Townsville, Queensland, Australia, Contribution 65, p. 12.
- Lang, J.R., Lueck, B., Mortensen, J.K., Russell, J.K., Stanley, C.R. and Thompson, J.F.H. (1995a): Triassic-Jurassic silica-undersaturated and silica-saturated alkalic intrusions in the Cordillera of British Columbia: implications for arc magmatism; *Geology*, v. 23, p. 451–454.
- Lang, J.R., Stanley, C.R. and Thompson, J.F.H. (1995b): Porphyry copper deposits related to alkalic igneous rocks in the Triassic-Jurassic arc terranes of British Columbia; *in Porphyry Copper Deposits of the American Cordillera*, F.W. Pierce and J.G. Bolm (ed.), Arizona Geological Society, Digest 20, p. 219–236.
- Logan, J.M. and Mihalynuk, M.G. (2005): Regional geology and setting of the Cariboo, Bell, Springer and Northeast porphyry Cu-Au zones at Mount Polley, south-central British Columbia; *in Geological Fieldwork 2004*, BC Ministry of Energy, Mines, and Petroleum Resources, Paper 2005-1, p. 249–270.
- Logan, J.M., Mihalynuk, M.G., Ullrich, T. and Friedman, R.M. (2007): U-Pb age of intrusive rocks and ⁴⁰Ar-³⁹Ar plateau ages of copper-gold-silver mineralization associated with alkaline intrusive centres at Mount Polley and the Iron Mask batholith, southern and central British Columbia; *in Geological Fieldwork 2006*, BC Ministry of Energy, Mines, and Petroleum Resources, Paper 2007-1, p. 93–115.
- Mortensen, J.K. Ghosh, D.K. and Ferri, F. (1995): U-Pb geochronology of intrusive rocks associated with copper-gold porphyry deposits in the Canadian Cordillera; *in Porphyry Deposits of the Northwestern Cordillera of North America*, T.G. Schroeter (ed.), Canadian Institute of Mining and Metallurgy, Special Volume 46, p. 142–158.
- Mortimer, N. (1987): The Nicola Group: Late Triassic and Early Jurassic subduction-related volcanism in British Columbia; *Canadian Journal of Earth Sciences*, v. 24, p. 2521–2536.
- Panteleyev, A., Bailey, D.G., Bloodgood, M.A. and Hancock, K.D. (1996): Geology and mineral deposits of the Quesnel River-Horsefly map area, central Quesnel Trough, British Columbia (NTS 93A/5, 6, 7, 11, 13; 93B/9, 16; 93G/1; 93H/4); *BC Ministry of Energy, Mines, and Petroleum Resources, Bulletin 97*, 156 p.
- Pass, H.E., Cooke, D.R., Chamberlain, C., Simpson, K., Rees, C., Ferreira, L., McAndless, P. and Robertson, S. (2007): Infill paragenesis and hydrothermal alteration in the Northeast zone of the Mt. Polley magmatic-hydrothermal breccia complex, British Columbia; *Proceedings of the 9th Biennial meeting of the Society for Geology Applied to Mineral Deposits*, Irish Association for Economic Geology, p. 423–426.
- Rees, C., Bjornson, L., Blackwell, J., Ferreira, L., McAndless, P., Robertson, S., Roste, G., Stuble, T. and Taylor, C. (2005): Geological report on the Mount Polley property and summary of exploration in 2003–2004; Imperial Metals Corporation, internal report, 211 p.
- Rees, C., Ferreira, L., Bjornson, L., Blackwell, J., Roste, G., Stuble, T. and Taylor, C. (2006): Geological report on the Mount Polley property and summary of 2005 exploration; Imperial Metals Corporation, internal report, 169 p.
- Seedorff, E., Dilles, J.H., Proffett, J.M., Jr., Einaudi, M.T., Zucher, L., Stavast, W.J.A., Johnson, D.A. and Barton, M.D. (2005): Porphyry-related deposits: characteristics and origin of hypogene features; *in Economic Geology 100th Anniversary Volume*, J. Hedenquist, J., J.F. Thompson and J.

- Richards, (ed.), Society of Economic Geologists, p. 251-298.
- Serrano, L., Vargas, R., Stambuk, V., Aguilar, C., Galeb, M. Holmgren, A., Contreras, A., Godoy, S., Vela, I., Skewes, M.A. and Stern, C.A. (1996), The late Miocene to early Pliocene Rio Blanco–Los Bronces copper deposit, central Chilean Andes; *in* Andean Copper Deposits: New Discoveries, Mineralization, Styles, and Metallogeny, F. Camus, R.W. Sillitoe and R. Petersen (ed.), Society of Economic Geologists, Special Publication 5, p. 119–130.
- Sketchley, D.A., Rebagliati, C.M. and DeLong, C. (1995): Geology, alteration, and zoning patterns of the Mt. Milligan copper-gold deposits; *in* Porphyry Deposits of the Northwestern Cordillera of North America, T.G. Schroeter (ed.), Canadian Institute of Mining and Metallurgy, Special Volume 46, p. 650–665.
- Sillitoe, R.H., (1985): Ore-related breccias in volcanoplutonic arcs; *Economic Geology*, v. 80, p. 1467–1514.
- Wilson, A., Cooke, D.R. and Harper, B.L. (2003): The Ridgeway gold-copper deposit: a high-grade alkalic porphyry deposit in the Lachlan Fold Belt, NSW, Australia; *Economic Geology*, v. 98, p. 1637–1656
- Zweng, P.L., and Clark, A.H. (1995): Hypogene evolution of the Toquepala porphyry copper-molybdenum deposit, Moquegua, southeastern Peru; *in* Porphyry Copper Deposits of the American Cordillera, F.W. Pierce and J.G. Bolm (ed.), Arizona Geological Society, Digest 20, p. 566–612.

Mapping the Structure of the Nechako Basin Using Passive Source Seismology

J.F. Cassidy, Geological Survey of Canada, Sidney, BC; University of Victoria, School of Earth and Ocean Sciences, Victoria, BC; JCassidy@NRCan.gc.ca

I. Al-Khoubbi, Geological Survey of Canada, Sidney, BC

H.S. Kim, University of Victoria, School of Earth and Ocean Sciences, Victoria, BC

Cassidy, J.F., Al-Khoubbi, I. and Kim, H.S. (2007): Mapping the Structure of the Nechako Basin Using Passive Source Seismology; in Geoscience BC Summary of Activities 2007, Geoscience BC, Report 2008-1, p. 115–120.

Introduction

The key objective of this project is to help assess the hydrocarbon and mineral potential of the Nechako Basin area in central British Columbia, using passive source seismology. The Nechako Basin has been the focus of limited hydrocarbon exploration since the 1930s. Seven exploratory wells were drilled, and oil stains on drill chip samples, as well as the presence of gas in drill stem tests, attest to some hydrocarbon potential. Seismic data collected in the 1980s were of variable quality, mainly due to the effects of volcanic cover. This study will utilize recordings of distant earthquakes and background noise to map the sediment thickness, crustal thickness and overall geometry of the Nechako Basin. An array of seven seismic stations was deployed in September 2006 (Table 1, Figure 1) to sample a large area of the basin. The results of this study will complement independent active-source seismic studies that are planned for the region by providing images using waves coming from within the earth and providing constraints on the shear-wave velocity. The results of this research will also complement magnetotelluric (MT) studies that are currently underway, providing critical new information on porosity, fractures and fluids. This paper describes the methods that will be used, the progress of the data collection to date, some preliminary results and future work.

Methodologies

Receiver Function Analysis

The primary technique used in this study will be receiver function analysis, in order to constrain the shear-wave velocity structure. In this method, locally generated P- to S-wave conversions (Figure 2; Cassidy, 1992, 1995; Eaton and Cassidy, 1996) will be used to map major discontinuities beneath the seven three-component seismic stations

Keywords: geophysics, Nechako Basin, seismology, S-wave velocity

This publication is also available, free of charge, as colour digital files in Adobe Acrobat® PDF format from the Geoscience BC website: <http://www.geosciencebc.com/s/DataReleases.asp>.

Table 1. Location of broadband seismic stations in the Nechako Basin.

Seismic Station Location	Code	Latitude	Longitude	Elevation (km)
Anahim Lake, BC	ALRB	52.5103	-125.0844	1.237
Cack lake ¹ seismic station, BC	CLSB	52.7587	-122.5551	0.792
Fletcher Lake, BC	FLLB	51.739	-123.1059	1.189
southwest Quesnel, BC	RAMB	52.632	-123.1227	1.259
south of Vanderhoof, BC	SULB	53.2786	-124.3576	1.171
Tatla Lake, BC	TALB	52.0147	-124.2536	1.127
Thunder Mountain, BC	THMB	52.5489	-124.1323	1.126

¹ unofficial place name

deployed across the Nechako Basin (covering an area of approximately 33 000 km²). This method typically requires recording for approximately a two-year period in order to collect enough recordings sampling a wide range of directions and distances. The advantages of this method include site-specific information (mapping discontinuities directly beneath the recording site); S-velocity information (difficult to obtain from other studies); interface geometry, including dip angle and direction; and images obtainable for structure beneath strong near-surface reflectors, as the teleseismic energy is coming from below these near-surface reflectors, thereby providing images of both near-surface and crustal-scale structure. A similar study, conducted across the northern Coast Mountains of BC to image the coastal batholith, shows a pronounced change in crustal structure at the boundary between the batholith and the westernmost edge of the Nechako Basin. This attests to the capacity of this imaging method to resolve crustal architecture in this region.

The receiver function method has recently been applied in studies of sedimentary basins around the world. In the Bohai Bay Basin (China), Zheng et al. (2005) used receiver functions to map the sedimentary thickness (2–12 km) and velocities to better understand the petroleum potential of this region. In the Mississippi embayment, Julia et al. (2004) combined results from detailed geotechnical, seismic reflection and receiver function studies to determine the velocity structure and density profiles of the sedimentary column, as well as sedimentary thickness. In Chile, Lawrence and Wiens (2004) combined receiver function

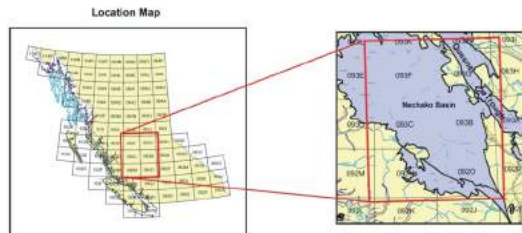
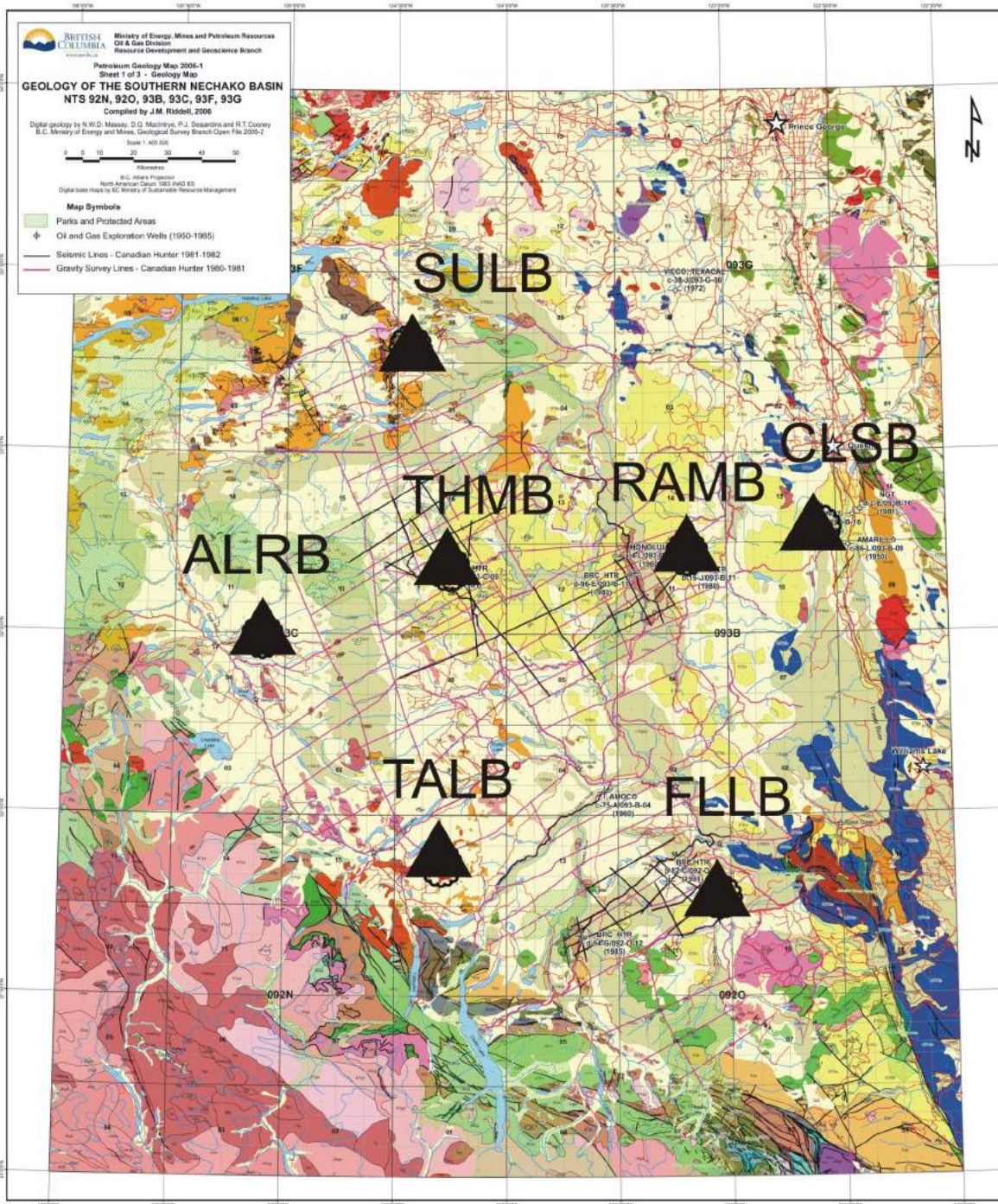


Figure 1. Location of the study area. Filled triangles (and four-character station codes) indicate the locations of the seven broadband seismic stations. Base map from Riddell (2006).

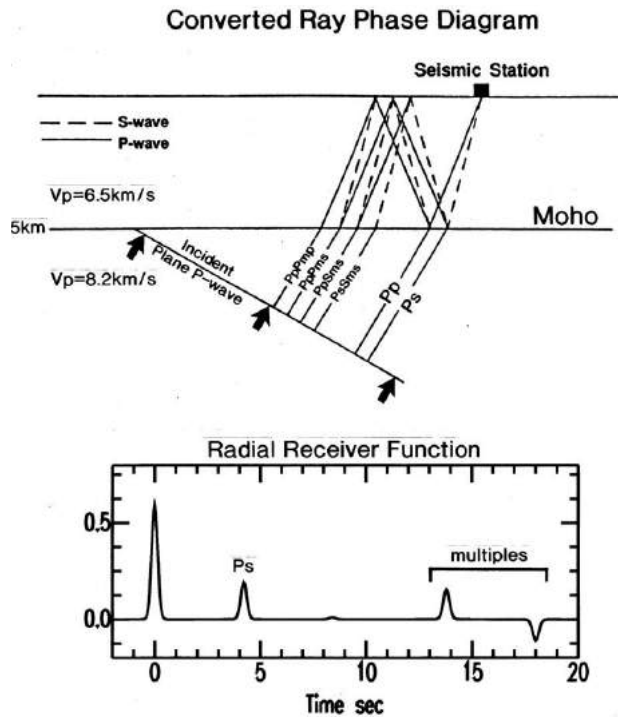


Figure 2. Diagram illustrating the receiver function method. When incident P waves from distant earthquakes encounter S-wave velocity boundaries beneath a seismic station (top), some of the energy is converted to an S wave (Ps). The amplitude and arrival time of the Ps phase, relative to the direct P wave, provides constraints on the velocity contrast and depth to the interface.

data with surface wave data to map the sedimentary rocks in Rocas Verdes Basin of Patagonia.

Surface-Wave Tomography Using Ambient Noise

Analysis of seismic ‘noise’ is being undertaken to constrain the velocity structure of the Nechako Basin. This method has been successfully used to map sedimentary basins in southern California (e.g., Sabra et al., 2005; Shapiro et al., 2005) and numerous other locations around the world. In this type of study, ambient noise recordings made at stations 20–100 km apart (or more) are compared and aligned. These recordings, typically dominated by Rayleigh waves, are modelled to constrain the velocity structure at various depths. This ‘ambient noise’ study will complement the receiver function technique (which provides site-specific information beneath the recording stations) by providing models that average the velocity structure between pairs of stations. By combining all possible station-pairs, a tomographic image beneath the basin will be obtained.

Data

In September 2006, seven three-component broadband seismic stations were deployed across the Nechako Basin area of central BC. The sites were chosen to sample a large portion of the basin, and to be close to existing boreholes



Figure 3. Photograph of Nechako seismic station RAMB, showing the typical station layout, with solar panels and satellite dish (seismic vault is not visible).

(Figure 1). These stations utilize solar power and satellite data transmission, in order that ground shaking can be recorded continuously and the data transmitted in real time and archived at data collection centres in Sidney, BC and Ottawa, ON. A typical station setup, consisting of solar panels, a seismic vault and a satellite dish with associated electronics, is shown in Figure 3.

During the first twelve months of operation, more than 100 large, distant earthquakes (teleseisms) were recorded (Figure 4). These data will be useful for the receiver function analysis described above. These events cover a wide range of azimuth and distance, providing a suitable dataset for examining geometry (dip angle and direction) of the structural boundaries beneath the seismic stations. In addition,

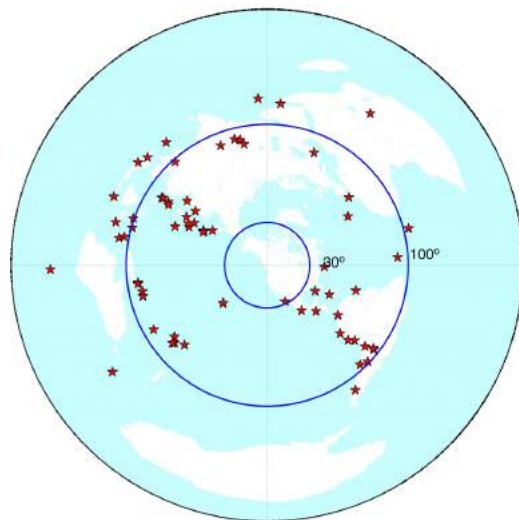


Figure 4. Distribution of teleseisms recorded during the first year of array operation. Stars indicate large (magnitude >6), distant earthquakes. The map is centred on the Nechako Basin seismic array, with distances of 3360 km (30°) and 11200 km (100°) indicated. This is the useful distance range for receiver function studies.

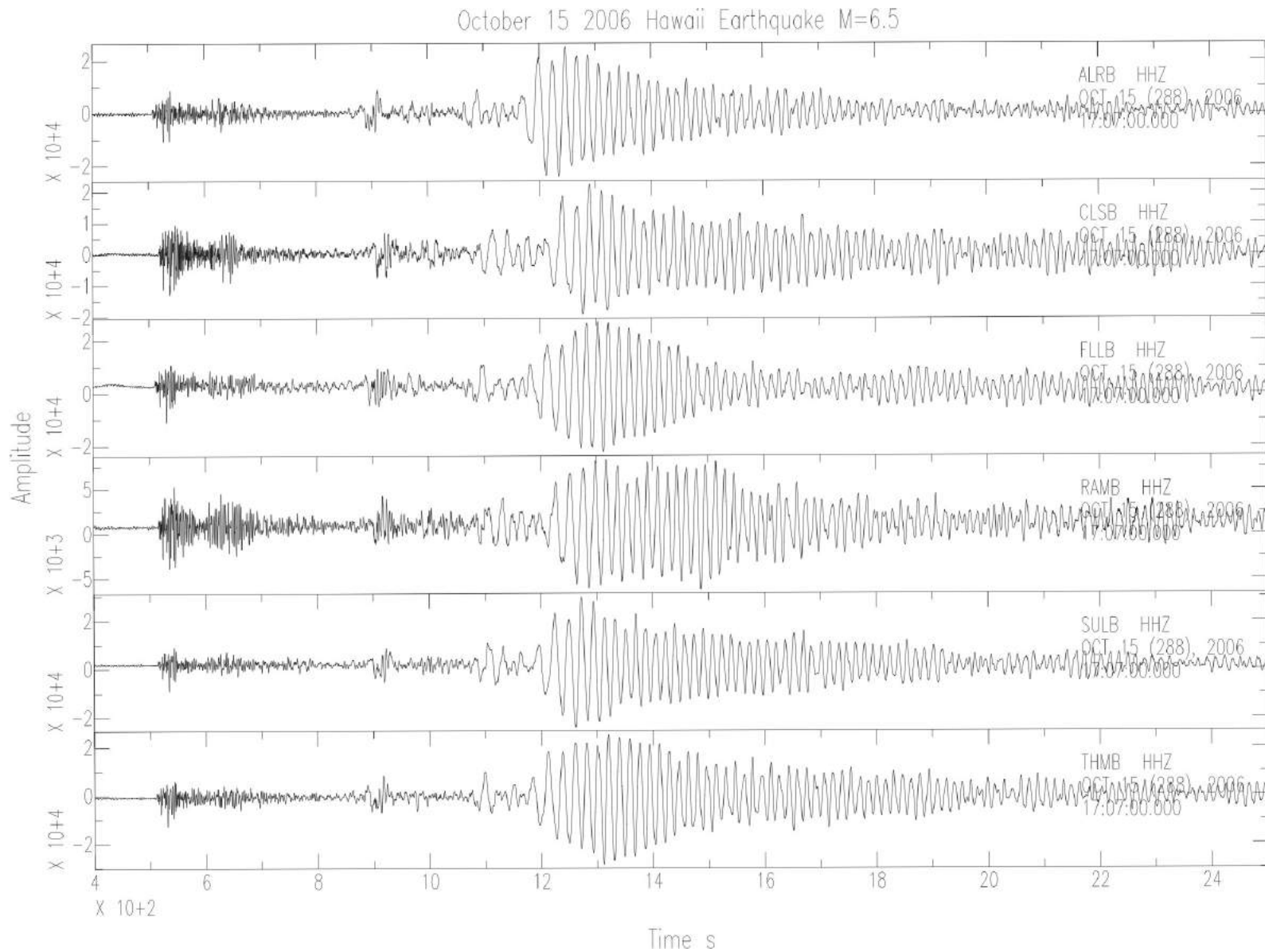


Figure 5. Sample waveforms (magnitude 6.3 earthquake near Hawaii) recorded on the Nechako seismic stations. These waves contain information on the subsurface structure of the Nechako Basin.

background noise (recorded continuously) is being used for the surface-wave tomography noise study sampling of the basin. Sample waveforms of a teleseism are provided in Figure 5.

Preliminary Results

To date, only a small number of receiver functions have been computed for stations within the Nechako Basin. These preliminary receiver functions, however, are consistent, and show arrivals indicative of sedimentary rocks in the basin and crustal thickness variations. For example, the receiver functions for the magnitude 8.1 Kuril Islands earthquake on January 13, 2007 is shown in Figure 6. The arrival at Time '0' is the direct P wave, other arrivals are locally generated P- to S-wave converted phases and free-

surface multiples. The Ps-converted phase near 4 s is associated with the continental Moho (as are the multiples at 12–17 s). The earlier arrivals (i.e., the arrivals within the first 2 s) are associated with near-surface, low-velocity sedimentary rocks. As many dozens of receiver functions are processed in the near future, S-wave velocity models will be developed for each of these sites.

Future Work

Over the next six months, receiver functions will be computed for all suitable events recorded to date. These will be stacked into distance and azimuth bins and used to identify the robust phases that will be modelled for shear-wave velocity structure. Amplitudes and arrival times will be used to constrain the S-wave velocity contrast and depth of the

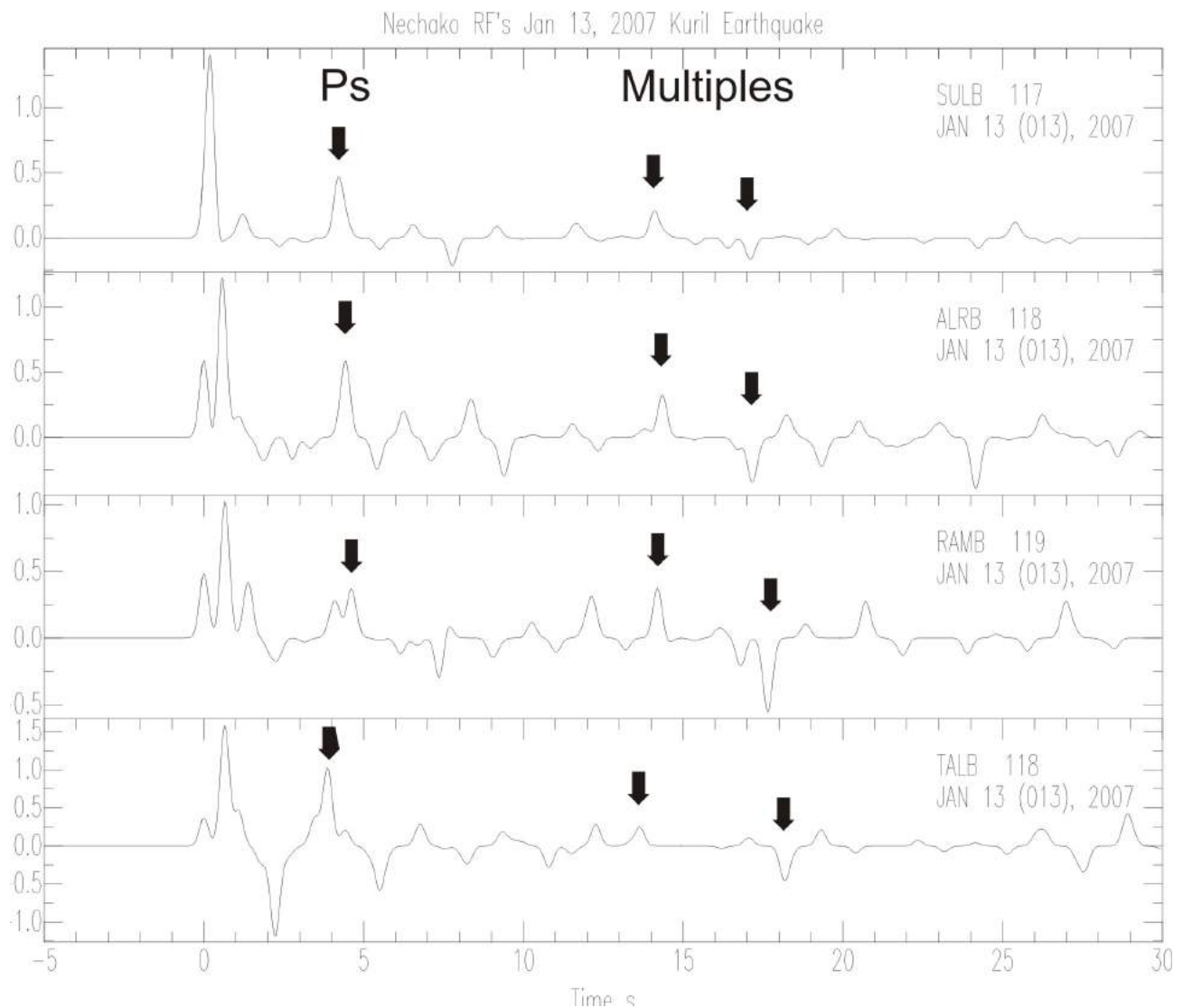


Figure 6. Sample receiver functions for select Nechako Basin stations. The arrival at Time '0' is the direct P wave. Subsequent arrivals are locally generated P- to S-wave converted phases and free-surface multiples. A small-amplitude arrival at T = 0, followed immediately by large-amplitude arrivals, is indicative of near-surface, low-velocity sedimentary rocks. The large arrivals indicated by arrows are consistent with a Ps conversion from the continental Moho (near T = 4 s) and free-surface multiples of this phase near T = 12–17 s.

boundary, and azimuth variations in the receiver functions will help constrain the geometry (dip angle and direction) of the interfaces. This research is being undertaken by a University of Victoria M.Sc. student (H. Kim). The regional surface wave tomography ambient noise study is now underway, being conducted by a University of Manitoba M.Sc. student. Initial results and interpretations, including shear-wave velocity models, will be presented in 2008.

Acknowledgments

The authors gratefully acknowledge the financial support of the BC Ministry of Energy, Mines and Petroleum Resources, the Geological Survey of Canada and Geoscience BC in deploying and operating this seismic network. J. McCutcheon of the University of Manitoba, and S. Williams of the Geological Survey of Canada are thanked for their assistance deploying this seismic array, and I. Asudeh and the POLARIS team for maintaining these instruments. H. Kao and R. Currie are thanked for providing a thorough review of this manuscript.

Geological Survey of Canada contribution 20070361.

References

- Cassidy, J.F. (1992): Numerical experiments in broadband receiver function analysis; *Bulletin of the Seismological Society of America*, v. 82, p. 1453–1474.
- Cassidy, J.F. (1995): A comparison of the receiver structure beneath stations of the Canadian National Seismograph Network; *Canadian Journal of Earth Sciences*, v. 32, p. 938–951.
- Currie, C.A., Cassidy, J.F. and Hyndman, R.D. (2001): A regional study of crustal shear wave splitting above the Cascadia subduction zone: margin parallel crustal stress; *Geophysical Research Letters*, v. 28, p. 659–662.
- Eaton, D.W. and Cassidy, J.F. (1996): A relict subduction zone in western Canada: evidence from seismic reflection and receiver function data; *Geophysical Research Letters*, v. 23, p. 3791–3794.
- Julia, J., Herrmann, R.B., Ammon, C.J. and Akinici, A. (2004): Evaluation of deep sediment velocity structure in the New Madrid seismic zone; *Bulletin of the Seismological Society of America*, v. 94, p. 334–340.
- Lawrence, J.F. and Wiens, D.A. (2004): Combined receiver-function and surface wave phase-velocity inversion using a niching genetic algorithm: application to Patagonia; *Bulletin of the Seismological Society of America*, v. 94, p. 977–987.
- Riddell, J.M. (2006): Geology of the Southern Nechako Basin NTS 92N, 92O, 93B, 93C, 93F, 93F; BC Ministry of Energy, Mines and Petroleum Resources, Petroleum Geology Map 2006-1, 3 sheets at 1:400 000 scale.
- Sabra, K.G., Gerstoft, P., Roux, P., Kuperman, W.A. and Fehler, M.C. (2005): Surface wave tomography from microseisms in Southern California; *Geophysical Research Letters*, v. 32, doi: 10.1029/2005GL023155.
- Shapiro, M.C., Campillo, M., Stehly, L. and Ritzwoller, M.H. (2005): High-resolution surface wave tomography from ambient seismic noise; *Science*, v. 37, doi: 10.1126/science.1108339.
- Zheng, T., Zhao, L. and Chen, L. (2005): A detailed receiver function image of the sedimentary structure of the Bohai Bay Basin; *Physics of the Earth and Planetary Interiors*, v. 152, p. 129–143.

Ashman Ridge Section Revisited: New Insights for the Evolution of the Bowser Basin, Northwestern British Columbia (NTS 93L/13)

J-F. Gagnon, Department of Earth and Atmospheric Sciences, University of Alberta, Edmonton, AB, jfgagnon@ualberta.ca

J.W.F. Waldron, Department of Earth and Atmospheric Sciences, University of Alberta, Edmonton, AB

Gagnon, J-F. and Waldron, J.W.F. (2008): Ashman Ridge section revisited: new insights for the evolution of the Bowser Basin, northwestern British Columbia (NTS 93L/13); in Geoscience BC Summary of Activities 2007, Geoscience BC, Report 2008-1, p. 121–128.

Introduction

The Bowser Basin is a large sedimentary basin deposited above basement of the Stikine Terrane in the Intermontane Belt of northwestern British Columbia (Figure 1). It was the site of deposition of a large volume of siliciclastic sedimentary rocks during Middle Jurassic through Early Cretaceous time. Approximately 6 km of marine to nonmarine sedimentary rocks, mainly assigned to the Bowser Lake Group, were deposited onto the Early to Middle Jurassic volcano-sedimentary assemblage of the Hazelton Group (Ricketts et al., 1992; Evenchick and Thorkelson, 2005). The boundary between these units marks a major change in depositional style, from a volcanic arc setting to a subsiding sedimentary basin. The transition zone hosts significant mineralization (e.g., Eskay Creek Au-Ag deposit; Anderson, 1993; Barrett and Sherlock, 1996; Roth et al., 1999) as well as dark organic shale with significant potential as a petroleum source rock (Ferri et al., 2004; Ferri and Boddy, 2005). A clear understanding of the nature of this stratigraphic transition at basin scale could provide new insights for both mineral and hydrocarbon exploration.

The aim of this study is to provide new detailed stratigraphic observations of the Ashman Ridge section, which exhibits continuous exposure across the Hazelton Group–Bowser Lake Group transition. In a future paper, this stratigraphic column will be integrated in a regional basin analysis study and compared with equivalent stratigraphic units previously described in the northern part of the Bowser Basin (Waldron et al., 2006; Gagnon et al., 2007).

Ashman Ridge is located approximately 40 km west of Smithers, BC (Figure 1). The section was originally described as part of a project involving regional stratigraphic mapping of north-central British Columbia by Tipper and Richards (1976), who defined the Ashman Formation of

the Bowser Lake Group and proposed Ashman Ridge as the type section. Stratigraphically lower units of the Hazelton Group are also well exposed along the section and provide a complete record of the change in depositional environment.

Stratigraphic Units

Volcanic Rocks

The lowest stratigraphic units exposed at Ashman Ridge consist of amygdaloidal andesitic to dacitic flows and associated pyroclastic rocks of the Hazelton Group. This predominantly volcanic succession was previously assigned to the Howson Subaerial Facies of the Late Sinemurian to Early Pliensbachian Telkwa Formation by Tipper and Richards (1976). According to them, the Howson Facies consists of a thick suite of calcalkaline basalt to rhyolite flows and derived pyroclastic rocks. The volcanic flows identified in the current study are typically 5–15 m thick, and autobrecciated near the top. Most are aphanitic, but the section contains minor amounts of feldspar-phyric andesite. The presence of highly indurated ignimbrite containing flattened pumice suggests that these volcanic rocks were mostly deposited in a subaerial environment (Figure 2). The occurrence of a unit of light grey packstone in the dominantly volcanic succession, however, indicates that marine conditions existed locally. This fossiliferous fine-grained limestone contains well-preserved silicified burrows and ooids, indicating deposition in a relatively warm shallow sea (Figure 3). These carbonate units are capped by a very thick rusty-weathered vesicular basalt flow with epidote-bearing quartz veins.

The uppermost dominantly volcanogenic unit of the section consists of maroon to bright red, fine-grained crystalline tuff. Tipper and Richards (1976) included this unit in the Red Tuff Member of the Nilkitkwa Formation and estimated its age to be Middle Toarcian or younger, based on paleontological control in underlying and overlying units. On Ashman Ridge, units of the Red Tuff Member comprise well-bedded, welded ash flow tuff, poorly sorted rubbly lapilli tuff, and lahar. Rounded bombs up to 30 cm in diameter are common in a very fine grained matrix. In the Smithers area, this extensive subaerial pyroclastic unit con-

Keywords: stratigraphy, sedimentology, Hazelton Group, Smithers Formation, Ashman Formation, Bowser Lake Group

This publication is also available, free of charge, as colour digital files in Adobe Acrobat® PDF format from the Geoscience BC website: <http://www.geosciencebc.com/s/DataReleases.asp>.

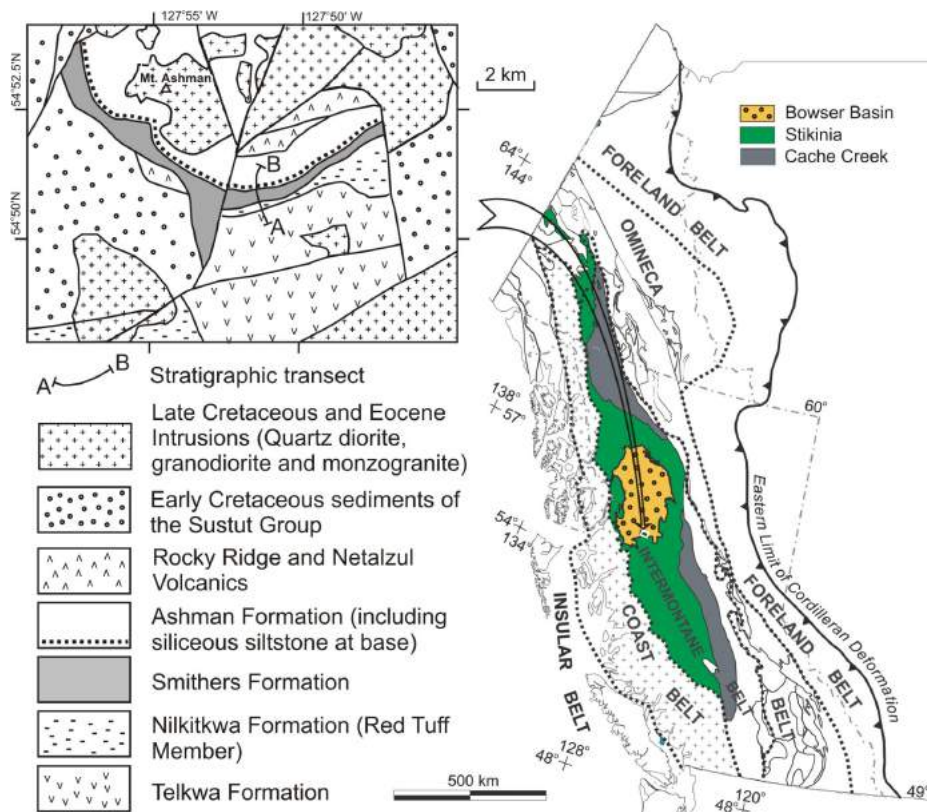


Figure 1. Simplified geology of the Ashman Ridge area, showing the location of the stratigraphic transect described in this study. Right side of the figure shows the location of the Bowser Basin in relation to principal tectonic belts of the Canadian Cordilleran Orogen (*modified from* Tipper and Richards, 1976; Evenchick and Thorkelson, 2005).

stitutes the last major preserved volcanic eruption related to the Hazelton arc before widespread sedimentation of the Smithers Formation was initiated.

Sedimentary Rocks

Establishment of a subsiding sedimentary basin on the Hazelton arc occurred around the Middle Toarcian and is recorded by the deposition of sandstone, assigned by Tipper and Richards (1976) to the Smithers Formation. As de-

finied by these authors, the Smithers Formation consists of a mixture of fossiliferous, light grey-brown, lithic sandstone and tuffaceous siltstone.

At Ashman Ridge, the fossil-rich calcareous sandstone unconformably overlies the subaerial, oxidized pyroclastic units of the Red Tuff Member (Figure 4). The basal contact is erosive but no angular discordance was observed at the outcrop scale. A high concentration of volcanic-derived clasts in the tuffaceous sandstone suggests recycling of the



Figure 2. *Fiamme* structures in a unit of densely welded ignimbrite.



Figure 3. Silicified burrows in a unit of fine-grained oolitic limestone.

underlying Red Tuff Member and/or contemporaneous volcanism. Even though the hiatus associated with the unconformity remains poorly constrained due to the lack of precise dating of the Red Tuff Member, paleontological control below and above it suggests a gap of only a few million years.

Detailed stratigraphic observations of the lower, sandstone-dominated section taken along the exposed section at Ashman Ridge are shown in Figure 5, on which this interval is distinguished as unit A. The unit comprises mostly medium- to fine-grained, greenish brown sandstone with abundant marine fauna, including belemnites, gastropods, corals, ammonoids and a wide variety of ornate bivalves such as *Trigonia* (Figure 6). Bioturbation is omnipresent and tends to be particularly well displayed in occasional beds of green glauconitic sandstone (Figure 7). This rich faunal assemblage and common occurrence of wave-generated sedimentary structures suggest that the unit was deposited in relatively shallow marine conditions, confirming the previous interpretation of the Smithers Formation by Tipper and Richards (1976).

Fossiliferous calcareous sandstone of unit A is conformably overlain by a unit of thinly bedded blocky siliceous mudstone with recessive units, typically only millimetres to a few centimetres thick, of pale orange-weathered tuff (unit B in Figure 5). This unit contrasts with the underlying sandstone in that it lacks abundant bivalves, shows only sparse bioturbation and is significantly finer grained. The contact is easily mappable. Well-preserved ammonites, including *Kepplerites* sp. and *Cobbanites* sp., were collected during this study approximately 66.5 m below the top of the thinly bedded unit (Figure 8: corresponds to GSC location 85413; Tipper and Richards 1976). Belemnites and calcareous concretions are abundant in the upper half of this unit, which totals 221 m in thickness (Figure 5). The fine grain size, laterally continuous bedding, and lack of current-generated structures indicate that this unit accumulated mostly from suspension.

The siliceous, fine-grained succession is overlain with a sharp but apparently conformable boundary by brown- and white-weathering arkosic sandstone with thick limy concretions, marking the base of unit C (Figure 5). Even though the contact is conformable, field observations indicate that there is an ~10 m dextral offset along a steep normal fault close to the point where this contact crosses the crest of the ridge. The overlying medium-grained, arkosic sandstone contains abundant mud rip-up clasts at the bases of the 40–70 cm thick beds. Parallel horizontal laminations are common and there are local concentrations of fossil wood debris. The depositional environment for this sand-

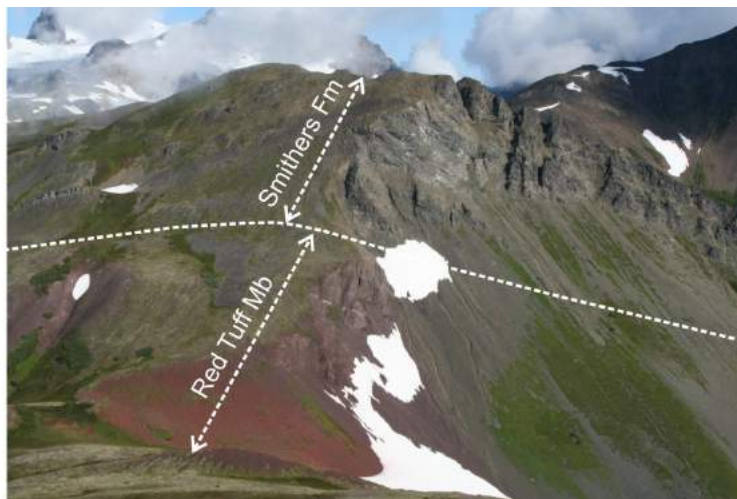


Figure 4. Stratigraphic contact between the Red Tuff Member and the Smithers Formation at Ashman Ridge.

rich unit is interpreted to be one of high energy, contrasting with conditions that prevailed during the deposition of the underlying belemnite-rich, siliceous argillite of unit B.

Higher in unit C, a 50 m succession of finely laminated fine-grained sandstone and siltstone overlies the coarser feldspathic sandstone. It contains few belemnites and calcareous concretions. This recessive, fine-grained unit is capped by a thin bed of dark shale that probably corresponds to a flooding surface. Immediately above it, multiple coarsening-upward sequences were identified in fine-grained to pebbly sandstone. Hummocky cross-stratification, trough crossbedding and climbing ripples are common sedimentary structures in this unit. Abundant trace fossils are found in the finer grained sections and multiple *Trigonia* bivalves were also collected. At 760 m in the measured stratigraphic section, a coarsening-upward conglomerate interval is overlain by a 10 cm thick bed of wood debris. These regressive cycles could be interpreted as progradation of a deltaic system into a shallow marine environment. Recessive intervals of fissile shale and very fine silt are interbedded with the coarser progradational shoreface deposits and are interpreted by the authors to represent lateral embayments. Flaser laminations are common in the finer grained units, which suggests that the sediments were reworked by tidal processes. Occasional thin layers of reworked pale-weathering ash tuff at the base of sandstone beds attest to distal volcanism. Relatively good exposure enabled the authors to measure sedimentary strata up to 1145 m and no significant lithological change was observed.

Discussion

Tipper and Richards (1976) divided the Ashman Ridge section into a number of units. Above the predominantly volcanic rocks of the Telkwa and Nilkitkwa formations, they

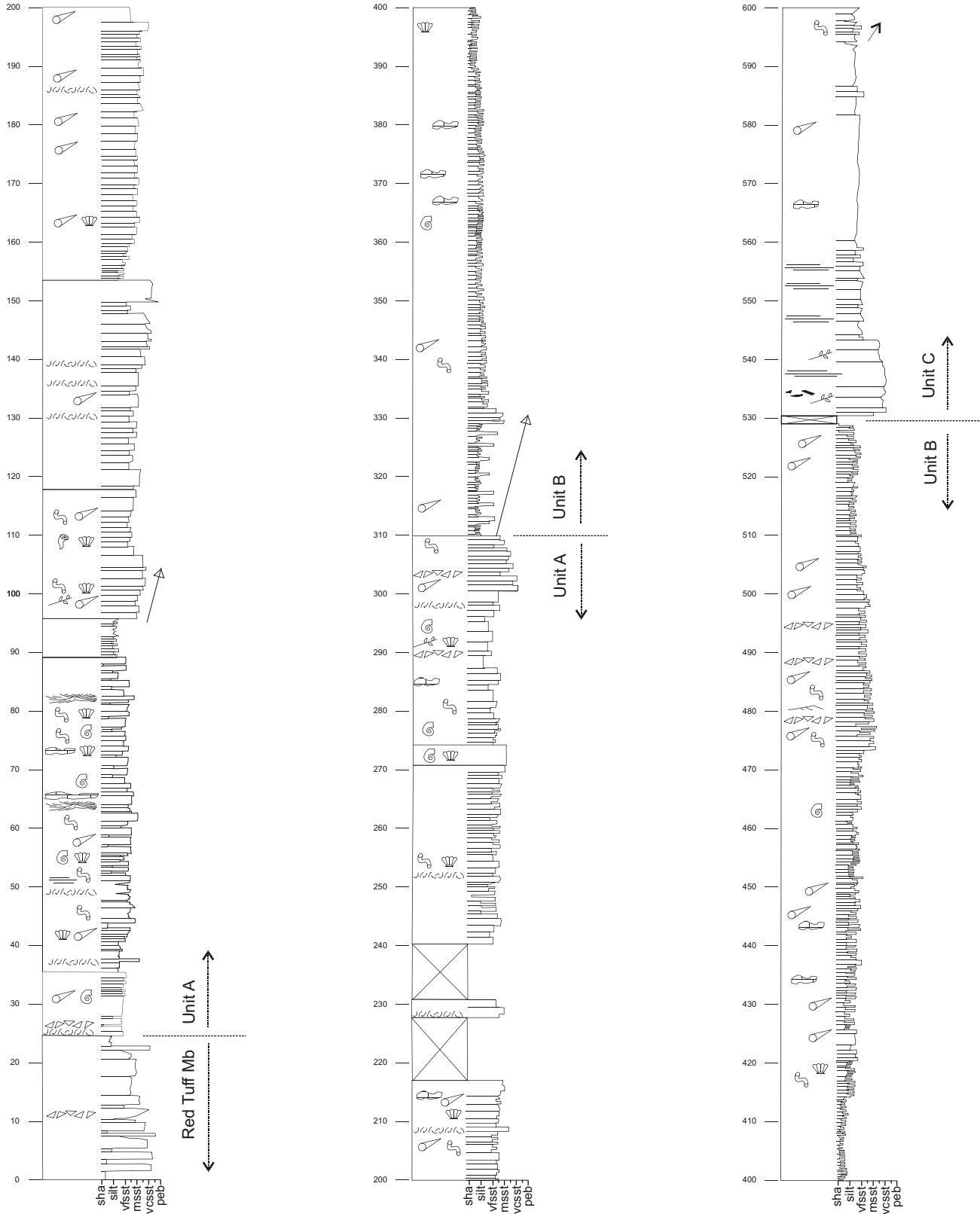


Figure 5. Detailed stratigraphic section at Ashman Ridge, showing the different units identified in this study.

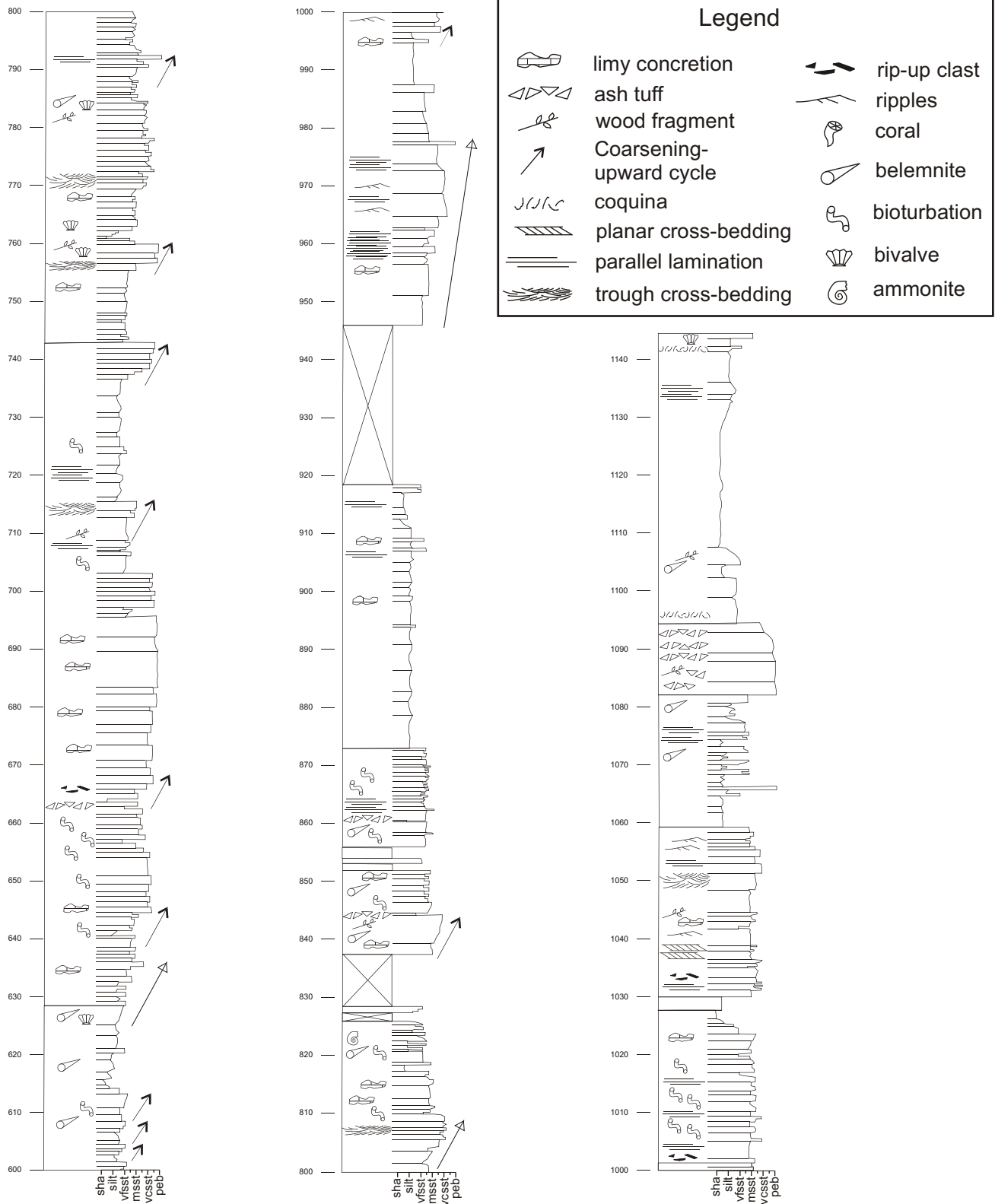


Figure 5 (continued)



Figure 6. *Trigonina* bivalve of the Smithers Formation, indicating deposition in a shallow marine environment. Observed at 102 m on the stratigraphic section.



Figure 7. Trace fossils in a glauconitic fine-grained sandstone of the Smithers Formation. Observed at 78 m on the stratigraphic section.



Figure 8. Well-preserved ammonite fossil collected near the top of the 'pyjama beds' unit. Observed at 463 m on the stratigraphic section.

assigned sandstone of unit A and the basal part of unit B of this study to their Smithers Formation. Most of the remainder of unit B of this study was assigned by Tipper and Richards to the Ashman Formation. The highest part of their section was assigned to undifferentiated Bowser Lake

Group. Tipper and Richards (1976) placed the top of the Ashman Formation at the top of a 659 m thick unit, tentatively identified at 980 m in the section measured for this study, although they give no indication of the lithological criteria for distinguishing the Ashman Formation from undifferentiated units of the Bowser Lake Group.

Based on work by the current authors (Waldron et al., 2006; Gagnon et al., 2007), that of others farther north in the Bowser Basin (Thomson et al., 1986; Anderson and Thorkelson 1990; Greig 1991), and the definitions for the Smithers Formation of Tipper and Richards (1976), the authors suggest a different subdivision (Figure 9). Unit A is a clearly mappable unit of bioturbated fossiliferous sandstone that corresponds closely, in lithological character, to the Tipper and Richards (1976) definition of the Smithers Formation. The current study therefore suggests that the top of the Smithers Formation should be set at the top of the uppermost heavily bioturbated calcareous sandstone bed observed at 310 m in the section measured for this study (Figure 5).

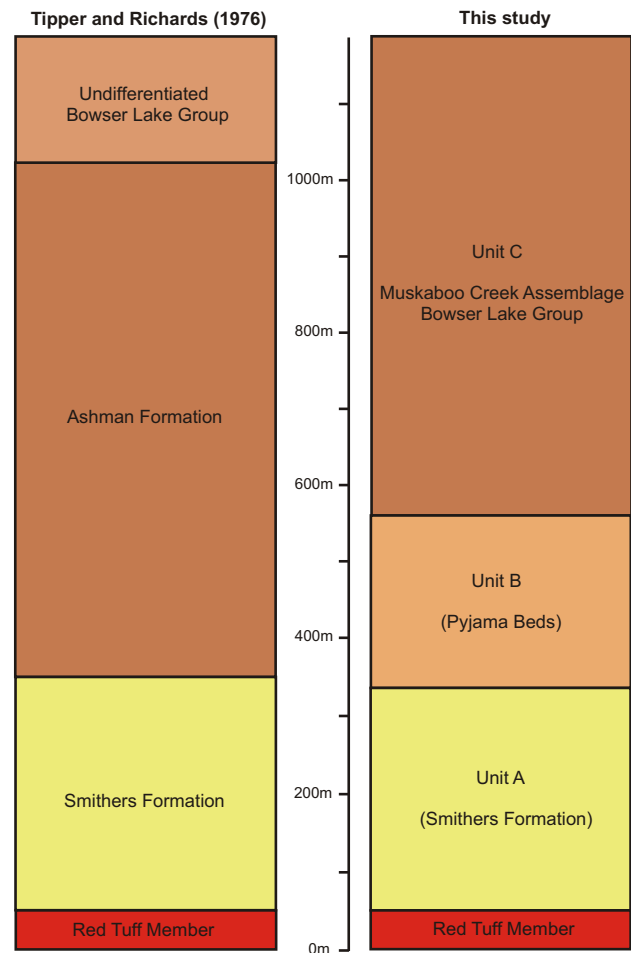


Figure 9. Stratigraphic correlations between the detailed section of this study and the original type section of the Ashman Formation (Tipper and Richards, 1976).

Following the same logic, the next important lithological boundary occurs at 531 m, where interbedded siliceous mudstone and tuff of unit B are overlain by laminated, medium- to very coarse grained arkosic sandstone beds with abundant mud rip-up clasts and wood fragments of unit C. This marks a significant change in depositional environment within the basin. Interbedded siltstone and thin tuff units similar (though not everywhere identical) to unit B are widespread in the Middle Jurassic of the Bowser Basin, though they are referred to by a variety of names. In the Joan Lake area, they are referred to as the Quock Formation of the Spatsizi Group by Thomson et al. (1986). The Quock Formation was later lowered to the Quock Member of the Spatsizi Formation by Evenchick and Thorkelson (2005). Elsewhere, similar units are referred to as the Troy Ridge Facies of the Salmon River Formation by Anderson and Thorkelson (1990). Informally, correlative units have been referred to widely as ‘pyjama beds’ (Anderson and Thorkelson, 1990; Anderson, 1993; Ferri et al., 2004; Ferri and Boddy, 2005; Evenchick and Thorkelson, 2005). The authors use this informal name pending future formal revision of the lithostratigraphy.

Overlying, nonsilicified clastic sedimentary rocks of unit C of this study, assigned to the Ashman Formation by Tipper and Richards (1976), bear a close field resemblance to widespread shallow marine units of the Bowser Lake Group assigned to the Muskaboo Creek assemblage of Evenchick et al. (2001). The upper boundary of this facies is not seen at Ashman Ridge, and the authors see no justification for placing an upper boundary at the top of the Tipper and Richards (1976) section.

The authors propose that the name Ashman Formation be abandoned, as it does not represent a clearly defined mappable unit. Instead, it is suggested that unit A of this study is equivalent to the Smithers Formation of the Upper Hazelton Group as regionally mapped. Unit B is yet to be formally named, but is correlative with the ‘pyjama beds’ mapped elsewhere as Upper Hazelton Group (Anderson, 1993; Waldron et al., 2006; Gagnon et al., 2007). The overlying unit C, equivalent to the bulk of the Ashman Formation as defined by Tipper and Richards (1976), is equivalent to the Muskaboo Creek Assemblage of the Bowser Lake Group (Evenchick et al., 2006).

The transition from unit A to unit B probably represents a deepening associated with subsidence at the onset of basin formation. The transition from the ‘pyjama beds’ of unit B to the Bowser Lake Group is unusual, because there is no interval of submarine fan or slope sediments (Ritchie-Alger or Todagin Assemblage) below shallow-marine sediments of the Muskaboo Creek Assemblage, as is typical of Bowser Basin successions farther north (Evenchick and Thorkelson, 2005). This suggests that the initial subsidence of the Bowser Basin was less profound at Ashman Ridge

than elsewhere, and the accommodation space generated in basin formation was filled relatively rapidly by sediment in this area.

The new stratigraphic framework proposed in this study confirms the presence of a mappable ‘pyjama beds’ unit conformably underlying sedimentary rocks of the Bowser Lake Group at the basin scale. This has important implications for both petroleum and mineral exploration, as equivalent stratigraphic units in the northern part of the Bowser Basin host volcanogenic massive sulphide mineralization (Barrett and Sherlock, 1996; Roth et al., 1999) and have proven petroleum source rock properties (Ferri et al., 2004; Ferri and Boddy, 2005).

Acknowledgments

The authors would like to thank Geoscience BC for supporting this research. Additional field costs were supported by Natural Sciences and Engineering Research Council of Canada (NSERC) Discovery Grant A8508 to the senior author. Helicopter support was provided by Highland Helicopters. D. Dockman assisted in the field. M. Gingras and W. Loogman provided helpful comments on an earlier version of the manuscript.

References

- Anderson, R.G. (1993): A Mesozoic stratigraphic and plutonic framework for northwestern Stikinia (Iskut River area), northwestern British Columbia, Canada; *in* Mesozoic Paleogeography of the Western United States II; Dunne, G.C. and McDougall, K.A. (ed.), Pacific Section, Society of Economic Paleontologists and Mineralogists, Publication 71, p. 477–494.
- Anderson, R.G. and Thorkelson, D.J. (1990): Mesozoic stratigraphy and setting for some mineral deposits in Iskut River map area, northwestern British Columbia; *in* Current Research, Part E, Geological Survey of Canada, Paper 90-1A, p. 131–139.
- Barrett, T.J. and Sherlock, R.L. (1996): Geology, litho-geochemistry and volcanic setting of the Eskay Creek Au-Ag-Cu-Zn deposit, northwestern British Columbia; *Exploration and Mining Geology*, v. 5, no. 4, p. 339–368.
- Evenchick, C.A., Poulton, T.P., Tipper, H.W. and Braidek, I. (2001): Fossils and facies of the northern two-thirds of the Bowser Basin, British Columbia; Geological Survey of Canada, Open File 3956, 103 p.
- Evenchick, C.A. and Thorkelson, D.J. (2005): Geology of the Spatsizi River map area, north-central British Columbia; Geological Survey of Canada, Bulletin 577, 276 p.
- Evenchick, C.A., Mustard, P.S., McMechan, M.E., Ferri, F., Ritcey, D.H. and Smith, G.T. (2006): Compilation of geology of Bowser and Sustut basins draped on shaded relief map, north-central British Columbia; Geological Survey of Canada, Open File 5313.
- Ferri, F., Osadetz, K.G. and Evenchick, C.A. (2004): Petroleum source rock potential of Lower to Middle Jurassic clastics, intermontane basins, British Columbia; *in* Summary of Activities 2004, BC Ministry of Energy, Mines and Petroleum

- Resources, URL <<http://www.em.gov.bc.ca/subwebs/oilandgas/pub/reports/summary2004.htm>>, p. 87–97.
- Ferri, F. and Boddy, M. (2005): Geochemistry of Early to Middle Jurassic organic-rich shales, intermontane basins, British Columbia; *in* Summary of Activities 2005, BC Ministry of Energy, Mines and Petroleum Resources, URL <<http://www.em.gov.bc.ca/subwebs/oilandgas/pub/reports/summary2005.htm>>, p. 132–151.
- Gagnon, J-F., Loogman, W., Waldron, J.W.F., Cordey, F. and Evenchick, C.A. (2007): Stratigraphic record of initiation of sedimentation in the Bowser Basin (NTS 104A, H), northwestern British Columbia; *in* Geological Fieldwork 2006, BC Ministry of Energy, Mines and Petroleum Resources, Paper 2007-1 and Geoscience BC, Report 2007-1, p. 275–283.
- Greig, C.J. (1991): Stratigraphic and structural relations along the west-central margin of the Bowser Basin, Oweegee and Kinskuch areas, northwestern British Columbia; *in* Current Research, Part A, Geological Survey of Canada, Paper 91-1A, p. 197–205.
- Ricketts, B.D., Evenchick, C.A., Anderson, R.G. and Murphy, D.C. (1992): Bowser Basin, northern British Columbia: constraints on the timing of initial subsidence and Stikinia-North America terrane interactions; *Geology*, v. 20, p. 1119–1122.
- Roth, T., Thompson, J.F.H. and Barrett, T.J. (1999): The precious metal-rich Eskay Creek deposit, northwestern British Columbia; *in* Volcanic-Associated Massive Sulfide Systems: Processes and Examples in Modern and Ancient Settings, Barrie, C.T. and Hannington, M.D. (ed.), *Reviews in Economic Geology*, v. 8, p. 357–373.
- Tipper, H.W. and Richards, T.A. (1976): Jurassic stratigraphy and history of north-central British Columbia; *Geological Survey of Canada, Bulletin* 270.
- Thomson, R.C., Smith, P.L. and Tipper, H.W. (1986): Lower to Middle Jurassic (Pliensbachian to Bajocian) stratigraphy of the northern Spatsizi area, north-central British Columbia; *Canadian Journal of Earth Sciences*, v. 23, p. 1963–1973.
- Waldron, J.W.F., Gagnon, J-F., Loogman, W. and Evenchick, C.A. (2006): Initiation and deformation of the Jurassic–Cretaceous Bowser Basin: implications for hydrocarbon exploration in north-central BC; *in* Geological Fieldwork 2005, BC Ministry of Energy, Mines and Petroleum Resources, Paper 2006-1 and Geoscience BC, Report 2006-1, p. 349–360.

Structure of the Southeastern Nechako Basin, South-Central British Columbia (NTS 092N, O; 093B, C): Preliminary Results of Seismic Interpretation and First-Arrival Tomographic Modelling

N. Hayward, Department of Earth Sciences, Simon Fraser University, Burnaby, BC, nhayward@sfu.ca

A.J. Calvert, Department of Earth Sciences, Simon Fraser University, Burnaby, BC

Hayward, N. and Calvert, A.J. (2008): Structure of the southeastern Nechako Basin, south-central British Columbia (NTS 092N, O; 093B, C): preliminary results of seismic interpretation and first-arrival tomographic modelling; *in* Geoscience BC Summary of Activities 2007, Geoscience BC, Report 2008-1, p. 129–134.

Introduction

The Nechako Basin is an Upper Cretaceous to Oligocene basin located in the Interior Plateau of southern British Columbia (Figure 1), between the Rocky and Coast mountains. The sedimentary basin formed over, and in part from, the accreted terranes of the western Canadian Cordillera, where the oceanic Cache Creek Terrane separates the Stikine and Quesnel volcanic arc terranes (Struik and MacIntyre, 2001). Westward-directed thrusting at the boundary between the Stikine and Cache Creek terranes occurred prior to 165 Ma (Schiarizza and MacIntyre, 1999). Transpressional tectonic processes were dominant until the Eocene (Best, 2004), when there was a shift to a dextral transtensional regime (Price, 1994) and accompanying volcanism. The basin is bounded by the Cretaceous Skeena Arch to the north, the Coast Mountains and Eocene Yalakom fault to the west, the Cretaceous Tyaughton Basin to the south and the Eocene Fraser fault to the east. The major Yalakom and Fraser faults are associated with the episode of Eocene transtension.

The basin is extensively blanketed by volcanic rocks of the Eocene Endako and Ootsa Lake groups and the Neogene Chilcotin Group (Figure 2), and Pleistocene glacial deposits (e.g., Riddell, 2006), making interpretation of the basin's stratigraphy and structure difficult. The Endako and Ootsa Lake groups consist, respectively, of basaltic to andesitic and intermediate to felsic flows, accompanied by

Keywords: seismic reflection, structural geology, seismic stratigraphy, first-arrival tomography, velocity models, magnetic anomaly, gravity anomaly

This publication is also available, free of charge, as colour digital files in Adobe Acrobat® PDF format from the Geoscience BC website: <http://www.geosciencebc.com/s/DataReleases.asp>.

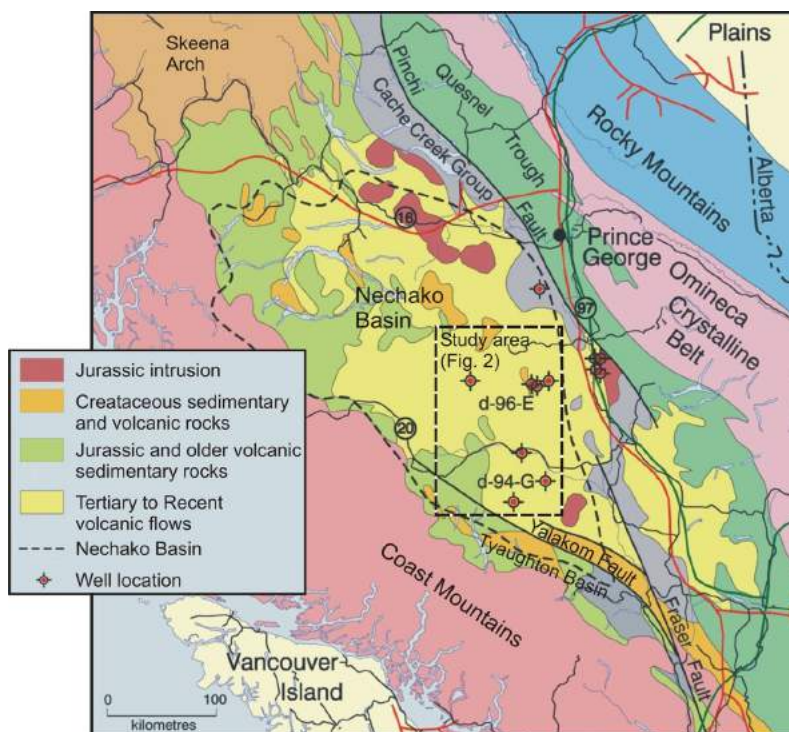


Figure 1. Location of the Nechako Basin and simplified geology of its western Canadian Cordillera setting. Black dashed box shows the study area. Red dashed box shows the focus region of this report.

tuff, breccia and sedimentary rocks. The Chilcotin Group consists primarily of basaltic flows (Riddell, 2006). However, isolated outcrops (e.g., Riddell, 2006), eight wells (drilled by Canadian Hunter Exploration Limited, Esso, Honolulu Oil Corporation Limited and Hudson's Bay Oil and Gas exploration companies) and seismic reflection interpretation in the 1980s by Canadian Hunter reveal the basin to contain Lower Jurassic to Upper Cretaceous sedimentary rocks. These rocks are folded and faulted as a result of the basin's complex tectonic history.

The interpretation of the seismic reflection and well data, on which this study is primarily based, reveals four blocks

of different geological structure and stratigraphy (Figure 2):

- 1) Block A (southern Redstone area), in the southern part of the study area, is centred on the Canadian Hunter Redstone wells b-82-C and d-94-G, and seismic lines 160-01 to 160-19.
- 2) Block B (western Redstone area), centrally located, includes the single seismic line 160-17, which intersects Hudson's Bay well c-75-A.
- 3) Block C (Chilcotin area), in the northwestern part of the study area, contains the Canadian Hunter Chilcotin well b-22-K and seismic lines 161-01 to 161-09.

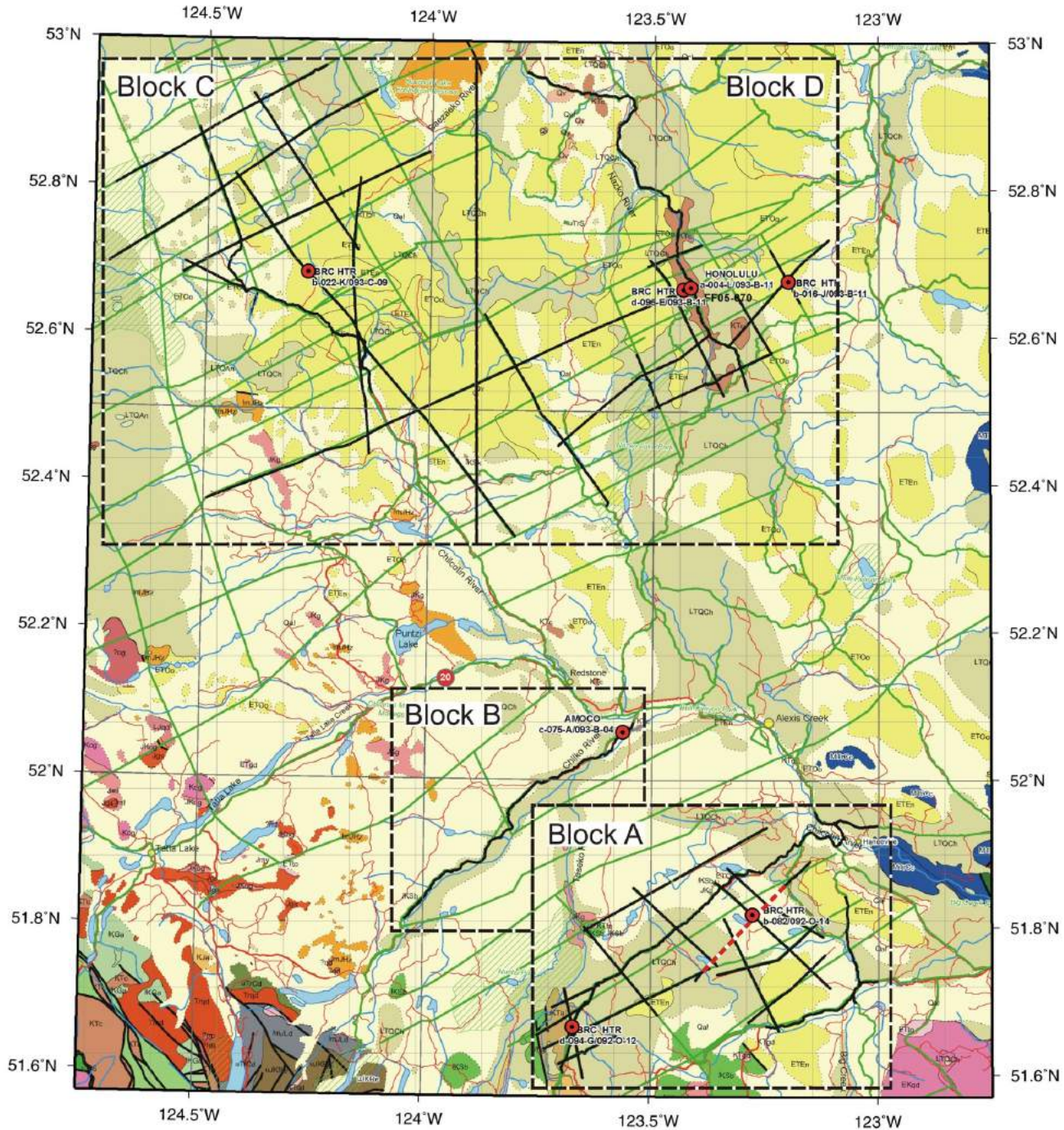


Figure 2. Geology of the study area (Riddell, 2006) and location of seismic reflection profiles (heavy black lines). Volcanic and surficial units: EtEn, Endako Group; EtOo, Ootsa Lake Group; LTQCh, Chilcotin Group; Qal, Quaternary cover; IKsb, Spences Bridge Group. Red dashed box shows the location of block A. Other blocks are shown by a black dashed box. Heavy red dashed line shows the location of the first-arrival tomographic velocity model shown in Figure 5.

- 4) Block D (Nazko area), in the northeastern part of the study area, includes wells Honolulu Nazko a-4-L, Canadian Hunter Nazko d-96-E and Canadian Hunter-Esso Nazko b-16-J, and seismic lines 159-01 to 159-15 and 162-02.

This study re-evaluates the stratigraphy and structure of the southeastern Nechako Basin, primarily from the reinterpretation, including tomographic velocity modelling, of more than 1650 km of Canadian Hunter seismic reflection profiles. These interpretations are aided by their integration with all relevant geological and geophysical information, including well logs, geology and potential field data. This paper presents a preliminary interpretation of the block A area (Figure 2).

Seismic Interpretation of Block A

Seismic reflection profiles form the basis for the re-examination of the structure and stratigraphy of the southeastern Nechako Basin. The seismic reflection data acquired by Canadian Hunter in the 1980s were recovered and reprocessed in 2006 by Arcis.

Surface mapping (e.g., Riddell, 2006) does not provide a usefully long stratigraphic section, due to the extensive veneer of Tertiary volcanic and Pleistocene glacial deposits (Figure 2). Therefore, data from the Canadian Hunter Redstone wells b-82-C and d-94-G provide the primary stratigraphic control.

Integration of Well Data with Seismic Profiles

Stratigraphic, structural, geophysical and material property data from wells in the southeastern Nechako Basin aided in the interpretation of seismic profiles. To correlate the data with the seismic profiles, thicknesses were converted to seismic traveltimes using the well sonic logs and the Petrel software package (Schlumberger Ltd.). The measured depth (2169 m) of well d-94-G was calculated to correspond to a two-way traveltimes of ~1.02 s. For well b-82-C, the total depth of 1719 m was calculated to correspond to a two-way traveltimes of ~1.1 s.

Synthetic seismograms were generated from density and sonic log data, also using the Petrel software package, to aid in seismic-to-well correlation. For well b-82-C, an estimate of the density variation through the well was derived from the neutron porosity log, assuming an intergranular fluid density of 1030 kg/m³ and a grain density of 2670 kg/m³, as the well's density log only covered a short interval of ~520 m. The synthetic seismograms show a general correlation with changes in reflection character, but the matching of specific reflections was not possible.

Well stratigraphy and geochronology have been re-evaluated by Ferri and Riddell (2006) and Riddell et al. (2007). Stratigraphic columns (Ferri and Riddell, 2006) were converted to time via the sonic logs, in order that more accurate correlations could be drawn with seismic reflections (e.g., Figure 3).

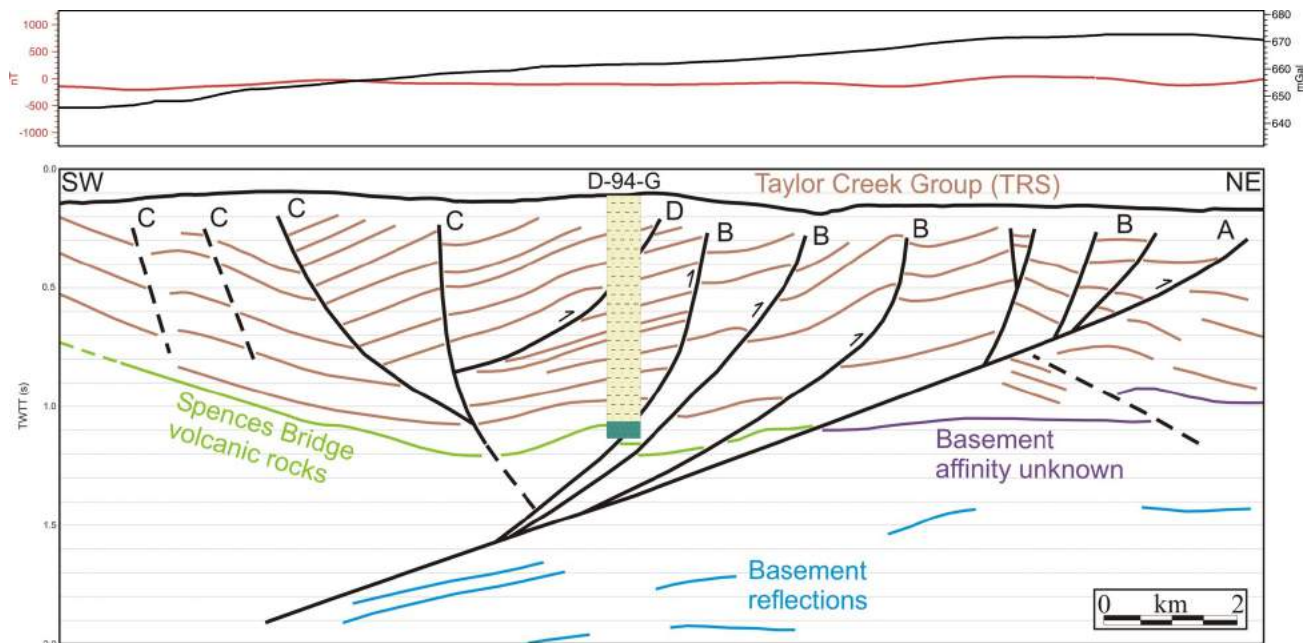


Figure 3. Structural and stratigraphic interpretation of a seismic reflection section from block A. Well d-94-G stratigraphic columns (time converted) from Ferri and Riddell (2006). Upper box shows the Bouguer gravity (black line) and total field magnetic (red line) anomalies. Abbreviation: TRS, Taseko River strata.

Structure of Nechako Basin Block A

The preliminary interpretation of the structure and stratigraphy of block A is shown in Figure 4. Magnetic anomalies (Figure 4) are dominated by the Tertiary volcanic rocks, but many anomalies indicate subsurface structural grain. Magnetic anomalies guided the interpretation of the orientation of structures, especially where only intersected by a single seismic profile.

Structure and Stratigraphy Adjacent to Well d-94-G

Near well d-94-G, a sub-basin containing ~2 km of middle/late Albian to Cenomanian sedimentary rocks of the Taylor Creek Group overlies the Spences Bridge (Riddell et al., 2007) andesite basement (Figure 3). This sub-basin has a corresponding Bouguer gravity low of ~660 mGal, relative to highs of ~670 mGal to the north and east. The Taylor Creek Group and Spences Bridge volcanic rocks are truncated against basement of unknown affinity by a southwest-dipping, low-angle primary fault (A; Figures 3, 4), which maybe of a compressive origin. The orientation of the contact of the Spences Bridge volcanic rocks with the

fault plane is oblique to the surface trace of the fault (Figure 4).

Several high-angle, southwest-dipping reverse faults sole into the primary fault (B; Figures 3, 4). The rocks of the Taylor Creek Group form a broad faulted anticline that plunges to the northwest. To the southwest, the Taylor Creek Group rocks thin and are cut (Figure 4) by a number of northeast-dipping faults that show a component of reverse or undetermined sense (C; Figure 3) and a concave trace (C; Figure 4). The outcrop of Spences Bridge volcanic rocks (Figure 2) and faulting (e.g., Riddell, 2006) just beyond the western extent of the seismic profiles marks the western edge of the sub-basin.

Although faults near well d-94-G are interpreted as partly compressive, the relative offset across the structures suggests a strong strike-slip component and possible reactivation. This motion was likely coincident with Eocene dextral transtension (Struik, 1993; Price, 1994), which included the Yalakom and Fraser fault systems, and suggests that motion was directed to the northwest (Figure 4).

A low-angle fault (D; Figure 3), trending oblique to previously discussed structures, is truncated by younger rocks of

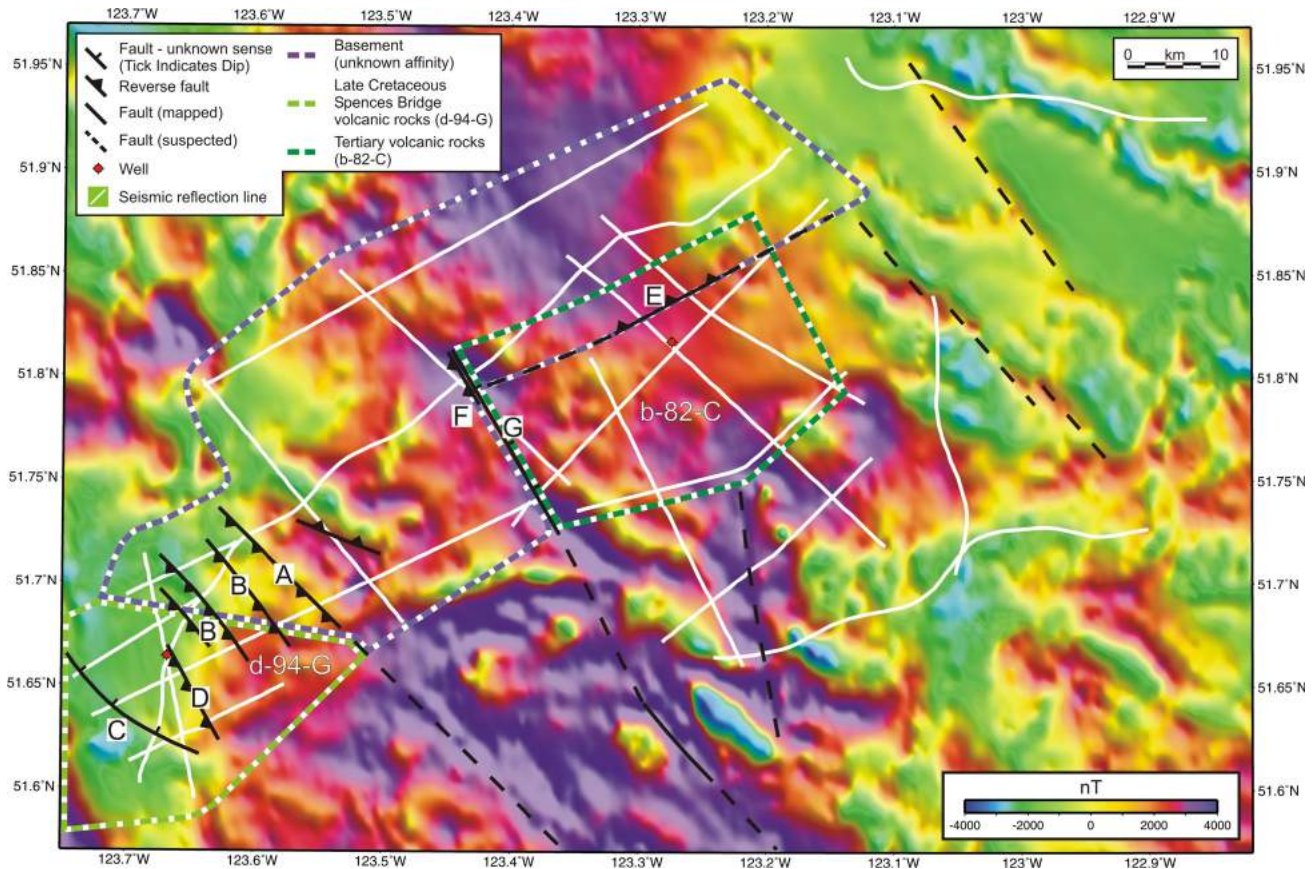


Figure 4. Structure of block A, overlain on the total magnetic field (illumination from the southwest). See legend for feature explanations. Letters mark structures shown in Figure 3. Heavy dashed coloured lines indicate basement affinity. Heavy black lines show regional faults from geological mapping (Riddell, 2006). Heavy black dashed lines show possible extension of these faults based on magnetic anomalies.

the Taylor Creek Group near the surface on some seismic profiles. This structure intersects and may be truncated at depth by steeply dipping faults (C; Figure 3), thus suggesting an earlier origin, perhaps related to pre-Eocene transpression.

Structure and Stratigraphy Adjacent to Well b-82-C

To the east of fault A (Figure 4), Albian sedimentary rocks of uncertain affinity (either Taylor Creek Group, Skeena Group or Silverquick Formation), sampled by well b-82-C (Riddell et al., 2007), are not as intensely deformed as the Taylor Creek Group rocks to the west. Broad folds have a generally northeasterly strike. In the region of well b-82-C, the sampled Albian granitic basement, which predates the Spences Bridge volcanic rocks, is not clearly imaged by seismic profiles. However, late Albian to Cenomanian (Riddell et al., 2007), fine-grained sedimentary and volcanic rocks that overlie the granitic basement produce reflections that are mapped with confidence on seismic profiles adjacent to the well.

Northwest of well b-82-C, basement rocks of unknown affinity are thrust (E; Figure 4) southeast over the late Albian sedimentary rocks. This boundary coincides with a reduction of the Bouguer gravity anomaly to the southeast from a high of ~670 mGal to a low of ~650 mGal. Several high-angle reverse or transpressive faults to the southeast appear to be contemporaneous with the basement thrust. The character of total field magnetic and gravity anomalies suggests that the rocks to the north may be intrusive; however, the structural contact implies intrusion prior to faulting. To the west, the thrust fault appears to be truncated by a pair of northwest-striking faults (F and G; Figure 4) that may be connected to faults mapped to the south (Figures 2, 4; Riddell, 2006). The faults divide a plateau of shallow basement to the west, related to high Bouguer gravity anomalies (~670 mGal), from the sedimentary basin and gravity low (~650 mGal) to the east. The northeast-striking thrust may indicate the presence of a compressional transfer zone between Eocene dextral strike-slip faults. This conclusion would be contrary to northeast-trending extensional faults that commonly link northwest-trending, dextral strike-slip faults (e.g., Struik, 1993) in the Canadian Cordillera.

First-Arrival Tomographic Velocity Modelling

First-arrival tomographic velocity modelling derives an estimate of the seismic P-wave velocity from the traveltimes of the first arrivals from the source to each receiver of a seismic reflection profile. Variations in velocity can reveal structures in near-surface rocks that may be poorly imaged by seismic reflection profiles. First-arrival tomographic velocity models have been used effectively to examine the structure of the Tofino Basin (Hayward and Calvert, 2007),

the Seattle fault (Calvert et al., 2003) and the Devil's Mountain fault (Hayward et al., 2006).

Method

First-arrival (the direct wave and subsurface refractions) tomographic-inversion velocity models were calculated (e.g., Calvert et al., 2003) for all straight seismic profiles (Figure 2). First arrivals picked during seismic reflection processing by Arcis were manually edited in the ProMAX™ software package (Landmark Graphics Corporation) in order to correct picking errors.

The Pronto software (Aldridge and Oldenburg, 1993) was used to model the seismic velocity. First-arrival times to all locations in a subsurface velocity grid (25 m grid spacing) were derived from a finite-difference solution to the eikonal equation. Source to receiver ray paths along the steepest direction of descent were created through the traveltimes grid. A one-dimensional (1-D) starting model was estimated from the results of a few trial inversions, setting the top of the model to 1700 m/s¹ with a gradient of 1.5 (m/s¹)/m¹. A perturbation in the velocity model was calculated from the difference between the calculated and observed first-arrival traveltimes for each of 15 iterations.

Although ray penetration often exceeded 1000 m, the highest density of rays (Figure 5a) was typically in the near-surface, leading to a well-constrained estimate of the P-wave velocity (Figure 5b) for depths of up to ~500 m.

Preliminary Velocity Model Results in the Vicinity of Well b-82-C1

Well b-82-C sampled ~220 m of the Endako volcanic rocks (Ferri and Riddell, 2006) that blanket this part of the basin. In the area of well b-82-C, the modelled rays are focused on the base of the volcanic layer (Figure 5a) at a depth of ~220 m, where the velocity model has a velocity of ~3200 m/s¹ (Figure 5b). Ray density and velocity models may thus be useful for constraining the thickness and velocity of the volcanic overburden.

Conclusions and Further Investigations

Preliminary seismic reflection interpretation in the block A region of the southeastern Nechako Basin has provided a new and detailed interpretation of the stratigraphy and structure of this region. The sub-basin in the vicinity of well d-94-G has the form of a highly faulted and northwest-plunging faulted anticline that is bounded by faulting and shallow basement to the northeast and southwest, respectively. In contrast, the sub-basin adjacent to well b-82-C is more poorly deformed, with broad open folding. Faulting is concentrated at the northwest and southeast margins, which are marked by basement and Bouguer gravity highs.

Work underway will further integrate this interpretation with additional geophysical and geological information and expand the interpretation to the other blocks (Figure 2). Seismic velocity models for the crooked seismic reflection lines, which require a 3-D model approach, will be created and used in combination with the existing models to provide information on the near-surface structure and volcanic overburden.

Acknowledgments

The authors wish to thank B. Struik for his detailed review and structural insight. They are grateful to Geoscience BC and the Natural Sciences and Engineering Council of Canada (NSERC) for funding this research.

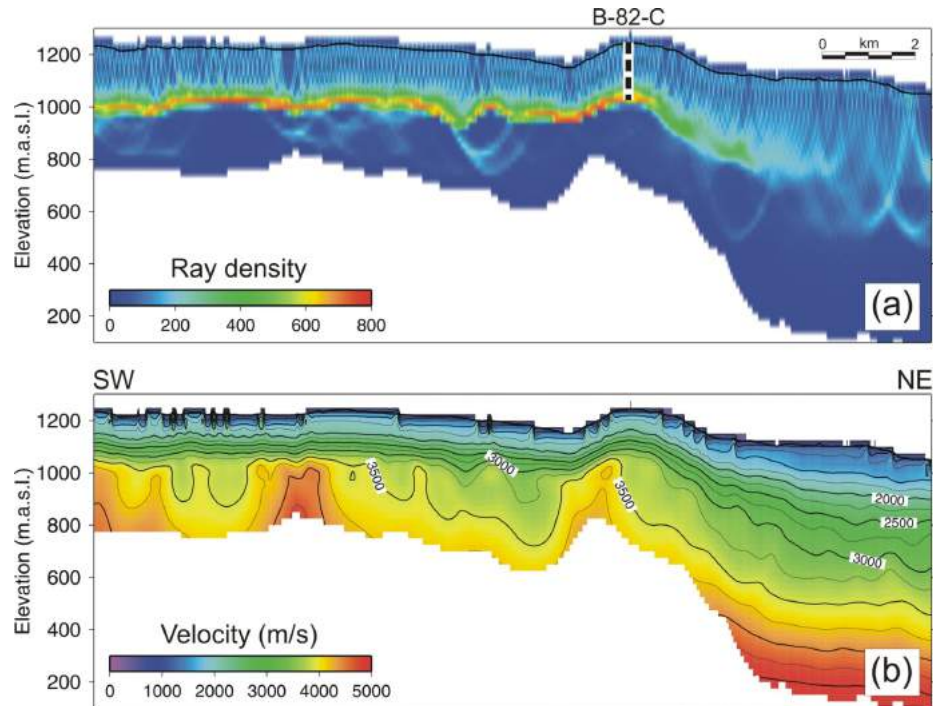


Figure 5. First-arrival tomographic ray density (a) and velocity model (b) derived from seismic reflection data in the vicinity of well b-82-C. See Figure 2 for model location.

References

- Aldridge, D.F. and Oldenburg, D.W. (1993): Two dimensional tomographic inversion with finite difference traveltimes; *Journal of Seismic Exploration*, v. 2, p. 257–274.
- Best, M.E. (2004): Qualitative interpretation of potential field profiles, southern Nechako Basin; *in* Summary of Activities 2004, BC Ministry of Energy, Mines and Petroleum Resources, p. 73–78.
- Calvert, A.J., Fisher, M.A., Johnson, S.Y. and SHIPS Working Group (2003): Along-strike variations in the shallow seismic velocity structure of the Seattle fault zone: evidence for fault segmentation beneath Puget Sound; *Journal of Geophysical Research*, v. 108, doi:10.1029/2001JB001703.
- Ferri, F. and Riddell, J. (2006): The Nechako Basin project: new insights from the southern Nechako Basin; *in* Summary of Activities 2006; BC Ministry of Energy and Mines and Petroleum Resources, p. 89–124.
- Hayward, N. and Calvert, A.J. (2007): Seismic reflection and tomographic velocity model constraints on the evolution of the Tofino forearc basin, British Columbia; *Geophysical Journal International*, v. 168, p. 634–646.
- Hayward, N., Nedimović, M.R., Cleary, M. and Calvert, A.J. (2006): Structural variation along the Devil’s Mountain fault zone, northwestern Washington; *Canadian Journal of Earth Sciences*, v. 43, p. 433–446.
- Price, R.A. (1994): Cordilleran tectonics in the evolution of the Western Canada Sedimentary Basin; Chapter 2 *in* Geological Atlas of the Western Canada Sedimentary Basin, G. Mossop and I. Shetsin, (comp.), Canadian Society of Petroleum Geologists, Calgary, Alberta and Alberta Research Council, Edmonton, Alberta.
- Riddell, J.M., compiler (2006): Geology of the southern Nechako Basin, NTS 92N, 92O, 93B, 93C, 93F, 93G; BC Ministry of Energy and Mines and Petroleum Resources, Petroleum Geology Map 2006-1, 3 sheets, 1:400 000 scale.
- Riddell, J., Ferri, F., Sweet, A. and O’Sullivan, P. (2007): New geoscience data from the Nechako Basin project; *in* Nechako Initiative Geoscience Update 2007, BC Ministry of Energy and Mines and Petroleum Resources, Petroleum Geology Open File 2007-1, p. 59–98.
- Schiarizza, P. and MacIntyre, D.G. (1999): Geology of Babine Lake–Takla Lake area, central British Columbia (93K/11, /12, /13, /14; 93N/3, /4, /5, /6); *in* Geological Fieldwork 1998, BC Ministry of Energy and Mines, Paper 1999-1, p. 33–68.
- Struik, L.C. (1993): Intersecting intracontinental Tertiary transform fault systems in the North American Cordillera; *Canadian Journal of Earth Sciences*, v. 30, p. 1262–1274.
- Struik, L.C. and MacIntyre, D.G. (2001): Introduction to the special issue of *Canadian Journal of Earth Sciences*: The Nechako NATMAP Project of the central Canadian Cordillera; *Canadian Journal of Earth Sciences*, v. 38, p. 485–494.

New Studies of the Lower Cretaceous Jackass Mountain Group on the Southern Margin of the Nechako Basin, South-Central British Columbia: Progress and Preliminary Observations

Peter S. Mustard, Department of Earth Sciences, Simon Fraser University, Burnaby, BC, pmustard@sfu.ca

J. Brian Mahoney, Department of Geology, University of Wisconsin–Eau Claire, WI

J. Russell Goodin, Department of Earth Sciences, Simon Fraser University, Burnaby, BC

Catherine I. MacLaurin, Department of Earth Sciences, Simon Fraser University, Burnaby, BC

James W. Haggart, Geological Survey of Canada, Pacific Division, Vancouver, BC

Mustard, P.S., Mahoney, J.B., Goodin, J.R., MacLaurin, C.I. and Haggart, J.W. (2008): New studies of the Lower Cretaceous Jackass Mountain Group on the southern margin of the Nechako Basin, south-central British Columbia: progress and preliminary observations; *in* Geoscience BC Summary of Activities 2007, Geoscience BC, Report 2008-1, p. 135–144.

Introduction

The Nechako Basin (Figure 1) is part of the Interior Plateau physiographic region of British Columbia, and has been variously defined in terms of extent and age (Ferri and Riddell, 2006). Accurate assessment of the petroleum potential of the Nechako Basin requires a comprehensive understanding of the basin architecture developed within Cretaceous strata, which represent the most prospective targets in the subsurface. Modeling the subsurface distribution of these Cretaceous units requires a detailed stratigraphic analysis of coeval, laterally adjacent strata exposed along the basin margins (Mustard and Mahoney, 2007).

The age and general lithological character of strata in the subsurface of the Nechako Basin are broadly known from industry drillholes (located on Figure 1) as well as through examination of isolated outcrops of Cretaceous intervals exposed beneath extensive Cenozoic volcanic and glacial cover (Ferri and Riddell, 2006; Mustard and MacEachern, 2007; Riddell et al., 2007). Regional facies patterns and basin architecture within the Nechako Basin are poorly understood, however, and even the stratigraphic affinities of subsurface units are unclear. For example, Hunt (1992) identified some subsurface strata as possible Jackass Mountain Group, a Lower Cretaceous succession that is exposed along the southern margins of the Nechako Basin, and that most pre-

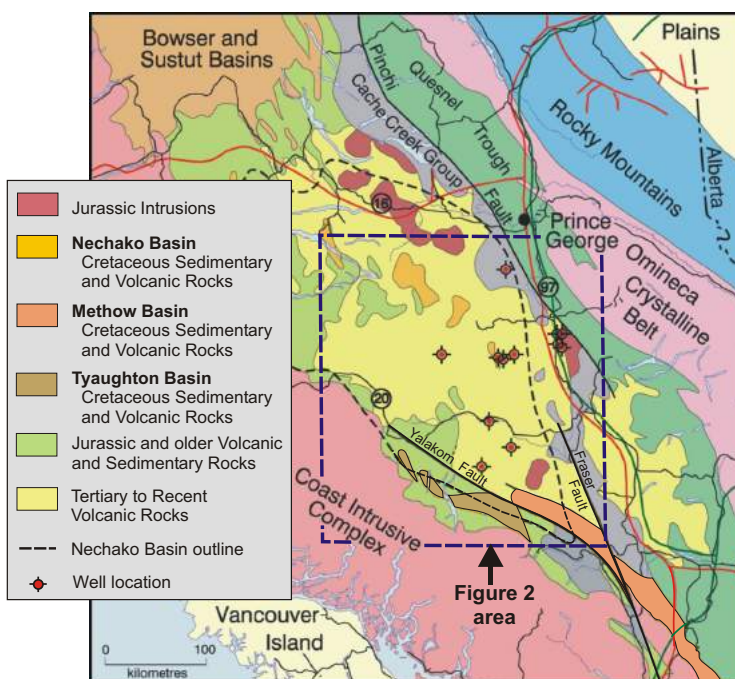


Figure 1. Regional geology, showing major Cretaceous units of the Nechako, Methow and Tyaughton basins and the outlined area of Figure 2 (modified from BC Ministry of Energy, Mines and Petroleum Resources, 2002; used with per-

vious studies have suggested is dominated by submarine fan deposits. In contrast, Hannigan et al. (1994) assigned these rocks to the Skeena ‘assemblage’ (more commonly termed the Skeena Group), a generally nonmarine Lower Cretaceous succession exposed along the northern margins of the Nechako Basin.

This confusion illustrates the poorly constrained nature of the subsurface strata in this region (for a more thorough discussion of the stratigraphic problems, see Ferri and Riddell, 2006) and the lack of understanding of the original extent of what is now termed the Nechako Basin. More recently, Rid-

Keywords: sedimentology, stratigraphy, Jackass Mountain Group, Nechako, Methow, Tyaughton, Cretaceous

This publication is also available, free of charge, as colour digital files in Adobe Acrobat® PDF format from the Geoscience BC website: <http://www.geosciencebc.com/s/DataReleases.asp>.

dell et al. (2007) have provided new palynological and radiometric age controls from subsurface drill cuttings of the existing hydrocarbon exploration wells. These change the suggested ages of some subsurface intervals considerably (e.g., expanding the amount of known Albian–Cenomanian subsurface strata). In addition, Mustard and MacEachern (2007) conducted a sedimentological and ichnological description and interpretation of the existing cored intervals from the archived wellcores. Most extant core from these wells represents either shallow marine or nonmarine environments of deposition, including those from Cretaceous strata. No deep marine facies were cored, although significant thicknesses of marine turbidites (presumably sub-wave-base depths) are interpreted to be present, based on geophysical well log profiles (Riddell et al., 2007).

At the southern end of the Nechako Basin, Lower Cretaceous Jackass Mountain Group (JMG) strata are unconformably overlain by Cenozoic volcanic rocks (Figure 2). The Cretaceous strata are generally classified as part of the Methow Basin, but are clearly the surface expressions of strata that continue northward into the subsurface beneath the Cenozoic rocks that form most of the exposed strata of the Nechako Basin (Hickson et al., 1994; Mahoney et al., pers. comm.). The JMG and associated strata include thick (>1000 m), laterally extensive (>10 km) sandstone successions that overlie and interfinger with mudstone. Previous studies have interpreted them as the deposits of large submarine fan deposystems (Kleinspehn, 1982, 1985), although Schiarizza et al. (1997) identified some areas of nonmarine strata, which they considered to be part of the JMG.

The authors' emphasis on the Jackass Mountain Group reflects the hypothesis that this unit is probably the best candidate for major reservoir systems in the subsurface of the Nechako Basin. It is suggested that JMG strata represent the closest surface analogue and the most likely direct correlative to the 'Skeena assemblage' of the subsurface, which has been interpreted by Hannigan et al. (1994, p. 140) to contain "the most significant petroleum plays in this assessment". This confusion regarding stratigraphic nomenclature also highlights the confusion of 'basin' names traditionally assigned to different stratigraphic successions in the region. The authors suggest that the separation of stratigraphic successions of similar age and type into separate 'Nechako,' 'Methow,' and possibly 'Tyaughton' basins likely reflects the history of different researchers studying the same rocks in different areas, rather than discrete depositional basins. These studies will test the hypothesis that the Nechako, Methow and perhaps the Tyaughton 'basins' constituted one extensive and continuous regional area of deposition during at least Early Cretaceous time (a basin that may have been linked with Early Cretaceous deposition of the southern Skeena 'Basin' as well, although the

current studies will not directly test this hypothesis). If these individual 'basins' were originally laterally continuous and thus represent a single Early Cretaceous depocentre, there would be major implications for the hydrocarbon potential of the Nechako 'Basin', greatly increasing both the volume of potential reservoir rocks and potential source rocks, such as the extensive black shale of the Ladner Group in the Methow Terrane (Ray, 1990).

A brief regional reconnaissance study in 2006 identified two major areas of well-exposed JMG suitable for detailed stratigraphic and sedimentological studies (Mustard and Mahoney, 2007). These detailed studies commenced in summer 2007, and form the basis for two M.Sc. research projects (Goodin and MacLaurin). Fieldwork will continue in 2008 on both of these studies and several regional studies on Cretaceous strata in the area, including the Nechako Basin.

Summer 2007 Field Research

Jackass Mountain Group in the Camelsfoot Range Area

During summer 2007, Goodin conducted a detailed examination of sections of the JMG in the Camelsfoot Range (Figure 2, locality A; Figure 3). The JMG is well exposed on several ridges in this area and is volumetrically the most significant geological unit in the central and eastern Camelsfoot Range (Hickson et al., 1994; Schiarizza et al., 1997; Mahoney et al., pers. comm.). The study area extends northwest along the Yalakom fault from the confluence of the Fraser and Bridge rivers, to the geographic junction between Nine Mile Ridge and the Yalakom River (Figure 3). The northern boundary is delineated by the northeast-trending Nine Mile Ridge. The study area is focused on the central part of an approximately 150 km long, southward-tapering wedge of mainly medium- to coarse-grained sandstone and polymictic conglomerate exposed between the Yalakom and Fraser fault systems. It is part of a broad, asymmetric synclorium with the base of the JMG exposed in steeply dipping beds on the western limb east of the Yalakom River, and the upper part exposed in moderately west-dipping beds in the eastern limb.

Within this study area, five detailed stratigraphic sections were measured (Figure 3). Forty-five lithological, 10 detrital zircon, 12 mudstone geochemistry, 11 microfossil and 3 macrofossil samples were collected, most from the stratigraphic sections. Section thicknesses include approximately 1500 m on Yalakom Mountain (A on Figure 3), 130 m on eastern Nine Mile Ridge (B on Figure 3), 130 m on western Nine Mile Ridge (C on Figure 3), 125 m on Madson Creek (D on Figure 3), and 70 m on a low-lying ridge in the central study area (E on Figure 3). Several additional traverses were conducted to collect general lithological, structural and fossil information.

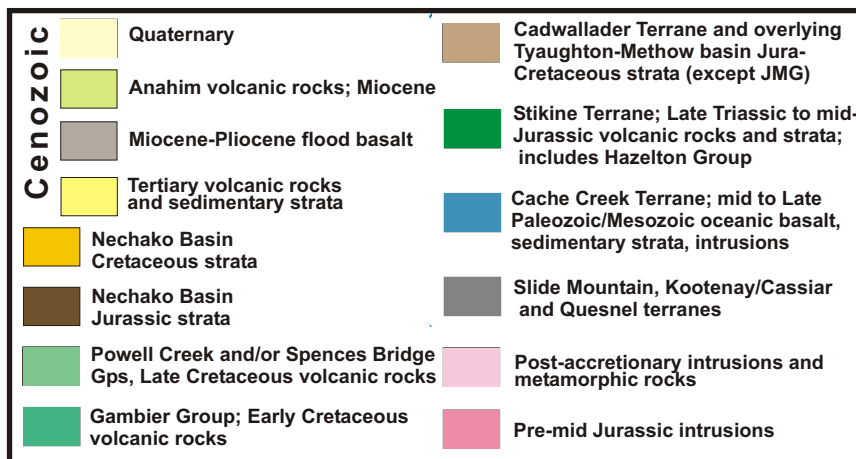
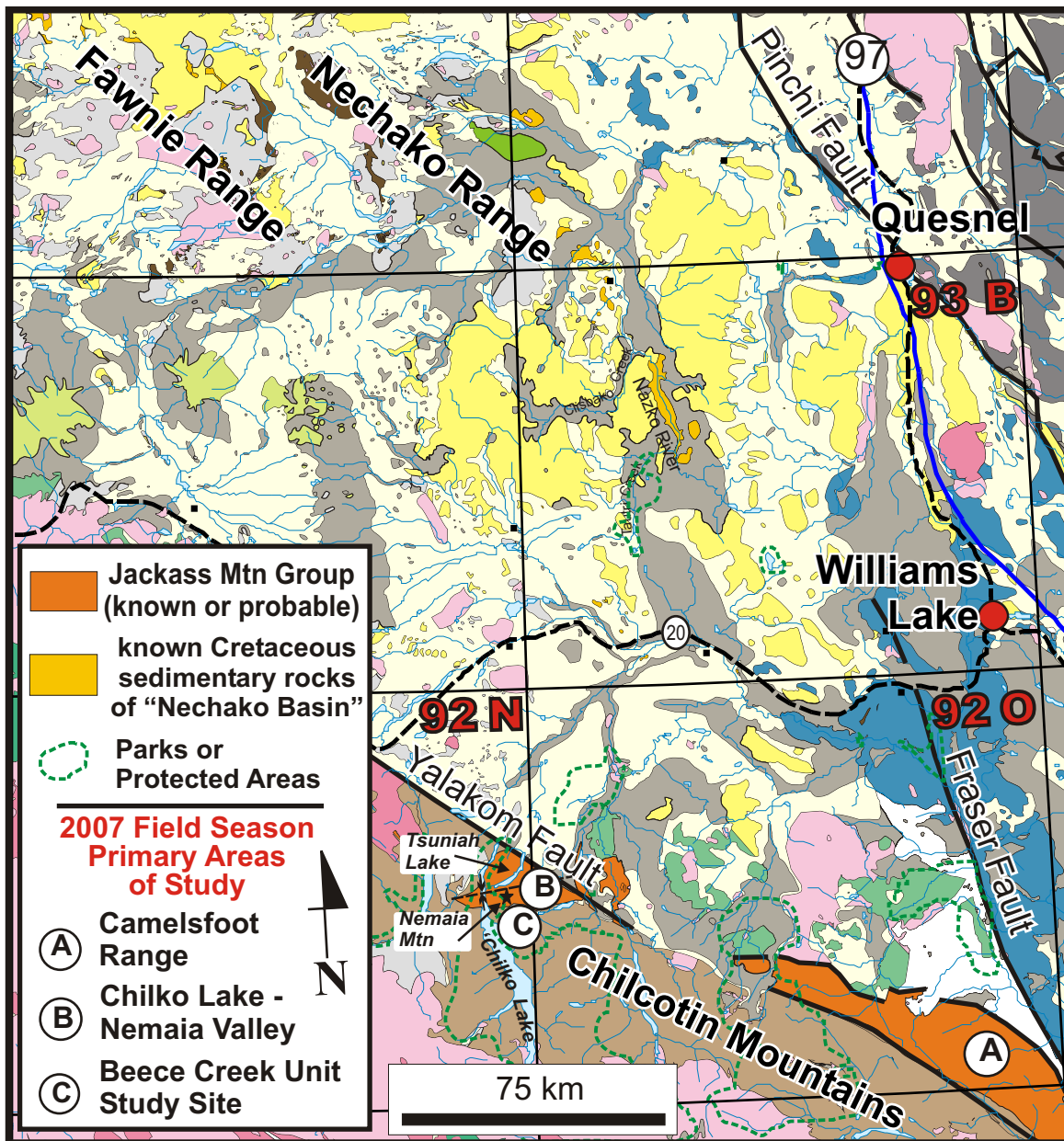


Figure 2. Regional geological framework and location of major areas of study discussed in this paper (modified from Ferri and Riddell, 2006 and Riddell, 2006; used with permission).

At and near Yalakom Mountain (A on Figure 3), northwest-trending JMG strata dip steeply and are slightly overturned towards the north in some areas. Jackass Mountain Group units in this area overlie Middle Jurassic rocks of the Ladner Group (Mahoney, 1993; Schiarizza et al., 1997). These basal JMG rocks are dominated by massive, green, medium- to coarse-grained, lithic-rich feldspathic sandstone and interbedded siltstone. These form a >1500 m thick unit on Yalakom Mountain (Figure 3) that is correlative with the volcanic sandstone unit described by Schiarizza et al. (1997). Jackass Mountain Group strata containing fossils of probable Barremian age are present about 200 m below the base of this section, but above the basal unconformity with the underlying Lower to Middle Jurassic Dewdney Creek Formation (GSC Locality Number 74815; unpublished data provided by Poulton et al., 1994 included in Schiarizza et al., 1997). New fossil collections from the upper part of the stratigraphic section north of Yalakom Mountain are of Albian age (*Brewericeras hulenense* zone). Thus, the full stratigraphic section of the JMG in the Yalakom Mountain area appears to range in age from Barremian to Albian.

The Madson Creek section (D on Figure 3) includes the best exposures of the most readily identifiable unit within the JMG of the Camelsfoot Range (Figure 3). These striped, dark grey and pale olive 'zebra beds', composed of rippled and syndimentary folded, silt-sized and fine- to medium-grained sandstone units, respectively, form a 125 m thick succession bounded above and below by massive, medium- to coarse-grained, green lithic-rich feldspathic sandstone (Figure 4, with legend as Figure 5). Although the thickest observed outcrop of this lithofacies is in the Madson Creek area, the zebra beds are present throughout the central part of the study area, are considered to be laterally continuous for many kilometres, and form part of a sedimentary unit at least several hundreds of metres thick. These beds dominate the stratigraphic succession to the northeast of Hogback Mountain; however, further west, although still present, the beds seem to be in transition to, and become interbedded with, more massive and thicker sandstone beds. This suggests an interfingering relationship between the zebra beds and thick lithofeldspathic sandstone beds similar to those of the Yalakom Mountain area. While no fossils have yet been identified from the zebra beds, strata structurally underly-

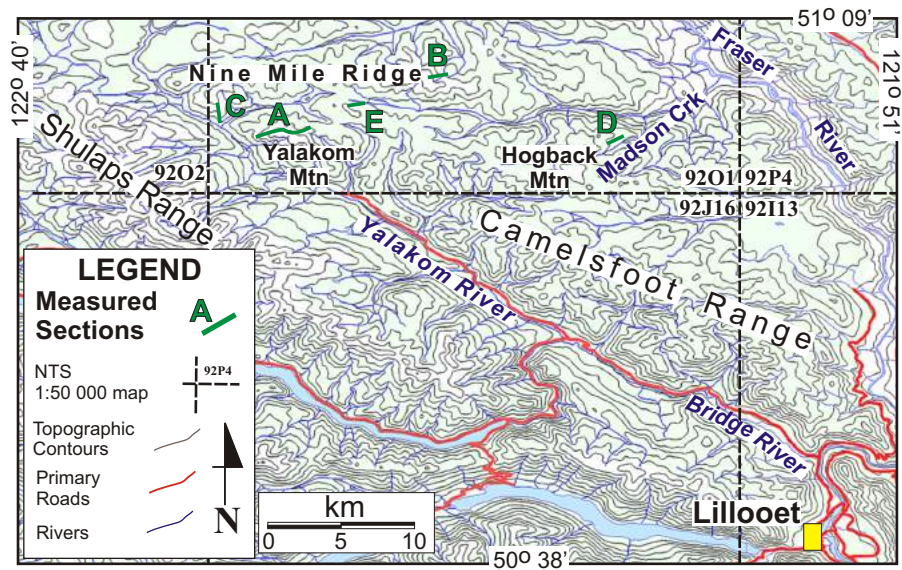


Figure 3. Location map for Camelsfoot Range study, showing main geographic features and the locations of sections measured during 2007.

ing these beds in the Madson Creek area contain the belemnoid fossil *Acroteuthis*, suggesting a pre-Albian Cretaceous age.

Rocks on Nine Mile Ridge (B and C on Figure 3) comprise a unit several kilometres thick of repeated successions of <40 m thick bed sets consisting of abundant trough crossbeds of moderately- to well-sorted, medium-grained sandstone and rare pebbly sandstone at the base of some sets. These are separated by sections of poorly exposed siltstone, mudstone and lesser fine-grained sandstone units that are tens to hundreds of metres thick. In a few places, the finer packages include fine-grained, sandstone thin beds that are regular and rhythmically repeated, and dark grey mudstone interbeds that gradationally coarsen up to one of the crossbedded sandstone bed sets described above. The repeated more than 100 m thick successions of decimetre-thick trough cross-stratified sandstone separated by siltstone-rich intervals suggest accumulation in a fluvial environment, with river systems building across and into floodplains that may have included lacustrine areas (with rhythmically deposited fresh-water turbidites) and small, fresh-water deltaic successions.

The JMG strata in the Camelsfoot Range can be subdivided into three major facies associations, which roughly correspond to southern, central and northern geographic areas, as described above. In the south, directly northeast of the Yalakom fault, the thick succession includes massive sandstone units that were deposited as sediment gravity flows (mostly turbidites) in a sub-wave-base, marine environment. These correspond to the submarine fan deposits that Kleinspehn (1982, 1985) interpreted to be the dominant depositional environment for the entire JMG. In the central portion of the study area, the interbedded turbiditic sand-

stone and siltstone comprising the zebra beds of the Madson Creek area were most likely deposited near or within the migrating lobes of an active submarine fan system. Common wave reworking of the upper parts of many turbidites, however, indicates that depth was typically above the storm wave base, suggesting a relatively shallow shelf environment, possibly transitional to a marginal marine shoreline regime. It is considered likely that these shallow shelf turbidites comprise distal (e.g., prodeltaic units) deposits of river-dominated delta or fan delta systems, rather than as parts of deeper water submarine fan systems. The facies exposed on Nine Mile Ridge are indicative of nonmarine fluvial, floodplain and possible lacustrine environments. Unfortunately, poor exposure in the valleys near Nine Mile Ridge means that it is not possible to trace this nonmarine unit directly into the marine facies of the rest of the JMG in this region.

Assuming that the JMG study area in the Camelsfoot Range is all part of the same structural block (Mahoney et al., pers. comm.), these three major facies associations likely represent both lateral and vertical changes in basin depositional patterns over time. The southern submarine fan sandstone may represent the base of a relative marine regression, whereas the central facies of shallow marine turbidites may reflect either progressive shallowing of the basin over time or a time-equivalent, but more proximal, marine facies in the northern part of the study area. The Nine Mile Ridge nonmarine succession represents either a more proximal part of the basin or a progressive shallowing of JMG deposition over time. The current lack of age control on the nonmarine unit and possibility of structural separation from the other facies makes either interpretation feasible at this stage of the study.

Jackass Mountain Group in the Nemaia Mountain Area

MacLaurin began a similar detailed stratigraphic study of JMG and related strata in the Chilko Lake–Nemaia Valley area (locality B on Figure 2), a study that will continue during the summer of 2008. The JMG and other Cretaceous and Jurassic sedimentary successions are well exposed in this area, especially on Nemaia Mountain and surrounding ridges (Figure 2; Schiarizza et al., 2002). These strata are exposed immediately southwest of the Yalakom fault and traditionally are considered part of the Tyaughton Basin, which Garver (1992) described as a discrete sub-basin from the Methow Basin, with different sedimentation patterns and source areas. Restoration of ~115 km of dextral offset on the Yalakom fault (as suggested *in* Schiarizza et al., 1997), however, restores the JMG of the Camelsfoot Range directly adjacent to the Chilko Lake–Nemaia exposures, suggesting original depositional continuity.

The JMG and underlying Jurassic strata in this area are well exposed in a northeast-plunging syncline whose axis runs beneath and parallel to Tsuniah Lake (Figure 2; Schiarizza et al., 2002). Reconnaissance traverses of the area revealed dominantly undeformed JMG strata unconformably overlying the Jurassic Nemaia Formation in most areas. In other localities, JMG strata unconformably overlie the Jurassic Relay Mountain Group. Based on this reconnaissance work, five localities were identified as suitable for measuring detailed stratigraphic sections. These comprise two well-exposed ridges on the northern limb, two on the southern limb and one on the furthest southwest portion of the syncline.

During the summer of 2007, work on four of the stratigraphic sections was initiated, comprising the four sections on the northern and southern syncline limbs. One 2.2 km thick measured section on the northeastern side of the syncline documents a 1.9 km thick JMG succession of predominantly well-sorted sandstone with minor mudstone intervals (Figure 6, with legend as Figure 5). Above the JMG–Nemaia Formation contact in this section, a massive sandstone unit containing rare swaley cross-stratification and conglomeratic lenses fines upwards into a sandy siltstone. A 100 m thick mudstone succession, containing wave- and combined-flow ripple lamination, sandy interbeds and abundant fossil and organic material, overlies this sandy unit and coarsens upward into an interval of extensive, well-sorted sandstone bodies that display abundant very low angle cross-stratification and (in some localities) distinct trough- and hummocky cross-stratification. This unit is overlain by massive to planar stratified sand bodies and interbedded mudstone. The lower 800 m of a 1.2 km thick section on which measurement is in progress on the northwest side of the syncline exhibits similar stratigraphy with minor changes in unit thickness.

The upper 800 m of an 1.4 km thick stratigraphic section on which measurement is in progress on the southeast limb of the syncline is distinctly finer grained, with a higher percentage of mudstone in the middle sandstone unit, but is capped by an anomalous conglomeratic facies. Well-sorted sandstone dominates this unit, displaying abundant low-angle cross-stratification and soft-sediment deformation. The basal 200 m is composed dominantly of silty mudstone with minor fine-grained sandstone. The age of these basal JMG strata is poorly constrained, but the underlying Nemaia Formation strata contain ammonites of Bathonian age (*Iniskinites* sp.), whereas the upper part of this unit contains ammonites that appear to be referable to Hauterivian forms. The upper 200 m of the fourth section, located on the southwest limb of the syncline, is composed of well sorted, massively bedded sand intercalated with finer-grained intervals. This section is tentatively correlated to the upper portion of the measured section on the northeast limb of the

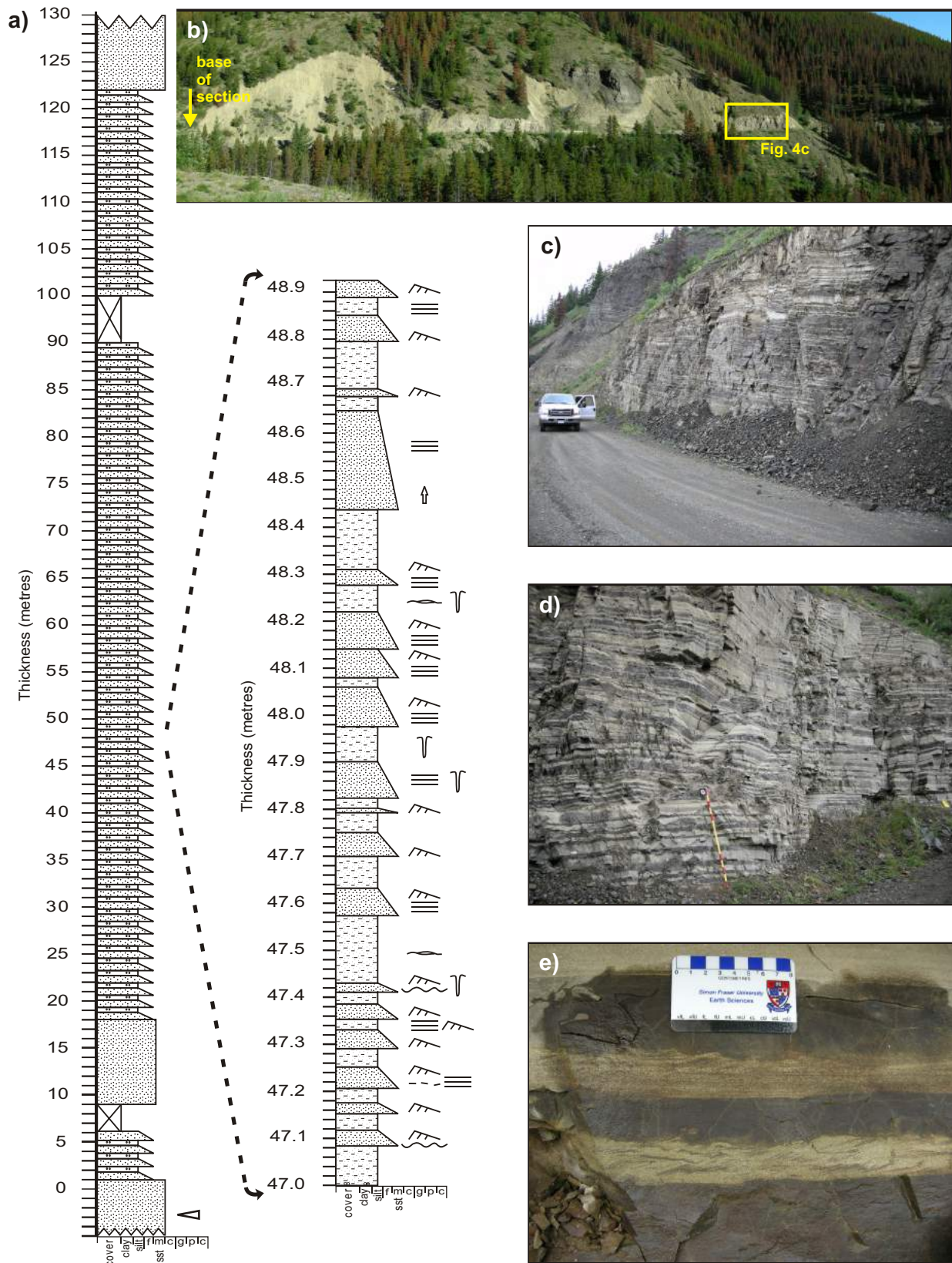


Figure 4. a) Measured stratigraphic section located on Madson Creek (D on Figure 3), Figure 5 provides a common legend for Figures 4 and 6; b) roadcut of the lower part of the section on the west side of Madson Creek; c) middle portion of the section, showing typical sheet-like sandstone-mudstone couplets; d) closer view of sandstone-mudstone couplets where a detailed section from 47 to 48.9 m was measured; e) close-up view of two sandstone beds displaying aggradational current ripple forms, some possible reworking of upper ripples and trace fossils at the sand-mud interface and above.

syncline and contains probable Albian-aged fossils in its uppermost part.

Extensive sampling of rock types keyed to stratigraphic position will facilitate detailed petrological, organic maturation and porosity and permeability analyses. Approximately 70 rock samples, distributed between the four measured sections, were collected for petrological analyses. Ten detrital zircon sandstone samples and 17 mudstone geochemical samples were collected for isotopic provenance studies. One thermal maturation sample of a carbonized wood fragment found in the southeastern section and one total organic carbon mudstone sample were also taken.

Several new fossil locations were identified in this area. A distinctive 100 m thick, dark grey mudstone unit present in both measured sections on the northern limb yielded common fossil specimens, including ammonites, gastropods and bivalves of probable Hauterivian age. The conglomeratic unit beneath the mudstone unit also yielded bivalves and a few ammonite and gastropod fossils, presently under study.

Primary observations indicate that correlations between these four sections can be undertaken, and preliminary interpretations suggest an overall deepening of the basin over time from a shallow marine environment to an outer shelf or slope environment. The northern limb of the syncline is interpreted to be a storm-dominated lower to upper shoreface environment with intermittent, but moderate, deltaic influ-

ence. The southern limb shows significant dissimilarities to the northern limb, including a distinctly finer-grained basal unit. A very preliminary study of the section suggests it represents a shallow marine depositional environment that underwent transgression from lower shoreface to outer shelf conditions. The conglomeratic facies may be associated with a deltaic influence.

Regional Studies

In addition to the focused graduate student studies summarized above, several regional sampling programs were initiated. Sampling of Lower Cretaceous strata in the areas between the Camelsfoot Range and Chilko Lake region was initiated to compare the detrital zircon and other geochemical characteristics of these strata to those of the main study areas, and to test suggestions made in previous studies that Methow and Tyaughton basins were distinct sub-basins during Early Cretaceous time (e.g., Garver, 1992).

South of the synclinorium in the Nemaia Mountain area, across a series of high-angle faults, strata of probable Albian age are exposed on the northern flanks of Mt. Tatlow (C on Figure 2). This unit consists of black silty mudstone, lithic sandstone and chert-pebble conglomerate, which unconformably overlies the Upper Jurassic Relay Mountain Group. These rocks have been assigned to the Beece Creek succession of the mid-Cretaceous Taylor Creek Group in several previous studies and published geological maps (e.g., Schiarizza and Riddell, 1997; Schiarizza et al., 2002). Preliminary stratigraphic analysis indicates these strata conformably overlie both the middle to late Albian Dash and Lizard formations of the Taylor Creek Group, and that these strata may be directly correlative to part of the Jackass Mountain Group on Nemaia Mountain. If this interpretation is correct, this correlation would provide the earliest definitive tie between the Methow and Tyaughton basins, and would substantially increase the extent of the regional Early Cretaceous depocentre. The well-exposed stratigraphic section on the northern flanks of Mt. Tatlow will be examined in detail as part of a fourth year B.Sc. project (M. Forgette of University of Wisconsin–Eau Claire, one of the student assistants of the 2007 season). The section has been measured in detail and extensively sampled for thin section petrography, shale geochemistry, detrital zircon analysis, palynological and microfaunal studies and total organic carbon.

Summary and Regional Implications

The 2007 field season focused on detailed field investigations, measurement of stratigraphic sections and sample collection as part of two studies of well-exposed Jackass Mountain Group strata. In addition, some initial sampling was conducted for more regional studies of Early Cretaceous units in adjacent areas. Much of the final interpretation from these studies will follow further fieldwork in

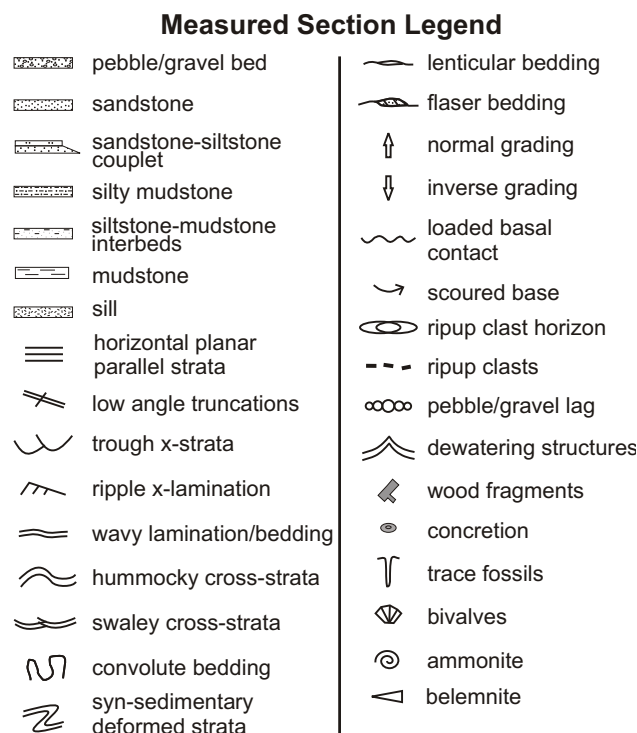


Figure 5. Common legend for measured sections of Figures 4 and 6.

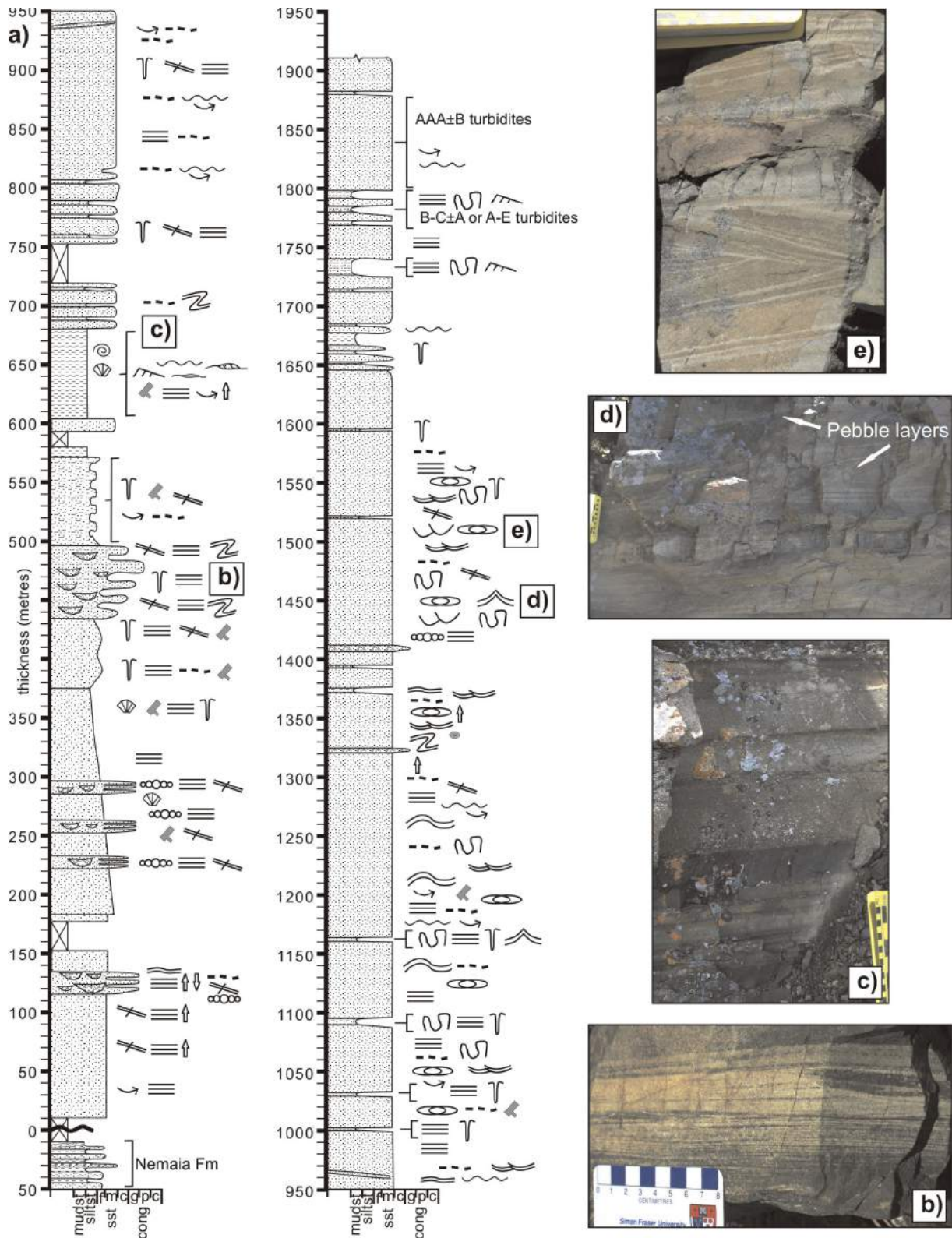


Figure 6. a) Simplified stratigraphic section through JMG from ridge north of Tsuniah Lake (common legend in Figure 5); **b)** fine-grained laminated sandstone displaying irregular wavy lamination and cross-laminated ripple forms, typical of the lower sand-rich unit; **c)** fine- to medium-grained sandstone beds (most are normally graded) with mudstone capping or between beds, probably constituting turbidites, although this unit also contains some shallow-water features; **d)** light and dark sandstone (mostly fine to medium grained) with rare pebbly layers in erosive-based troughs (central) and top bed, high-angle discontinuities are probably channel bases; **e)** medium-grained sandstone displaying high-angle cross-stratification typical of this upper sandstone unit (both swaley and trough cross-stratification occur in this unit).

2008 and extensive processing of geochemical samples, examination of thin sections from rock samples and analysis of new macrofossil collections. As well, extensive collections of mudstone samples processed for microfossils (palynology and foraminifers) will hopefully provide additional age constraints. Some preliminary implications are, however, apparent.

The presence in the Jackass Mountain Group of extensive and extremely thick facies intervals interpreted to represent shallow marine and nonmarine environments was surprising, given that the main previous study of the JMG interpreted it to be dominated by submarine fan deposition in relatively deep (sub-wave-base) environments (Kleinspehn, 1982, 1985; although Schiarizza et al., 1997 did recognize some nonmarine components within the JMG in their regional synthesis). In the Camelsfoot Range, sub-wave-base submarine fan facies are present as a thick succession immediately northeast of the Yalakom fault. The JMG in large areas of the northern Camelsfoot Range, however, comprises nonmarine fluvial and possibly lacustrine successions. In addition, the central Camelsfoot Range contains extensive exposures of sandstone-mudstone turbidites, but with common reworking of the tops of these turbidites by wave processes, indicating a relatively shallow marine environment of deposition. The precise age of the nonmarine facies is presently unknown, but detrital zircon samples from fluvial sandstone in this facies will at least provide a maximum age, and palynology samples will hopefully provide more specific age constraints and other biostratigraphic information. The implication is that a continuous, nonmarine to marine succession is preserved in this area, which possibly spans Barremian to Albian-Cenomanian time. The presence of thick and moderately well-sorted, cross-stratified fluvial sandstone packages in the northern Camelsfoot Range provides a new potential hydrocarbon reservoir system, which may have had better original porosity and permeability characteristics than the less well-sorted massive sandstone turbidites common to the southern Camelsfoot Range.

Detailed work in the Nemaia Mountain study area also suggests that much, if not most, of the JMG in this area lacks submarine fan turbidites. Thick successions of marine sandstone with swaley and, locally, hummocky and trough cross-stratification indicate shallow and relatively high-energy nearshore environments of deposition, as do associated heterolithic sandstone-mudstone packages containing wave and combined-flow ripple types. These shallow marine intervals appear to be more common in the northern and lower parts of the JMG succession in this area and change upward and southward to massive sandstone beds and interbedded mudstone successions that are more typical of deeper marine submarine fan systems, although the extent and thickness of these facies do not appear to be great. The presence of very thick successions of shallow

marine (shoreface or delta front) facies, which include extensive decimetre thick intervals of well-sorted sandstone, is an important new discovery. If these strata continue in the subsurface to the north, they may represent high priority targets to test as a hydrocarbon reservoir system.

The presence of significant thicknesses of shallow marine and terrestrial units within the JMG also increases support for correlation of this unit with similar subsurface Lower Cretaceous strata of the Nechako Basin. Shallow marine sandstone, in particular, is likely to serve as well-sorted and laterally extensive units with sufficient porosity and permeability to act as high-volume reservoir units for significant hydrocarbon accumulation. As well, this correlation greatly expands the extent of potential source rocks for the subsurface strata. Mud-rich source rocks of the Tyaughton and Methow basins include the extensive Ladner Group and Relay Mountain Group units. Both of these extensive units are current objects of study for source-rock potential, both as part of this project and the ongoing projects described in Ferri and Riddell (2006).

Acknowledgments

Funding is primarily from Geoscience BC Grant 2006-014. Additional financial support comes from Natural Science and Engineering Research Council (NSERC) Grant 611258 to Mustard; Simon Fraser University to Mustard, Goodin and MacLaurin; University of Wisconsin-Eau Claire to Mahoney; and the Geological Survey of Canada to Haggart. The King families of Bluff Lake are thanked for help and accommodation for the Nemaia Mountain project, with special thanks to Mike King of Whitesaddle Air Services for stellar helicopter support. The pilots and crew of CC Helicopters in Lillooet are also thanked for support for the Camelsfoot Range project, with special appreciation extended to the base manager, Scott Taylor. Alex Guy, Michelle Forgette and Liz Balgord, undergraduate students at the University of Wisconsin-Eau Claire, provided excellent assistance to the geologists. James MacEachern of Simon Fraser University, Lyn Anglin of Geoscience BC and Cathie Hickson of the Geological Survey of Canada are thanked for providing formal reviews of the manuscript.

References

- BC Ministry of Energy, Mines and Petroleum Resources (2002): Nechako Basin: oil and gas opportunities in central British Columbia; BC Ministry of Energy, Mines and Petroleum Resources, information brochure.
- Ferri, F. and Riddell, J. (2006): The Nechako Basin project: new insights from the southern Nechako Basin; *in* Summary of Activities 2006, BC Ministry of Energy, Mines and Petroleum Resources, URL <<http://www.em.gov.bc.ca/subwebs/oilandgas/pub/reports/summary2006.htm>>, p. 89-124 [November 2007].
- Garver, J.I. (1992): Provenance of Albian-Cenomanian rocks of the Methow and Tyaughton basins, southern British Colum-

- bia: a mid-Cretaceous link between North America and the Insular terranes; *Canadian Journal of Earth Sciences*, v. 29, p. 1274–1295.
- Hannigan, P., Lee, P.J., Osadetz, K.J., Dietrich, J.R. and Olsen-Heise, K. (1994): Oil and gas resource potential of the Nechako–Chilcotin area of British Columbia; BC Ministry of Energy, Mines and Petroleum Resources, Geofile 2001-6, 167 p., 5 maps at 1:1 000 000 scale.
- Hickson, C.J., Mahoney, J.B. and Read, P. (1994): Geology of Big Bar map area: facies distribution in the Jackass Mountain Group; *in* Current Research, Part A, Geological Survey of Canada, Paper 94-1A, p. 143–150.
- Hunt, J.A. (1992): Stratigraphy, maturation, and source rock potential of Cretaceous strata in the Chilcotin–Nechako region of British Columbia; M.Sc. thesis, The University of British Columbia, 447 p.
- Kleinspehn, K.L. (1982): Cretaceous sedimentation and tectonics, Tyaughton–Methow Basin, southwestern British Columbia; Ph.D. thesis, Princeton University, 184 p.
- Kleinspehn, K.L. (1985): Cretaceous sedimentation and tectonics, Tyaughton–Methow Basin, southwest British Columbia; *Canadian Journal of Earth Sciences*, v. 22, p. 154–174.
- Mahoney, J.B. (1993): Facies reconstructions in the Lower to Middle Jurassic Ladner Group, southern British Columbia; *in* Current Research, Part A, Geological Survey of Canada, Paper 93-1A, p. 173–182.
- Mahoney, J.B., Hickson, C.J. and Schiarizza, P. (pers. comm.): Geology, Taseko Lakes, British Columbia; Geological Survey of Canada, Open File Map, scale 1:250 000. 1 sheet.
- Mustard, P.S. and Mahoney, J.B. (2007): Stratigraphic analysis of Cretaceous strata flanking the southern Nechako Basin (parts of NTS 092M, O; 093B), British Columbia: constraining basin architecture and reservoir potential; *in* Geological Fieldwork 2006, BC Ministry of Energy, Mines and Petroleum Resources, Paper 2007-1 and Geoscience BC, Report 2007-1, p. 377–379.
- Mustard, P.S. and MacEachern, J.A. (2007): A detailed facies (sedimentological and ichnological) evaluation of archived hydrocarbon exploration drill core from the Nechako Basin, BC; *in* Nechako Initiative — Geoscience Update 2007, BC Ministry of Energy, Mines and Petroleum Resources, Petroleum Geology Open File 2007-1, p. 7–58.
- Ray, G.E. (1990): The geology and mineralization of the Coquihalla gold belt and Hozameen fault system, southwestern British Columbia (92H/611, 14); BC Ministry of Energy, Mines and Petroleum Resources, Bulletin 79, 97 p.
- Riddell, J.M., compiler (2006): Geology of the southern Nechako basin, NTS 92N, 92O, 93B, 93C, 93F, 93G; BC Ministry of Energy, Mines and Petroleum Resources, Petroleum Geology Map 2006-1, scale 1:400 000.
- Riddell, J., Ferri, F., Sweet, A. and O’Sullivan, P. (2007): New geoscience data from the Nechako Basin project; *in* Nechako Initiative — Geoscience Update 2007, BC Ministry of Energy, Mines and Petroleum Resources, Petroleum Geology Open File 2007-1, p. 59–98.
- Schiarizza, P. and Riddell, J. (1997): Geology of the Tatlayoko Lake–Beece Creek area; *in* Interior Plateau Geoscience Project: Summary of Geological, Geochemical and Geophysical Studies; BC Ministry of Energy, Mines and Petroleum Resources, Paper 1997-2 and Geological Survey of Canada, Open File 3448, p. 63–101.
- Schiarizza, P., Gaba, R.G., Glover, J.K., Garver, J.I. and Umhoefer, P.J. (1997): Geology and mineral occurrences of the Taseko–Bridge River area; BC Ministry of Energy, Mines and Petroleum Resources, Bulletin 100, 291 pages.
- Schiarizza, P., Riddell, J., Gaba, R.G., Melville, D.M., Umhoefer, P.J., Robinson, M.J., Jennings B.K. and Hick, D. (2002): Geology of the Beece Creek–Nuit Mountain area, B.C. (NTS 92N/8, 9, 10; 92O/5, 6, 12); BC Ministry of Energy, Mines and Petroleum Resources, Geoscience Map 2002-3, scale 1:50 000.

Designing a Test Survey in the Nechako Basin, South-Central British Columbia (NTS 092N, O; 093B, C, F, G) to Determine the Usefulness of the Magnetotelluric Method in Oil and Gas Exploration

J. Spratt, Geoscience BC, Vancouver, BC; jespratt@yahoo.com

J. Craven, Geological Survey of Canada, Ottawa, ON

S. Shareef, Geological Survey of Canada, Ottawa, ON

F. Ferri, British Columbia Ministry of Energy Mines and Petroleum Resources, Victoria, BC

J. Riddell, British Columbia Ministry of Energy Mines and Petroleum Resources, Victoria, BC

Spratt, J., Craven, J., Shareef, S., Ferri, F. and Riddell, J. (2008): Designing a test survey in the Nechako Basin, south-central British Columbia (NTS 092N, O; 093B, C, F, G) to determine the usefulness of the magnetotelluric method in oil and gas exploration; *in* Geoscience BC Summary of Activities 2007, Geoscience BC, Report 2008-1, p. 145–150.

Introduction

In response to the rapid spread and destructive effects of the mountain pine beetle (MPB), British Columbia is facing a challenge in developing economic diversification opportunities for forestry-based communities in the interior of the province. Geoscience BC is undertaking a number of projects that will help to assess the mineral and petroleum potential in the MPB-affected area. Although only limited exploration has been carried out, the potential for hydrocarbons has been observed within several interior basins of British Columbia, including the Nechako Basin. A 1994 estimate by the Geological Survey of Canada, based on very limited information, suggested that the Nechako Basin may contain as much as a trillion cubic metres of gas and a billion cubic metres of oil, although these estimates are qualified as being very speculative (Hannigan et al., 1994).

Recent examinations of 20-year-old magnetotelluric (MT) data collected from within the Nechako Basin have shown that the method can be useful in understanding the shallow structure of the subsurface beneath the basin and that additional MT data acquisition, using modern high-frequency and broadband instrumentation, may be an important tool in mapping the boundaries of the basin and the structures within it. This information will contribute to developing a better understanding of the potential for hydrocarbon resources in the region (Spratt et al., 2006). In the fall of 2007, a field campaign was designed to record more than 800 high-frequency and broadband MT sites from within the Nechako Basin. The primary objective of the survey is to

evaluate the technique as a tool both for oil and gas exploration and for geological characterization of the Nechako Basin.

Geological and Geophysical Background

Geology of the Nechako Basin

The Mesozoic Nechako Basin, located in the Intermontane Belt of the Canadian Cordillera, is a basin that includes overlapping sedimentary sequences deposited in response to terrane amalgamation to the western edge of ancestral North America (Monger et al., 1972; Monger and Price, 1979; Monger et al., 1982; Gabrielse and Yorath, 1991). Regional transcurrent faulting and associated east-west extension, beginning in the Late Cretaceous, were accompanied by the extrusion of basaltic lava during the Eocene and Miocene to form a sheet that covers much of the basin at thicknesses varying between 5 and 200 m (Mathews, 1989; Andrews and Russell, 2007), and possibly as much as 1 km in isolated locations. The main geological elements in the southern Nechako area include Miocene basalt, Tertiary volcanic and sedimentary rocks, Cretaceous sedimentary rocks and Jurassic sedimentary rocks (Figure 1).

Geophysical Studies

Results and interpretations of magnetotelluric (MT) surveys are often both complemented and constrained by geological information and models obtained from other types of geophysical surveys. Several different studies have been carried out within the Nechako Basin in the past, and several more are being planned for the near future. Existing models or data will be used to resolve the MT inversion models, providing the most accurate interpretation for the electrical resistivity structure in the subsurface.

In the early 1980s, a regional gravity survey was carried out by Canadian Hunter that identified a gravity low in the

Keywords: Nechako Basin, magnetotelluric, electromagnetic

This publication is also available, free of charge, as colour digital files in Adobe Acrobat® PDF format from the Geoscience BC website: <http://www.geosciencebc.com/s/DataReleases.asp>.

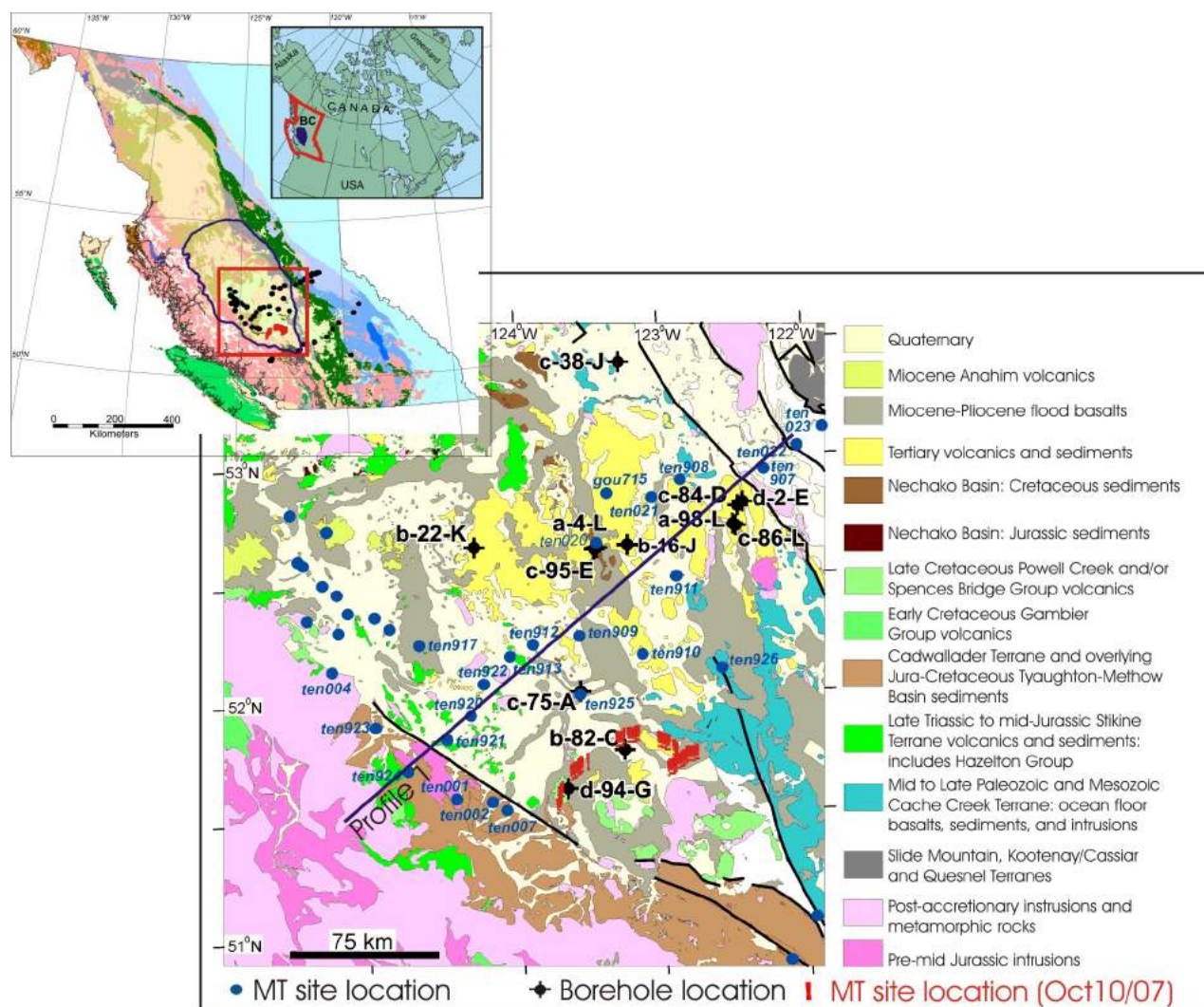


Figure 1. Location and geology of the Nechako Basin, showing the locations of the boreholes, old MT sites and the newly acquired MT sites. The blue outline on the location map in the upper left shows the outline and extent of the Nechako Basin. The blue line labelled 'Profile 1' is the surface trace of the two-dimensional model shown in Figure 3.

southern Nechako Basin. In early 2000s, Bemex Consulting International confirmed this anomaly with ground gravity and magnetic data collected in the southern tip of the basin (Figure 2). In addition to these regional surveys, several boreholes were drilled throughout the southern portion of the basin between 1960 and 1986 (Figure 1), providing detailed geological information as well as a variety of borehole logs that included natural gamma-ray spectroscopy, neutron porosity and resistivity. Due to absorption and reflection effects, the presence of the surface basaltic flows and Tertiary volcanic rocks covering most of the region has, to date, prevented uniform and consistent seismic-energy penetration and complicated the magnetic interpretations.

More than 100 rock samples have been sent to the Geological Survey of Canada's petrophysical laboratory in Ottawa for measurement of the resistivities and porosities of key lithological units in the Nechako Basin. The intent of this

analysis is to provide information on the primary electrical conduction mechanisms and level of electrical anisotropy of the different units. These, along with the resistivities from existing well logs, will place constraints on the conductivity models generated and make it possible to account for distortion due to anisotropy and static shift effects.

Finally, new seismic information will soon be available. Seven long-term teleseismic stations have recently been deployed within the Nechako Basin as part of a joint project involving the Geological Survey of Canada–Pacific (GSC), the BC Ministry of Mines, Energy and Petroleum Resources, and the University of Manitoba. In addition, Geoscience BC is acquiring Vibroseis® data and the GSC is planning to acquire explosive-source seismic reflection data in 2007–2008. These projects have been designed to account for the surface volcanic layers and will be an insightful addition to the magnetotelluric interpretations.

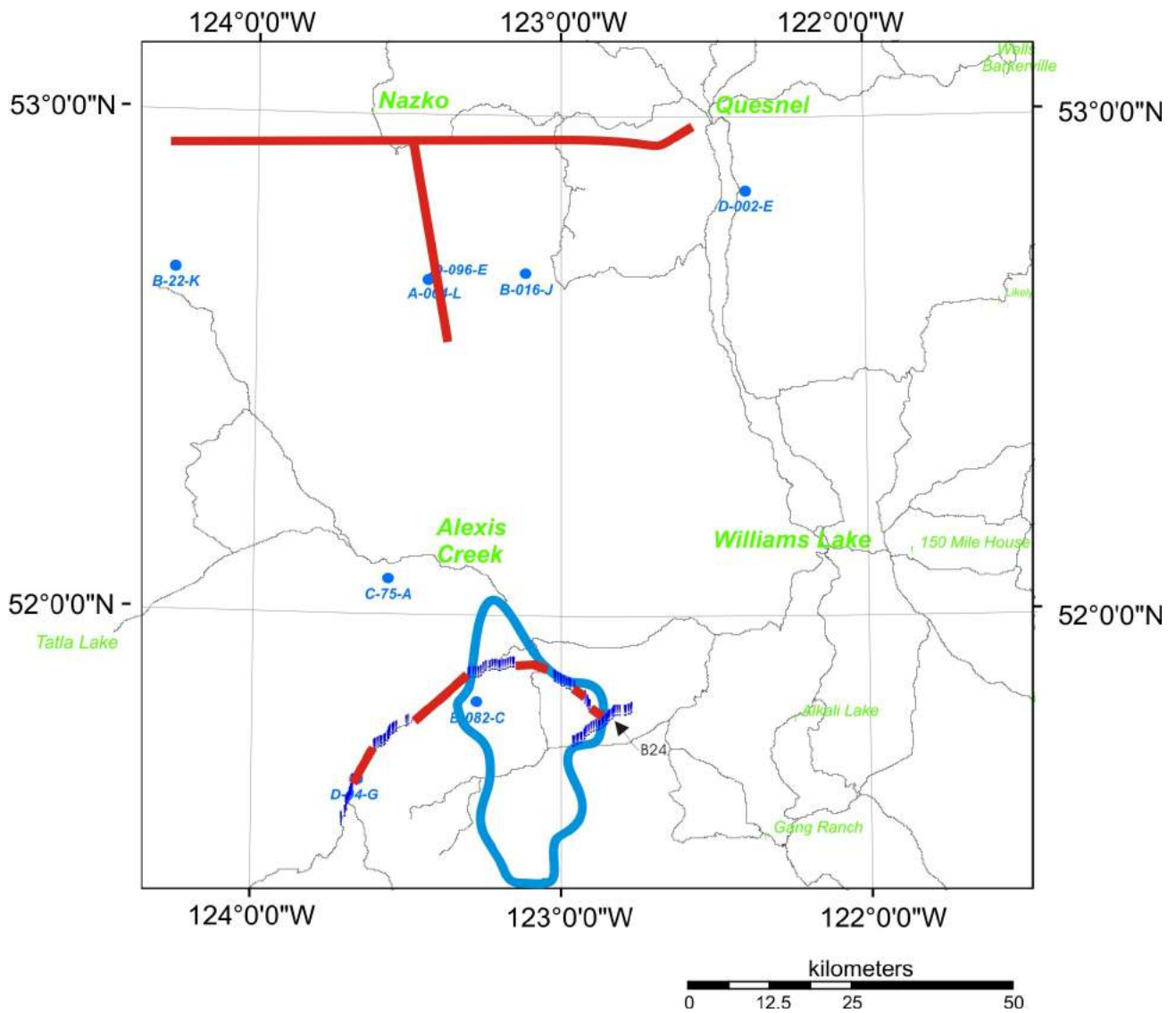


Figure 2. Locations of the MT profiles (thick orange lines) along which data is expected to be collected by the end of November 2007. The blue exclamation points show the locations of the sites collected to date, and the light blue line marks the outline of the observed gravity low. The light blue circles show borehole names and locations.

Magnetotelluric Method and Previous Studies

The magnetotelluric (MT) method provides information on the electrical conductivity of the subsurface of the Earth by measuring the natural time-varying electric (E) and magnetic (H) fields at its surface (Cagniard, 1953; Wait, 1962; Jones, 1992). The measurement of these mutually perpendicular electric and magnetic fields allows the calculation of phase lags and apparent resistivities at various frequencies, known as MT response curves, for each MT site recorded. Since the depth of penetration (or skin depth) of these fields is dependent on frequency (lower frequencies penetrate deeper) and the conductivity of the material (the lower the conductivity, the greater the depth), estimates of depth can be made from the response curves beneath each site (Kearey and Brooks, 1991).

As magnetotelluric (MT) data are sensitive to changes in the resistivity of materials, the method can distinguish between some lithological units. For example, basalt and igneous basement rocks typically have electrical resistivity values of >1000 ohm-m, whereas sedimentary rocks are more conductive, with values of 1–1000 ohm-m. Aside from lithology, other factors are known to affect the overall conductivity of a specific unit in the crust. The presence of saline fluids, changes in porosity, and the presence of graphite films and interconnected metallic ores are all factors that can substantially increase the conductivities of rocks (Haak and Hutton, 1986; Jones, 1992). As the method is sensitive to, but not impeded by, the surface volcanic rocks and can detect variations within the different units, it should prove useful in locating the boundaries of the Nechako Basin and defining the structure within.

In the early 1980s, the University of Alberta recorded MT data across the Nechako Basin between 52° and 53°N using short-period automatic MT system (SPAM) instruments that recorded data in the frequency range 0.016–130 Hz (Figure 1; Majorowicz and Gough, 1991). Initial analysis of these data revealed an anomalously conductive upper crust (10–300 ohm-m) in the eastern half of the northeast-southwest profile that was attributed to the presence of saline water in pore spaces and fractures. The western half of the profile showed the presence of an eastward-dipping resistive feature. The resistive body has been interpreted to represent granodiorite or other crystalline rocks of the Coast Belt that extend beneath a thin layer of basalt (Gough and Majorowicz, 1992; Majorowicz and Gough, 1994; Jones and Gough, 1995; Ledo and Jones, 2001).

Modern processing software and techniques, as well as modelling and interpretation packages, were applied to these original MT sites (Spratt et al., 2006). The new analysis included detailed strike analysis, distortion decomposition and two-dimensional modelling inversions. Using these advanced methods, it was shown that the MT data were capable of penetrating the Cenozoic volcanic rocks and imaging the shallow features of the Nechako Basin (Figure 3).

Magnetotelluric Data Acquisition

Design of the Survey

Borehole resistivity measurements were analyzed to assess the frequency range, expected resolution and site spacing that would be most appropriate for defining the structure of the Nechako Basin and for oil and gas exploration. Syn-

thetic MT response curves were calculated from existing borehole resistivity measurements for three different frequency bands: broadband (BBMT, 10 000–0.01 Hz), magnetotelluric (MT, 380–0.01 Hz) and audiomagnetotelluric (AMT, 10 000–5 Hz). One-dimensional Occam inversion models were then generated from these synthetic curves for each band at each well. These 1-D models indicate that the AMT frequency set produced the best models at most depths, showing a shallow and highly resistive layer. In some cases, the MT range appears to be necessary for imaging slightly deeper structure. From these results, it was decided that the most accurate basin structure could be imaged using a combination of AMT and MT data acquisition.

In order to accurately compare results and interpretations, the magnetotelluric profiles were originally designed to coincide as much as possible with those outlined in the proposed Geoscience BC Vibroseis[®] seismic-reflection survey to be undertaken in the region. The MT profiles have been altered due to accessibility. Figure 2 shows the current intended MT profiles in the southern Nechako Basin, with the southern lines running through a region of lower gravity anomalies. The total length of the profiles is approximately 355 km. Data were initially collected with a mix of daytime and night-time acquisition periods by three independent crews. The AMT data were collected at each site for 1 hour during the daytime, with a productivity of 6–8 sites/day per crew. At the end of each day, sufficient equipment was left in the field to record AMT and MT data overnight. The overnight data were significantly better than the daytime data due to the generally stronger source field at night (Garcia and Jones, 2002) and the longer recording time. It was

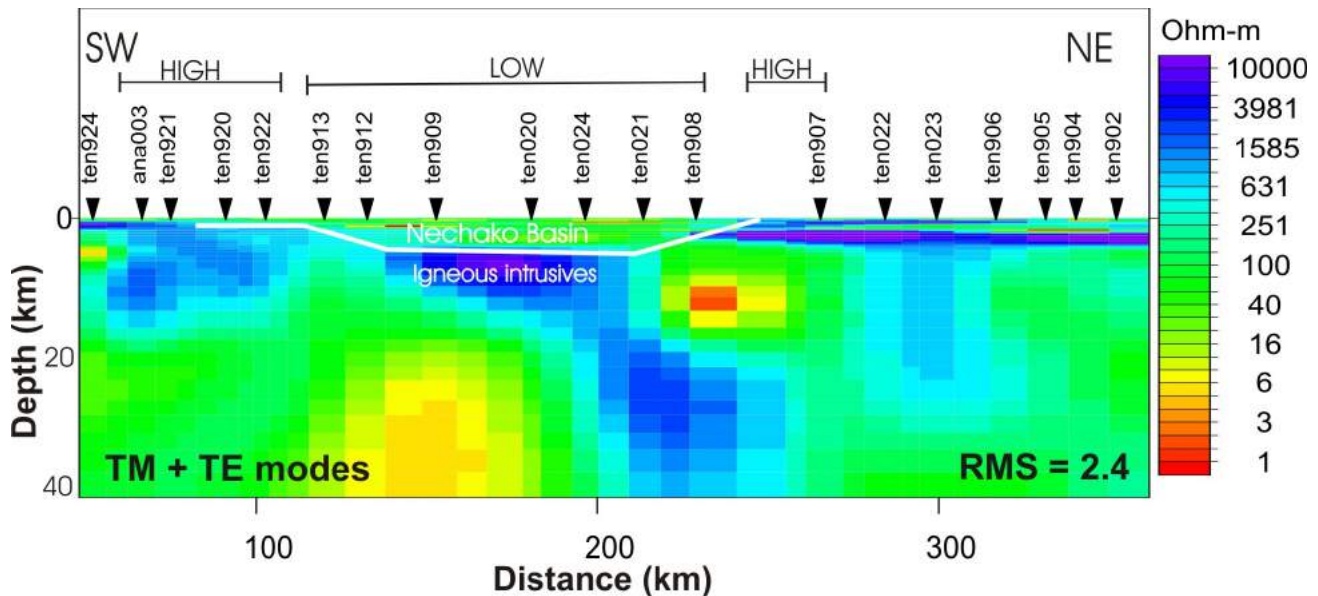


Figure 3. Two-dimensional conductivity model from 20-year-old MT data that were re-analyzed using modern techniques. The red and blue colours represent conductive and resistive regions, respectively. The white line (from Spratt et al., 2006) marks the interpreted boundary of the Nechako Basin.

therefore decided to switch to entirely overnight recordings. In such a scheme, the crews deploy equipment at 6 sites/day. After completion of the fall field campaign, a total of 880 combined AMT sites and BBMT sites are expected to be collected along these profiles.

Data Acquisition

The data are recorded using MTU-5A systems from Phoenix Geophysics Limited. A standard site layout is composed of five electrodes, either lead-lead-chloride porous pots or steel rods, to measure the electric fields in two perpendicular directions, and three separate coils to measure the magnetic fields in the horizontal and vertical directions (Figure 4). Currently, each of three separate teams installs 6 sites/day and leaves them to record overnight. Two of the six sites are telluric only, meaning that only the two telluric or electric field channels are deployed. Two of the sites are five-channel AMT sites, meaning that the telluric and AMT magnetic fields are measured. The remaining two sites are five-channel MT sites, meaning that the telluric and MT magnetic fields are recorded. The relatively tight station spacing of 500 m and the generally layered subsurface conditions mean that the magnetic field recordings (AMT or MT) at the different sites can be used with the telluric channels at all sites. The end result is that each crew is deploying six combined AMT and MT sites per day.

To date, more than 100 sites have been collected along the southernmost profiles (Figure 2). The data quality in general is very good, with combined AMT and BBMT sites yielding apparent-resistivity and phase response curves over a span of seven period decades (i.e., orders of magnitude; Figure 5a). The response curves at site B24 show a resistive layer (100 ohm-m to 0.005 s) above a slightly more conductive layer (~10 ohm-m); with increasing period, the response curves suggest the presence of a third bottom layer that is strongly two-dimensional, as indicated by the phase split between the two curves. An approximate depth estimate for the boundary between the second and third layers, using the skin depth equation, is 890 m. Although considerable analysis and depth modelling still need to be completed, this site shows a good indication that the method is imaging the resistive upper volcanic rocks, the more conductive sediment rocks, and a more complex deeper structure below.

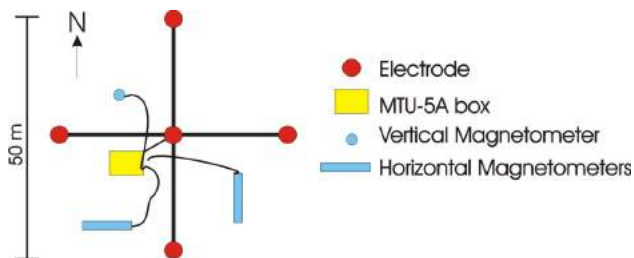


Figure 4. Plan view of a typical layout for an MT site.

Conclusions

The magnetotelluric method has proven to be useful in imaging lithographic structures of varying conductivities (e.g., distinguishing sedimentary units from volcanic and crystalline basement rocks). A magnetotelluric survey has been designed to assess the capabilities of the MT method in the exploration for hydrocarbons in the Nechako sedimentary basin and evaluate the extent to which the structure of the basin can be defined. Analysis of borehole resistivity

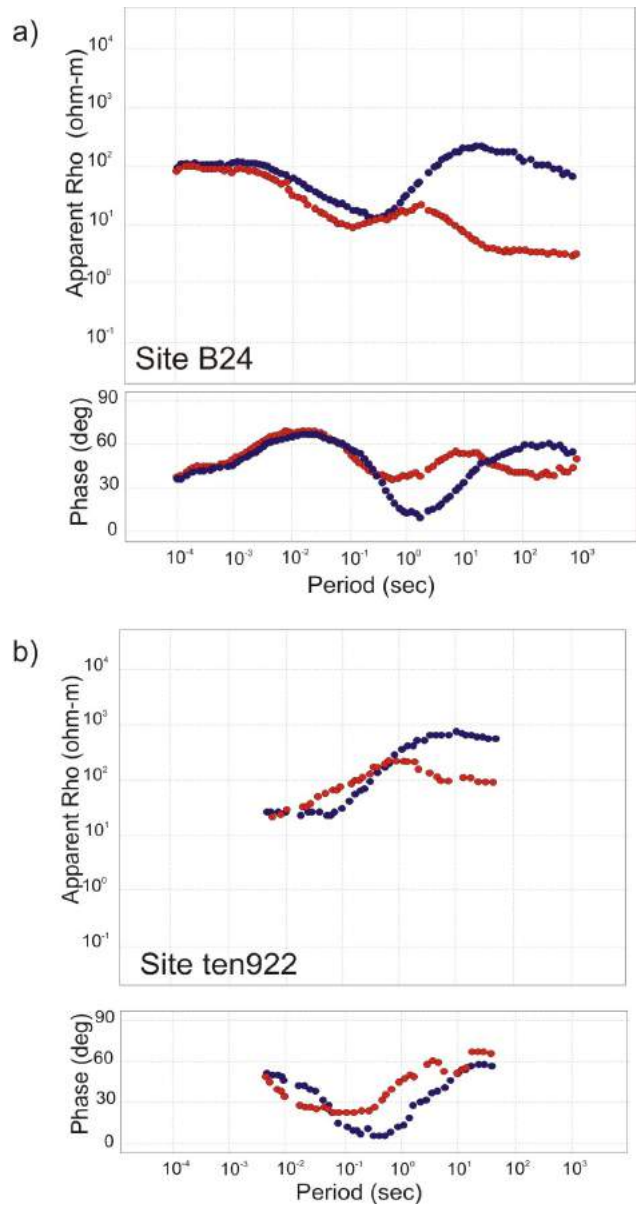


Figure 5. Examples of the apparent-resistivity and phase-versus-period response curves: **a)** data collected recently at a combined MT-AMT overnight site, and **b)** data quality at one of the 20-year-old sites. The quality of the data at the newer site is very good through seven decades, including the AMT dead band. The blue and red dots show the transverse magnetic and transverse electric modes, the difference in the curves indicating a difference in the north-south direction compared to the east-west direction.

data from the region has provided guidelines for data acquisition parameters, such as the most appropriate frequency ranges to record and site spacing. The planned survey consists of more than 800 AMT and BBMT sites that will be collected from within the Nechako Basin. Data acquisition began in mid-September, and initial results show excellent data quality. It is expected that all data will have been collected by the end of November 2007, after which detailed analysis, modelling and interpretations will be undertaken.

Acknowledgments

Financial support for this work comes from the Geological Survey of Canada, Geoscience BC and the BC Ministry of Energy Mines and Petroleum Resources. The authors wish to thank D. Snyder and P. Keating for their reviews, insightful comments and constructive suggestions.

Geological Survey of Canada contribution 20070349.

References

- Andrews, G.D.M. and Russell, J.K. (2007): Mineral exploration potential beneath the Chilcotin Group (NTS 092O, P; 093A, B, C, F, G, J, K), south-central British Columbia: preliminary insights from volcanic facies analysis; *in* Geological Fieldwork 2006, BC Ministry of Energy, Mines and Petroleum Resources, Paper 2007-1 and Geoscience BC, Report 2007-1, p. 229–238.
- Cagniard, L. (1953): Basic theory of the magnetotelluric method of geophysical prospecting; *Geophysics*, v. 18, p. 605–635.
- Gabrielse, J. and Yorath, C.J. editors (1991): *Geology of the Cordilleran Orogen in Canada*; Geological Survey of Canada, Geology of Canada, no. 4 (*also* Geological Society of America, *Geology of North America*, v. G-2).
- Garcia X. and Jones, A.G. (2002): Atmospheric sources for audio-magnetotelluric (AMT) sounding; *Geophysics*, v. 67, no. 2, p. 448–458.
- Gough, D.I. and Majorowicz, J.A. (1992): Magnetotelluric soundings, structure and fluids in the southern Canadian Cordillera; *Canadian Journal of Earth Sciences*, v. 29, p. 609–620.
- Haak, V. and Hutton, V.R.S. (1986): Electrical resistivity in continental lower crust; Geological Society of London, Special Publication 24, p. 35–49.
- Hannigan, P., Lee, P.J., Osadetz, K.G., Dietrich, J.R. and Olsen-Heise, K. (1994): Oil and gas resource potential of the Nechako-Chilcotin area of British Columbia; Geological Survey of Canada, GeoFile 2001-6, 38 p.
- Jones, A.G. (1992): Electrical conductivity of the continental lower crust; *in* *Continental Lower Crust*, D.M. Fountain, R.J. Arculus and R.W. Kay (ed.), Elsevier, p. 81–143.
- Jones, A.G. and Gough, D.I. (1995): Electromagnetic images of crustal structures in southern and central Canadian Cordillera; *Canadian Journal of Earth Sciences*, v. 32, p. 1541–1563.
- Kearey, P. and Brooks, M. (1991): *An Introduction to Geophysical Exploration (Second Edition)*; Blackwell Scientific Publications.
- Ledo, J. and Jones, A.G. (2001): Regional electrical resistivity structure of the southern Canadian Cordillera and its physical interpretation; *Journal of Geophysical Research*, v. 106, p. 30 755–30 769.
- Majorowicz, J.A. and Gough, D.I. (1991): Crustal structures from MT soundings in the Canadian Cordillera; *Earth and Planetary Science Letters*, volume 102, pages 444–454.
- Majorowicz, J.A. and Gough, D.I. (1994): A model of conductive structure in the Canadian Cordillera; *Geophysical Journal International*, v. 117, p. 301–312.
- Mathews, W.H. (1989): Neogene Chilcotin basalts in south-central British Columbia; *Canadian Journal of Earth Sciences*, v. 23, p. 1796–1803.
- Monger, J.W.H. and Price, R.A. (1979): Geodynamic evolution of the Canadian Cordillera — progress and problems; *Canadian Journal of Earth Sciences*, v. 16, p. 770–791.
- Monger, J.W.H., Price, R.A. and Tempelman-Kluit, D. (1982): Tectonic accretion of two major metamorphic and plutonic belts in the Canadian Cordillera; *Geology*, v. 10, p. 70–75.
- Monger, J.W.H., Souther, J.G. and Gabrielse, H. (1972): Evolution of the Canadian Cordillera — a plate tectonic model; *American Journal of Science*, v. 272, p. 557–602.
- Spratt, J.E., Craven, J., Jones, A.G., Ferri, F. and Riddell, J. (2006): Utility of magnetotelluric data in unravelling the stratigraphic-structural framework of the Nechako Basin, British Columbia from a re-analysis of 20-year-old data; *in* Geological Fieldwork 2006, BC Ministry of Energy, Mines and Petroleum Resources, Paper 2007-1 and Geoscience BC, Report 2007-1, p. 395–403.
- Wait, J.R. (1962): Theory of magnetotelluric fields; *Journal of Research of the National Bureau of Standards*, v. 66D, p. 509–541.